UNIVERSITAT DE BARCELONA

Proteomic profile in *postmortem* brain in chronic schizopfrenia

América Vera Montecinos

PROTEOMIC PROFILE IN *POSTMORTEM* BRAIN IN CHRONIC SCHIZOPHRENIA

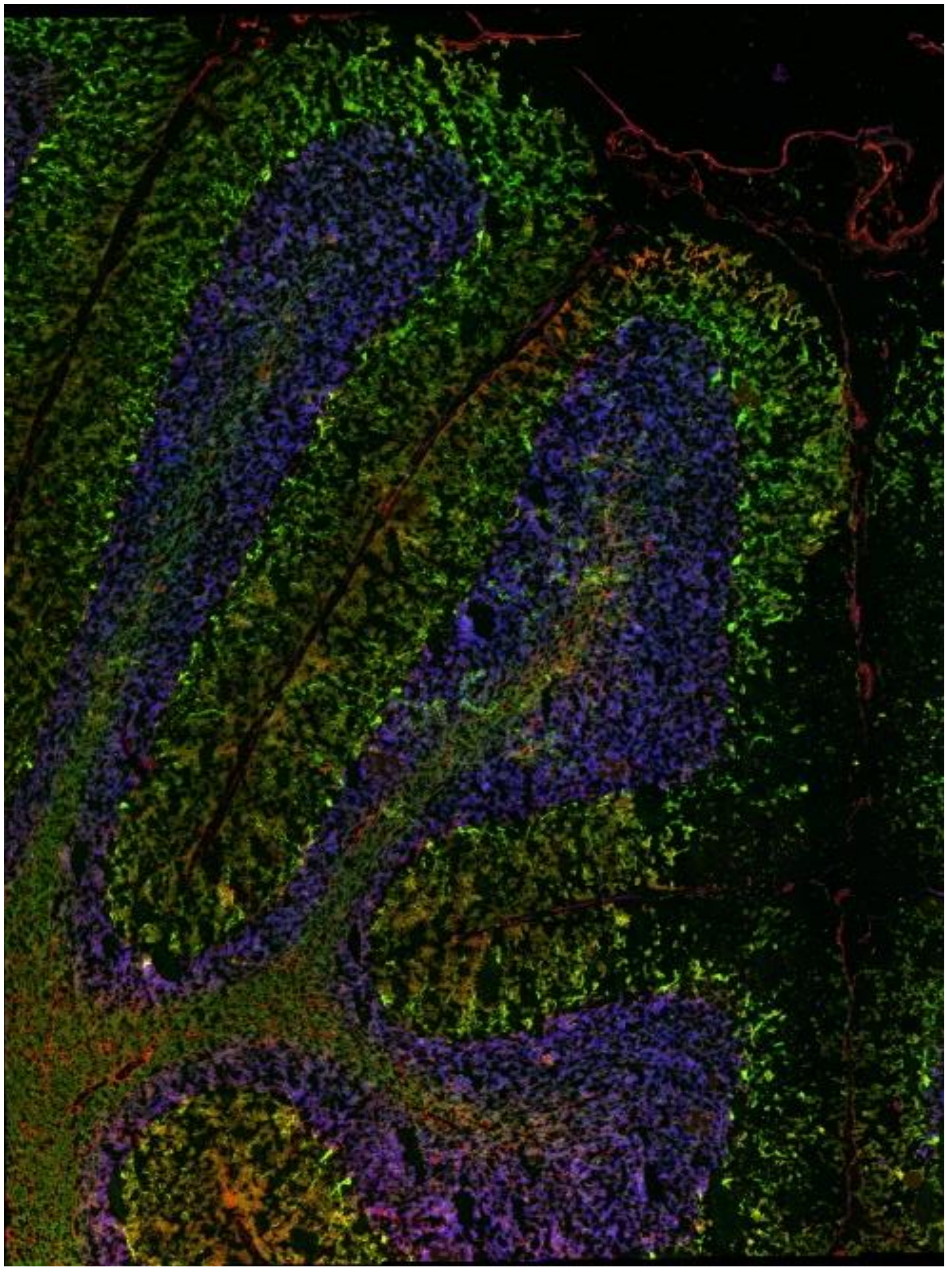

América Jennifer Vera Montecinos

Departamento de Bioquímica y Biología Celular

Facultad de Biología

Universidad de Barcelona

2020

UNIVERSITAT DE BARCELONA

FACULTAT DE BIOLOGIA

PROGRAMA DE DOCTORAT EN BIOMEDICINA

PROTEOMIC PROFILE IN *POSTMORTEM* BRAIN IN CHRONIC SCHIZOPHRENIA

Memoria realizada por América Vera Montecinos,

para optar al grado de Doctora por la Universidad de Barcelona

América Vera Montecinos

Autora

Dra. Belén Ramos Josemaria

Director

Dr. Isidre Ferrer Abizanda

Tutor

A mi madre Juanita Rosa, Osman, Manuel, Ale

Alexia, Anto, Seba, Fabi, Stephi y Maty

Todo hombre puede ser, si se lo propone, escultor de su propio cerebro

Santiago Ramón y Cajal

(1852-1934)

This Predoctoral research has been performed thanks to several subsidised projects:

1. The Predoctoral fellowship “Becas Chile”, 72160426 grant number. Gobierno de Chile to America Vera.

2. Miguel Servet grant (MS16/00153-CP16/00153) to BR financed and integrated into the National R + D + I and funded by the Instituto de Salud Carlos III (Spanish Ministry of Health) – General Branch Evaluation and Promotion of Health Research – and the European Regional Development Fund (ERDF).

This Thesis has been developed in the Molecular Psychiatry Laboratory of the Fundació Sant Joan de Déu (coordinator Dra Belén Ramos), part of the Unitat de Recerca del Parc Sanitari Sant Joan de Déu

Agradecimientos

Mis más sinceros agradecimientos van a mi tutora la Dra. Belén Ramos, quien me acogió en su laboratorio, recuerdo el primer día que le escribí para saber si podía realizar el doctorado en su laboratorio, desde ahí comenzó este viaje, gracias por compartir la ciencia, por inculcar que tomé mis propias decisiones y ser más exhaustiva con mi trabajo. Por su capacidad de ver los resultados de manera positiva, y la disponibilidad en este periodo de escritura de tesis. También agradecer a mi tutor Isidre Ferrer, por su disposición.

A mis compañeros de laboratorio, Elia, quien fue mi única compañera por un largo tiempo, gracias por repetirme tantas veces algunos protocolos y la ubicación de los reactivos, al principio todo me parecía tan extraño y por compartir tardes de experimentos. También, por las conversaciones interculturales que teníamos con palabras que más de una vez en catalán o español tenían otro significado, gracias Elia¡. A Fran, por compartir tardes de experimentos y por contribuir a mi risa con sus profundos pensamientos sobre algunas frases de papers. Como no mencionar a Ania, quien estuvo en el lab por un tiempo en su proyecto de máster y realización experimental posterior, gracias por tu compañía.

También dar las gracias los colaboradores que hicieron posible el desarrollo de esta tesis, Dra. Judit Villén y Dr. Ricard Rodríguez-Mias por su colaboración en proteómica. Dra. Karina MacDowell y Dr. Borja García-Bueno por su disponibilidad, disposición y contribución experimental con modelos de double-hit.

Muchas gracias a los donantes y a sus familias por darnos la posibilidad de investigar y de realizar esta tesis. Gracias por confiar en la ciencia.

Como no mencionar a Julieta, Mari, que a pesar de la distancia, siempre estuvieron y estarán presentes en mi vida, gracias por despertarme con mensajes de energía y cariño¡. A Claudio, amigo gracias por compartir tus conocimientos informáticos y por las largas conversaciones para resolver problemas “Omics” desde el master al doctorado¡

Siempre encontramos a personas que de algún modo nos acompañan en algún tramo de nuestra vida, aquí he encontrado aquellas personas que pasan por tu vida con un propósito, Isabel, gracias por tu cariño desde el momento que nos conocimos. A mi primera compañera de piso Reme, gracias por acogerme cuando recién llegue. Lus, por sus secretos botánicos¡. En especial a Seba, por hacerle este último tramo más llevadero a mis neuronas, has sido un gran apoyo en esta etapa, te lo agradezco de todo corazón, gracias por tu cariño. A Amelie y Lee por su cariño desinteresado y compañía.

A Teresa y Hernán, por enseñarme y por su motivación con la ciencia, ¡que recuerdos guardo con ustedes!

A mi familia, mi Network fundamental, gracias a ellos he podido llevar a cabo esta etapa, por su energía, amor incondicional, por creer en mi siempre. Por hacerme sentir cerca de ellos a pesar de la distancia y compartir cenas virtuales!. A mi mamá, por su valioso tiempo a cualquier hora que la necesitara estaba ahí al otro lado del teléfono, por sus consejos y por desafiar sus propios miedos para estar unos meses conmigo aquí, muchas gracias mamá. A Osman, sin duda este viaje no hubiese sido posible sin su enorme apoyo y sabias palabras, ¡por su incondicionalidad! Ale, por el apoyo y energía en este viaje a Alexia y Anto por su cariño e interés en todo! No tengo palabras para agradecerles! A Manuel, Fabi, Stephy y Mati por su cariño. ¡los quiero mucho Network!

Summary

Schizophrenia is a complex psychiatric disorder involving dysregulation of multiple pathways. In the last decades, the cortico-cerebellar-thalamo-cortical circuit has been proposed to play a key role in cognitive impairments in schizophrenia. The cerebellum is a brain area that forms part of this circuit that modulates synaptic responses of cortical regions, it has been proposed to play an important role in schizophrenia pathophysiology. Furthermore, the cerebellum, in connection with the dorsolateral prefrontal cortex, is involved in executive and working memory function. Thus, we hypothesized that the altered proteomic profile in the brain participates in the molecular network dysfunction in chronic schizophrenia. In this doctoral thesis we aimed to compare the proteomic profile in the *postmortem* cerebellar cortex and the prefrontal cortex of individuals with chronic schizophrenia by using (i) mass spectrometry, (ii) bioinformatic analyses to identify altered molecular networks, (iii) two double-hit schizophrenia murine models induced by maternal deprivation combined with an additional stressor for the hit proteins from the altered network in the cerebellum, (iv) immunohistochemistry techniques and (v) 3D projection analysis for unexplored candidate hits in human cerebellum.

First, we performed a pilot proteomic analysis on *postmortem* human cerebellar tissue from patients with schizophrenia (n=4) and control (n=4) subjects in a pool design using differential isotope peptide labelling followed by liquid chromatography tandem mass spectrometry (LC-MS/MS). Our results showed 1412 quantified proteins and 99 significantly altered proteins. 11 candidate proteins were selected as the most robust candidates from the enriched biological functions comprising cell communication/signal transduction in schizophrenia. In this study we report 68 new proteins altered in schizophrenia. In our individual proteomic study of the cerebellum, we analysed 12 cerebellar samples of subjects with schizophrenia and 14 healthy control individuals using one-shot liquid- tandem mass spectrometry. We identified a proteomic signature composed of 2578 identified proteins and 1474 quantified proteins with 250 significantly dysregulated proteins. This study reported 167 new proteins that are altered in the cerebellum in schizophrenia. Moreover, our study allowed us to identify the proteome profile and molecular networks altered in the cerebellum in chronic schizophrenia. Hierarchical clustering allowed schizophrenia subjects to be segregated from controls. Furthermore, our analyses showed that the 250 altered proteins could be under the transcriptional control of only11 transcription factors. The pathways regulated by these 11 transcription factors were related to transport, signalling, inflammation, and apoptosis.

Our network generation analysis in the cerebellum showed two well-defined networks. The network generated from the up-regulated proteins showed a mixed module with enriched pathway interactions. This module consisted of proteins from vesicle-mediated transport and axon guidance pathways. In the axon guidance pathway, CLASP1 was a hit protein that we further studied in two independent *double-hit* murine models for schizophrenia. Our results showed CLASP1 to be down-regulated in the murine model of maternal deprivation combined with social isolation, while our proteomic study showed it to be up-regulated. The second network was formed by two modules generated from proteins that were found to be down-regulated in the cerebellum: an energy module and a neutrophil degranulation module. The energy module was well defined in our analysis, with NDUFB9 found to be a down-regulated hit protein in our proteomic study and in the double-hit murine model of maternal deprivation combined with social isolation. The second module was neutrophil degranulation. METTL7A was found to be a hit protein in this pathway. In our study, we found . and METTL7A was found to be consistently down-regulated both in schizophrenia subjects and murine models for schizophrenia. We demonstrated for the first time the expression of METTL7A in Bergmann glia cells in the human cerebellum. We also detected METTL7A in one of its canonical localizations, in lipid droplets in white matter cells.

The prefrontal cortex analysis revealed 4407 identified proteins, 1989 quantified proteins and 43 significantly altered proteins. The enriched pathways were mainly related to the immune system. The network generated from the enriched pathway showed a mixed module with interactions between MHC class II antigen presentation, membrane trafficking, Golgi-to-ER retrograde transport, Nef-mediated CD8 down-regulation and the immune system.

Together, the results presented in this Thesis suggest an imbalance in the immune system in two brain regions, the cerebellum and the prefrontal cortex. This suggests that the nervous system could be susceptible to an imbalance in the immune system in schizophrenia subjects. Moreover, the vesicle-mediated transport pathway was found to be altered in both the cerebellum and the prefrontal cortex, two brain areas that participate in the cortico-cerebellar thalamo-cortical circuit. This result suggests a possible alteration in synaptic efficacy and communication between these areas in schizophrenia.

Abbreviations

SZ	Schizophrenia
GBD	Global Burden of Disease
YLDs	Age-standardized years lived with disability
CNS	Central nervous system
DA	Dopamine
NMDA	N-methyl-D-aspartate
PCP	Phencyclidine
MK-801	Dizocilpine
DSM	Diagnostic and Statistical Manual of Mental Disorders
PPI	Pre-pulse inhibition
CB	Cerebellum
CCTCC	Cortico-cerebellar-thalamic-cortical circuit
PFC	Prefrontal cortex
DLPFC	Dorsolateral prefrontal cortex
OFC	Orbitofrontal cortex
CC	Corpus callosum
ACC	Anterior cingulate
PMD	*Postmortem* delay
CSF	Cerebrospinal fluid
LC-MS/MS	Liquid chromatography tandem mass spectrometry
LFQ	Label free quantitative
MD/Iso	Maternal deprivation with isolation
MD/RS	Maternal deprivation with restraint stress
ML	Molecular layer
GL	Granular layer
PL	Purkinje layer
WM	White matter
SP1	Transcription factor SP1
SP4	Transcription factor SP4
KLF7	Krüppel-like factor 7
EGR1	Early growth response protein 1
HNF4A	Hepatocyte nuclear factor 4-alpha
CTCF	Transcriptional repressor CTCFL
GABPA	GA-binding protein alpha chain
NRF1	Endoplasmic reticulum membrane sensor NFE2L1
NFYA	Nuclear transcription factor Y subunit alpha
MEF2A	Myocyte-specific enhancer factor 2A
YY1,	Transcriptional repressor protein YY1
β-actin	Beta-actin
ARRB1	Beta-arrestin-1
SNX5	Sorting nexin-5
DCTN1	Dynactin subunit 1
DTNBP1	Dysbindin 1
GFAP	Glial Fibrillary Acidic Protein
METTL7A	Methyltransferase-like 7A
NDUFB9	NADH dehydrogenase [ubiquinone] 1 beta subcomplex subunit 9
CLASP1	CLIP-associating protein 1
YWHAZ	14-3-3 protein zeta/delta

FIGURES

TABLES

TABLE OF CONTENTS

I. INTRODUCTION

1.1. Prevalence of schizophrenia.

Schizophrenia is a complex polygenic psychiatric disorder that has a substantial impact on the quality of life of patients and their families. According to the Global Burden of Disease (GBD) study (Murray *et al.*, 1996), psychiatric disorders constitute 14% of the age-standardized years lived with disability (YLDs) (James *et al.*, 2018). According to the World Health Organization, schizophrenia affects 20 million people worldwide (World Health Organization., 2019) with a prevalence of 4 per 1000 and a lifetime morbid risk of 7.2 per 1000 (McGrath *et al.*, 2008). Moreover, the GBD study showed that from 2007 to 2017 the 20 top YLDs were attributable to schizophrenia, which increased 16.7% in males while in females it rose by 17.7% (James *et al.*, 2018). The prevalence of schizophrenia in Spain is 3 per 1000 individuals per year in men and 2.8 per 1000 in women, with an estimated age of 15 to 54 years (Ayuso-Mateos *et al.*, 2006). Although schizophrenia has a low incidence, it is a disorder with high disabling power that has a profound impact on affected individuals, their families and society.

1.2. Origins of the concept of schizophrenia

Historically, the first bases of the clinical concept of this disorder were proposed by psychiatrists Emil Kraepelin, Eugen Bleuler and Kurt Schneider. In the 1890s Kraepelin was the first to use the term *dementia praecox* as an umbrella term to describe the symptoms of affective deterioration, apathy, disorganization of thought and psychic hallucinations. Kraepelin also established the first nosology for this set of symptoms (Andreasen, 1997; Hoff, 2015). Furthermore, Kraepelin also thought that the origin of this disorder could be due to anatomical or toxic processes in the brain. His observations on the evolution of the disease allowed Kraepelin to postulate that this disease could be neurodegenerative due to the observed loss of cognitive functions. However, it was Bleuler who in 1908 introduced the term *schizophrenia*, using it later in his 1911 work *Dementia*

Praecox oder gruppe der schizophrenien. Bleuler proposed the division of the symptoms in two categories: fundamental symptoms (or negative symptoms) and accessory symptoms. Bleuler focussed more on psychopathology and "split personality", unlike Kraepelin, who concentrated on the symptoms of the disease and its evolution (Bleuler and Bleuler, 1986; Moskowitz and Heim, 2011). Kraepelin's and Bleuler's observations contributed to the knowledge of the same subtypes of schizophrenia reported today in the Diagnostic and Statistical Manual of Mental Disorders (DSM) (Lawrie, Hall and Johnstone, 2010). In 1940 the German psychiatrist Kurt Schneider took Kraepelin and Bleuler's information but considered only the clinical observation criteria, focussing on the psychotic processes more than the symptoms and evolution of the disease. In this way, Schneider proposed and called "first-rank symptoms" those psychotic processes (Whalley *et al.*, 1984; Andreasen, 1997) which were considered essential for the diagnosis of schizophrenia. However, Schneider later recognized that "first-rank symptoms" were related to a "loss of ego-bound". The observations carried out by Kraepelin, Bleuler and Schneider were the first bases for the diagnosis of schizophrenia. After several years of debate on the symptomatology used for the diagnosis of schizophrenia, today two main symptoms are used around the world (Lawrie, Hall and Johnstone, 2010): psychosis and hallucinatory experience or delusional idealization. At the same time, the duration of disease can be between one and six months. While these symptoms are described in the DSM-IV-V (Center for Behavioral Health Statistics and Quality, 2016), the diagnosis and treatment of schizophrenia are still today being constantly debated.

1.3. Etiopathology and pathophysiology of schizophrenia

Schizophrenia is a complex polygenic psychiatric disorder involving dysregulation of multiple signalling pathways, neuronal plasticity and thus showing altered neuronal connectivity (Zhang *et al.*, 2015; Rosato *et al.*, 2019). As one of several of

neurodevelopment disorders, schizophrenia has been proposed to have four phases, namely premorbid, prodromal, onset/deteriorative and chronic/residual (Lieberman, 1999a; Lieberman *et al.*, 2002).

i. Premorbid phase

This phase may develop during gestation and from infancy to early adolescence (**Figure 1**), with the main features being physical anomalies, altered motor coordination, and also cognitive and social deficits, the latter of which could be due to synaptogenic dysfunction (Lieberman *et al.*, 2002).

ii. Prodromal phase

This initial phase often manifests itself in adolescents and young adults (Skokou *et al.*, 2012). This phase is the focus of continued debate due to the presence of nonspecific symptoms (Remington *et al.*, 2016). Interest in the prodromal phase (**Figure 1**) has led to the development of several diagnostic tools to identify symptoms, enabling early intervention in subjects at risk (Gourzis, Katrivanou and Beratis, 2002). However, the symptoms that characterize this phase are mainly negative symptoms, positive-prepsychotic symptoms and positive-disorganization symptoms, as shown in **Table 1.**

Table 1. Symptoms of the prodromal phase in schizophrenia. *Modified from Gourzis, Katrivanou and Beratis, 2002.*

Negative symptoms	Positive-prepsychotic	Positive-disorganization
Marked isolation	Odd beliefs/magical thinking	Marked peculiar behaviour
Marked withdrawal	Suspiciousness	Inappropiate affect
Marked impairment in role functioning	Belief in clairvoyance	Disgressive speech
Marked impairment in personal hygiene and grooming	Telepathy	Vague speech
Blunted affect	Sixth sense	Overelaborate speech
Flat affect	Belief that others can feel one's feelings	Circumstantial speech
Poverty of speech	Overvalued ideas	Poverty of speech content
Marked lack of initiave, interests, or energy	Ideas of reference	
Impairment in concentration	Unusual perceptual experiences/perceptual Aberration/body image aberration	

In this regard, Lieberman (1999) proposed that these clinical features could be due to maturation processes in adolescence interacting with altered biological processes that

occurred during development, such as synaptic pruning and myelinization. During this phase, no clear therapeutic guidelines are available other than emotional support and stress reduction together with the use of GABA agonist, NMDA allosteric modulators, antioxidants and atypical antipsychotics could also help in this stage.

iii. Onset/progressive, active or acute phase

This phase is the most evident in schizophrenia and is characterized by positive and negative affective symptoms and cognitive impairment (Lyne *et al.*, 2014, 2018) (**Figure 1**). This phase of first-episode psychosis includes hallucinations and delusions (Byrne, 2007). The pathophysiological processes that could be involved in this phase include the sensitization of dopaminergic and glutamatergic systems in the mesolimbic-cortical circuit (Lieberman *et al.*, 2002).

iv. Chronic or residual phase

The symptoms that prevail during this period include psychosis, negative symptoms and significant cognitive impairment (Fujimaki *et al.*, 2018) (**Figure** 1). The altered pathophysiological processes are related to loss of cell processes, while possible apoptotic events may affect cortical-limbic striatal neurons. During the residual phase, the use of antipsychotics is not completely effective. Therefore, a treatment needs to be found that improves the quality of life of patients (Lieberman *et al.*, 2002).

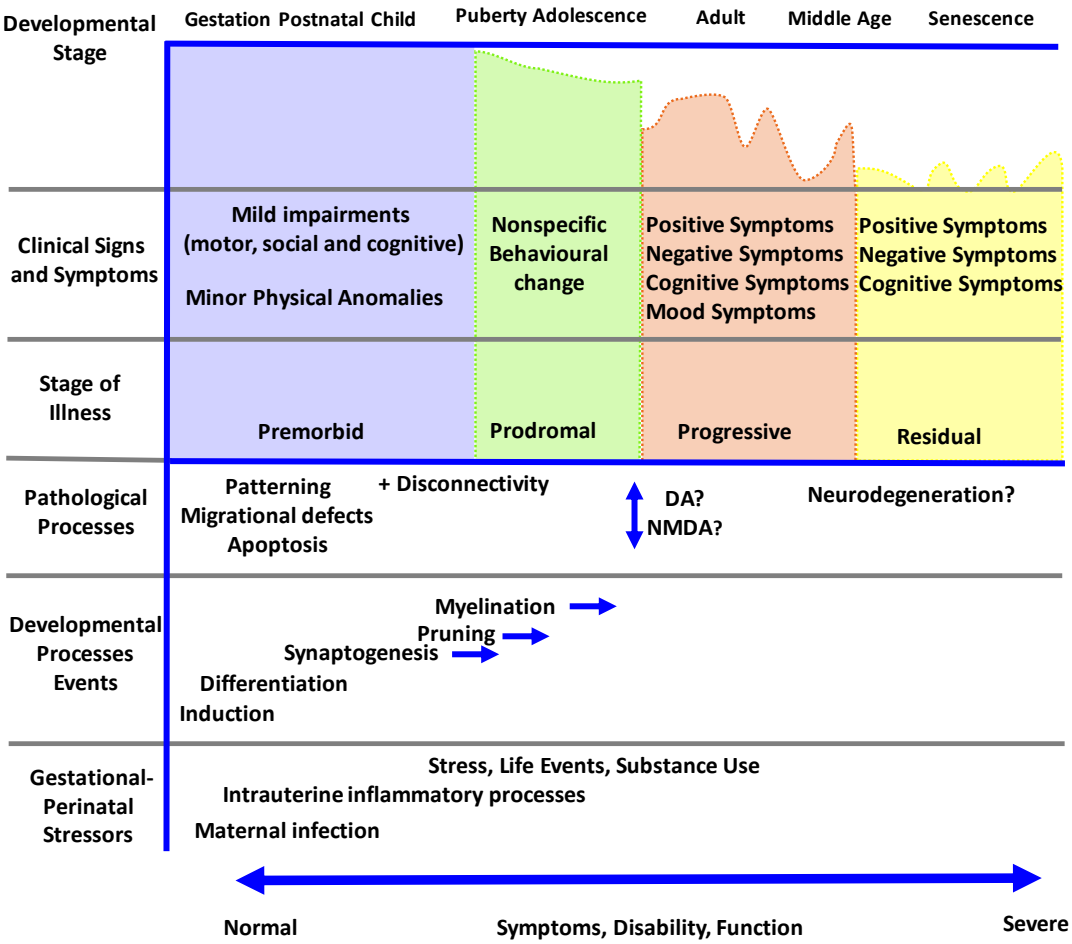

Figure 1.A diagram of the clinical phases of schizophrenia and developmental processes and stages. This diagram integrates the many clinical and pathophysiological phases of schizophrenia. From the top: The developmental stage is the period of life in which the illness phases occur. These phases include the premorbid, prodromal, progressive and residual phases. Symptoms are described. The pathological processes are related to the hypotheses that may underlie this disorder. Developmental process events are those processes that may be implicated in the onset of schizophrenia. **DA**: Dopamine, **NMDA**: N-methyl-D-aspartate. Adapted from Lieberman *et al*., 2002.

1.3.1. Genetic risk for schizophrenia

Genetic factors play an important role in schizophrenia. This disorder is characterized by high heritability, which is estimated to be 79% (Hilker *et al.*, 2018). The first bases of the high genetic component of schizophrenia come from twin studies (Sullivan, Kendler and Neale, 2003; Hilker *et al.*, 2018). The risk for schizophrenia in the general population is approximately 1% (McGrath *et al.*, 2008), while for first-degree schizophrenia subjects the risk increases to 6.5% and for monozygotic twins, who share close to 100% of their genomic sequence, the risk is between 50% and 60% (Kendler *et al.*, 1993).

Nowadays, the Human Genome Project (Avramopoulos, 2010) is the main tool used to study the molecular genetics of psychiatric disorders such as schizophrenia. Two postulates on variation in the DNA sequence could explain the high genetic risk of schizophrenia. First, susceptibility genes (Moran *et al.*, 2016) in which small effects are cumulative, thereby increasing the risk for schizophrenia. Second, single rare gene mutations that have a significant effect on the pathophysiology of schizophrenia. This postulates have their bases in studies on copy number variants (CNV) (Doherty, O'Donovan and Owen, 2012; Marshall *et al.*, 2017) in which cumulative effects were associated with gene loci abnormalities that could be inherited or that could be the result of interaction with environmental factors which have a high impact in the development of this disorder.

Several studies have associated certain genes with a genetic risk to manifest schizophrenia. Such genes include NRG1 (Mostaid *et al.*, 2017); KT1 (Thiselton *et al.*, 2008); COMT (Owen, Williams and O'Donovan, 2004); ZNF804A (O'Donovan *et al.*, 2008; Riley *et al.*, 2010); DISC1 (Millar *et al.*, 2000); DR2D (Lawford *et al.*, 2005); GRIA1 (Kang *et al.*, 2012); and *DTNBP1* (Straub *et al.*, 2002).

1.3.2. Pathophysiology models of schizophrenia

1.3.2.1. Dopaminergic hypothesis

The dopaminergic hypothesis, formulated in the 1970s (Seeman, 1987) due to the discovery of antipsychotic drugs and the studies of Carlsson and Lindqvist (1963) on the metabolism of dopamine, was the first hypothesis proposed for schizophrenia. It is based on the affinity of antipsychotics for dopamine receptors (Version I hypothesis), with the antipsychotics blocking the reuptake of dopamine, leading to an improvement in psychosis (Carlsson, Lindqvist and Magnusson, 1957). However, this first version of the hypothesis is not clear about the origin of the negative symptoms. It was not until 1991 that a second version of this hypothesis was proposed in which contributions from studies in *postmortem* animals and image data focussed on cortical-subcortical signalling. The new evidence suggested that the effects of the dopaminergic dysfunction could be region-dependent (Davis *et al.*, 1991). Furthermore, dopaminergic neuron injury in the frontal area increased dopamine levels in the striatum (Pycock, Kerwin and Carter, 1980), suggesting hypodopaminergia in the frontal cortex and hyperdopaminergia in the striatum. In this second version, Davis *et al.*, 1991 proposed that frontal hypodopaminergia could be related to the negative symptoms observed in schizophrenia, while hyperdopaminergia in the striatum could be associated with the positive symptoms. However, this hypothesis does not go deeply into the aetiology of schizophrenia.

The latest version of the dopaminergic hypothesis (version III) was proposed by Howes and Kapur in 2009. First, they hypothesized that altered dopamine levels are the result of the interaction of multiples “hits” which converge on a common point that leads to psychosis in schizophrenia. Second, the main alteration is the change in presynaptic dopaminergic levels. Third, altered dopamine levels are related more to psychosis than to schizophrenia. Fourth, altered dopaminergic signalling could be related to aberrant salience, which means that a person can define inappropriately common situations (Howes and Nour, 2016). This revised third hypothesis postulates the interaction of

environmental and genetic risk factors which could converge in presynaptic striatal hyperdopaminergic signalling.

1.3.2.2. Glutamatergic hypothesis: a system alteration

NMDA receptors are widely distributed in the brain and are involved in several processes during brain development (Ewald and Cline, 2009). Blocking NMDA receptors mainly reflects its function in the CNS because of its wide distribution (Watanabe *et al.*, 1992; Akazawa *et al.*, 1994; Takai *et al.*, 2003). NMDA receptors consist of three subunits, NR1, NR2 and NR3 (Flores-Soto *et al.*, 2012). The functional NMDA receptors are heterodimers and have at least two NR1 subunits. It has also been reported that different combinations of subunits could give different proprieties to NMDA receptors (Hansen *et al.*, 2014). From the 1970s glutamate was recognized as being the main excitatory neurotransmitter in vertebrate brains (Meldrum, 2000). Glutamate acts upon two types of receptors: (1) metabotropic, G protein-coupled receptors (mGluR1-5) and (2) ionotropic, ligated-gated ion channels, which have three types of receptors: N-methyl-D-aspartate (NMDA), α-amino-3hydroxy-5methyl-4 isoxazolepropionic acid (AMPA) and kainite (Reiner and Levitz, 2018). The first evidence for the role of N-methyl-D-aspartate (NMDA)-type glutamate receptors in schizophrenia came in the 1990s (Javitt, 1991). Evidence on the alteration of NMDA receptors came from studies on phencyclidine (PCP) and ketamine, which are NMDA receptor antagonists (Javitt, 1991, 2010). The results revealed that blocking these receptors led to schizophrenia-like symptoms such as psychosis and cognitive disturbances (Krystal *et al.*, 1994). Evidence on NMDA receptors antagonists such as phencyclidine and ketamine supports the glutamate hypofunction hypothesis in schizophrenia (Uno and Coyle, 2019).

1.3.2.3. Interaction of the glutamatergic system with the dopaminergic and GABAergic system

The origin of schizophrenia is multifactorial and may involve several signalling pathways. In this regard, NMDA dysfunction could affect dopamine regulation (Nair, Savelli and Mishra, 1998; Jang and Lee, 2001) and alter GABAergic signalling. In the context of schizophrenia, studies in healthy subjects under the effects of ketamine (an NMDA receptor antagonist) showed altered dopamine regulation that could be a consequence of dysfunctional NMDA signalling (Frohlich and Van Horn, 2014). Furthermore, studies demonstrated that altered parvalbumin-positive GABAergic interneurons in the cerebral cortex and hippocampus are related to NMDA receptor dysfunction (Cohen *et al.*, 2015). The parvalbumin-positive interneurons participate in gamma and beta neuronal oscillations (Metzner, Zurowski and Steuber, 2019). Gamma neuronal oscillations constitute a mechanism that regulates neuronal response throughout the cortex brain (Bartos, Vida and Jonas, 2007). Beta neuronal oscillations are involved in sensory gating (Limanowski, Litvak and Friston, 2020) and attention (Güntekin *et al.*, 2013). Studies in schizophrenia subjects showed a reduction in the synchronization phase due to decreases in the amplitude of gamma oscillations in the frontal region during executive and working memory tasks (Cho, Konecky and Carter, 2006; Haenschel *et al.*, 2009). Thus, the synchronization phase could have a role in integrating neuronal response in the cortical area (Varela *et al.*, 2001). These studies suggest that an altered synchronization phase could affect cortical connectivity in schizophrenia.

1.3.2.4. Inflammation and Neurodegenerative hypothesis

Inflammation and degenerative hypotheses have also been suggested and hybrid models between these hypotheses and the neurodevelopmental hypothesis have even been proposed, generating extensive debate in this field (Woods, 1998; Meyer *et al.*, 2009; Altamura *et al.*, 2013).

The involvement of immune dysfunction and inflammation in schizophrenia is supported by emerging evidence suggesting aberrant immune mechanisms (O'Donnell *et al.*, 1995; Kroken *et al.*, 2019; Comer *et al.*, 2020). A genome-wide association study reported a major histocompatibility complex (MHC) locus and Toll-like receptors (TLRs), both involved in innate immunity, as genetic risks for schizophrenia (Schizophrenia working group and psychiatric genomics consortium, 2014). *Postmortem* studies of schizophrenia subjects showed altered expression of elements of TLR4 signalling (García-Bueno *et al.*, 2016; MacDowell *et al.*, 2017). Moreover, several studies found high inflammatory cytokine levels in schizophrenia subjects (Miller *et al.*, 2011; Orlovska-Waast *et al.*, 2019). Cytokines are molecules implicated in the immune system response in peripheral central nervous system and the CNS (Zhang and An, 2009).

Furthermore, maternal infection during the gestational period could increase the risk for schizophrenia in offspring exposed to viral or bacterial infections in intrauterine life (Brown *et al.*, 2004). In this regard, high levels of IL-8 during pregnancy have been implicated in a decrease in brain volume and an increase volume of ventricles in schizophrenia subjects (Ellman *et al.*, 2010). Cytokines such as Interferon-ϒ can modulate and inhibit the differentiation of oligodendrocytes and alter myelinization processes (Chew *et al.*, 2005). Thus, inflammatory processes could alter myelinization and lead to neuronal connectivity dysfunction. In addition, studies on cerebrospinal fluid (CSF) revealed an increased CSF/serum albumin ratio, high levels of cytokines and vascular endothelial growth factor, a protein that increases blood-brain barrier permeability in schizophrenia patients (Müller and Ackenheil, 1995; Müller *et al.*, 1997; Najjar *et al.*, 2017). Thus, the accumulation of cytokines in the CSF could have an impact on the integrity of the brain parenchyma in schizophrenia patients due to altered blood-brain barrier permeability.

The neurodegenerative models are supported by evidence of disseminated apoptotic events in the CNS and cognitive decline in the later phases of schizophrenia. However, although evidence of gliosis, a marker typical of neurodegeneration, has not been found,

graded apoptosis in *postmortem* tissue from schizophrenia patients has been observed (Lieberman, 1999b; Jarskog *et al.*, 2005). This graded apoptosis could be due to "synaptic apoptosis" in which apoptotic events occur only in synapses in distal neurites though without immediate neuronal death (Mattson, Keller and Begley, 1998), something which may occur in schizophrenia. Moreover, apoptotic events could be due to the altered expression of the anti-apoptotic protein *bcl-2* in schizophrenia (Jarskog *et al.*, 2000).

1.3.2.5. Neurodevelopment hypothesis

In 1988, Weinberger proposed the neurodevelopment hypothesis. This hypothesis proposed two critical periods of neurodevelopmental vulnerability, early life and adolescence, with an environmental *double hit* in a genetically predisposed individual being required for the emergence of the disease (Fatemi and Folsom, 2009; Davis *et al.*, 2016). Several environmental injuries such as obstetric complications, maternal infection and stress have been proposed as risk factors for schizophrenia. However, these injuries must occur during specific and transcendental "time windows" for correct brain development (Marín, 2016). Thus, time windows are critical periods for neurodevelopment disorders. A critical period could be the maturation of oligodendrocytes, which are responsible for myelination in the CNS (Flynn *et al.*, 2003) or alteration in complement C4 signalling involved in synaptic pruning (Druart and Le Magueresse, 2019). The alteration in complement C4 signalling could lead to an excessive elimination of neurons during the synaptic pruning phase in adolescence (Maynard *et al.*, 2001). Similarly, myelination damage could lead to neural connection dysfunction. These alterations, if they occur during intrauterine development (Fatemi and Folsom, 2009; Rapoport, Giedd and Gogtay, 2012), could remain latent until adolescence or young adulthood. Based on this hypothesis, cumulative damage in different molecular pathways required for the early development of the CNS together with traumatic experiences during childhood or adolescence could contribute to the failure of axonal assembly connections and normal synaptic transmission (Weinberger, 1988; Martínez-Téllez *et al.*, 2009; Holtzman *et al.*,

2013). Adolescence is an active phase of remodelling of neuronal networks and synaptic activity in which significant energy is required for the correct building of functional circuits (Choi *et al.*, 2015). Thus, an additional stressor in adolescence such as psychosocial stress could impact on these vulnerable pathologic neural circuits and compromise this active phase of remodelling of circuits, altering their functioning and promoting disease emergence. Schizophrenia has several biological components and the many hypotheses proposed should not be considered as being mutually exclusive. These hypotheses could be unified, allowing a better understanding of this complex disorder.

1.3.2.6. Integration of different altered network hypotheses

Altered neuronal networks underlie schizophrenia and several hypotheses could be unified to understand this dysfunction. Genetic predisposition together with insults during the perinatal and postnatal periods could lead to the accumulation of errors during neurodevelopment, which could therefore negatively affect the balance of neurotransmitters such as dopamine, glutamate, GABA in CNS. Moreover, the energy imbalance proposed for schizophrenia could enhance dysregulation in the release of neurotransmitters and lead to dysfunction of synapses and multiple pathway signalling. Altered signalling could also alter the immune response and consequently lead to the release of proinflammatory molecules. These molecules would alter cerebral barriers (detailed in *section 5.1.2*) and lead to molecules entering the cerebral parenchyma, thus altering the homeostatic balance in the brain and contributing to the global dysregulation of neuronal networks in schizophrenia.

1.4. Neuronal circuits in schizophrenia

1.4.1. Cortico-thalamo-cortico cerebellar circuit

The cerebellum connects with the medial prefrontal cortex (Watson 2009), the dorsolateral prefrontal cortex (Kelly and Strick, 2003) and the anterior prefrontal cortex (Krienen and

Buckner, 2009). The cortex-cerebellar afferent projections pass through the pontine nuclei at the intermediated cerebellar peduncle (Palesi *et al.*, 2017). The cerebello-cortical efferent projections pass through ventrolateral (VL) thalamic nuclei (Middleton, 2002). The cortex-cerebellar loops are complex interconnections that also involve the basal ganglia, the limbic system and subcortical areas (Bostan and Strick, 2018; Milardi *et al.*, 2019). During neurodevelopment, the cerebellum evolves in parallel with the associative region but not with motor or sensory regions. This could be part of the evidence explaining the involvement of the cerebellum in cognitive function. The cerebellum associates with cortical areas such the medial prefrontal cortex, which is involved in cognitive control (Ridderinkhof *et al.*, 2004), and the dorsolateral prefrontal cortex, which is implicated in working memory (Petrides, 2000) and learning (Pascual-Leone *et al.*, 1996). Furthermore, the prefrontal cortex has been associated with psychosis (Dolan and Bench, 1993), while the anterior prefrontal cortex is involved in decision-making, reasoning and cognitive branching (Koechlin and Hyafil, 2007).

It has been proposed that dysconnectivity between the frontal cortex, the thalamus and the cerebellum, called the cerebello-thalamo-cortical circuit (CTCC) (**Figure 2**), underlies "cognitive dysmetria", which involves alterations in prioritizing, coordination and responding to information processing, functions that are related to cognitive deficits in schizophrenia (Andreasen *et al.*, 1999, 2018; Andreasen and Pierson, 2008; Picard *et al.*, 2008). In the last decades, the cortico-cerebellar-thalamo-cortical circuit (CCTC) has been proposed to play a key role in cognitive impairments and symptoms in both ultra-high risk individuals for schizophrenia and in individuals that have transited to schizophrenia (Andreasen and Pierson, 2008; Bernard, Orr and Mittal, 2017; Parker *et al.*, 2017). Since the cerebellum is a brain area that forms part of this cortical region synaptic response-modulating circuit, it has been proposed to play an important role in the pathophysiology of the disease (Andreasen *et al.*, 1999; Picard *et al.*, 2008; Bernard, Orr and Mittal, 2017). Nowadays, clinical and neuroimaging studies suggest that the cerebellum supports

cognitive and executive functions in schizophrenia (Wiser *et al.*, 1998; Crespo-facorro *et al.*, 2001; Koziol *et al.*, 2014). Moreover, computerized analyses showed dysfunction of the prefrontal-thalamic-cerebellar circuit in schizophrenia individuals during complex narrative tasks in comparison with healthy controls (Andreasen *et al.*, 1996). Along this same line, a recent study showed reduced functional connectivity between the thalamus, the left vestibulocerebellar area, right cerebellar Crus I and the frontal pole in early schizophrenia. Furthermore, a positive correlation was reported between the size of the left thalamus and the decrease in the functional connectivity of the thalamus and the right cerebellum (Chen *et al.*, 2020). Furthermore, hyperactivity of the CTCC in subjects with psychosis or high predisposition to psychosis has been recently reported (Cao *et al.*, 2018). These authors argued that this hyperactivity could be due to a compensatory mechanism involving increased error input from the cerebral cortex area. This evidence supports the role of the cerebellum in the pathophysiology of schizophrenia.

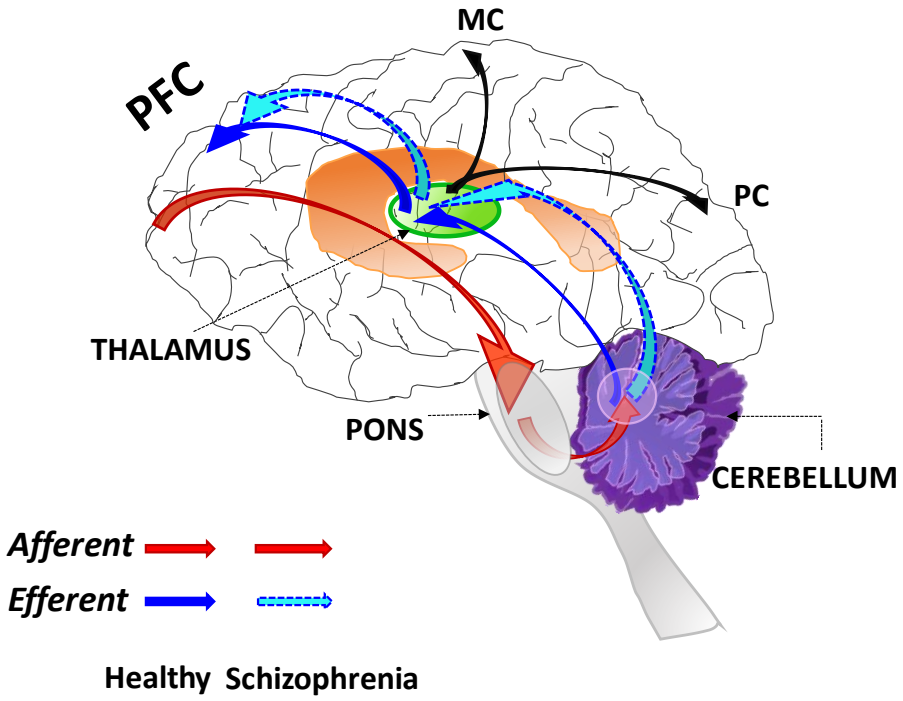

Figure 2. Cerebello-thalamo-cortical circuits in cognition. The cerebellum is connected to cortical areas by the cortico-cerebellar-thalamic-cortical circuit (CCTCC). Afferent projections from the prefrontal cortex pass through the pons to the cerebellum. Efferent projections pass from the cerebellum through the thalamus to the prefrontal cortex. The dotted arrow shows the altered CCTCC in schizophrenia. The cerebellum is also connected to the motor cortex and the parietal cortex (black arrows). **PFC**: Prefrontal cortex, **MC**: Motor cortex, **PC**: Parietal cortex. Adapted from Perez-Garcia, 2002.

1.5. Brain abnormalities in schizophrenia

Several morphological abnormalities have been related to schizophrenia (Ribolsi *et al.*, 2014). Studies have shown reduced cortical volume in the brain (Zhang *et al.*, 2016), Broca's area (Wisco *et al.*, 2007), and the *corpus callosum* (Whitford *et al.*, 2010), and ventricular enlargement (Kempton *et al.*, 2010). Moreover, morphological brain changes during the early stage of psychosis in schizophrenia have also been reported (Takahashi and Suzuki, 2018).

1.5.1. The cerebellum in schizophrenia

The cerebellum plays an essential role in integrating input signals from the cortical areas to generate an output signal back to the same area in the cortex, which is essential to detect and correct errors during the execution of motor movements. However, it could also be involved in the regulation of cognitive functions. The cerebellar cortex has four times more neurons than the cerebral cortex (Barton, 2012), which could be important for the integrative function of the cerebellum. These extra neurons are acquired thanks to active neuronal expansion during development (Lewis *et al.*, 2004). This lengthy maturation phase of the cerebellum means that it is highly vulnerable to accumulating errors during its development, which could have a significant impact in schizophrenia. Thus, molecular alterations in the cerebellum in schizophrenia could constitute an attractive biological substrate as a possible reservoir of failures in multiple pathways through development and during the disease. Moreover, the cerebellum consists of a homogeneous neuronal population with granular cells making up approximately 90% of the population (Pfaff, 2013). This feature makes the cerebellum a useful model to study molecular alterations that could alter internal circuits.

The cerebellum has been traditionally implicated only in motor coordination (Manto *et al.*, 2012). However, in the last decades several studies have supported the notion that the cerebellum participates in other biological processes such as cognitive processes, sensorimotor processes and emotion (Schmahmann, 2010; Buckner, 2013; Baumann *et al.*, 2015; Overwalle *et al.*, 2020). It has also been implicated in cerebellar cognitive affective syndrome (Schmahmann, 2004). In the last decades, an increasing body of evidence has suggested that the cerebellum plays a role in the aetiology of schizophrenia, contributing to cognitive and affective deficits. As described in *section 4.1*, the cerebellum performs its functions through CCTC circuits, which connect the cerebellum to several regions of the cerebral cortex (Andreasen and Pierson, 2008). Functional and structural

analyses of tissue from schizophrenia subjects have shown abnormalities in the cerebellum, such as altered blood circulation during executive tasks (Andreasen *et al.*, 1996; Crespo-facorro *et al.*, 2001) and reduced cerebellar cortex and grey matter volume (Laidi *et al.*, 2015; He *et al.*, 2019).

Studies in *postmortem* cerebellum from schizophrenia subjects revealed altered protein expression related to inflammatory processes via TLR4 signalling (MacDowell *et al.*, 2017). Altered expression of SP4 and SP1 transcription factors has also been reported in the cerebellum (Pinacho *et al.*, 2013; Pinacho, Saia, Meana, *et al.*, 2015).

Recently, proteomic studies from *postmortem* cerebellum have shown altered functional processes related to the cytoskeleton, cellular junctions, migration of Purkinje cells, transport and cell communication functions with relevance in altered calcium-binding expression (Vidal-Domènech *et al.*, 2020) and inflammation processes (Reis-de-Oliveira *et al.*, 2020). These studies support the interest of studying the cerebellum in order to understand its role and find possible targets for a better quality of life.

1.5.1.1. Transcriptional programs in the cerebellum

During cerebellar development, each regionalization and neuronal precursor migration process is controlled by genetic networks formed of transcription factors and their target genes (Leto *et al.*, 2016). In the context of schizophrenia, several signalling pathways are known to be dysregulated. Therefore, it is necessary to identify the transcriptional programs that regulate these differentially expressed genes. In this context, studies have associated altered expression of several transcription factors such as TCF4 with a high risk of schizophrenia (Blake *et al.*, 2010), probably due to its function during development where it is essential for neuronal migration during cortex cerebellar development (T. Chen *et al.*, 2016), which is interesting from the perspective of the neurodevelopment hypothesis for schizophrenia. Furthermore, it is known that altered dendritic organization could be affected in schizophrenia. In this context, altered protein expression in *postmortem*

cerebellum of certain SP/KLF-like factors such as specificity proteins (SPs) and Kruppel-like family of transcription factors (KLFs) during neuronal morphogenesis (Ye *et al.*, 2011) has been associated with altered dendritic organization and neuronal growth in schizophrenia (Ramos *et al.*, 2007; Pinacho *et al.*, 2014). This evidence suggests that altered processes related to cytoskeletal organization and/or assembly could be under the transcriptional control of certain SP/KLF-like factors. On the other hand, transcriptional dysregulation of NKX2-1 and EGR1 has been associated with altered GABAergic neurotransmission in schizophrenia (Malt *et al.*, 2016), which could lead to altered synaptic processes and the poor cognitive function described in schizophrenia. Finally, the accumulative effect of altered expression of these transcription factors could lead to dysregulation of the transcription network, which could compromise neuronal structure, synaptic efficiency and lead to the dysfunction of signalling pathways in schizophrenia.

1.5.1.2. Cerebellum-glia limitans-pia mater-cerebrospinal fluid barrier

The cerebellum is separated from cerebrospinal fluid by a barrier formed by the pia mater and the end-feet of astrocytes that form the glia limitans (**Figure 3**)**.** The pia mater is the inner meningeal layer formed by leptomeningeal cells that cover the outer brain and the cerebellum (Weller *et al.*, 2018). Recent studies have demonstrated that meninges not only have a protective role but are also involved in the cellular homeostasis of the CNS (Radakovits *et al.*, 2009; Ichikawa-tomikawa *et al.*, 2012). During intrauterine development, the meninges secrete trophic factors such as retinoic acid, main in the neural migration and in the establishing of the pial basement membrane (Siegenthaler and Pleasure, 2011; Decimo *et al.*, 2012), which is an anchor point for glia limitans end-feet (Feig and Haberly, 2011). In the cerebellum, the cells comprising the *glia limitans* are also called Bergmann glia cells (Koirala and Corfas, 2010) and form an intimate contact layer between with the cerebellar parenchyma and the pia mater (Decimo *et al.*, 2012). In the context of schizophrenia it has been reported that the cerebellum could have altered

barrier permeability (Margari *et al.*, 2013). However, the molecular and structural mechanisms involved in the alteration of the cerebellar barrier have not been clearly established.

In addition, Bergmann glia carry out several functions during cerebellar development. For example, they are essential for the correct migration of granular cells (Hatten 1999) and participate in the formation of the dendrites in the Purkinje cells (Lippman *et al.*, 2008), suggesting an extensive contribution to synaptic stabilization. Bergmann glia are also involved in the homeostasis of the CNS through neurotransmitter uptake, glutamine production, regulation of ions and synaptic neuromodulation (Bordey and Sontheimer, 2003).

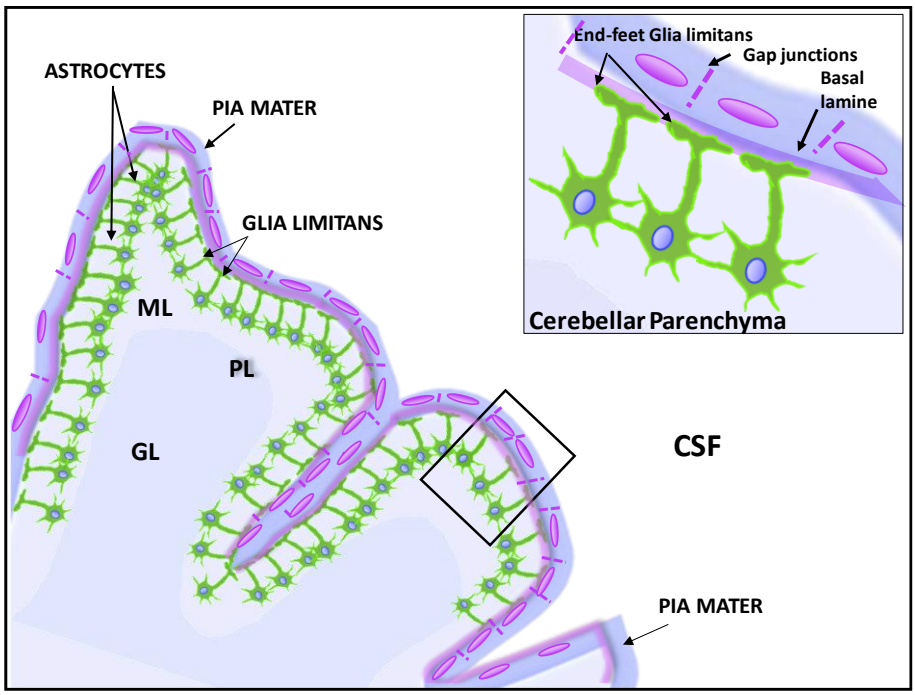

Figure 3.The cerebellum and the cerebrospinal fluid barrier. The cerebellar parenchyma is separated from cerebrospinal fluid by the pia mater and end-feet of the glia limitans. A magnified view is shown in the upper right panel. **ML**: Molecular layer, **PL**: Purkinje layer, **GL**: Granular layer, **CSF**: Cerebrospinal fluid.

1.5.2. The prefrontal cortex in schizophrenia

The prefrontal cortex is the association area in the anterior part of the frontal lobe (Goyal *et al.*, 2008). Evolutionarily, it is the last brain region to develop (Teffer and Semendeferi, 2012). The prefrontal cortex governs executive functions (Kouneiher, Charron and Koechlin, 2009), which involve all rational thinking cognitive processes such as attention, behaviour, cognitive flexibility and impulse inhibition (Logue and Gould, 2014). In the context of schizophrenia, studies have shown cognitive, social, and emotional impairments (Russell *et al.*, 2000; Ragland *et al.*, 2007; Ursu *et al.*, 2011). Altered cognitive functioning in schizophrenia could be due to the dysfunction in the maturation of connectivity between the prefrontal cortex and other brain areas. Studies have demonstrated that maturation of connectivity occur in two periods, the first during the prenatal and perinatal phases and the second during the global maturation of the circuit to establish functional networks, which lasts until early adulthood (Teffer and Semendeferi, 2012). Dysfunction in dopaminergic (Meyer-Lindenberg *et al.*, 2002; Slifstein *et al.*, 2015), GABAergic (Lewis *et al.*, 1999; Tanaka, 2008) and glutamatergic (Li, Yang and Lin, 2019) signalling has been reported in the prefrontal cortex in schizophrenia. Prefrontal cortex sends its projections to the cerebellum (Middleton and Strick, 2001), while the cerebellum sends projections to dorsal area 46, medial area 9, and lateral area 9 in the prefrontal cortex (Middleton and Strick, 2001). This connectivity is supported by functional neuroimaging studies that demonstrated the co-activation of these two areas during verbal fluency tasks (Schlösser *et al.*, 1998) and working memory (Desmond *et al.*, 1997). These findings support the existence of crosstalk between the prefrontal cortex and the cerebellum and the involvement of these areas in executive functions. Furthermore, these two regions have a lengthy maturation phase, which means they are particularly vulnerable to the accumulation of errors during their development.

1.6. Animal models in schizophrenia

In the last decades, several animal models have been developed to explain the etiopathology of schizophrenia. Furthermore, they represent more rapid models for understanding the biology and evolution of complex disorders such as schizophrenia.

1.6.1. Genetic models

1.6.1.1. Disrupted in schizophrenia 1

Disrupted in schizophrenia-1 (DISC-1) was the first risk gene identified for mental disorders (Millar *et al.*, 2000). DISC-1 is involved in multiple processes in the CNS that occur from embryonic development to early adulthood (Jaaro-Peled, 2009). These processes are related to the cytoskeleton, dendritic structure (Glantz and Lewis, 2000) and centrosome organization (Morris *et al.*, 2003). DISC-1 may participate in synaptic plasticity and dendritic spine stability (Tropea *et al.*, 2018). Mice with a loss of DISC-1 function showed an altered brain morphology that included enlarged ventricles, reduced cortical thickness (Pletnikov *et al.*, 2008) and a decrease in the spontaneous inhibitory transmission of parvalbumin interneurons in the medial prefrontal cortex. This study also showed the disruption of feedforward inhibition from the medial thalamus to the medial prefrontal cortex (Delevich *et al.*, 2020). These changes in brain morphology are consistent with schizophrenia. However, this model could not reproduce the negative symptoms of this disorder.

1.6.1.2. *22q11.2* deletion

In humans, deletion of the chromosomal region *22q11.2* is common (Saito *et al.*, 2020). This deletion affects approximately 1 in 4000 births (Scambler, 2000). In 90% of the subjects affected, a 3.0 Mb region is deleted. Moreover, deletion of *22q11.2* has been associated with schizophrenia (Marshall *et al.*, 2017). It has been estimated that approximately 25% of subjects who have this deletion could develop schizophrenia (Van,

Boot and Bassett, 2017). Moreover, subjects with a hemizygous *22q11.2* deletion have a 40% probability of developing schizophrenia (Schneider *et al.*, 2014). Such observations support the high genetic component of schizophrenia. Subjects with a *22q11.2* deletion suffer neurocognitive and social deficits (Peyroux *et al.*, 2019). The animal models developed to study the *22q11.2* deletion exhibited anatomical alterations in cortical and grey matter volumes, reduced size in the spine, abnormal dendritic architecture (Stark *et al.*, 2008) and dysfunctional prepulse inhibition (PPI) (Karayiorgou, Simon and Gogos, 2010). However, most of the models have a 1.5 Mb deletion and do not replicate the 3.0Mb deletion observed in humans. In this context, Saito *et al.*, 2020 developed a mouse model with a 3.0 Mb deletion. This model exhibited impaired early visual processes, an impairment that is related to schizophrenia. It has also been proposed that deletion of *22q11.2* could be the first hit, with a second hit required for development schizophrenia. This second hit could lie outside of the region affected by the deletion of 22q11.2, in this region there are potential genes involved in schizophrenia and could contribute to psychosis (Michaelovsky *et al.*, 2019).

1.6.1.3. Dysbindin 1

Dysbindin 1 (DTNBP1) has been proposed as a risk gene for schizophrenia (Van Den Oord *et al.*, 2003; Funke *et al.*, 2004). Dysbindin has several functions related to synapses, exocytosis, vesicle biogenesis and excitatory neurotransmission processes (Ghiani and Dell'Angelica, 2011). In the context of schizophrenia, studies performed in schizophrenia cohorts showed that the genetic variation of DTNBP1 is related to cognitive ability and emotional behaviour (Burdick *et al.*, 2006; Donohoe *et al.*, 2007; Wolf *et al.*, 2011). To study the role of DTNBP1 in schizophrenia, a DTNBP1 mutant Sandy (Sdy) animal model was developed. Studies with this model revealed a decrease in the volume of cortical areas mainly related to the auditory cortex (Lutkenhoff *et al.*, 2012). Moreover, studies with DTNBP1-deficient mice suggest that DTNBP1 could modulate dopamine signalling in the

medial prefrontal (Papaleo *et al.*, 2012). This study showed working memory dysfunction and altered behaviour with traits observed in schizophrenia subjects related to the disruption of dopamine signalling. Furthermore, a recent investigation studied the impact the interaction between genes and the environmental could have on the risk of developing schizophrenia. This study used the Sdy model (genetic factor) and Polyl: C infection in the postnatal stage (environmental factor). The results showed that adult mice developed inflammation, increased microglial population and alteration in the subventricular zone development in comparison to wild-type mice or wild-type mice injected with Polyl:C. Thus, DTNBP1 may regulate the immune response during infection with Polyl:C (Al-Shammari *et al.*, 2018).

1.6.2. Pharmacological models

1.6.2.1. Phencyclidine, ketamine and dizocilpine

Several studies in animals have used non-competitive antagonists of NMDA receptors such as phencyclidine (PCP), ketamine or dizocilpine (MK-801) to understand the effects of the hypofunction of this receptor in the aetiology of schizophrenia. PCP binding to NMDA receptors leads to altered PPI and altered dopaminergic signalling in the frontal lobe, fronto-cortical and mesolimbic regions, observations that have been reported in schizophrenia (Jentsch and Roth, 1999; Neill *et al.*, 2010). Ketamine treatment of animals revealed increases aggressive social behaviour, which is on of the negative symptoms in schizophrenia (Becker *et al.*, 2003). Animals treated with MK-801 displayed altered PPI, behaviour, impaired cognitive functioning and working memory (Bast *et al.*, 2000; Mabunga *et al.*, 2019). The pharmacological models were not able to replicate all the symptoms of this complex disorder. However, a study of pharmacological models could be used to determine the effects on symptoms.

1.6.3. Neurodevelopmental models: Prenatal and postnatal injuries

1.6.3.1. Immune challenge

The first evidence of the effects of infection on the development of schizophrenia comes from the study carried out by Mednick *et al.*, 1988. Her study reported that individuals exposed to A2 influenza in the second trimester of intrauterine development have high risk of schizophrenia. This led to the development of several animal models of prenatal and neonatal infection. Prenatal infections carried out using the human influenza virus showed the dysregulation of structural genes and deficits in PPI (Fatemi *et al.*, 2005). Maternal immune activation by lipopolysaccharide infection resulted in altered dendritic morphology in the medial prefrontal cortex and the hippocampus (Baharnoori, Brake and Srivastava, 2009). Other models involving prenatal and neonatal infections include immune activation by polyriboinosinic-polyribocytidilic acid (PolyI:C), which showed an increase in dentate gyrus and basolateral amygdala of GABAA receptor α2 (Nyffeler *et al.*, 2006), and neonatal exposure to the Borna virus (Eisenman *et al.*, 1999), which showed alteration in the levels of serotonin in the cerebellum (Eisenman *et al.*, 1999) and hippocampal synaptogenesis (Hans *et al.*, 2004).

1.6.3.2. Prenatal and perinatal stress

Prenatal stress has been proposed as one of the risk factors for developing schizophrenia. Several models have been developed that include prenatal or perinatal stress. Prenatal models may consist of different types of stressors such as restraint of movement together with water and/or food deprivation (Martínez-Téllez *et al.*, 2009) and foot-shocks (Shalev and Weiner, 2001) to the mother. Supporting these animal models are other findings in animal experiments that showed that prenatal exposure to stressors leads to learning deficits (Lemaire *et al.*, 2000; Gi *et al.*, 2006). Furthermore, a study found that post-weaning social isolation induces altered adult behaviour through hyperactivity of the hypothalamic-pituitary-adrenal axis, which could be related to negative symptoms in

schizophrenia (Weiss *et al.*, 2004). Another type of animal model used to understand the origin of schizophrenia is the double-hit model in which two hits are required for the emergence of this disorder: first, a hit in the prenatal or perinatal phase and a second hit during adolescence (Giovanoli *et al.*, 2016; Monte *et al.*, 2017). This rodent animal model is based on the exposure of animals to the first hit of immune challenge with poly(I:C) from postnatal day (PN) 5–7, which corresponds the end of the third trimester in human pregnancy, and the exposure to the second hit from PN 40–48, which corresponds to human age 12–18 (adolescence). This second hit corresponds to unpredictable peripubertal stress, which includes different stressful situations. These results revealed PPI deficits, working memory impairment, high levels of lipidic peroxidation in the prefrontal cortex, low levels of glutathione as an oxidative stress marker, and social impairment (Monte *et al.*, 2017). The double-hit model also includes NMDA receptor inhibition with a single injection of MK-801 at PN 7 and a second hit of social isolation from post-weaning to adulthood. These results showed a decrease in the volume of the medial prefrontal cortex and hippocampus, altered gene expression and structural alterations related to schizophrenia (Gilabert-Juan *et al.*, 2013).

1.7. Proteomic approaches in psychiatric disorders

The development of '-omics' technologies such as quantitative proteomics has allowed us to study the proteomic profile of the brain areas implicated in several psychiatric disorders such as schizophrenia. The proteomic approaches have allowed the protein signature and molecular mechanisms involved in specific brain areas in schizophrenia to be investigated. These areas include the anterior cingulade (Clark *et al.*, 2006, 2007; Smalla *et al.*, 2008); the prefrontal cortex (Prabakaran *et al.*, 2004; Pennington *et al.*, 2008; Smalla *et al.*, 2008; Martins-De-Souza *et al.*, 2009; Chan *et al.*, 2011; Jane A. English *et al.*, 2011; Pinacho *et al.*, 2016); the thalamus (Martins-de-Souza *et al.*, 2010); the hippocampus (Föcking *et al.*, 2011; Schubert, Föcking and Cotter, 2015); the temporal lobule (Saia-Cereda *et al.*, 2017); the auditory cortex and the corpus callosum (Jane A English *et al.*, 2011; Saia-Cereda *et*

al., 2015a); the dorsolateral prefrontal cortex (Martins-de-Souza, Gattaz, Schmitt, Maccarrone, *et al.*, 2009; Wesseling *et al.*, 2013; Pinacho *et al.*, 2016); the orbitofrontal prefrontal cortex (Velásquez *et al.*, 2017); Wernicke's area (Martins-de-Souza, Gattaz, Schmitt, Novello, *et al.*, 2009); the insular cortex (Pennington *et al.*, 2008); and the cerebellum (Reis-de-Oliveira *et al.*, 2020; Vidal-Domènech *et al.*, 2020). We used one-shot liquid chromatography tandem mass spectrometry (LC-MS/MS), which is currently one of the main techniques used in proteomics to understand biochemical pathways due to its capacity to profile large numbers of proteins simultaneously (Saia-Cereda et al., 2017). Furthermore, such a large number of proteins allowed us to integrate the information to identify signalling pathways. Thus, this latest generation of proteomic technologies represents an incompletely explored area in psychiatry in terms of determining altered molecular brain networks and could allow a map to be drawn of accumulated errors in multiple pathways (neurotransmission, development, the immune system and homeostasis) that occur in the cerebellum and the prefrontal cortex in schizophrenia to provide a global view of altered networks in the brain. These analyses applied in these two highly connected areas would provide extremely valuable information about altered networks involved in the disruption of coordination of executive functions and the emergence of symptoms in schizophrenia. Together, the identification of altered networks will contribute to the understanding of this complex disorder and will provide novel biomarkers

II. HYPOTHESIS

III. OBJECTIVES

II. HYPOTHESIS

According to the evidence set out in the introduction, we hypothesized that **proteomic profiles in the brain allow i) to identify altered molecular networks in chronic schizophrenia that could be related to stress and ii) to discover novel altered proteins with an unknown role in the brain.**

III. OBJECTIVES

1. To analyse the proteomic profile from pooled samples from *postmortem* cerebellar tissue in chronic schizophrenia compared to healthy controls.

2. To analyse proteomic signatures in individual samples in *postmortem* cerebellar tissue in chronic schizophrenia compared to healthy controls.

3. To analyse proteomic signatures in individual samples in *postmortem* dorsolateral prefrontal cortex tissue in chronic schizophrenia compared to healthy controls.

4. To determine protein levels of selected altered candidates in chronic schizophrenia in stress rodent models.

5. To characterize the cell-specific localization in human brain of a selected candidate with an unknow expression in the brain.

IV. MATERIAL AND METHODS

4.1. Proteome of pooled protein lysates from *postmortem* cerebellum from schizophrenia and healthy controls

4.1.1. *Postmortem* human cerebellum tissue

Samples of cerebellum in schizophrenia committed suicide (n = 4) and control subjects who had died in a traffic accident and who had had no history of psychiatric episodes (n = 4) were obtained at autopsies in the Basque Institute of Legal Medicine, Bilbao, Spain, in compliance with the policies of the research and ethical boards for post-mortem studies. Toxicological screening for antipsychotics, antidepressants, and other drugs was performed at the National Institute of Toxicology, Madrid, Spain. All deaths were subjected to retrospective analysis for previous medical diagnosis. Subjects with ante-mortem criteria for paranoid schizophrenia according to the Diagnostic and Statistical Manual of Mental Disorders (DSM-IIIR and DSM-IV) were matched to control subjects who had died from accidental causes in a paired design, based on gender, age, and *postmortem* delay (PMD) (**Table 1**).

Specimens of the lateral cerebellar cortex from the posterior lobe, extending from the pial surface to white matter and only including grey matter, were dissected from coronal slabs stored at -80 ˚C. Protein extracts were prepared from tissue samples using NP40 lysis buffer as described previously (Pinacho *et al.*, 2011). Protein concentration was determined by Bradford assay (Biorad).

4.1.2. Mass spectrometry screening and data processing

Our screening strategy combined differential isotopic labelling of peptides via reductive dimethylation with offline fractionation by SCX and liquid chromatography coupled to tandem mass spectrometry (LC-MS/MS) on a hybrid linear ion trap orbitrap mass spectrometer (LTQ-Orbitrap). 400 μg of total protein extracts from four pooled control (100 μg/each) and four pooled schizophrenia (100 μg/each) lysates, for more details to see https://doi.org/10.1371/journal.pone.0230400.s008. Briefly, the digested peptides were

dimethyl-labelled with either hydrogen (light peptides, control) or deuterium (heavy peptides, schizophrenia) isotopes through a reductive dimethylation reaction as described previously (Khidekel *et al.*, 2007). Differentially labelled peptides were then mixed 1:1. Dimethylated peptide mixtures were separated by strong cation exchange (SCX) chromatography on a polysulphoethyl A column. Peptide mixtures were analysed by LC-MS/MS. Each peptide fraction was separated by reverse phase chromatography on a capillary column and analysed online on a hybrid linear ion trap orbi- trap (LTQ-Orbitrap XL, Thermo Scientific) mass spectrometer for identification and relative quantification of isotopically labelled peptide pairs. MS/MS spectra were searched against a concatenated target-decoy Uniprot human protein database (UP000005640 version 05-23- 2017, n = 71,567 target sequences) using the Comet search algorithm (version 2015025) and specific search parameters (see S1 File). The mass spectrometry proteomics data have been deposited in the ProteomeXchange Consortium via the PRIDE partner repository with the dataset identifier PXD008216 (Vizcaíno *et al.*, 2016). Peptide matches were filtered to <1% False-Discovery Rate (FDR) and protein groups were filtered at 90% probability score. The log2 heavy/light ratio for each protein was determined and transformed to a z-score (Graumann *et al.*, 2008). A significance value (p-value) for each protein ratio was calculated from the complementary error function for the normalized distribution of the z-scores (Graumann *et al.*, 2008). The FDR was computed for all the p-values using the Benjamini and Hochberg method (Hochberg, 1995). The FDR threshold was set at 0.1 for selected significant proteins with consistent changes amongst peptides. Proteins were classi- fied according to their biological function using the Human Protein Reference Database (HPRD-http://www.hprd.org).

4.1.3. Ontology gene analysis from proteome of pooled protein lysates from *postmortem* cerebellum from schizophrenia and healthy controls

Significant proteins with consistent changes amongst peptides were then selected. Proteins were classified according to their biological function using the Human Protein Reference Database (HPRD-http://www.hprd.org). Up-regulated proteins were those with a z-score >0 and an FDR p value <0.1 and down-regulated proteins were those with a z-score <0 and an FDR p value <0.1. From these significantly altered proteins a panel of candidate proteins was then selected to be further validated by immunoblot following these criteria: (i) the change had been identified in more than 4 peptides; (ii) a greater than 2-fold increase or decrease.

4.2. Quantitative proteomic analyses in the cerebellum in individual samples of chronic schizophrenia and healthy controls

4.2.1. *Postmortem* human cerebellum tissue

Samples from the cerebella of subjects with chronic schizophrenia (n=12) and healthy controls (n=14) were obtained from the neurologic tissue collection of the *Parc Sanitari Sant Joan de Déu* Brain Bank (Roca, M., Escanilla, A., Monje, A., Baño, V., Planchat, L., Costa, J., 2008) and the Institute of Neuropathology of the *Universitari de Bellvitge* Hospital respectively. All SZ subjects were institutionalized donors with long-term illness who had no history of neurological episodes. We matched SZ and control groups by gender (only male patients were included), age, *postmortem* delay (PMD) and pH (Table S1). Experienced clinical examiners interviewed each donor *antemortem* to confirm SZ diagnosis according to the Diagnostic and Statistical Manual of Mental Disorders (DSM-IV) and International Classification of Diseases 10 (ICD-10). All deaths were due to natural causes. The study was approved by the Institutional Ethics Committee of Parc Sanitari Sant Joan de Déu. A written informed consent was obtained from each subject. The last

daily chlorpromazine equivalent dose for the antipsychotic treatment of patients was calculated based on the electronic records of the last drug prescriptions administered up to death as described previously (Gardner *et al.*, 2010). Human cerebellar lateral cortex was dissected from coronal slabs stored at - 80ºC, extending from the pial surface to white matter only including grey matter.

4.2.2. Protein reduction, Alkylation, LysC digestion, and desalting

Protein extracts were prepared from tissue samples using NP40 lysis buffer as described previously (Pinacho *et al.*, 2011). Protein concentration was determined by Bradford assay (Biorad, Hercules, CA, USA). 200 µg of total protein was lyophilized (Telstar, Lyoquest-55) per sample for mass spectrometry analysis. 200 µg of total protein extracts lyophilized from control and SZ lysates were resuspended in 100 µl 8M Urea, 50 mM Tris pH 8.2, 100 mM NaCl. The lysate was reduced with 3 mM dithiothreitol at 55 ºC for 30 min, alkylated with 20 mM iodoacetamide at room temperature for 30 min and quenched with additional 3mM dithiothreitol for 30 min at room temperature. The extract was digested with the endoproteinase LysC at 10 ng/µl at 30ºC overnight. Peptides were desalting with OASIS MCX cartridge (Waters): cartridge was conditioned with Methanol, 5% ammonium hydroxide in Methanol, and 0.1% TFA; acidified peptides were loaded on the column and washed with TFA 0.1% and 0.1% Formic acid in Methanol, finally peptides were eluted using 5% ammonium hydroxide in Methanol. Eluted peptides were acidified with formic acid. and dried before re-suspending in MS Buffer composed of 3% formic acid, and 4 % acetonitrile in water.

4.2.3. Liquid chromatography coupled to tandem mass spectrometry

The LC/MS-MS analysis was performed in a Q-Exactive mass spectrometer(Thermofisher Scientific, CA, USA) coupled to an Easy nLC II liquid chromatography system. Peptides were loaded onto a 100 µm ID × 3 cm precolumn packed with Reprosil C18 3 µm beads (Dr. Maisch GmbH), and separated by reverse-phase chromatography on a 100 µm ID × 30 cm analytical column packed with Reprosil C18 1.9 µm beads (Dr. Maisch GmbH). A gradient of 3% to 30% acetonitrile in 0.125% formic acid was used delivered at 225 nl/min over 130 minutes, with a total 180-minute acquisition time. Peptides were analyzed online on the orbitrap mass analyser using a top 20 data-dependent acquisition with all MS spectra being acquired and stored in centroid mode. Full MS scans were acquired from 300 to 1500 m/z at 70,000 FWHM resolution with a fill target of 3E6 ions and maximum injection time of 100 ms. The 20 most abundant ions on the full MS scan were selected for fragmentation using 2 m/z precursor isolation window and beam-type collisional-activation dissociation (HCD) with 26% normalized collision energy. MS/MS spectra were collected at 17,500 FWHM resolution with a fill target of 5E4 ions and maximum injection time of 50 ms. Fragmented precursors were dynamically excluded from selection for 35 s.

4.2.4. Data analysis

Raw files were processed and analysed using MaxQuant (version 1.5.3.8). MS/MS spectra were searched with Andromeda against UniProt fasta UP000005640 (Downloaded: 2015-06-30) with common contaminants added. The precursor mass tolerance was set to 7 ppm, and the fragment ion tolerance was set to 20 ppm. Search parameters included full LysC enzyme specificity with up to three missed cleavages permitted. The target-decoy database search strategy was used to guide filtering and estimate false discovery rates (FDR). Peptides matches were filtered to an FDR of ≤0.01. Proteins with at least one

peptide were considered identified. Label-free quantification (LFQ) was selected for individual protein comparisons between control and schizophrenia groups. A quality cut-off for protein determination was the presence of the protein in at least 7 samples per group. The normalized LFQ intensity was referred to media of the controls. A significance value for each quantified protein was calculated using Student's t-test and the correction of significance values of the quantified protein data set was performed following the Benjamini and Hochberg methods (Yosef, 1995). An FDR was computed for all significant values and the FDR threshold was set to 0.1.

The quantified proteins were imported into Perseus software platform (version 1.6.1.3) to check data quality obtained by LC/MS/MS and to visualize the data distribution (Tyanova *et al.*, 2016). We performed the following analyses. 1. Correlation matrix: the normalized LFQ intensity data were used to estimate a correlation coefficient matrix between controls and schizophrenia patients. For easy visualization, the correlation coefficient data were plotted as a heat map. 2. Hierarchical Clustering: This was carried out on Z-score transformed normalized LFQ intensity data for each protein using Euclidean distance.

4.3. Quantitative proteomic analyses in the prefrontal cortex in chronic schizophrenia and healthy controls

4.3.1. Postmortem prefrontal cortex brain tissue

Samples from prefontal cortex of subjects with chronic schizophrenia (n=20, left hemisphere), and healthy controls (n=20, 10 left hemispheres and 10 right hemispheres). The samples of chronic schizophrenia were obtained from the collection of neurologic tissue of *Parc Sanitari Sant Joan de Déu* Brain Bank (Roca, M., Escanilla, A., Monje, A., Baño, V., Planchat, L., Costa, J., 2008). For healthy controls the samples of prefrontal cortex from right hemispheres (n=10) were obtained from the Institute of Neuropathology of Hospital *Universitari de Bellvitge* and the samples from healthy controls of prefrontal cortex from left hemispheres were obtained from NavarraBiomed Biobank (n=7) and

Hospital Clinic IDIBAPS Biobank (n=3). All schizophrenia subjects were institutionalized donors with a long duration of the illness who had no history of neurological episodes. We matched schizophrenia and control groups by gender (only male patients were included), age, *postmortem* delay (PMD) and pH (**Table 5**). Experienced clinical examiners interviewed each donor *antemortem* to confirm SZ diagnosis according to the Diagnostic and Statistical Manual of Mental Disorders (DSM-IV) and International Classification of Diseases 10 (ICD-10). All deaths were due to natural causes. The study was approved by the Institutional Ethics Committee of Parc Sanitari Sant Joan de Déu. A written informed consent was obtained from each subject. The last daily chlorpromazine equivalent dose for the antipsychotic treatment of patients was calculated based on the electronic records of last drug prescriptions administered up to death as described previously (Gardner *et al.*, 2010). Human Brodmann area 9 from prefrontal cortex was dissected from coronal slabs stored at - 80ºC extending from the pial surface to white matter only including grey matter.

4.3.1.2. Protein reduction, Alkylation, LysC digestion, and desalting

Protein extracts were prepared from tissue samples using buffer lysis containing ammonium bicarbonate 50 mM, B-glycerophosphate 1M, sodium orthovanadate 100 mM, sodium pyrophosphate 200 mM, sodium fluoride 200 mM, tris 100 mM and Rapi Gest surfactant (Waters). Protein concentration was determined by Bradford assay (Biorad, Hercules, CA, USA) and 200 µg of total protein per each sample from control and SZ were used for mass spectrometry analysis. The lysate was reduced with 3 mM dithiothreitol at 55 ºC for 30 min. and alkylated with 20 mM iodoacetamide at room temperature for 30 min. and quenched with additional 10mM dithiothreitol for 30 min at room temperature.

Peptide samples for mass spectrometer analysis were prepared from reduced and alkylated lysate by adapting a single-pot solid-phase enhanced sample preparation (SP3)

similar to Hughes *et al.*, 2014 and using a KingFisher™ Flex (Thermo Fisher) automated robotic magnetic bead handler (Leutert *et al.*, 2019).

Specifically, 50 ug of lysate protein was diluted to 0.5 mg/ml concentration in 80% EtOH and loaded onto 500ug of conditioned magnetic carboxylated sp3 beads. Beads were subsequently washed 3 times with 100uL of 80% EtOH prior to on bead digestion/elution using 75 uL of 50mM AMBIC buffer and LysC at 10ng/ul. Digestion was carried out for 4 hours at 37C, beads were further washed with 75 ul of water and wash was combined with eluate. Eluate was acidified with formic acid and freeze dried prior to resuspending in MS sample buffer. Peptides were resuspended in 3% Formic acid and 4% acetonitrile in water at a 1ug/uL concentration.

4.3.1.3. Liquid chromatography coupled to tandem mass spectrometry

The LC/MS-MS analysis was performed in Q-Exactive instrument (Thermofisher Scientific, CA, USA) using data-dependent Top 20 acquisition method. Peptides were loaded onto a 100 µm ID × 3 cm precolumn packed with Reprosil C18 3 µm beads (Dr. Maisch GmbH), and separated by reverse-phase chromatography on a 100 µm ID × 30 cm analytical column packed with Reprosil C18 1.9 µm beads (Dr. Maisch GmbH). A gradient of 3% to 30% acetonitrile in 0.125% formic acid was used delivered at 225 nl/min over 130 minutes, with a total 180-minute acquisition time. Peptides were analyzed online on the orbitrap mass analyser using a top 20 data-dependent acquisition with all MS spectra being acquired and stored in centroid mode. Full MS scans were acquired from 300 to 1500 m/z at 70,000 FWHM resolution with a fill target of 3E6 ions and maximum injection time of 100 ms. The 20 most abundant ions on the full MS scan were selected for fragmentation using 2 m/z precursor isolation window and beam-type collisional-activation dissociation (HCD) with 26% normalized collision energy. MS/MS spectra were collected at 17,500 FWHM resolution with a fill target of 5E4 ions and maximum injection time of 50 ms. Fragmented precursors were dynamically excluded from selection for 35 s.

4.3.1.4. Data analysis

Raw files were processed and analyzed by MaxQuant (version 1.6.2.10). MS/MS spectra were searched with Andromeda against the uniprot_UP000005640_20180526.fasta with common contaminants added. The precursor mass tolerance was set to 7 ppm, and the fragment ion tolerance was set to 20 ppm. Search parameters included fully LysC enzyme specificity with up to three missed cleavages permitted. The minimum required peptide length was seven residues. The target-decoy database search strategy was used to guide filtering and estimate false discovery rates (FDR). Peptides matches were filtered to ≤ 0.01 FDR. Proteins with at least one peptide were considered identified. Label free quantification (LFQ) was selected for individual protein comparisons between control and schizophrenia groups. A quality cut off for protein determination was the presence of the protein in the 20 samples per group. The normalized LFQ intensity was referred to media of the controls. A significance value for each quantified protein was calculated from Student´s t-test and correction of significance values of the quantified protein data set was performed following the Benjamini and Hochberg methods (Yosef, 1995). A False Discovery Rate (FDR) was computed for all significant values and FDR threshold was set to 0.1. The quantified proteins were imported into Perseus software platform (version 1.6.1.3) to check data quality obtained by LC/MS/MS and to visualize the data distribution (Tyanova *et al.*, 2016). We performed the following analyses. 1. Correlation matrix: the normalized LFQ intensity data were used to estimate a correlation coefficient matrix between controls and schizophrenia patients. The correlation coefficient data were plotted as a heat map. 2. Hierarchical Clustering: This was carried out on Z-score transformed normalized LFQ intensity data for each protein using Euclidean distance.

4.4. Bioinformatic analysis

4.4.1. Proteomic data analysis in individual samples in the cerebellum and prefrontal cortex in schizophrenia

To analyze the profile of cerebellar proteome, we used the Log_2 of the fold change of normalized LFQ Intensity between schizophrenia and controls samples and FDR adjusted $-Log_{10}$ (*q*-value). To perform Disease, Gene Ontology (GO), and Pathways analysis we used Webgestalt support by Fisher`s exact test (Wang *et al.*, 2013). Diseases terms were obtained from PharmacoGenetics Knowledge Base (PharmGKB) and GLAD4U Gene List Automatically Derived For You (GLAD4U) databases (Hewett *et al.*, 2002; Jourquin *et al.*, 2012). For GO analysis, we performed non-redundant enriched categories analysis, for pathways analysis we used the Reactome database and for network generation, we used String version 11.0. To perform the screening on protein expression in the cerebellum we used the human protein atlas (Uhlén *et al.*, 2015). The enrichment analyses were set to FDR=0.1.

4.4.1.2. Chromosomic distribution analysis

To perform the chromosomal distribution analysis, we used Webgestalt (WEB-based GEne SeT AnaLysis Toolkit), and for enrichment analysis, we used the method of Over-Representation Analysis (ORA) supported by Fisher's exact test. For this analysis, we used the extension Chromosomal Location database. The loci identified in this analysis were crossed with genome-wide association study (GWAS) catalogue for risk loci in schizophrenia previously report by Ripke *et al.*, 2013, a study in a Europe population, and Wong *et al.*, 2014, a study in Chinese ancestry.

4.4.1.3. Transcription factor analysis

For the transcription factor analysis of chronic SZ cerebellum and prefrontal cortex, we used prioritized altered proteins and performed the enrichment analysis using FunRich Tool v.3.1.3 (Pathan *et al.*, 2015).

To perform Gene Ontology and the pathways analysis, we used Webgestalt and the method of Over-Representation Analysis. For the gene ontology analysis, we performed non-redundant enriched categories analysis, while for the pathways analysis, we used the Reactome database. The enrichment analyses were set to FDR=0.1. To represent enrichment analysis, we generated a heat map using the Perseus software platform (version 1.6.1.3).

4.4.1.4. Screening for proteins previously reported in cerebellum in schizophrenia

Using the Schizophrenia Database (Wu, Yao and Luo, 2017), we performed a screening in which we compared altered proteins with those previously reported in other gene expression studies. For proteins previously reported in proteomic studies, we performed a screening based on the gene symbol. For the representation of these results, we used FunRich Tool v.3.1.3 (Pathan *et al.*, 2015)

4.5. Murine model for schizophrenia

Three pregnant Wistar rats (Harlan Ibérica, Spain) at gestation days 14-16 were individually housed in a temperature/humidity-controlled environment in a 12h light/dark cycle with free access to food and water. The litter sizes varied between 7 and 11 animals. One was used as a control group and the others as part of a double-hit model. After birth, at postnatal day 9 (PD9), both double-hit litters were exposed to maternal deprivation for 24hrs as a first hit; this early stressful life event has an impact on prepulse inhibition in rats, similar to the alterations seen in schizophrenic patients. On PD21, the pups were weaned and one of the litters was exposed to isolation for 5 weeks as a second hit (PD21-56); although the pups were housed separately (1/cage), they could smell, hear and see their siblings, but they could not come into physical contact with them. Following isolation, the animals were regrouped (DM/Iso). Meanwhile, the second hit for the other litter

exposed to maternal deprivation involved restraint stress between PD 72 to 78 for 6 hours every day (DM/RS). These conditions represent suitable rodent models for the study of neuropsychiatric dysfunctions (Bailoo *et al.*, 2016; van Zyl, Dimatelis and Russell, 2016). Group sample sizes were CT, n=11; DM/Iso, n=9; DM/RS, n=7. All experimental protocols adhered to the guidelines of the Animal Welfare Committee of the Complutense University in accordance with European legislation (D2010/63/UE). All efforts were made to reduce the number of animals used and minimize animal suffering in the experiments.

4.5.1. Preparation of biological samples

The animals were subjected to cervical dislocation. The brain was removed from the skull and, after careful removal of the meninges and blood vessels, the cerebellum were excised and frozen at -80°C until assayed.

4.5.1.1. Western Blot Analysis

Brain cerebellum samples were homogenized by sonication in PBS (pH=7) mixed with a protease inhibitor cocktail (Complete®, Roche, Spain). After determining and adjusting protein levels, homogenates of cerebellum tissue were mixed with Laemmli sample buffer (Bio-Rad, USA) and β-mercaptoethanol (50 µl/ml Laemmli), 15µg were loaded into an electrophoresis gel. Once separated on the basis of molecular weight, proteins from the gels were blotted onto a nitrocellulose membrane with a semi-dry transfer system (Bio-Rad) and were incubated with specific antibodies against: (1) Methyltransferase-like protein 7A (METTL7A, 1:750 in BSA 1%; ABclonal A8201); (2) NADH dehydrogenase (ubiquinone) 1 beta subcomplex, 9 (NDUFB9, 1:1000 in BSA 0,5%; sc398869, SCT); (3) cytoplasmic linker associated protein 1 (CLASP1, 1:1000 in BSA 0,5%; sc390159, SCT); (4) tyrosine 3-monooxygenase/tryptophan 5-monooxygenase activation protein zeta (YWHAZ, 1:1000 in BSA 0,5%; sc293415, SCT); (5) β-actin (1:10000; A5441, Sigma). Primary antibodies were recognized by the respective horseradish peroxidase-linked

secondary antibodies. Blots were imaged using an Odyssey Fc System (Li-COR, Biosciences, Germany) and were quantified by densitometry (NIH ImageJ software). In all the WB analyses, the housekeeping protein β actin was used as a loading control, and each western blot was performed at least three times in separate assays. The data were presented as fold change from the control group.

4.6. Immunohistochemistry of human cerebellar tissue

Immunohistochemistry was performed from frozen healthy adult human cerebellar tissue. The tissue was embedded in optimal cutting temperature compound (OCT) and cut in cryostat (Microm HM 525, Thermo Scientific). The frozen block was oriented to obtain 7 µm thick sagittal sections. The frozen sections were fixed in 4% paraformaldehyde for 30 min at room temperature and were washed in Phosphate-Buffered Saline (PBS pH 7.4 (Sigma). The sections were incubated with blocking solution (PBS containing 15% goat serum, 0.05% BSA, 0.05% Triton X-100) for 1 hour at RT. Sections were immunostained with rabbit anti-METTL7A (ABclonal A8201, dilution 1:75), mouse anti-METTL7A (AB128017 (Clone 87.1_1E7), dilution 1:75), mouse anti-Tuj1 (Covance MMS435P, dilution 1:500) and mouse anti-GFAP (Millipore MAB360, dilution 1:400). These antibodies were diluted in PBS containing 1% goat serum, 0.05% BSA, 0.05% Triton X-100. For double immunostaining of METTL7A and GFAP, we preformed sequential incubation, first with anti-METTL7A overnight at 4ºC and subsequently for 45 minutes with anti-GFAP at 4ºC. For secondary antibodies, we used goat anti-rabbit Cy3 (Amersham, dilution 1:500) and goat anti-mouse Dye Light 488 (Invitrogen 35503, dilution 1:500). Nuclei were visualized with Hoechst 33342 stain (Invitrogen, dilution 1:400). For lipid droplet staining, we performed immunostaining without permeabilization, first with anti-METTL7A for 48 hours at 4ºC and then with the secondary antibody for 1 hour followed by a final incubation for 30 minutes with bodipy 493/503 (dilution 1:50) and Hoechst staining at RT. The sections were mounted with prolong diamond antifade mountant (Invitrogen P36970).

4.6.1. Confocal microscopy

Confocal microscopy analysis was performed using a Leica TCS SP8 STED 3X equipped with a white light laser confocal microscope with hybrid detectors (Leica Microsystems, Wetzlar, Germany). For extended-volume imaging at low magnification (HC PL APO CS2 10x/0.4 dry), a high-precision motorized stage was used to collect the large-scale 3D mosaics of each tissue section. The software automatically generates a list of 3D stage positions covering the volume of interest, which are computed using the dimensions of a single image in microns and degree of overlap between adjacent images. Individual image tiles were 696 × 696 pixels and the z-step was 2.5 µm. A total of 49 stacks were captured for each extended image. Brain tissues was excited sequentially at three different wavelengths: 405 nm, 488 nm, 552 nm, which respectively excite Hoechst 33342, GFAP/TUJ1 and BODIPY, and METTL7A. Hoechst 33342 was detected in the 420–465 nm range, GFAP/TUJ1 and BODIPY were detected in the 500-550 nm range, and METTL7A was detected in the 565–700 nm range. Z-stacks were acquired with at 20x, 63x or 100x magnification, with a 0.4 and 1.4 numerical aperture objective lens, respectively. At low- magnification, 10 sections were acquired every 1 µm across the tissue thickness. For volume rendering, it was necessary to optimize z-sectioning and the z-step size was set to 0.3 µm. The images were then deconvolved using Huygens software (SVI, Leiden, the Netherlands). 3D models were generated with Imaris x64 v7.2.1 software (Bitplane, Zurich Switzerland) with Surpass Mode. Maximum projections were created using LAS AF™ software (Leica Microsystems, Heidelberg, Germany

V. RESULTS

5.1. Proteome of pooled protein lysates from *postmortem* cerebellum of schizophrenia and healthy controls

Results published in Vidal-Domènech F, Riquelme G, Pinacho R, Rodriguez-Mias R, ***Vera A,*** *et al. Calcium-binding proteins are altered in the cerebellum in schizophrenia, PLoS ONE, 15(7), pp. 1–22. doi: 10.1371/journal.pone.0230400.*

We performed a pilot proteomic analysis of pooled protein lysates from the cerebellum from four subjects with paranoid schizophrenia and four control subjects matched for gender, age and *postmortem* delay (**Table 2**). For this analysis, the peptides were dimethyl-labelled with either hydrogen (light peptides, control) or deuterium (heavy peptides, schizophrenia), with offline fractionation by SCX and liquid chromatography coupled to tandem mass spectrometry (LC-MS/MS) on a hybrid linear ion trap orbitrap mass spectrometer (LTQ-Orbitrap). This strategy allowed us to obtain a mix of labelled peptides from pools as shows the experimental design (**Figure 4**). This experimental procedure allowed us to identify proteins significantly altered in the cerebellum in schizophrenia.

Table 2. Demographic, clinical- and tissue-related features of cases in pooled samples

Cohort I Subgroup (n=8)				
	Schizophrenia[a](n=4)	**Control (n=4)**	**Statistic**	***p* -value**
Gender				
Male	100% (n=4)	100% (n=4)	N/A	N/A
Age (years)	42 ± 11	42 ± 12	[b]7.50	1.000
PMD (hours)	8.25 ± 4.50	13.25 ± 7.59	[b]4.50	0.384
pH	6.68 ± 0.47	7.02 ± 0.29	[b]4.50	0.353
Toxicology			N/A	N/A
Atypical AP	50% (n=2)	N/A		
Other	50% (n=2)	50% (n=2)		
Drug free	N/A	50% (n=2)		

Mean ± standard deviation or relative frequency are shown for each variable; PMD, *postmortem* delay; SZ, schizophrenia; C, healthy control group; AP, antipsychotics; N/A, not applicable. [a]Paranoid schizophrenia (n=4). [b]Mann-Whitney U is shown for non-parametric variables. *Published in Vidal et al. 2020. PLOS ONE.*

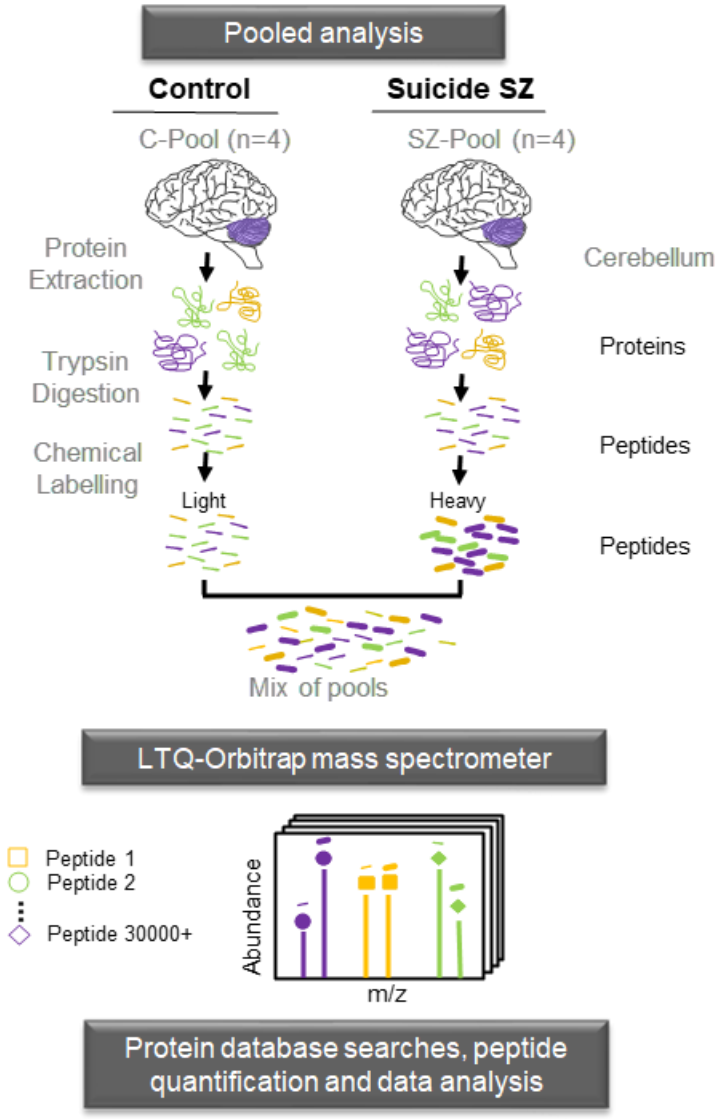

Figure 4.Experimental strategy for large-scale quantitative proteomic analysis and identification of differentially expressed proteins in cerebellum in schizophrenia. Protein lysates from the postmortem cerebellum of control (n = 4) and suicide schizophrenia (SZ, n = 4) subjects. In the analysis in pools, samples from the same group were pooled. Subsequently, protein database searches, peptide quantification and data analysis were performed as described in the experimental procedures section. Published in Vidal et al. 2020. PLOS ONE.

5.1.1. Quantitative proteomic analyses of pooled protein lysates

Our results from the pilot proteomic analysis of pooled samples from the cerebellum showed 2289 quantified proteins and 1412 quantified proteins with a Protein Prophet probability score of more than 90% (for more details, see **Dataset 1** (https://doi.org/10.1371/journal.pone.0230400.s006). 641 (45%) proteins were identified with more than 6 peptides, and all quantified proteins showed a normalized distribution (**Figure 5A-B**). The distribution of protein heavy-to-light (H/L) ratios revealed that some proteins of the cerebellar proteome were altered in schizophrenia. Our proteomic analysis found 99 (7%) significantly altered proteins with a false discovery rate (FDR) of 10% and a protein sequence coverage greater than 5% (for more details, see **Dataset 2** https://doi.org/10.1371/journal.pone.0230400.s007S2). Moreover, 31 proteins were previously reported in other brain areas in schizophrenia (**Table 3**). Thus, in this study 68 new proteins were found to be altered in schizophrenia. Gene ontology analysis of altered proteins showed that the biological functions transport and cell communication/signal transduction were more enriched in pooled protein lysates from the cerebellum (**Figure 6**). Furthermore, in this pilot proteomic study 11 candidate proteins (**Table 4**) were selected as the most robust candidates from the enriched biological functions of cell communication and transport according to two criteria: (i) the protein had been quantified with more than 4 peptides; and (ii) the protein showed a greater than 2-fold increase or decrease.

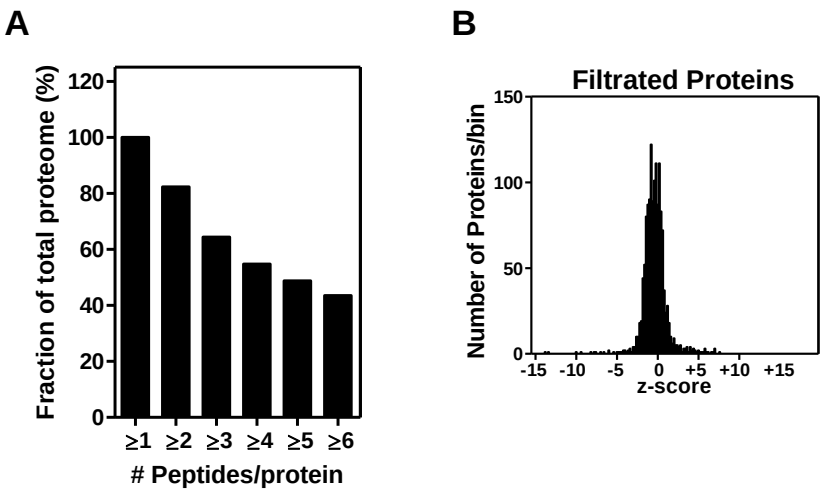

Figure 5.Quantified protein profile in pooled samples in the cerebellum in schizophrenia A. Distribution of the number of peptides quantified per protein from the data set of 2289 quantified proteins. **B.** Normalized distribution of z-scores for confidently quantified proteins (>2 peptide sequences) (n = 1148).

Table 3. List of altered proteins previously reported in other brain regions in proteomic studies in schizophrenia

Brain region	Gene Symbol	Reference*
DLPFC	GNB1, NDUFA12	(Behan et al. 2009)
	GNB1, MAG	(Chan et al. 2011)
	VIM	(English et al. 2009)
	GNB1, TF	(Martins-de-Souza, Gattaz, Schmitt, Maccarrone, et al. 2009)
	ATP6V0D1, SORBS1, VIM	(Martins-De-Souza et al. 2009)
	PNP	(Novikova et al. 2006)
	TF	(Pennington et al. 2008)
	BCL2L13, PHB2, SORBS1, SV2B, TMEM30A	(Pinacho et al. 2016)
	TF	(Prabakaran et al. 2004)
	PVALB	(Smalla et al. 2008)
OFC	DMTN, PGAM5, VDAC2	(Velásquez et al. 2017)
ACC	GNB1, TF	(Clark et al. 2006)
	AP2B1, ATP6V0A1, BAIAP2, CALM2, CCT6A, HSD17B4, NAPA, SRPRB, VDAC2	(M Föcking et al. 2015)
	GNB1	(Martins-de-Souza, Schmitt, et al. 2010)
CC	GNB1, HAPLN2, VIM	(Saia-Cereda et al. 2015)
	BAIAP2	(Saia-Cereda et al. 2016)
	CDC42	(Saia-Cereda et al. 2017)
Thalamus	VIM	(Martins-de-Souza, Maccarrone, et al. 2010)
Hippocampus	PVALB	(Melanie Föcking et al. 2011)
	ACOT7, CCT6A	(Schubert, Föcking, and Cotter 2015)
	VIM	(Nesvaderani, Matsumoto, and Sivagnanasundaram 2009)
Temporal lobe	HAPLN2	(Martins-de-Souza, Gattaz, Schmitt, Rewerts, et al. 2009)
	CADM1, CDC42, H3F3A, PPP3R1, VIM	(Saia-Cereda et al. 2017)
	PHB2, VIM	(MacDonald et al. 2015)

DLPFC: Dorsolateral prefrontal cortex, **OFC:** Orbitofrontal cortex, **ACC:** Anterior cingulate, **CC: Corpus callosum** *Complete reference information is detailed in **Dataset 1** https://doi.org/10.1371/journal.pone.0230400.s006. *Published in Vidal et al. 2020. PLOS ONE*

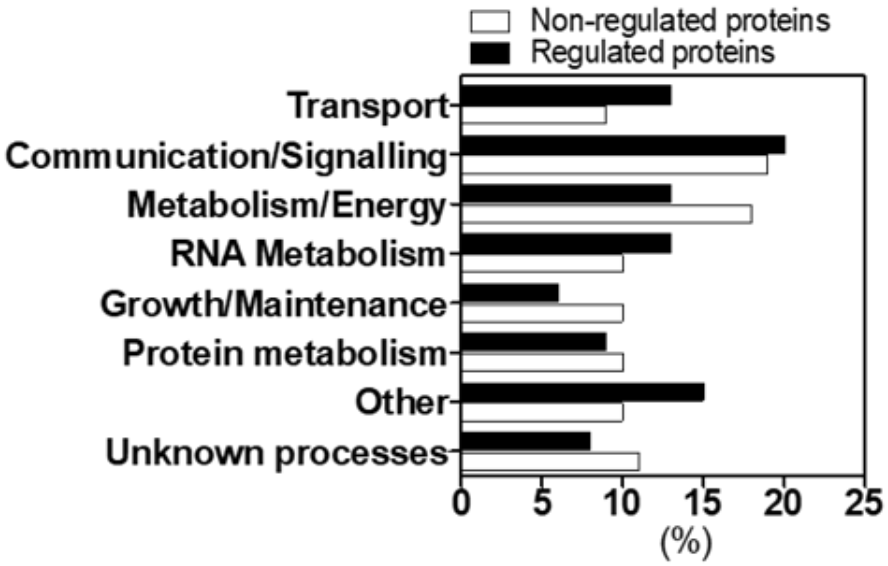

Figure 6.Gene ontology classification of biological functions for non-significantly and significantly altered proteins in the cerebellum in schizophrenia compared to control Transport (GO:0006810); Cell communication (GO:0007154); Signal transduction (GO:0007165); Metabolism (GO:0008152); Energy pathways (GO:0006091); Regulation of nucleobase, nucleoside, nucleotide and nucleic acid metabolism (GO:0019219); Cell growth and/or maintenance (GO:0008151); Protein metabolism (GO:0019538); Biological process unknown (GO:0000004). Published in Vidal et al. 2020. PLOS ONE.

Table 4. List of proteins filtrated from enriched and most representative functions in the postmortem cerebellum in schizophrenia

Function	Acc. Number	Gene Symbol	Protein Description	Quantified Peptides	Ratio H/L	log_2Ratio H/L
Transport	Q93050	ATP6V0A1	V-type proton ATPase 116 kDa subunit a isoform 1	5	0.09	-3.46
	A0A0A0MR02	VDAC2	Voltage-dependent anion-selective channel protein 2	16	0.13	-2.97
	Q86UR5	RIMS1	Regulating synaptic membrane exocytosis protein 1	11	0.46	-1.12
	M0R0Y2	NAPA	Alpha-soluble NSF attachment protein	6	3.90	1.97
	Q01469	FABP5	Fatty acid-binding protein, epidermal	6	5.20	2.38
Cell Comunication / Signal transduction	E7EMB3	CALM2	Calmodulin-2	18	2.56	1.36
	P37235	HPCAL1	Hippocalcin-like protein 1	9	2.64	1.40
	O00533	CHL1	Neural cell adhesion molecule L1-like protein	17	3.01	1.59
	Q8WUD1	RAB2B	Ras-related protein Rab-2B	6	3.17	1.66
	Q96FQ6	S100A16	Protein S100-A16	7	3.53	1.82
	P20472	PVALB	Parvalbumin alpha	8	3.65	1.87

Access number from Uniprot database; H/L ratio between heavy (schizophrenia) and light (control) peptide areas. *Published in Vidal et al. 2020. PLOS ONE.*

5.2. Proteomic analysis of *postmortem* cerebellum in individual protein lysates from schizophrenia and healthy controls

These results are part of the manuscript Analysis of networks in the cerebellum in chronic schizophrenia: reduction of METTL7A linked to stress and novel localization in glia cells. Vera-Montecinos et al., submitted to Molecular Psychiatry in 2020.

This proteomic analysis was performed on individual protein extracts from human cerebellar lateral cortex of 12 male patients with schizophrenia and 14 control individuals using Q-Exactive Orbitrap tandem mass spectrometer and label-free quantification to identify altered proteins related to schizophrenia. The experimental design is showed in **Figure 7**. (Proteomic analysis was performed in collaboration with Dr Villen and Dr Rodriguez Mias from the University of Washington, Seattle). No differences were observed in the demographic- or tissue-related variables analysis between schizophrenia and control groups matched for gender, age and *postmortem* delay (**Table 5**).

Table 5. Demographic, clinical- and tissue-related features of cases

	Schizophrenia (n=12)	Control (n=14)	Statistic	*p*- value
Gender				
Male	100% (*n* =12)	100% (*n* =14)	N/A	N/A
Age (years)	72 ± 9	69 ± 11	78.5[a]	0.56
PMD (hours)	5.48 ± 2.29	5.46 ± 1.81	0.02; 25 [b]	0.98
pH Cerebellum	6.88 ± 0.49	6.61 ± 0.63	1.25; 25 [b]	0.22
SZ diagnosis				
Chronic residual	66.67% (n= 8)			
chronic paranoid	16.67% (n=2)			
chronic disorganized	8.33% (n=1)			
chronic catatonic	8.33% (n= 1)			
Age of onset of SZ (years)	22 ± 8	N/A	N/A	N/A
Duration of illness	50 ± 9	N/A	N/A	N/A
Toxicology				
Daily AP dose (mg/day) [c]	609 ± 507.10	N/A	N/A	N/A
First generation AP	16.67% (n=2)			
Second generation AP	58.33% (n=7)			
First and Second generation AP	8.88% (n=1)			
AP free	16.67% (n=2)			

Mean ± standard deviation; PMD, *postmortem* delay; SZ, schizophrenia; AP, antipsychotics; N/A, not applicable. [a]Mann-Whitney U for non-parametric variables. [b]T-statistic and degree of freedom for parametric variables. [c]Last daily Chlorpromazine equivalent dose was calculated based on the electronic records of drugs prescriptions of the patients as described (Gardner et al., 2010).

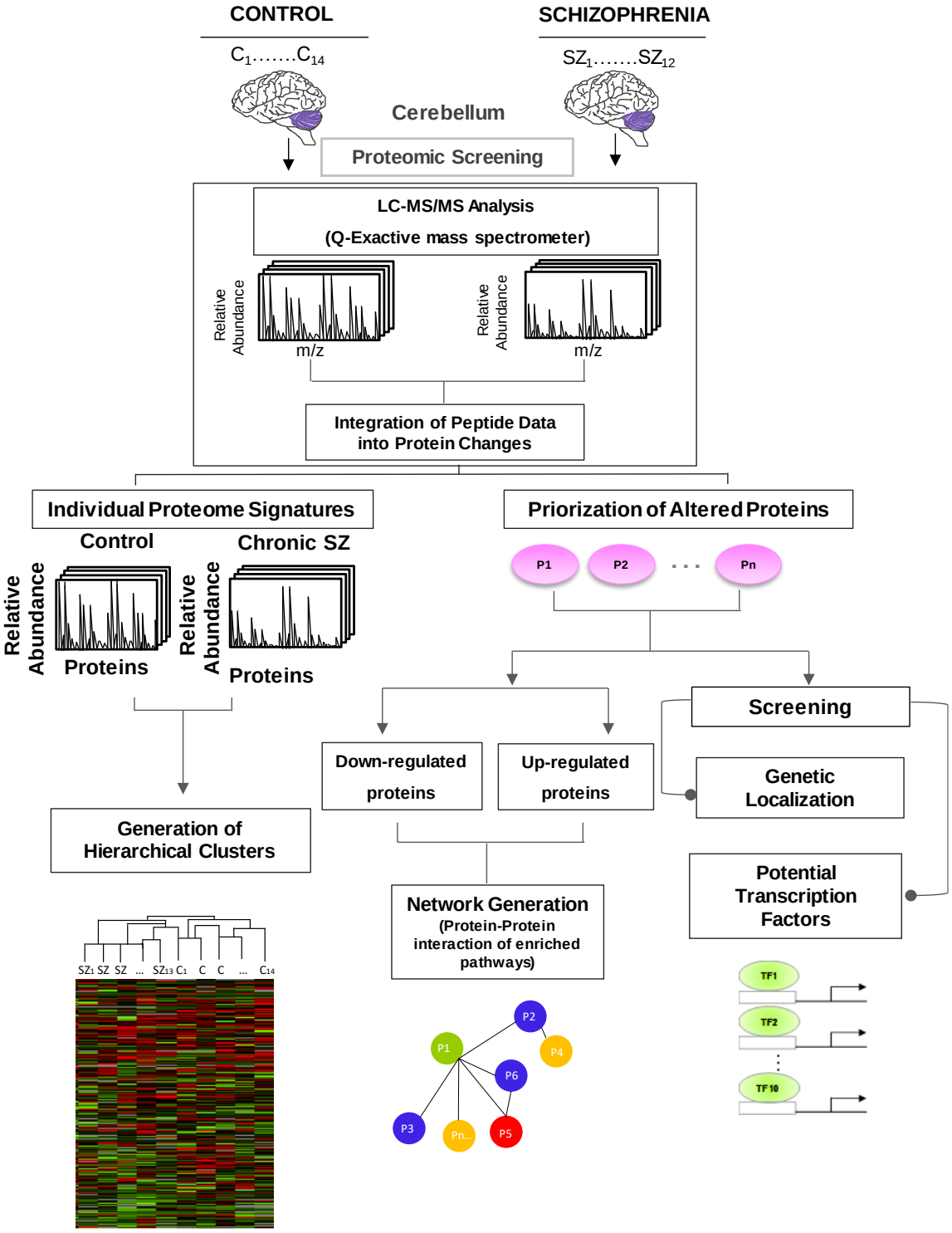
CONTROL
C1.....C14
SCHIZOPHRENIA
SZ1.....SZ12
Cerebellum
Proteomic Screening
LC-MS/MS Analysis
(Q-Exactive mass spectrometer)
Relative Abundance
m/z
Relative Abundance
m/z
Integration of Peptide Data into Protein Changes
Individual Proteome Signatures
Control
Chronic SZ
Relative Abundance
Proteins
Relative Abundance
Proteins
Priorization of Altered Proteins
P1
P2
Pn
Screening
Down-regulated proteins
Up-regulated proteins
Genetic Localization
Generation of Hierarchical Clusters
Potential Transcription Factors
Network Generation
(Protein-Protein interaction of enriched pathways)
SZ1 SZ SZ ... SZ13 C1 C C ... C14
P1
P2
P3
P4
P5
P6
Pn...
TF1
TF2
TF10

Figure 7. Experimental design for the proteomic analysis to identify altered pathways in schizophrenia. Protein lysates from the postmortem cerebellum of control (C) (n=14) and chronic schizophrenia (SZ) patients (n=12) were processed as described. The peptides were separated and analysed by Liquid Chromatography (LC) coupled to a Q-Exactive Orbitrap tandem mass spectrometer. The relative fold change of the peptides was integrated into protein changes. The individual protein signatures for each case and control were used to generate hierarchical clusters. The prioritization of altered proteins (P1-Pn represents generic proteins) in SZ was obtained by comparing protein fold changes between control and SZ groups (significant proteins adjusted using an FDR of 0.1). We performed four analyses for these altered proteins in SZ: i) Unsupervised hierarchical clustering analysis generated from quantified proteins in 12 SZ and 14 healthy control samples of postmortem cerebellum; ii) Genetic localization; iii) Transcription factor enrichment; iv) Generation of networks from significantly enriched pathways by protein-protein interaction. These analyses were performed using Perseus, Webgestalt, FunRich and String, respectively.

5.2.1. Quantitative proteomic analyses in the cerebellum in individual chronic schizophrenia subjects

We quantified a total of 2578 proteins. 1474 proteins (57%) were quantified in at least 7 individuals per group and kept for the other analyses (Dataset 1 Annex). 97.8% of the proteins were identified with 2 or more peptides and 46.5% with five or more peptides. For the individual proteome signature analysis, we examined the similarity of the individual proteome through a correlation matrix. To assess the similarity between the proteomes of the different individuals, we calculated Pearson correlation coefficients and visualized the results in a correlation matrix (**Figure 8**). All correlations were above 0.7. To assess the similarity between the SZ and control groups we calculated the Pearson correlation coefficient of the protein intensity mean calculated for each group. This correlation was 0.989, indicating that globally the cerebellar proteomes of SZ and control individuals were highly similar.

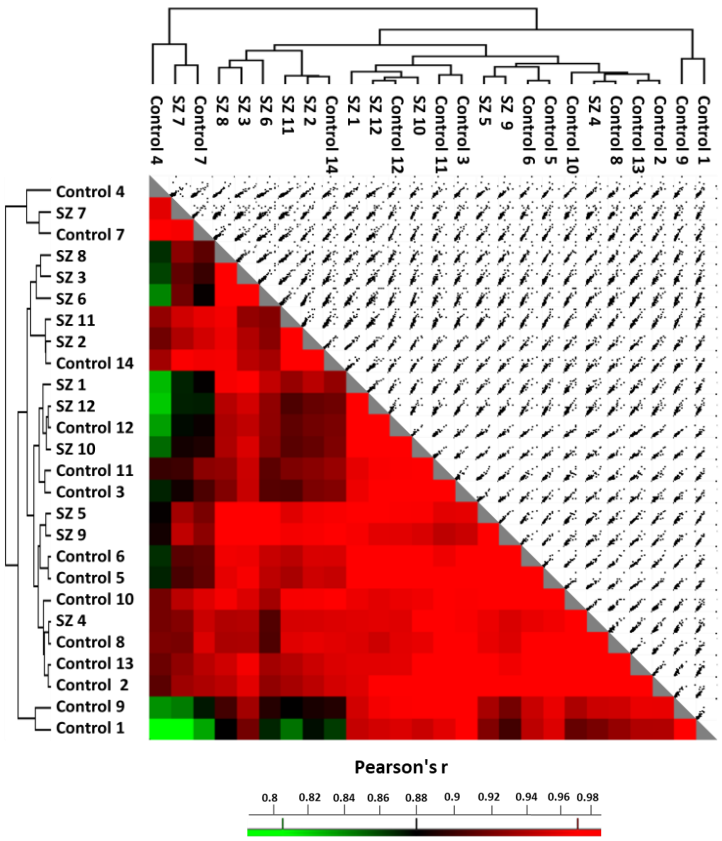

Figure 8. Quality control analysis for quantified proteins in the cerebellum. The correlation matrix shows the correlation coefficiency between the 1474 quantified proteins in each compared pair of samples.

Unsupervised hierarchical clustering analysis of the proteomic profiles was able to segregate controls and SZ samples, with the exception of five controls (#8, #7, #4, #12 and #14) (**Figure 9**). We further investigated whether the demographic- and tissue-related features could explain the differential clustering of these controls and observed that although four of these controls segregated together, none of the variables influence this segregation (**Figure 10**).

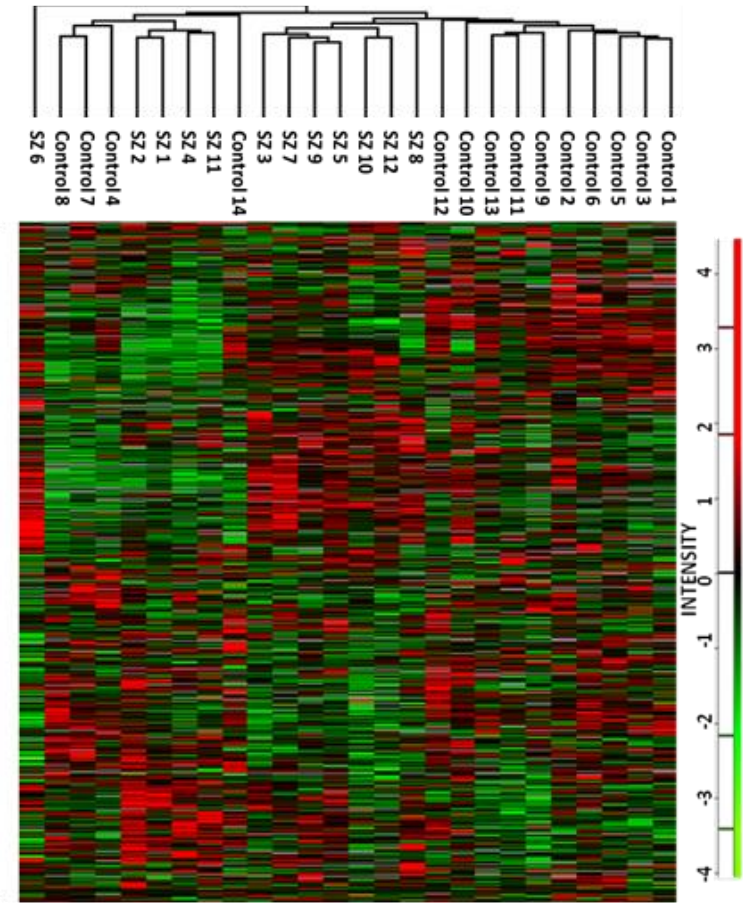

Figure 9. Unsupervised hierarchical clustering analysis. This analysis was performed using matrix processing according to the Euclidean distance and z-score aggregation method. Protein profiles were generated from 1474 quantified proteins in 12 SZ and 14 healthy control samples of postmortem cerebellum and were clustered according to the z-score and displayed as a heat map. Green colour clusters represent down-regulated proteins. Red colour clusters represent up-regulated proteins.

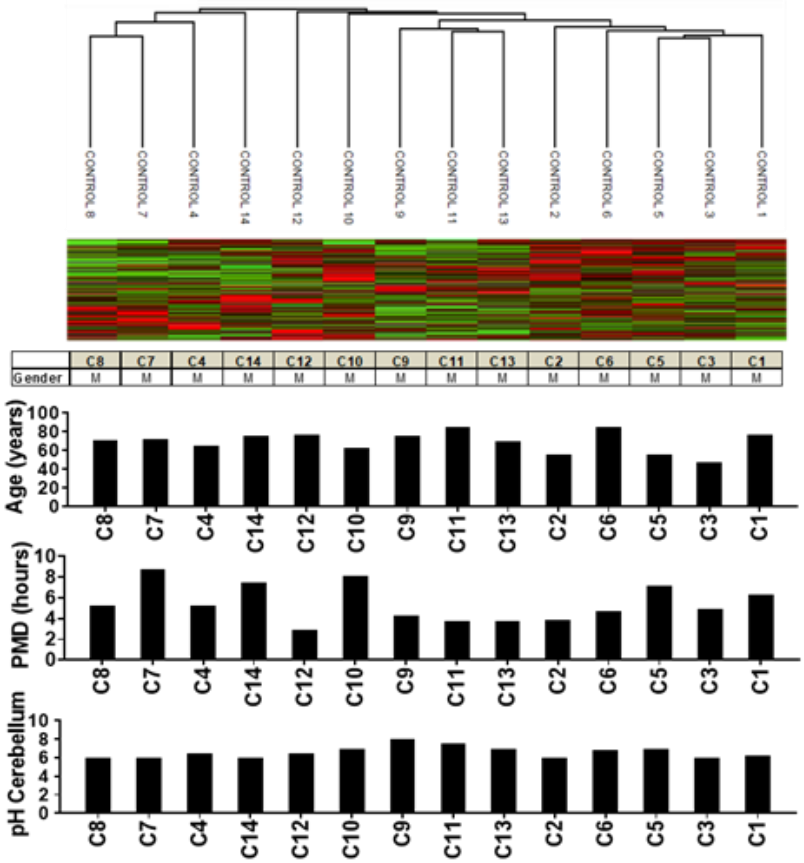

Figure 10.Unsupervised hierarchical clustering analysis for controls and demographic and tissue-related features of each control. Unsupervised hierarchical clustering analysis for quantified proteins from postmortem cerebellum of 14 healthy control samples. The table below it shows the gender. The graphs show the tissue-related features of each healthy control sample. **M**: Male, **PMD**: Postmortem delay.

Our results revealed 250 significantly deregulated proteins (16.9%) in schizophrenia with an FDR of <0.1 (Dataset 2 Annex). None of the regulated proteins showed significant correlation with PMD or pH (FDR<0.1) (Annex 3 and 4) was found for any altered protein. A screening in which the 250 significantly altered proteins were compared with those previously reported in gene expression studies from the Schizophrenia Database found that only 56 of the altered proteins had been previously reported at the gene expression level in an iPSC model of schizophrenia subjects, while only 16 altered proteins had been previously reported in a microarray assay in human cerebellum (**Figure 11,** Dataset 2 Annex). Additionally, 86 altered proteins in the cerebellum had been previously reported as altered in other brain regions in schizophrenia and 20 proteins have been reported in two recent cerebellar proteomic studies (**Table 6** and Dataset 2 Annex). Thus, our study reported 167 new altered proteins in the cerebellum in schizophrenia.

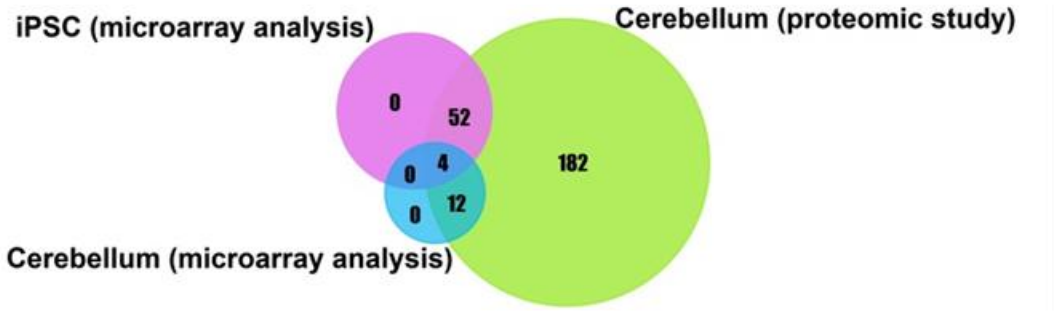

Figure 11. Screening of proteins previously reported in schizophrenia. This Venn diagram shows the comparison between the number of proteins previously reported in schizophrenia through gene expression analysis obtained from the Schizophrenia Database (human cerebellum and iPSC) and our proteomic study in the cerebellum.

Table 6. Proteins previously reported in proteomic studies in schizophrenia

Cerebral area	Proteins previously reported in schizophrenia	References
Cerebellum	CAMK4; C11orf58; NDUFA12; AHCY; ERP44; PAFAH1B1; PRDX6; NCKAP1; LCP1; MYH9; NAXE; ACLY; CYB5R1; NAPA; CCT7; HSD17B4; BCL2L13; RAB21; RIMS1; UBE2I	Vidal-Domènech et al., 2020; Reis-de-Oliveira et al., 2020
Anterior cingulade	CS; GPD1; AHCY; CBR1; UCHL1; PGAM1	Clark et al., 2007
Anterior cingulade cortex	CS; ACAT2; SOD1;DDAH1;DCTN2; IDH2; HNRNPK; IARS; METTL7A; ACTR2; PPIA; LIN7A; PIP4K2A; NAPA; SPTAN1; SCRN1; TPM1; ARHGDIA; YWHAZ; YWHAB; COMT; HSD17B4; AP2M1; UCHL1	Clark et al., 2007; ClarK et al., 2006; Föcking et al., 2015; Martins de Souza et al., 2010; Smalla et al., 2008; English et al., 2011
Anterior hippocampus	UCHL1 ; DDAH1 ; SOD1 ; CAPZA2 ; YWHAE; YWHAZ ;PRDX6	Nesvaderani et al., 2009
Posterior hippocampus	PGAM1	Nesvaderani et al., 2009
Anterior temporal lobe	YWHAQ; YWHAZ; HSPD1; NDUFB5; SPTAN1; YWHAH; YWHAE; MYH9; PURA; HNRNPK; MOG	Saia-Cereida et al., 2017; Martins de Souza et al., 2009[b]
Auditory cortex	GNAQ; ATP1A3; UCHL1	Mc Donald et al., 2015
Corpus callosum	YWHAZ; UCHL1; MOG; NPM1; DDAH1; YWHAE; YWHAB; ANK3; SOD1; DDT; HP1BP3; HNRNPR; YWHAH	English et al., 2011; Saia-Cereida et al., 2015; Sivagnanasundaram et al., 2007; Saia-Cereida et al., 2016
Dorsolateral prefrontal cortex	DPYSL5; NDUFS1; HSPD1; SPTAN1; YWHAE; PGAM2; MOG; RAP2A; NDUFA12; GDAP1; NDUFB10; SIRPA; HP1BP3; DPYSL4; ADH5; GSTM3; IGSF8; CLSTN1; MAP6; PRDX6; TKT; ERP29; PGAM1; PURA; YWHAZ; CBR1; TCP1; HSPA9; BCL2L13; UCHL1; ARPC1A; ITGAV; SCRN1; GPM6A; MARCKS; TXN2; TPT1; CYB5A; RTN1; GNAQ; ATP5PD; PPA2	Saia-Cereida et al., 2015; Martins de Souza et al., 2009[a]; English et al., 2009; Martins de Souza et al., 2009[c]; Chan et al., 2011; Behan et al., 2009; Pinacho et al., 2016; Pennington et al., 2008; English et al., 2011; Wesseling et al., 2013; Novikova et al., 2006; Smalla et al., 2008; Prabakaran et al., 2004
Hippocampus	TPPP; UBE2M; YWHAE;SOD1; PRDX6; TCP1; UCHL1	Schubert et al., 2015; Föcking et al., 2011
Mediodorsal thalamus	YWHAZ; CBR1; SYN3; PGAM1; NDUFB9; TKT; MOG; HSPD1; PPIA; PITPNA	Martins de Souza et al., 2010
Orbitofrontal prefrontal cortex	RAB35; ATP2B3; PGAM1; RTN1; DDAH1; ATP1A1; MARCKS; MOG; YWHAH; SYN3; GPM6A; ATP1A3	Velasquez et al., 2017
Wernicke's area	DLD; PRDX6; PGAM1; NDUFS1	Martins de Souza et al., 2009[d]
Insular cortex	SNCG; ERLIN2; NPM1; COPS4	Pennington et al., 2008

5.3. Genetic localization of altered proteins in the proteomic profile in the cerebellum

These results are part of the manuscript Altered transcriptional programs in the cerebellum in chronic schizophrenia Vera et al. in preparation, to be submitted in 2021.

We analysed the chromosomal distribution of the 250 altered proteins in the cerebellum. Our results showed a total of 185 loci with altered proteins, 54 of them previously reported to be risk loci for schizophrenia (**Annex 3**). Our analysis showed 139 loci with one altered protein, 33 loci with two altered proteins, and 9 loci with three altered proteins. The most abundant loci with altered proteins were 12q13.3, 16p13.3, 22q12.3 and Xq28, with four altered proteins each. **Table 7** show the loci with 3 and 4 altered proteins. This result shows that 43 altered proteins distributed in 13 loci (7% of the total) encompass 17.2% of the altered proteins in the cerebellum in schizophrenia.

Table 7. Chromosomal distribution of altered proteins in the cerebellum in chronic schizophrenia

Chromosomic region	Protein name	Previously report in SZ
1p36.22	LZIC;CLSTN1;TARDBP	
6q25.3	SOD2;TCP1;ACAT2	
7p13	DBNL;PPIA;PGAM2	
9q34.11	CRAT;SPTAN1;SET	
11q13.4	RPS3;NUMA1;ARRB1	
11p15.5	HRAS;CEND1;SLC25A22	
12q13.3	CS;NACA;LRP1;DCTN2	Yes[a]
12q13.12	GPD1;METTL7A;DIP2B	
16p13.3	UBE2I;ELOB;NDUFB10;TRAP1	Yes[b]
17p13.3	YWHAE;PAFAH1B1;PITPNA	Yes[a-b]
22q11.21	CRKL;COMT;BCL2L13	
22q12.3	SYN3;MYH9;TXN2;YWHAH	
Xq28	ATP6AP1;BCAP31;ATP2B3;CD99L2	

[a] Previously reported in schizophrenia by Ripke et al., 2014 (from European ancestry); [b] Previously reported in schizophrenia by Li Z. et al., 2017 (from Chinese ancestry). This analysis was performed using the Webgestalt Chromosomal Location database.

5.4. Putative transcriptional programs responsible of changes in the proteomic profile in the cerebellum

These results are part of the manuscript Altered transcriptional programs in the cerebellum in chronic schizophrenia, Vera et al. in preparation, to be submitted in 2021.

To investigate the transcriptional program that could be controlling the 250 altered proteins in schizophrenia, we performed an enrichment analysis of transcription factors. Our enrichment analysis for the targets of each transcription factor showed only 11 potential transcription factors that controlled the 250 altered proteins (**Figure 12**). These were: SP1, KLF7, SP4, EGR1, HNF4A, CTCF, GABPA, NRF1, NFYA, YY1, and MEF2A. This analysis revealed that the top 3 most significant transcription factors were SP1, YY1, and EGR1, with 125, 37, and 60 targets, respectively (**Table 8)**. Furthermore, this analysis showed that the transcription factors with the largest percentage of target

proteins were SP1, KFL7 (76 targets gene) and SP4 (66 targets gene), all of which belong to the Krüppel superfamily.

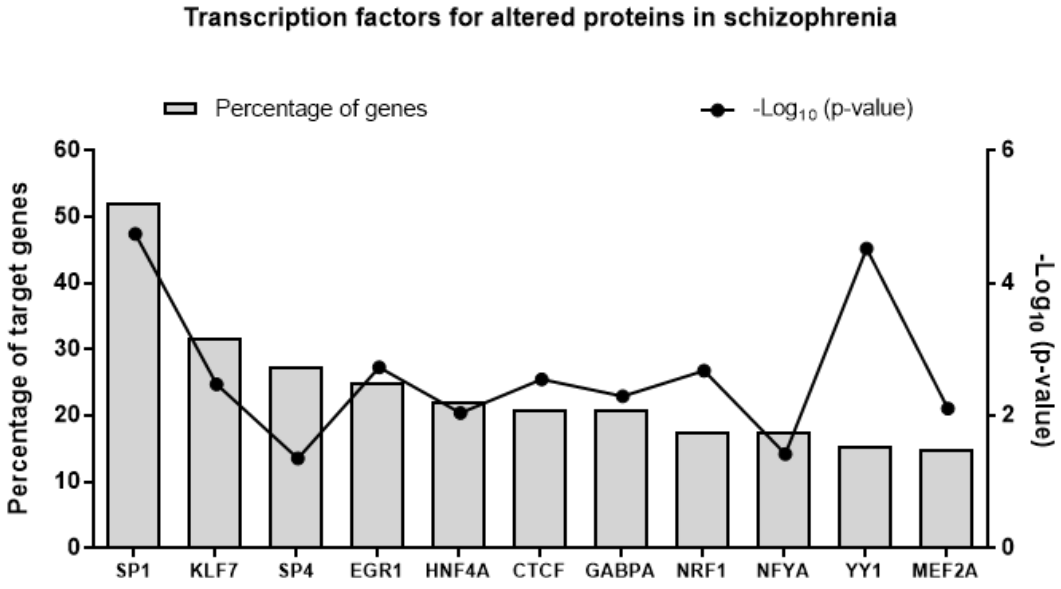

Figure 12.Potential transcription factors involved in the regulation of the altered proteins in the cerebellum of chronic schizophrenia patients. This graphic shows the 11 potential transcription factors in the cerebellum. For this analysis, we used FunRich.

Table 8. Target gene for each transcription factor

Transcription factor	Number of targets	Specific target genes for each transcription factor
SP1	125	_
KFL7	76	GGH
SP4	66	NCKAP1; MAPK1; NDUFB10
EGR1	60	CAMK4; TARDBP
HNF4A	53	ATP2B1; SH3GL3; SIRPA
CTCF	50	CAMKK2; OMG; NANS; PPA2; SNCG
GABPA	50	COPS3; GPS1; IDH3B; RAB12; RARS; RPS3; SF3B3
NRF1	42	_
NFYA	42	METTL7A; NDUFAF2
YY1	37	EIF4G2; HMGCL; SCRN1; SNX5
MEF2A	36	LCP1

5.4.1. Enrichment analysis for target genes of each transcription factor

5.4.1.1. Altered biological processes in the cerebellum in chronic schizophrenia

Our gene ontology analysis revealed 10 out of 11 transcription factors with enriched biological processes (FDR<0.05). No enriched biological functions were found for SP4. The most significant biological processes were regulated by SP1, KFL7, EGR1 and GABPA (**Figure 13**). In this analysis, SP1 and KFL7 target genes were enriched in functions related to cytoskeleton organization development, cellular and organelle organization and inflammation/immune response. KFL7 target genes showed significantly enriched processes related to neutrophil-mediated immunity and granulocyte activation. EGR1 targets were enriched in RNA processing such as mRNA metabolism and RNA catabolic processes. GABPA and YY1 targets were mainly involved in cellular and organelle organization and assembly, while targets of MEF2A, together to those of SP1, were enriched in the regulation of vesicle-mediated transport involved in synaptic functions.

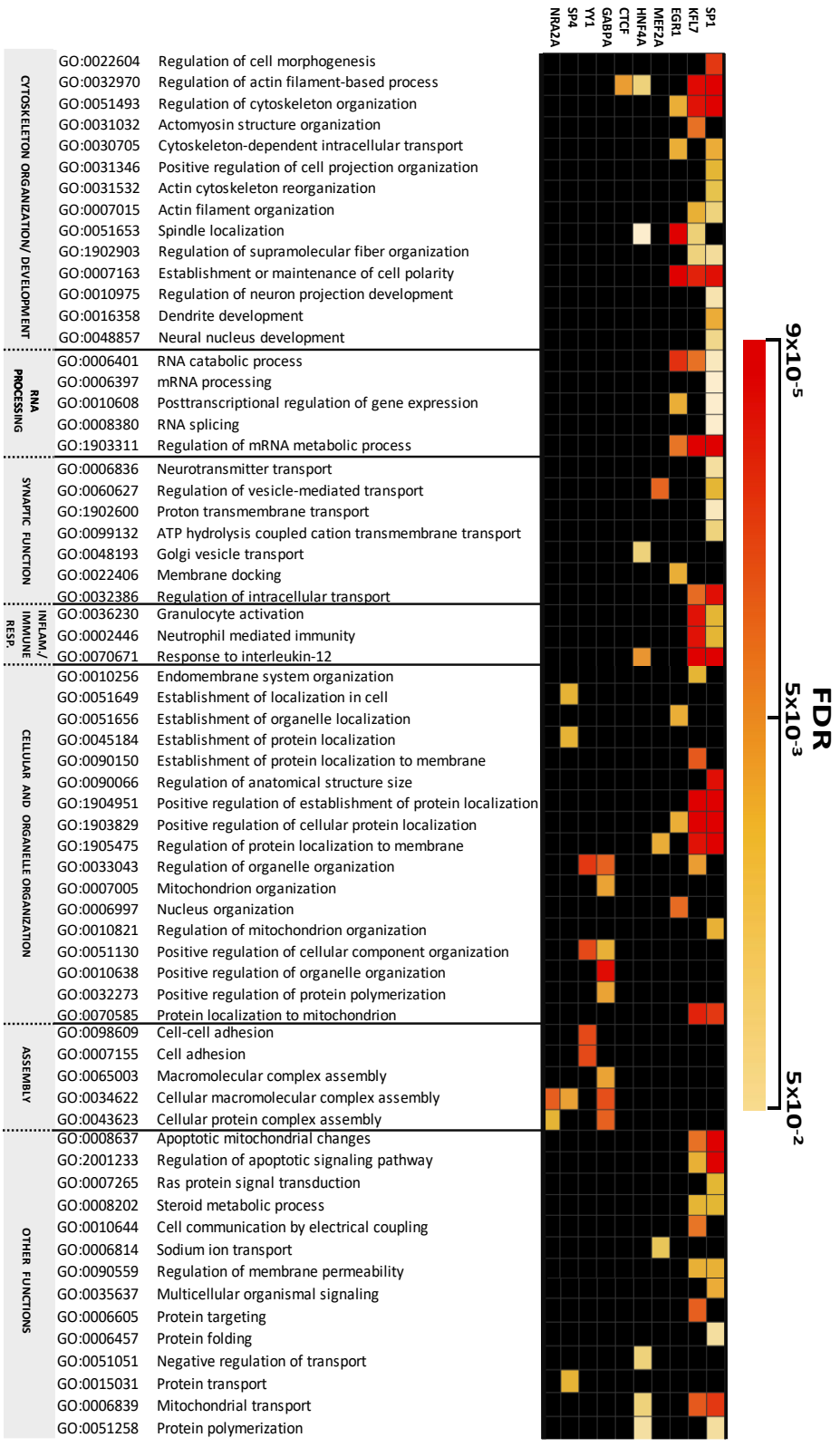

Figure 13. Non-redundant enriched biological process categories for altered targets of transcription factors. The enrichment analysis was performed using Webgestalt and Perseus

5.4.1.2. Altered pathway analysis in the cerebellum in chronic schizophrenia

Our results revealed pathways significantly enriched (FDR<0.05) in altered targets of 5 transcription factors: SP1, KLF7, EGR1, HNF4A and CTCF (**Figure 14**). The altered pathways were regulated mainly by targets of Krüppel TFs such as SP1 and KFL7, with 29 and 13 pathways being enriched for SP1 and KLF7 targets, respectively. SP1 targets showed enrichment in all pathways. The vesicle-mediated transport pathway was under the control of targets of 5 TFs. Other pathways were also enriched for targets of each TF. However, HNF4A-altered targets were only enriched in pathways related to vesicle-mediated transport and membrane trafficking pathways. CTCF targets were enriched in pathways involved in transport and processes associated with the Golgi complex. Moreover, SP1- and KLF7-altered targets showed an enrichment in pathways related to signalling, inflammation/immune response, apoptosis and energy (mitochondrial processes and glucose transport mediated by translocation of SLC2A4 (GLUT4) to the plasma membrane).

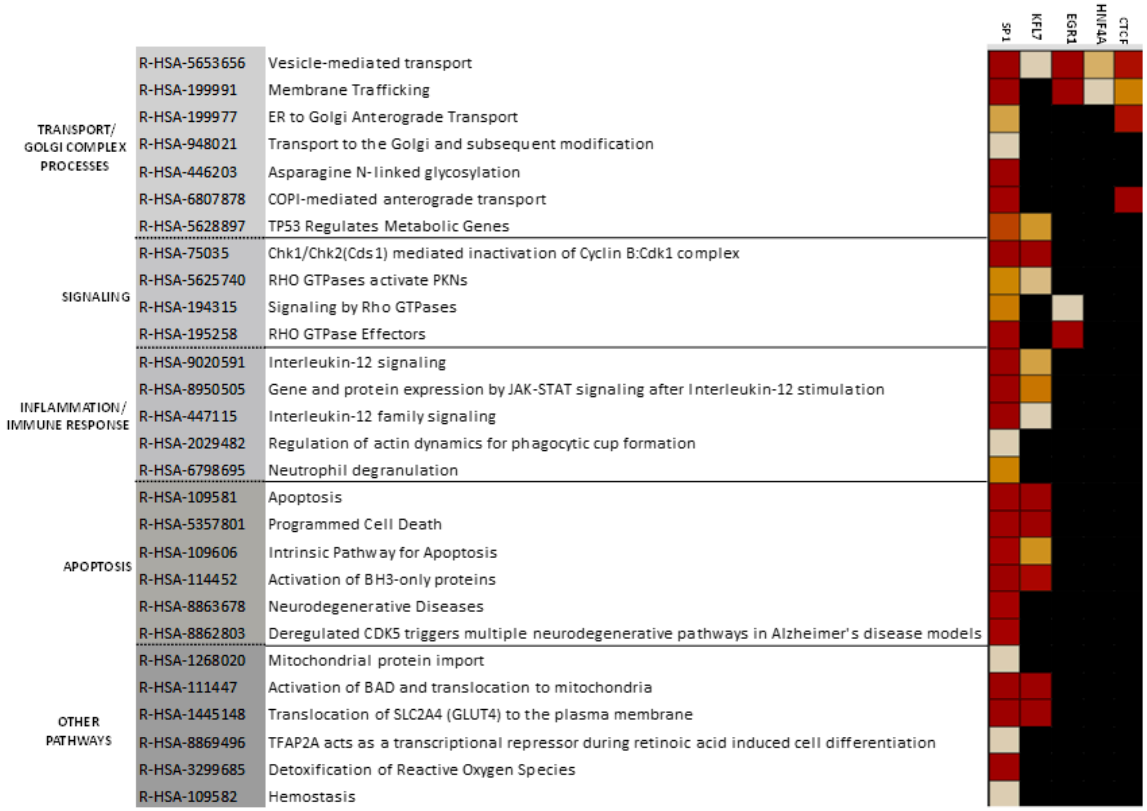

Figure 14. Non-redundant enriched pathways for altered targets of transcription factors. We used the Reactome database for enrichment pathway analysis and the results are displayed as a heat map created using Perseus.

5.5. Analysis of up-regulated and down-regulated proteins in the cerebellum

These results are part of the manuscript Analysis of networks in the cerebellum in chronic schizophrenia: Reduction of METTL7A linked to stress and novel localization in glia cells. Vera et al. submitted to Molecular Psychiatry in 2020

Our results showed 250 proteins significantly deregulated (16.9%) in the cerebellum of which 142 proteins were down-regulated and 108 were up-regulated. No significant correlation with PMD or pH (FDR<0.1%) (Dataset 4 Annex and Dataset 5 Annex) was found for any altered protein. A volcano plot was used to categorize proteins as up- or down-regulated based on the fold change (Log_2 FC) between schizophrenia and control cases and the significance corrected p-value ($–Log_{10}$ (q-*value*) was adjusted to FDR<0.1. This analysis revealed a wide range of changes in schizophrenia among the 250 altered proteins, with most of the altered proteins in schizophrenia registering a fold change of between 0.2 and 0.6 Log_{10}. (**Figure 15**).

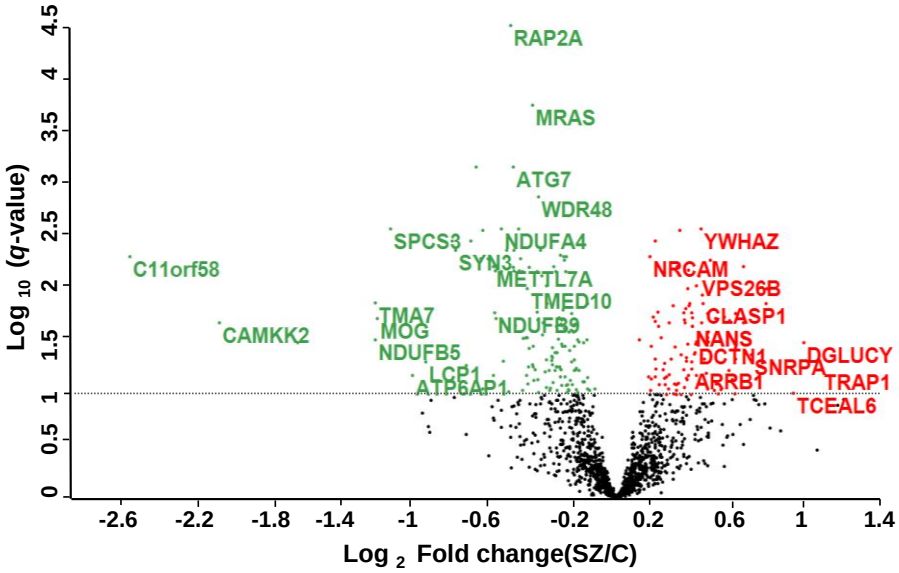

Figure 15. Volcano plot analysis of proteomic data in the cerebellum. The figure shows the volcano plot of the -$\log_{10}$ q-value (adjusted p-value; FDR≤0.1) versus the $\log_2$ fold change in the cerebellum in schizophrenia relative to healthy control. **SZ**, schizophrenia; **C**, control. Up-regulated and down-regulated significant proteins are represented in red and green, respectively. The grey line shows the FDR threshold.

5.5.1. Gene ontology enrichment analysis for diseases, biological processes and pathways

The gene ontology (GO) enrichment analysis showed enrichment in disease categories related to mitochondrial diseases and mental disorders for down-regulated proteins, but in stress, neurodegenerative diseases, and drug interaction with drug for up-regulated proteins (**Figure 16A and Table 9**). The biological processes analysis of the 142 down-regulated proteins revealed significant enrichment of terms referring mainly to energy metabolism (**Figure 16B and Table 9**). For the 108 up-regulated proteins, the enriched categories were related to structural and signalling functions (**Figure 16B and Table 9**). For the down-regulated proteins, two predominant pathways were enriched: the citric acid (TCA) cycle/respiratory electron transport and neutrophil degranulation (**Figure 16C**). For the up-regulated proteins, six pathways were enriched. From highest to lowest score of significance, these were: vesicle-mediated transport, apoptosis, Rho GTPase effectors, signalling by Rho GTPases, axon guidance, and cell cycle (**Figure 16C**).

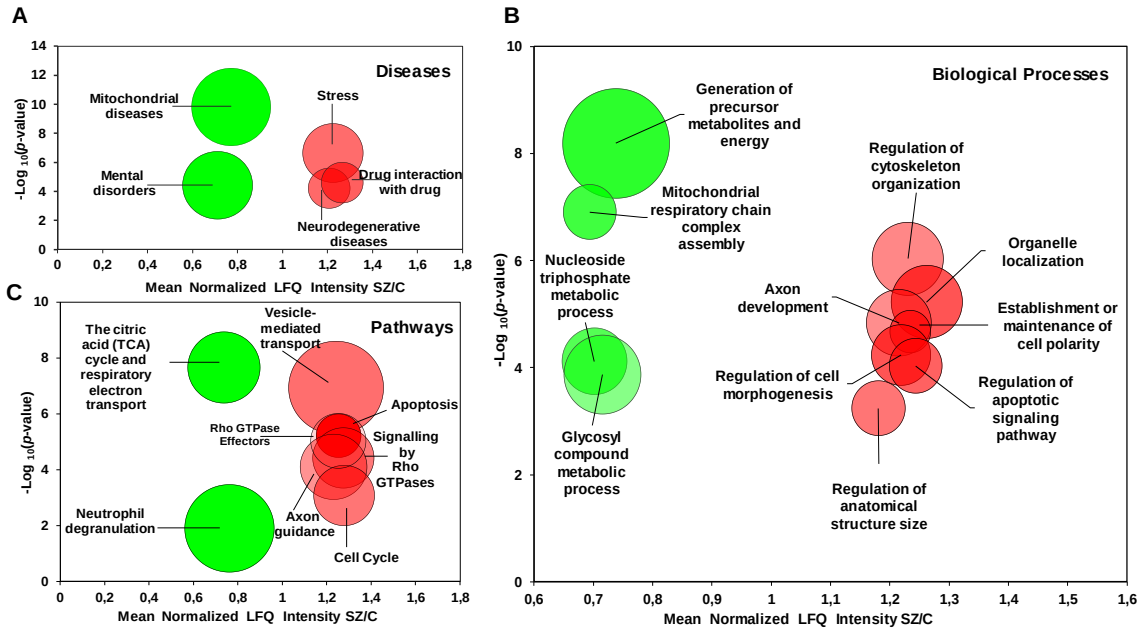

Figure 16. Enrichment analyses of the cerebellar proteome in chronic schizophrenia. The bubble chart shows enriched disease categories for 142 down-regulated proteins and 108 up-regulated proteins in schizophrenia. **A.** The enriched categories for the down-regulated proteins were: mitochondrial diseases (PA447172), mental disorders (PA447208), and for the up-regulated proteins: stress (PA445752), drug interaction with drug (PA165108622), and neurodegenerative diseases (PA446858). **B.** Non-redundant enriched biological processes categories for the down-regulated proteins in schizophrenia were: generation of precursor metabolites and energy (GO: 0006091), mitochondrial respiratory chain complex assembly (GO: 0033108), nucleoside triphosphate metabolic process (GO: 0009141), glycosyl compound metabolic process (GO: 1901657). For the up-regulated proteins, the enriched functions were: regulation of cytoskeleton organization (GO: 0051493), organelle localization (GO: 0051640), axon development (GO: 0061564), establishment or maintenance of cell polarity (GO:0007163), regulation of cell morphogenesis (GO:0022604), regulation of apoptotic signalling pathway (GO: 2001233), regulation of anatomical structure size (GO: 0090066), and microtubule-based movement (GO: 0007018). **C.** The enriched pathways categories in schizophrenia for the down-regulated proteins were: citric acid (TCA) cycle/respiratory electron transport (R-HSA-1428517) and neutrophil degranulation (R-HSA-6798695). The enriched pathways for the up-regulated proteins were: vesicle-mediated transport (R-HSA-5653656), apoptosis (R-HSA-109581), signalling mediated by Rho GTPase effectors (R-HSA-195258), signalling by Rho GTPases (R-HSA-194315), axon guidance (R-HSA-422475), and cell cycle (R-HSA-1640170). The X-axes show the mean of normalized LFQ intensity in schizophrenia relative to the control group for all the proteins that belonged to each category. The Y-axes show the -log$_{10}$ enrichment *p*-value. The bubble size is

directly proportional to the number of proteins represented in each enriched disease, biological process or pathway category. Red colour represents up-regulated proteins. Green colour represents down-regulated proteins. **SZ**, schizophrenia; **C**, control

Table 9. Non-redundant categories of disease, gene ontology and pathways among altered proteins

CLASSIFICATION	CATEGORY	PROTEIN OVERLAP IN CATEGORY	Total number	Observed number	E	*p*-value	FDR
	Down-regulated proteins						
DISEASES	Mitochondrial diseases	DLD;SLC25A4;SLC25A5;HSPD1;ACADVL;NDUFA4;NDUFB5;NDUFB6;NDUFB9;NDUFS1;NDUFA12;SOD2;UQCRB;SLC25A22;CAPN1;SLC25A12;NDUFAF2	353	17	2.32	1.53E-10	4.0E-07
	Mental disorders	ADH5;GABRA6;PCLO;ANK3;MARK1;MOG;ATP1A3;PIP4K2A;SLC17A7;PTPRD;SMS;SYP;SYN3;PICALM;SLC25A12	679	15	4.45	3.83E-05	2.01E-02
BIOLOGICAL PROCESSES	Generation of precursor metabolites and energy	COX17;CS;DLD;GPD1;SLC25A4;IDH3B;ACADVL;NDUFA4;NDUFB5;NDUFB6;NDUFB9;NDUFB10;NDUFS1;NDUFA12;UQCRB;UQCRC2;SLC25A12;NDUFAF2	365	18	3.36	6.47E-09	4.93E-06
	Mitochondrial respiratory chain complex assembly	COX17;NDUFB5;NDUFB6;NDUFB9;NDUFB10;NDUFS1;NDUFA12;UQCRB;NDUFAF2	290	11	2.67	7.61E-05	9.67E-03
	Nucleoside triphosphate metabolic process	DLD;GPD1;NDUFA4;NDUFB5;NDUFB6;NDUFB9;NDUFB10;NDUFS1;NDUFA12;UQCRB;UQCRC2	421	13	3.88	1.36E-04	1.48E-02
	Glycosyl compound metabolic process	DLD;AHCY;GPD1;NDUFA4;NDUFB5;NDUFB6;NDUFB9;NDUFB10;NDUFS1;GMPR2;NDUFA12;UQCRB;UQCRC2	34	4	3.13	2.59E-04	2.45E-02
	ATP hydrolysis-coupled transmembrane transport	ATP1A1;ATP1A3;ATP6V1C1;ATP6AP1	37	4	0.34	3.59E-04	3.04E-02
	Tricarboxylic acid metabolic process	CS;DLD;IDH3B;ACLY	37	4	0.34	3.59E-05	3.04E-03
PATHWAYS	The citric acid (TCA) cycle and respiratory electron transport	CS;DLD;IDH3B;NDUFA4;NDUFB5;NDUFB6;NDUFB9;NDUFB10;NDUFS1;NDUFA12;UQCRB;UQCRC2;NDUFAF2171	171	13	1.79	2.19E-08	3.50E-05
	Neutrophil degranulation	HUWE1;ARPC5;ACTR2;ATG7;SIRPA;ERP44;METTL7A;DBNL;RAB37;ACLY;PRCP;PSAP;RAP1B;CAPN1;GGH;CD47	487	16	5.07	4.0E-05	1.28E-02
	Up-regulated proteins						
DISEASES	Stress	SYNCRIP;COMT;TXN2;PDIA3;HSPA9;MYH9;NACA;MAPK1;RPS3;SOD1;YWHAE;YWHAZ;USP7	592	13	2.20	2.30E-07	6.02E-04
	Drug interaction with drug	HSPA9;LRP1;ARRB1;PPIA;MAPK1;DIABLO;TPT1;YWHAB;YWHAZ	423	9	1.57	2.56E-05	3.36E-02
	Neurodegenerative diseases	DCTN1;HSPA9;LRP1;MAP1B;RTN1;SNCG;SNRPD1;SOD1;UCHL1	473	9	1.76	6.11E-05	5.33E-02
BIOLOGICAL PROCESSES	Regulation of cytoskeleton organization	ARPC2;ARPC1A;DCTN1;CLASP1;ARHGDIA;LRP1;PAFAH1B1;MAPK1;RPS3;SPTAN1;TPM1;CAPZA2	414	12	2.08	9.29E-07	7.08E04
	Organelle localization	DCTN2;DCTN1;CLASP1;MAP1B;MYH9;NUMA1;PAFAH1B1;UCHL1;YWHAZ;CADPS;NAPA;LIN7A	495	12	2.49	5.91E-06	2.25E-03
	Axon development	RAB10;RAB21;ARHGDIA;MAP1B;NRCAM;PAFAH1B1;PITPNA;MAPK1;DPYSL5;SPTAN1;UCHL1	452	11	2.27	1.46E-05	3.71E-05
	Establishment or maintenance of cell polarity	RAB10;CLASP1;MAP1B;MYH9;NUMA1;PAFAH1B1;LIN7A	168	7	0.85	2.10E-05	4.0E-03
	Regulation of cell morphogenesis	ARPC2;RAB21;ARHGDIA;MAP1B;MYH9;NRCAM;PAFAH1B1;C1QBP;TPM1;YWHAH	433	10	2.18	5.78E-05	6.29E-03
	Regulation of apoptotic signalling pathway	PDIA3;HNRNPK;RPS3;SOD1;TPT1;YWHAB;YWHAE;YWHAH;YWHAZ	369	9	1.86	9.24E-05	8.80E-03
	Multicellular organismal signalling	NRCAM;ATP2B1;ATP2B3;PAFAH1B1;SOD1;YWHAE	472	9	2.38	5.74E-03	3.36E-02
	Regulation of anatomical structure size	ARPC2;ARPC1A;RAB21;MAP1B;NRCAM;PAFAH1B1;SOD1;SPTAN1;CAPZA2	472	9	2.36	5.74E-04	3.36E-02
	Cytosolic transport	VPS26B;DCTN1;RAB21;SNX5;MAPK1	138	5	0.69	6.46E.04	3.51E-02
	Microtubule-based movement	DCTN1;RAB21;MAP1B;PAFAH1B1;SOD1;UCHL1	226	6	1.14	9.50E-04	4.83E-02
PATHWAYS	Vesicle-mediated transport	ARPC2;DCTN2;ARPC1A;RAB10;DCTN1;RAB21;SNX5;LRP1;ARRB1;PAFAH1B1;COPS4;SPTAN1;YWHAB;YWHAE;YWHAH;YWHAZ;NAPA	670	17	3.84	1.17E-07	1.87E-04
	Apoptosis	PLEC;DIABLO;PSMB1;SPTAN1;YWHAB;YWHAE;YWHAH;YWHAZ	174	8	1	6.07E-03	1.57E-03
	Rho GTPase Effectors	ARPC2;ARPC1A;CLASP1;MYH9;PAFAH1B1;MAPK1;YWHAB;YWHAE;YWHAH; YWHAZ	311	10	1.78	9.32E-06	1.86E-03
	Signalling by Rho GTPases	ARPC2;ARPC1A;CLASP1;ARHGDIA;MYH9;PAFAH1B1;MAPK1;YWHAB;YWHAE;YWHAH;YWHAZ	446	11	2.56	3.82E-05	5.10E-03
	Axon guidance	ARPC2;ARPC1A;CLASP1;ARRB1;MYH9;NRCAM;PITPNA;MAPK1;PSMB1;DPYSL5;SPTAN1;YWHAB	573	12	3.28	8.00E-05	8.00E-03
	Cell Cycle	DCTN2;DCTN1;CLASP1;NUMA1;PAFAH1B1;MAPK1;PSMB1;YWHAB;YWHAE;YWHAH;YWHAZ	635	11	3.64	8.40E-04	5.60E-02

Disease classification was performed using the PharmMGKB database and genes associated with individual disease terms were inferred using GLAD4U. For the gene ontology analysis we used the Gene Ontology Consortium database: pathways were identified according to the Reactome database and proteins assigned to each pathway are listed. Total number: number of reference proteins in category/pathways; Observed number: proteins in the data set and also in category/pathways; E: expected in the category and adjusted *p*-value is corrected for test multiple, FDR=0.1. These analyses were carried out using Webgestalt.

5.5.2. Network generation from enriched pathways in the cerebellum

Network analysis of enriched pathways for the down-regulated proteins revealed two well-differentiated modules, one related to energy metabolism with proteins of TCA cycle/respiratory electron transport and the other related to neutrophil degranulation pathways (**Figure 17A**). The neutrophil degranulation proteins overlapped with proteins of secretory granular and secretory lumen pathways. For the enriched up-regulated pathways, the network analysis showed an overlap between several altered pathways that were mainly related to axonal development and functioning (**Figure 17B**). The vesicle-mediated transport pathway showed the highest overlap with other pathways, with 52% overlapping with signalling by Rho GTPases proteins, 35% with the cell cycle, 29% with apoptosis, and 23% with axon guidance proteins (**Figure 17B**). For each network module, we searched for the most or two most robust candidates based on the most prominent on LFQ-intensity fold change and coefficient of variation lower than 0.35 (**Figure 17**; **Annex 6**). In the mixed module, two candidate proteins were selected that belonged to at least three different pathways. The hit proteins were NDUFB9 for the energy module, METTL7A for the neutrophil degranulation module, CLASP1 (axonal guidance) and YWHAZ (vesicle-mediated transport) for the mixed module (**Figure 17B**; **Annex 6**). Next, for the proteins in the aforementioned modules, we used publicly available immunocytochemistry data to assess their expression in the different layers of the cerebellum and found that all the proteins were widely distributed throughout the cerebellar layers (**Figure 17**). with the exception of proteins: ARRB1, ATG7 and SNX5 which were only expressed in Purkinje cells, and CD47 which was only expressed in the granular layer no information was available for six altered proteins: NDUFA4, RAB37, METTL7A, RAP1B, MYH9 and DPYSL5.

A. Altered Network in down-regulated proteins

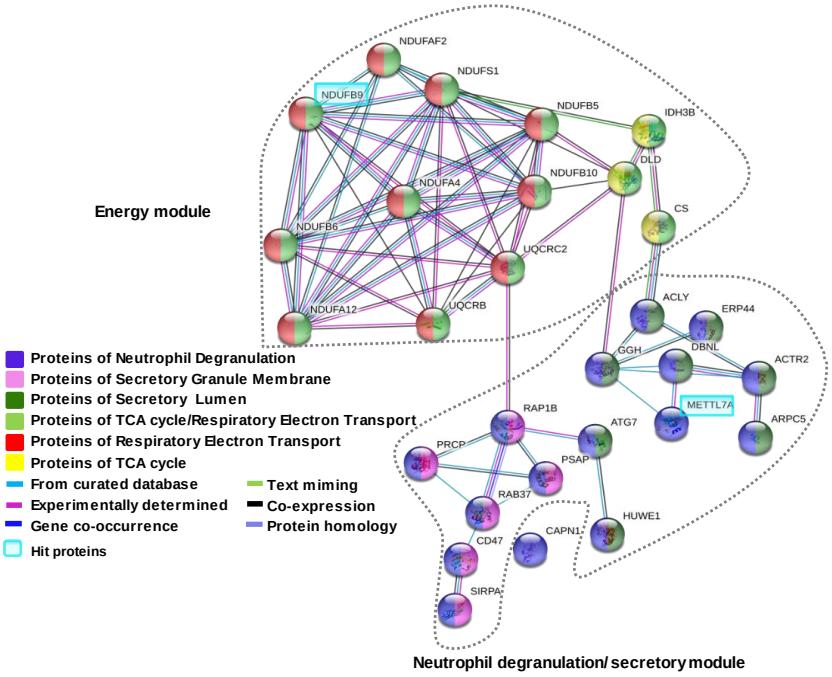

	Gene name	Granular layer	Purkinje cell	Molecular layer
Energy Module	UQCRB			
	IDH3B			
	DLD			
	NDUFB6			
	NDUFA12			
	CS			
	NDUFB10			
	NDUFB5			
	NDUFAF2			
	NDUFB9			
	UQCRC2			
	NDUFS1			
	NDUFA4	x	x	x
Neutrophil degranulation Module	PSAP			
	PRCP			
	SIRPA			
	ACLY			
	GGH			
	HUWE1			
	ERP44			
	ACTR2			
	ARPC5			
	DBNL			
	ATG7			
	CD47			
	RAB37	x	x	x
	METTL7A	x	x	x
	RAP1B	x	x	x
Not protein-protein interacction	CAPN1			

High protein expression
Medium protein expression
Low protein expression
Not detected
X Only detected by mRNA

B. Altered Network in up-regulated proteins

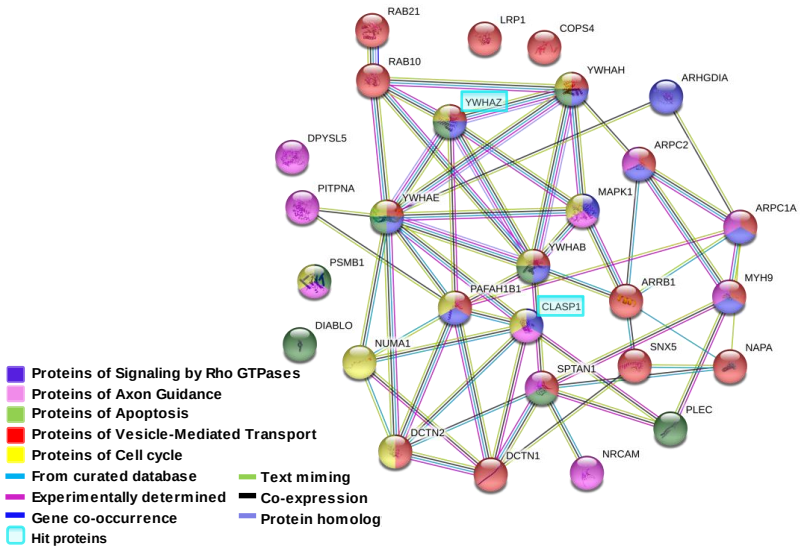

	Gene name	Granular layer	Purkinje cell	Molecular layer
Mixed Module	NUMA1			
	NAPA			
	ARCP2			
	ARPC1A			
	YWHAB			
	DCTN2			
	SPTAN1			
	YWHAE			
	YWHAZ			
	RAB21			
	YWHAH			
	MAPK1			
	CLASP1			
	PAFAHB1			
	ARRB1			
	DCTN1			
	NRCAM			
	RAB10			
	SNX5			
	MYH9	x	x	x
Not protein-protein interacction	COPS4			
	PSMB1			
	DIABLO			
	LRP1			
	DPYSL5	x	x	x

High protein expression
Medium protein expression
Low protein expression
Not detected
X Only detected by mRNA

Figure 17. Network generation formed by altered pathways in cerebellum in schizophrenia. **A** protein-protein interaction network illustrates the interaction and overlap between proteins of the down-regulated pathways. Two modules were generated, one related to energy metabolism and the other to the neutrophil degranulation/secretory module. **B.** protein-protein interaction network formed by the up-regulated pathways. The interaction overview shows how proteins overlap in the different pathways. The right-hand panels show the level of protein expression as determined by immunohistochemistry for each protein in the down- and up-regulated modules and their localization in the different layers in the cerebellum. These pathways were significantly enriched in the panel of 250 altered proteins in chronic schizophrenia cerebellum. Each node represents a protein. Colour denotes membership of the module. The coloured edge (connections between nodes) represents the type of interaction between nodes. Highlighted gene symbols represent the most robust hit protein for each module based on the most prominent fold change with a coefficient of variation lower than 0.35 for control and schizophrenia groups. In the mixed module, the candidate selected belonged to at least three different pathways. Both networks were generated using String V.11, while the Human Protein Atlas database was used for the levels of protein expression determined by immunohistochemistry.

5.6. Correlation analysis between proteins altered in the cerebellum and executive function

We performed an analysis of the Frontal battery (FAB) to investigate whether the proteins involved in the altered pathways were associated with executive function. However, our results showed a significant correlation ($r=0.833$, $FDR<0.1$) only between FAB and Dynactin subunit 1 (DCTN1), which is involved in the vesicle-mediated transport and axon guidance module (**Annex 7**). In addition, we performed a correlation analysis with negative symptoms but did not observe any significant correlation.

5.7. Quantitative proteomic analyses of *postmortem* prefrontal cortex from schizophrenia and healthy controls

These results are part of the manuscript Analysis of networks in the dorsolateral prefrontal cortex in chronic schizophrenia: Relevance of altered immune response. Vera-Montecinos et al. in preparation, to be submitted in 2021.

To identify altered proteins related to schizophrenia in the prefrontal cortex (Brodmann area 9), we used individual protein extracts from a larger cohort of schizophrenia subjects (n=20) and healthy controls (n=20) . In this proteomic analysis we used a Q-Exactive Orbitrap tandem mass spectrometer and label-free quantification (the proteomic analysis was performed in collaboration with Dr Villen and Dr Rodriguez Mias from the University of Washington, Seattle). The experimental strategy used in this proteomic study is shown in **Figure 18**. We performed this proteomic analysis using protein extracts from the left hemispheres of 20 male patients with schizophrenia and 20 control individuals (10 right hemispheres and 10 left hemispheres) matched for gender, age and postmortem delay. No differences were observed between the schizophrenia and control groups for any demographic- or tissue-related variables (**Table 10**).

Table 10. Demographic, clinical- and tissue-related features of cases

	Schizophrenia (n=20)	Control (n=20)	Statistic	*p*- value
Gender				
Male	100% (*n* =20)	100% (*n* =20)	N/A	N/A
Age (years)	74 ± 10	74 ± 9	0.06;38[a]	0.94
PMD (hours)	5.15 ± 2.59	6.07 ± 2.81	1.07; 38 [a]	0.29
pH PFC	6.76 ± 0.75	6.67 ± 0.48	0.42; 38 [a]	0.67
SZ diagnosis				
Chronic residual	70% (n= 14)			
chronic paranoid	15% (n=3)			
chronic disorganized	5% (n=1)			
chronic catatonic	5% (n= 1)			
Simple-type	5% (n= 1)			
Age of onset of SZ (years)	23.9 ± 10	N/A	N/A	N/A
Duration of illeness	50 ± 11	N/A	N/A	N/A
Toxicology				
Daily AP dose (mg/day) [b]	683.9 ± 925.9	N/A	N/A	N/A
First generation AP	20% (n=4)			
Second generation AP	40% (n=8)			
First and Second generation AP	25% (n=5)			
AP free	15% (n=3)			

Mean ± standard deviation; PMD, postmortem delay; SZ, schizophrenia; AP, antipsychotics; N/A, not applicable. [a] T-statistic and degree of freedom for parametric variables. [b]Last daily Chlorpromazine equivalent dose was calculated based on the electronic records of drug prescriptions of the patients as described (Gardner et al., 2010).

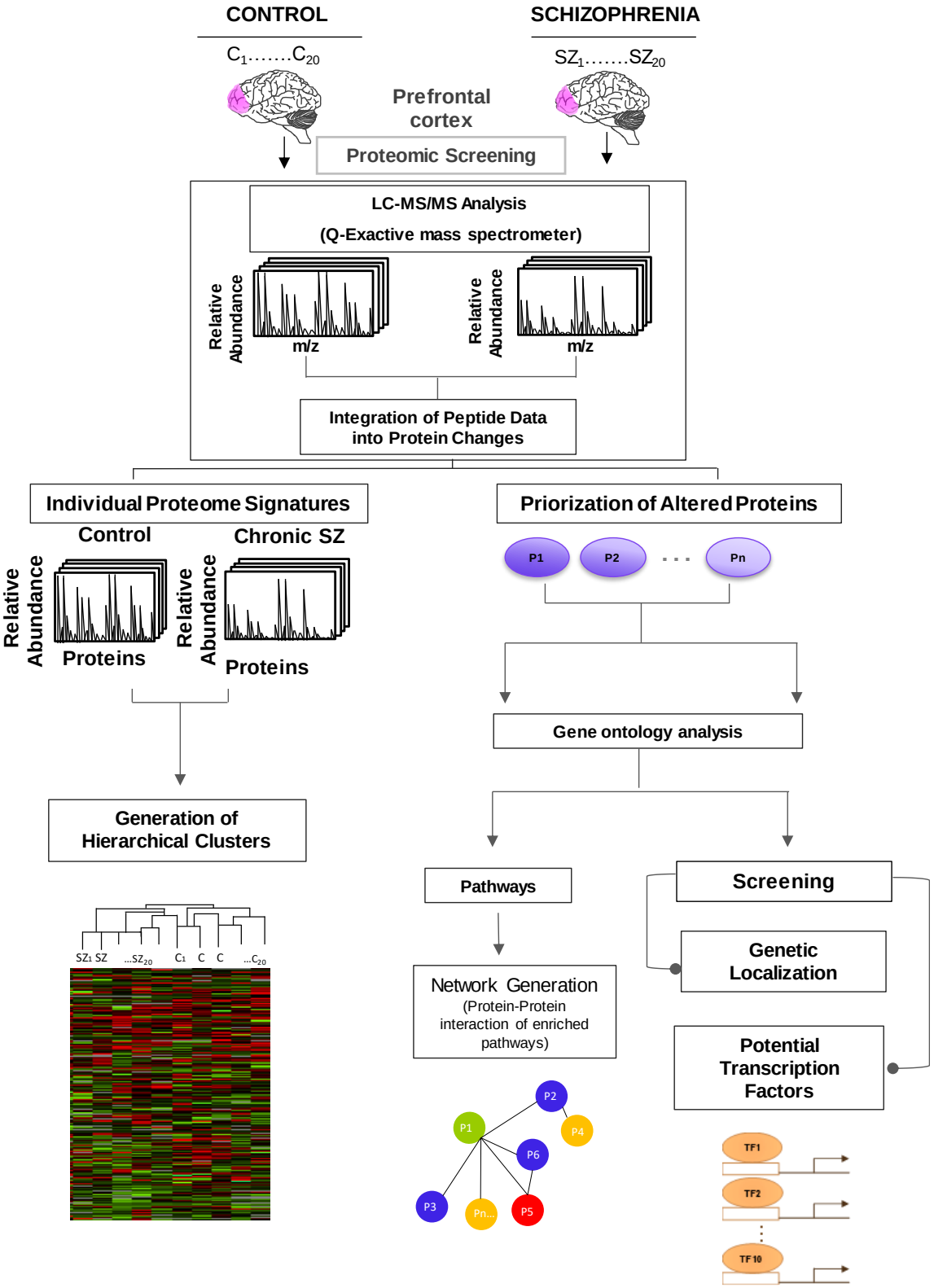
CONTROL
SCHIZOPHRENIA
C1.....C20
SZ1.....SZ20
Prefrontal cortex
Proteomic Screening
LC-MS/MS Analysis
(Q-Exactive mass spectrometer)
Relative Abundance
m/z
Relative Abundance
m/z
Integration of Peptide Data into Protein Changes
Individual Proteome Signatures
Control
Chronic SZ
Relative Abundance
Proteins
Relative Abundance
Proteins
Generation of Hierarchical Clusters
SZ1 SZ
...SZ20
C1
C
C
...C20
Priorization of Altered Proteins
P1
P2
Pn
Gene ontology analysis
Pathways
Network Generation
(Protein-Protein interaction of enriched pathways)
P1
P2
P3
P4
P5
P6
Pn...
Screening
Genetic Localization
Potential Transcription Factors
TF1
TF2
TF 10

Figure 18. Experimental design of the proteomic analysis to identify altered pathways in schizophrenia. Protein lysates from the postmortem prefrontal cortex of control subjects (C) (n=20) and chronic schizophrenia (SZ) patients (n=20) were processed as depicted. The peptides were separated and analysed by Liquid Chromatography (LC) coupled to a Q-Exactive Orbitrap tandem mass spectrometer. The relative fold change of peptides was integrated into protein changes. The individual protein signatures for each case and control were used to generate hierarchical clusters. The prioritization of altered proteins (P1-Pn represents generic proteins) in schizophrenia was obtained by comparing protein fold changes between control and schizophrenia groups (significant proteins adjusted to an FDR=0.1). We performed three analyses for these altered proteins in schizophrenia: i) Unsupervised hierarchical clustering analysis generated from quantified proteins in 20 schizophrenia and 20 healthy control samples of postmortem prefrontal cortex; ii) Genetic localization; iii) Transcription factor enrichment; iv) Enrichment analysis of biological processes and pathways; and v) Generation of networks from significantly enriched pathways by protein-protein interaction. These analyses were performed using Perseus, Webgestalt, FunRich and String, respectively

5.7.1 Quantitative proteomic analyses in the prefrontal cortex in chronic schizophrenia

Our results of the proteomic analysis in the prefrontal cortex revealed 4407 identified proteins and 1989 quantified proteins (**Annex 8**). The proteomic analysis revealed 99.9% of the proteins were identified with 2 or more peptides and 91.3% with five or more peptides. In addition, our analysis showed 43 significantly altered proteins in the prefrontal cortex (FDR=0.1) (**Annex 9**) of which 9 were up-regulated and 34 were down-regulated. 40 of the 43 altered proteins had been previously reported in gene expression analyses in schizophrenia from the Schizophrenia Database, two proteins had been related to schizophrenia in individual studies (Mouaffak *et al.*, 2011; Sun *et al.*, 2018) and one protein RBMXL2 has not been reported in SZ. For the individual proteome signature analysis, we first examined the similarity of the individual proteome in the prefrontal cortex through a correlation matrix (**Figure 19**). The results showed correlations above a Pearson correlation coefficient of 0.07 with an average coefficient of 0.994 between the schizophrenia and control samples. We then analysed any possible laterality effect on these results. However, we did not find any significant differences between the right and left hemispheres in the controls in our study and no segregation of clustering analysis by hemisphere (data not shown and **Figure 20**).

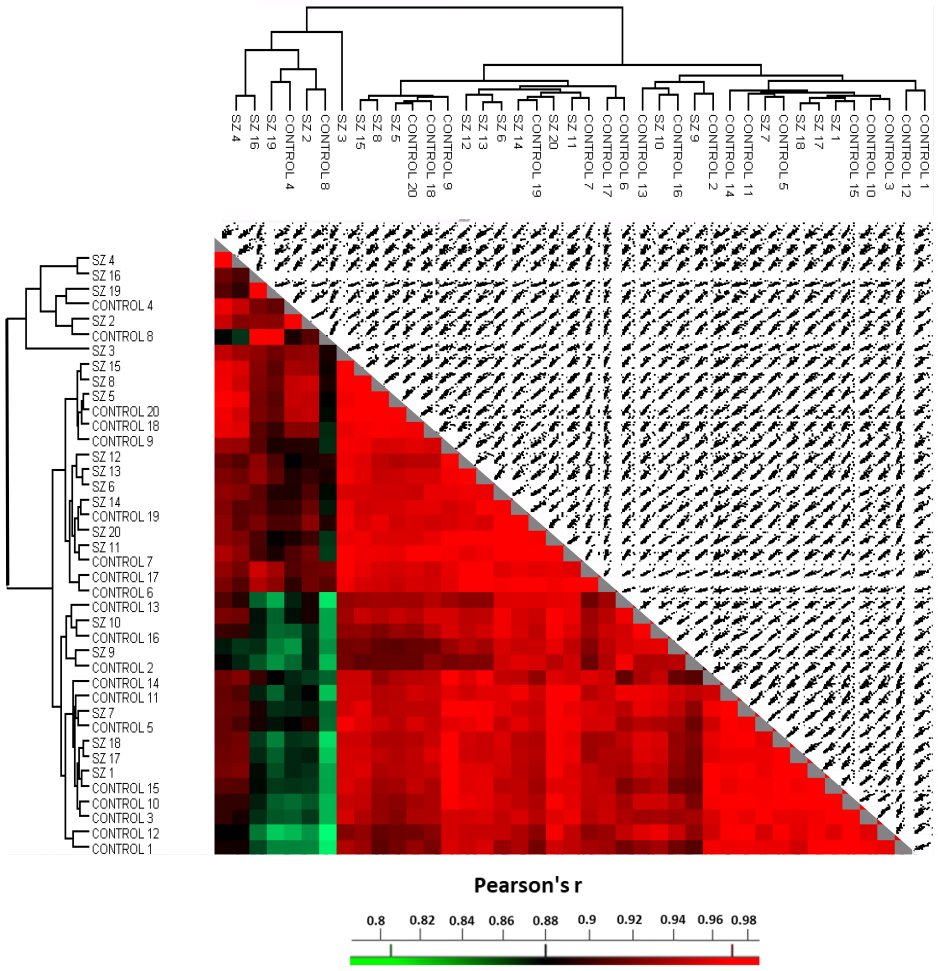

Figure 19. **Quality control analysis for quantified proteins in the prefrontal cortex**. **A.** The correlation matrix shows the correlation coefficiency between the 1989 quantified proteins in each compared pair of samples.

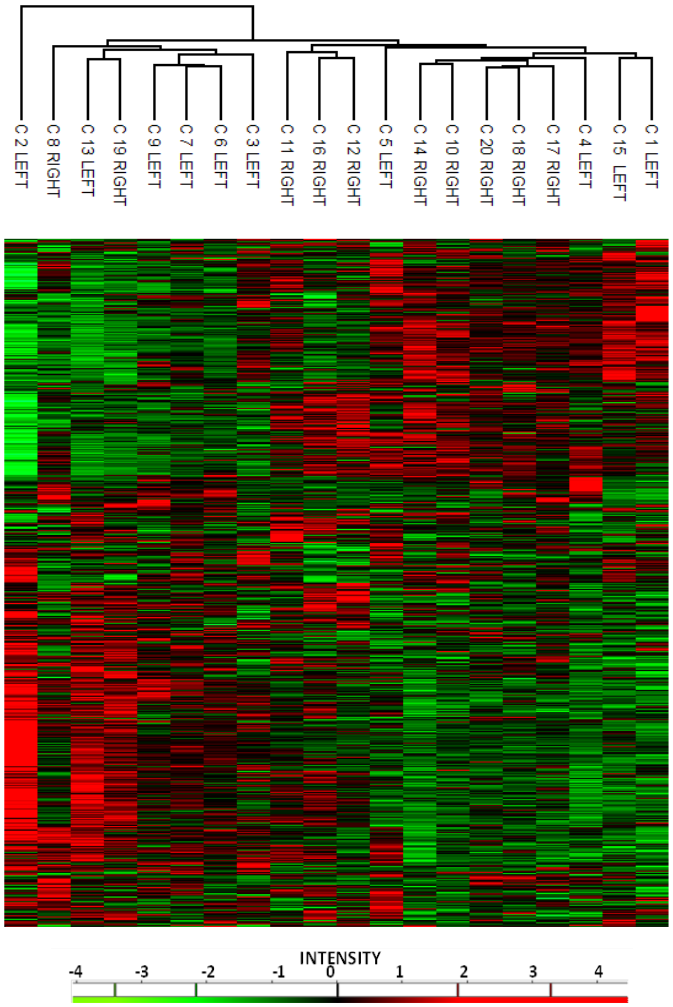

Figure 20. Laterality analysis between the right and left hemispheres from healthy controls. Hierarchical clustering for quantified proteins of 10 right hemispheres and 10 left hemispheres from postmortem prefrontal cortex of healthy control samples. Green colour clusters represent down-regulated proteins. Red colour clusters represent up-regulated proteins.

The unsupervised hierarchical clustering analysis revealed that the proteomic profile detected for each subject did not allow segregation between controls and schizophrenia samples (**Figure 21**). We further investigated whether laterality (**Figure 22**) or demographic and tissue-related features could influence this lack of segregation, but none of the variables was found to do so

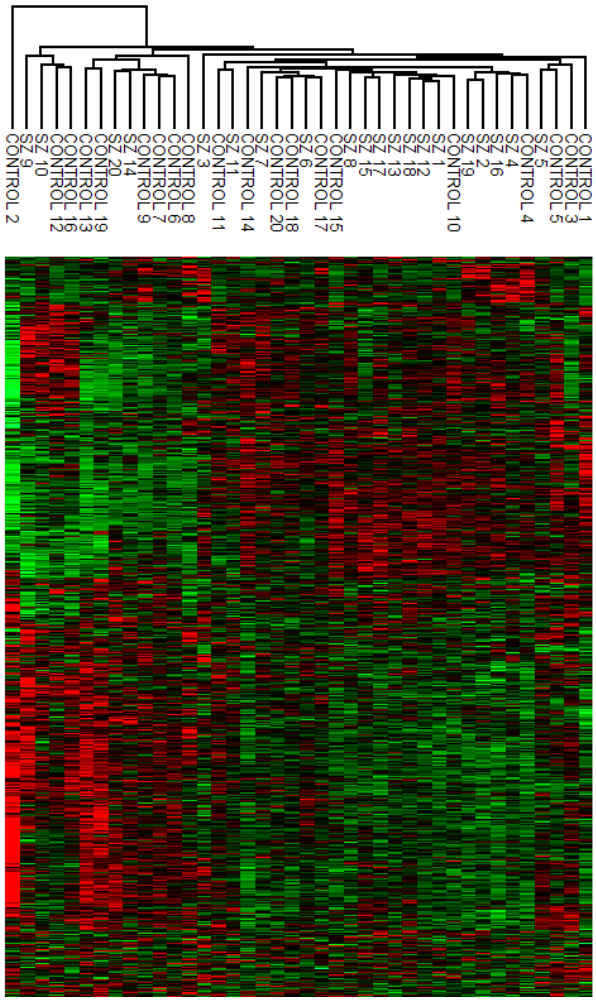

Figure 21. Unsupervised hierarchical clustering analysis from prefrontal cortex proteins. This analysis was performed with matrix processing according to the Euclidean distance and z-score aggregation method. We used 1989 quantified proteins. This analysis was not able to discriminate schizophrenia subjects from control individuals. Green colour clusters represent down-regulated proteins. Red colour clusters represent up-regulated proteins

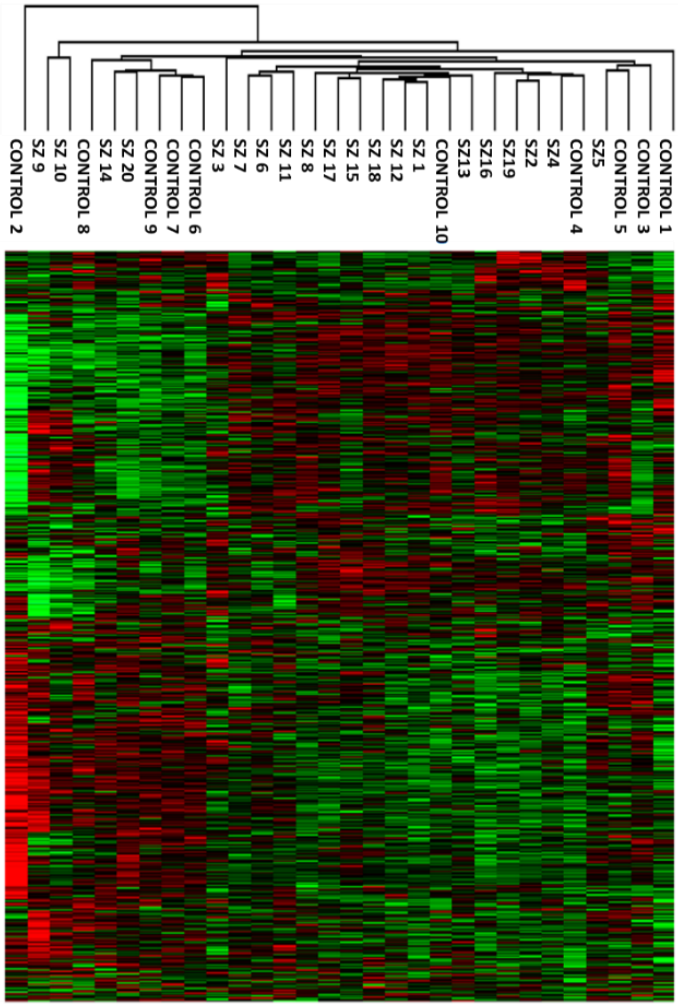

Figure 22. Laterality analysis between the left hemispheres of schizophrenia subjects and the left hemispheres of healthy controls. Unsupervised hierarchical clustering analysis for quantified proteins of 10 left hemispheres from the postmortem prefrontal cortex of healthy control samples and 20 left hemispheres from the postmortem prefrontal cortex of schizophrenia subjects. Green colour clusters represent down-regulated proteins. Red colour clusters represent up-regulated proteins

5.7.2. Genetic localization of altered proteins in the proteomic profile in the prefrontal cortex

We analysed the chromosomal distribution of the 43 altered proteins in the prefrontal cortex. Our results showed a total of 37 loci with altered proteins, 8 of them previously reported to be risk loci for schizophrenia (data not shown). Our analysis showed 35 loci with one altered protein and two loci with two altered proteins.

5.7.3. Transcription factors analysis in the prefrontal cortex

To investigate the transcriptional program that could be controlling the 43 altered proteins in prefrontal cortex in schizophrenia, we performed an enrichment analysis of transcription factors. However, we did not find enriched transcription factors for the proteins altered in the prefrontal cortex (data not shown).

5.7.4. Gene ontology enrichment analysis for biological processes and pathways

The gene ontology analysis with the 43 proteins that were altered in the prefrontal cortex showed an enrichment of several biological processes (FDR=0.1) (**Figure 23A** and **Table 11**) involved in vesicle-mediated transport, processing and antigen presentation via MHC class II, intracellular transport and selenium metabolism. The enriched pathways (**Figure 23B**) were directly related to the enriched biological processes observed. These pathways were related to MHC class II antigen presentation, vesicle-mediated transport, Golgi transport and immune system (**Figure 23B**). All these enriched pathways were found for the down-regulated proteins.

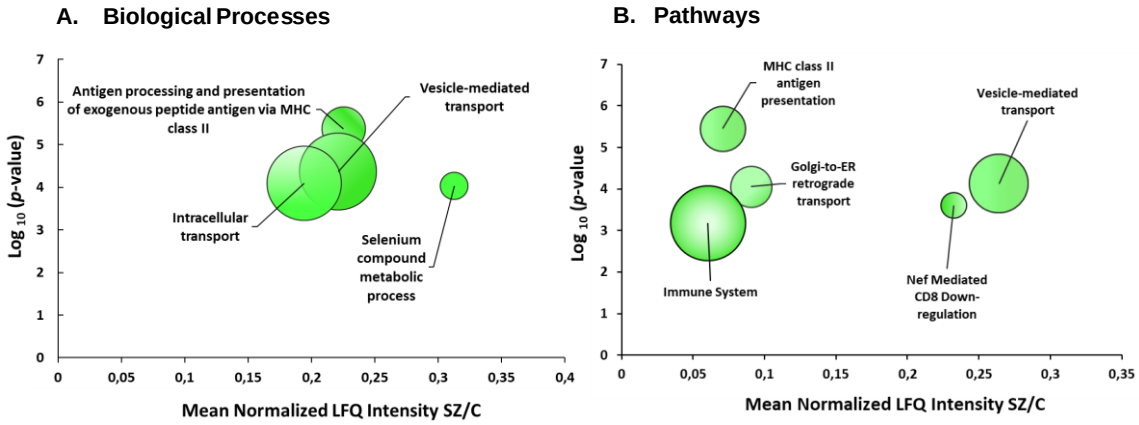

Figure 23. Enrichment analyses from the prefrontal cortex proteome in chronic schizophrenia. **A.** The bubble chart shows enriched categories from 43 altered proteins in schizophrenia. **A.** Non-redundant enriched biological processes categories were: antigen processing and presentation of exogenous peptide antigen via MHC class II (GO:0019886), vesicle-mediated transport (GO:0016192), intracellular transport (GO:0046907) and selenium compound metabolic process (GO:0001887). **B.** The enriched pathway categories in schizophrenia were: MHC class II antigen presentation (R-HSA-2132295), vesicle-mediated transport (R-HSA-5653656), Golgi-to-ER retrograde transport (R-HSA-8856688), Nef-mediated CD8 down-regulation (R-HSA-182218) and immune system (R-HSA-168256). The X-axes show the mean of normalized LFQ intensity in schizophrenia relative to the control group for all the proteins that belonged to each category. The Y-axes show the -$\log_{10}$ enrichment p-value. The bubble size is directly proportional to the number of proteins represented in each enriched category, biological process or pathway. The green colour represents down-regulated proteins. **SZ**, schizophrenia; **C**, control.

Table 11. Non-redundant gene ontology analysis of the 43 proteins altered in the prefrontal cortex

Classification	Category	Proteins overlap in the category	Total Number	Observed Number	E	*p*-value	FDR
BIOLOGICAL PROCESSES	Antigen processing and presentation of exogenous peptide antigen via MHC class II	ACTR1A;AP2M1;AP2S1;DCTN5;RAB7A	97	5	0.24	4.32E-06	0.02
	Vesicle-mediated transport	RAB6B;SYNJ1;ACTR1A;PLCG1;AP2M1;ACLY;AP2S1;ATG7;ARF3;DCTN5; GPI;RAB5C;CYFIP2;LIN7C;RAB7A	1942	15	4.89	4.28E-05	0.06
	Intracellular transport	RAB6B;RAN;SYNJ1;ACTR1A;AP2M1;AP2S1;ARF3;PPP1CC;NEFL;DCTN5; RAB5C;TIMM10;SRSF9;RAB7A	1803	14	4.54	8.06E-05	0.08
	Selenium compound metabolic process	SCLY;TXNRD1	6	2	0.02	9.24E-05	0.08
PATHWAYS	MHC class II antigen presentation	ACTR1A;AP2M1;AP2S1;TUBB3;DCTN5;RAB7A	121	6	0.42	3.55E-06	0.01
	Vesicle-mediated transport	ACTR1A;SYNJ1;RAB6B;AP2M1;AP2S1;TUBB3;ARF3;DCTN5;RAB5C;RAB7A;	667	10	2.33	7,39E-05	0.03
	Golgi-to-ER retrograde transport	ACTR1A;RAB6B;TUBB3;ARF3;DCTN5	131	5	0.46	8.72E-05	0.04
	Nef Mediated CD8 Down-regulation	AP2M1;AP2S1	7	2	0.02	2.47E-04	0.08
	Immune System	ACTR1A;PLCG1;PRKACA;AP2M1;ACLY;ATP6V1E1;AP2S1;TUBB3;ATG7; TRIM2;GPI;CYFIP2;LMNB1;DCTN5;RAB5C;RAB7A	1997	16	6.98	6.63E-04	0.09

For the gene ontology analysis we used the Gene Ontology Consorcium database: pathways were identified according to the Reactome database and proteins assigned to each pathway are listed. Total number: number of reference proteins in the category/pathway. Observed number: proteins in the data set and also in the category/pathway. E: expected in the category and adjusted p-value is corrected for test multiple, FDR=0.1. These analyses were carried out using Webgestalt.

5.7.4.1. Network generation from enriched pathways in the prefrontal cortex

Network analysis of significantly enriched pathways for proteins altered in the prefrontal cortex showed an overlap among the several altered pathways (**Figure 24**). A mixed module was observed in which the main overlap was generated by the immune system pathway. This pathway showed about 43% overlap with membrane trafficking proteins, 37% with MHC class II antigen presentation, 12% with Nef-mediated CD8 downregulation and 31% with Golgi ER retrograde transport.

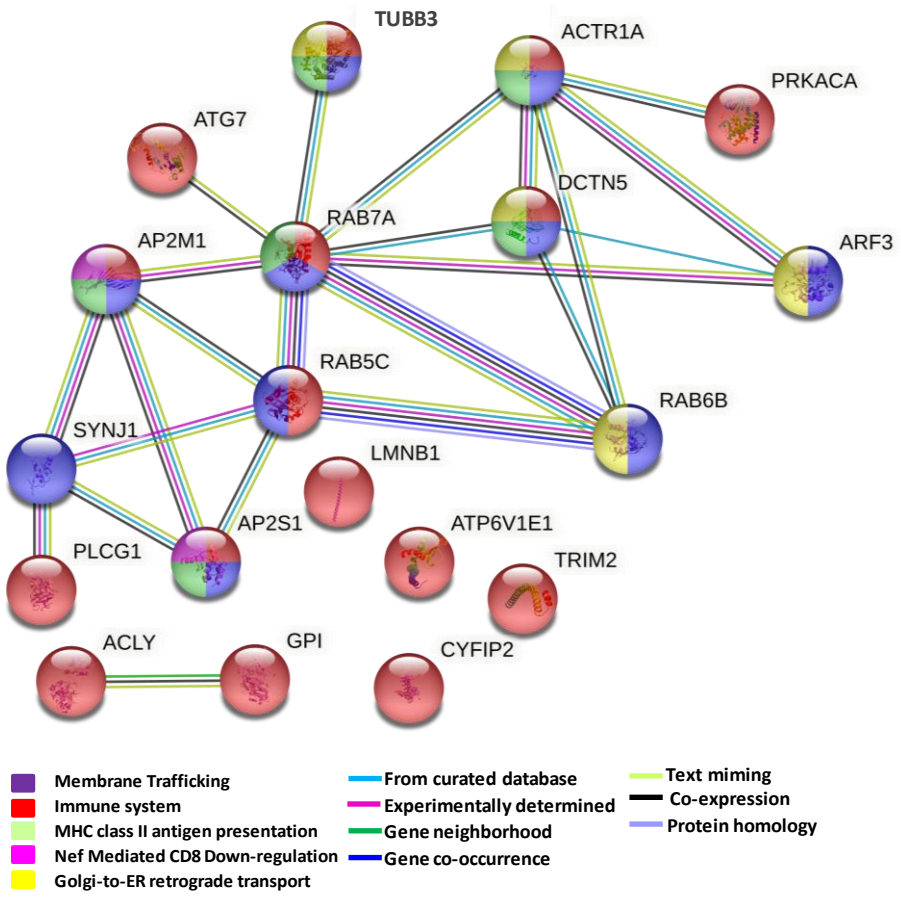

Figure 24. Network formed by altered pathways in the prefrontal cortex in schizophrenia. This protein-protein interaction network illustrates a mixed module with interactions and overlaps among proteins formed by down-regulated pathways in the prefrontal cortex. The interaction overview shows how proteins overlap in the different pathways. These pathways were significantly enriched in the panel of 43 altered proteins in the prefrontal cortex in schizophrenia. Each node represents a protein. The colour denotes membership of a module. The coloured edge (connections between nodes) represents the type of interaction between nodes. The network was generated using String V.11.

5.7.5. Correlation analysis between proteins altered in the prefrontal cortex and executive function

We performed an analysis of the Frontal battery (FAB) and negative symptoms to investigate whether the proteins involved in altered pathways were associated with executive function. However, we did not find any significant correlation between FAB and proteins altered in the prefrontal cortex (data not shown).

5.8. Validation of altered pathways in double-hit in murine models for schizophrenia

These results are part of the manuscript Analysis of networks in the cerebellum in chronic schizophrenia: reduction of METTL7A linked to stress and novel localization in glia cells. Vera et al. submitted to Molecular Psychiatry in 2020.

We investigated the most robust candidates from the network modules in the cerebellum of two double-hit schizophrenia murine models, maternal deprivation combined with an additional stressor: social isolation (MD/Iso) or chronic restraint stress (MD/RS). These candidates were: NDUFB9, METTL7A, CLASP1 and YWHAZ. Validation in the double-hit murine models analysis was performed in collaboration with the group of Dr Leza of the Autonomous University of Madrid (Madrid). We also included a comparison of the differences in protein levels detected by proteomic analysis of these candidates between the control and schizophrenia groups (**Figure25**). We observed that NDUFB9 levels were reduced in the human schizophrenia cohort and in the MD/Iso model, but not in the MD/RS model (**Figure 25A**). METTL7A showed a decrease in protein expression levels in the chronic schizophrenia cohort and in both murine models (**Figure 25B**). CLASP1 was down-regulated in the MD/Iso model but up-regulated in the schizophrenia cohort (**Figure 25C**). No significant changes were found in the DM/RS model for CLASP1. YWHAZ, which was up-regulated in the SZ cohort, did not show any change in either of the two SZ murine models (**Figure 25D**). Thus, METTL7A was the only one that was consistently deregulated in the human schizophrenia cohort and the two murine models.

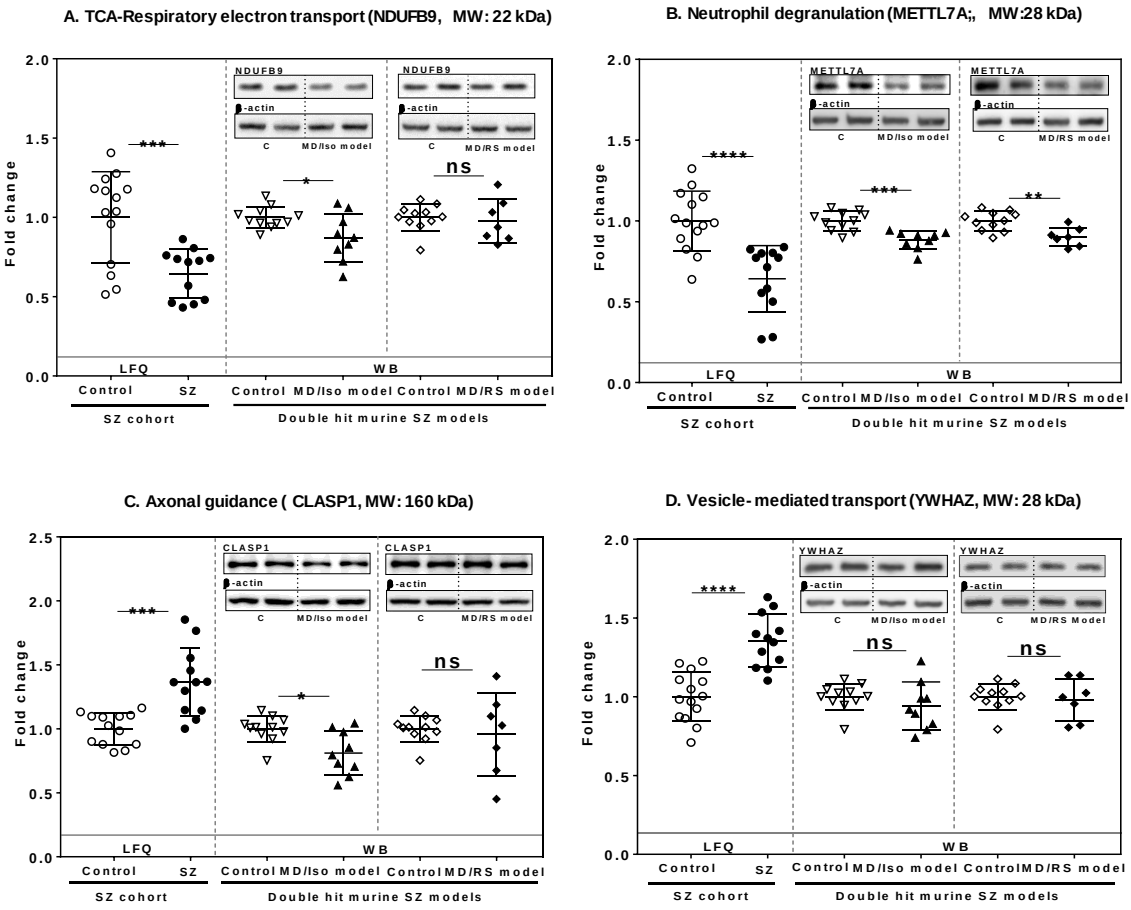

Figure 25. Analysis of hit proteins from altered pathways in the human schizophrenia cohort and the two double-hit schizophrenia murine models. Protein levels of candidate hit proteins METTL7A (**A**), NDUFB9 (**B**), CLASP1 (**C**) and YWHAZ (**D**) from the indicated enriched pathway in schizophrenia were analysed in the cerebellum of the human schizophrenia cohort compared to the two double-hit schizophrenia murine models, maternal deprivation combined with social isolation (MD/Iso) or chronic restraint stress (MD/RS). The protein fold change in the human schizophrenia cohort (control: n=14; SZ=12) was determined by proteomic analysis as explained in the methods and the relative fold change in the murine models was determined by immunoblot analysis (control: n=11; MD/Iso model: n=9; MD/RS model: n=8). TCA-RET: citric acid cycle-respiratory electron transport. VTM: vesicle-mediated transport. Statistical analysis was performed using the t-test for samples with normal distribution and non-parametric distribution was performed using the Mann-Whitney U test in the MD/RS model for NDUFB9, and the MD/Iso and MD/RS models for CLASP1 and YWHAZ. The protein levels were normalized to the mean of the controls. Individual values represent the protein levels for each subject or animal. Means and standard deviation are shown in the graphs. ns: not significant, *p<0.05, **p<0.01, ***p<0.001, ****p<0.0001

5.9. Characterization of METTL7A in human cerebellar tissue

These results are part of the manuscript Analysis of networks in the cerebellum in chronic schizophrenia: reduction of METTL7A linked to stress and novel localization in glia cells. Vera et al. submitted to Molecular Psychiatry in 2020.

We studied the expression of methyltransferase-like 7A (METTL7A) in the cerebellum due to it was the only one consistently down-regulated protein in the human SZ cohort and the two murine models for schizophrenia. Besides, very little information about METTL7A was available in the literature in the context of the brain and schizophrenia. For the immunohistochemical characterization of METTL7A, we used adult human cerebellar tissue from a healthy 47-year-old male subject (PMD=4.92 hours; pH=6). Using haematoxylin-eosin staining, we first confirmed the good preservation of human cerebellar tissue (**Figure 26A**). We optimized the blocking conditions to avoid background signal from secondary antibodies. No signal was detected in these negative controls (**Figure 26B**).

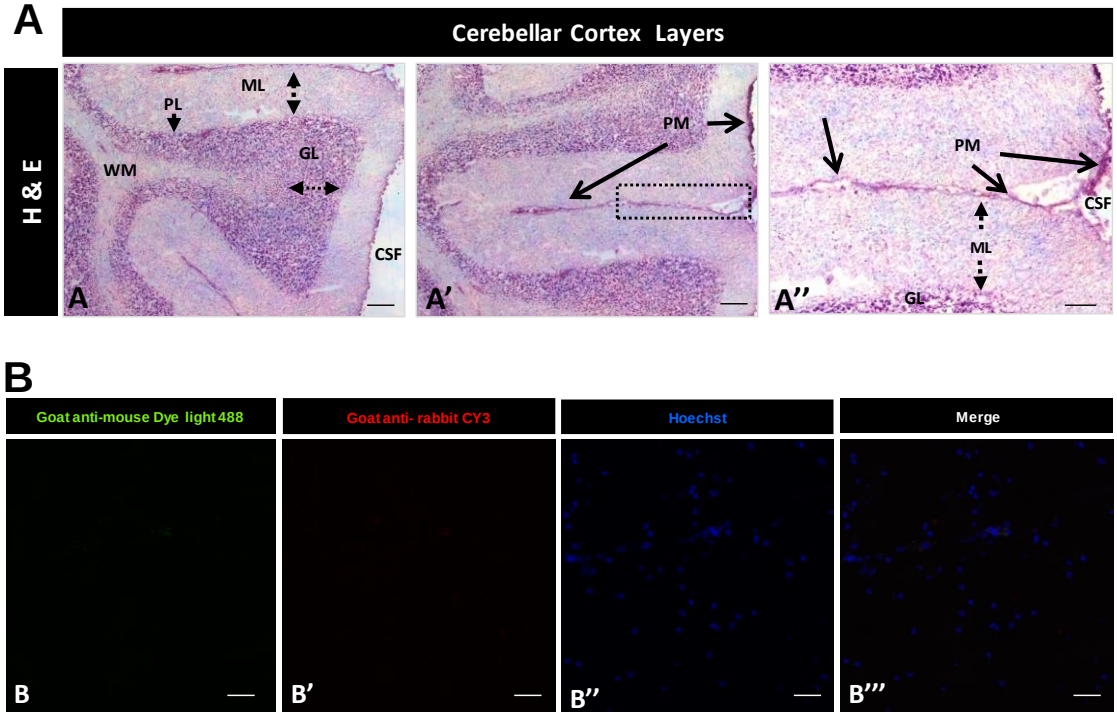

Figure 26. Haematoxylin-Eosine staining and negative control for secondary antibodies in human cerebellum. Panel A. **A-A'**. Image shows Haematoxylin-Eosine stain of human cerebellum showing the good preservation of the tissue and its layers. Image **A''** shows the 20x magnification of the square labelled in **A'**. **GL**: Granular layer; **PL**: Purkinje layer; **ML**: Molecular layer; **WM**: White matter; **PM**: Pia mater; **CSF**: Cerebrospinal fluid. A-A': Tissue thickness 7 µm. Scale bar 5 µm and 10x magnification. **A''**. Tissue thickness 7 µm. Scale bar 5 µm and 20x magnification. **Panel B**. Negative control for secondary antibody goat anti-mouse Dye light 488 and goat anti-rabbit Cy3 (**B'**) as negative control for rabbit anti-METTL7A, mouse anti-GFAP and mouse anti-Tuj1. Negative control of Figures 13, 15, 16, 17, 18. All negative controls were used without incubating tissues with the corresponding primary antibody. Nuclei stained with Hoechst (**B''**). The images were merged (**B'''**). **B-B'''**. Tissue thickness 7 µm. Scale bar 4 µm. Images were acquired at 20x magnification.

5.9.1. METTL7A expression pattern in human cerebellar tissue

To investigate the localization of METTL7A in human cerebellar tissue, we used two different antibodies that provide similar patterns of expression: a polyclonal antibody (**Figure 27**) and a monoclonal antibody (**Figure 28**). The **Figure 27 A-A''** shows a general view of a sagittal section of the cerebellum. From the innermost to outermost layer lie the white matter, the granular layer, and the Purkinje layer, which is between the granular and molecular layer is indicated with an asterisk**.** The image (**Figure 27A''**) shows the pia mater covering each cerebellar lobule. We found that the immunodetection of METTL7A was strong in the apical region of the molecular layer where it showed a fibrillary profile across the molecular layer in adult human cerebellum (**Figure 27B-B'**' for the polyclonal antibody and **Figure 28A-A''** for the monoclonal antibody). We observed moderate immunodetection for METTL7A in the Purkinje layer (**Figure 27A, C-C''**, **Figure 28B-B''**), low expression in the granular layer (**Figure 27A, D-D"**, **Figure 28C-C''**) and high immunoreactivity in white matter (**Figure 27A, E-E''**, **Figure 28D-D''**).

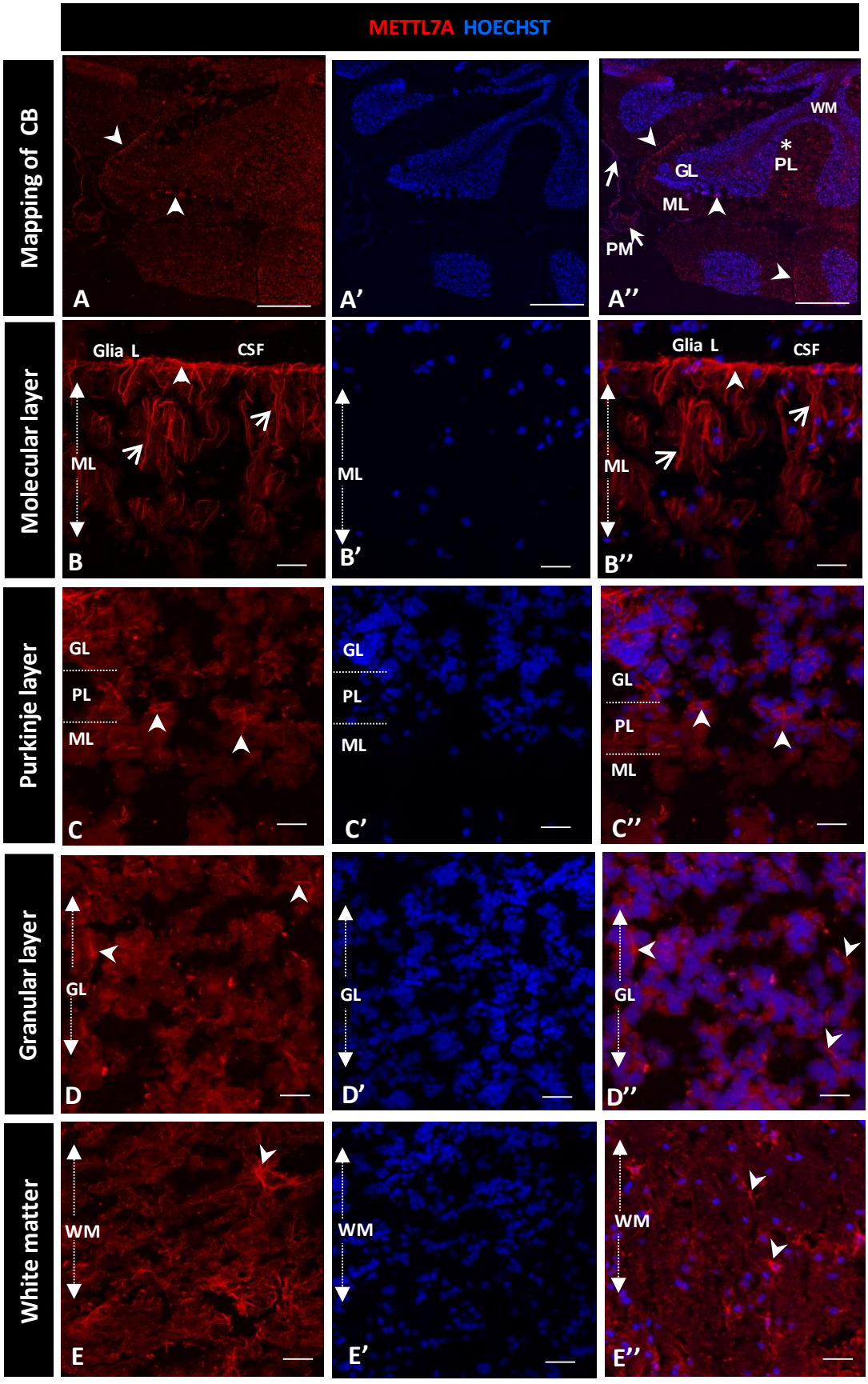
METTL7A HOECHST
Mapping of CB
Molecular layer
Purkinje layer
Granular layer
White matter
A
A'
A''
WM
GL
PL
ML
PM
Glia L
CSF
B
B'
B''
C
C'
C''
D
D'
D''
E
E'
E''

Figure 27. Immunohistochemistry of METTL7A in human cerebellum using a polyclonal antibody: **A-E** Images show the immunodetection of METTL7A using polyclonal antibody AB8021. **A-A''.** Mapping of adult human cerebellum and immunodetection of METTL7A, which is higher in the apical region (arrowheads). **B-B''.** Strong immunoreactivity of METTL7A in the molecular layer (arrows) and the apical region (arrowheads). **C-C''**. Image of the Purkinje layer shows reactivity of METTL7A possibly in the Bergmann glia cells (arrows). **D-D''**. The granular layer shows low immunoreactivity for METTL7A, but higher in some cells (arrowheads). **E-E''.** White matter shows high immunoreactivity in cells for METTL7A. **A', B', C', D'** and **E'.** Nuclei were stained with Hoechst. **CB**: Cerebellum; **GL**: Granular layer; **PL**: Purkinje layer; **ML**: Molecular layer; **WM**: White matter; **PM**: Pia mater; **CSF**: Cerebrospinal fluid. **A.** Tissue thickness 7 µm. Scale bar 1 mm and 10x magnification. **B-E**. Tissue thickness 7 µm. Scale bar 4 µm, 20x magnification

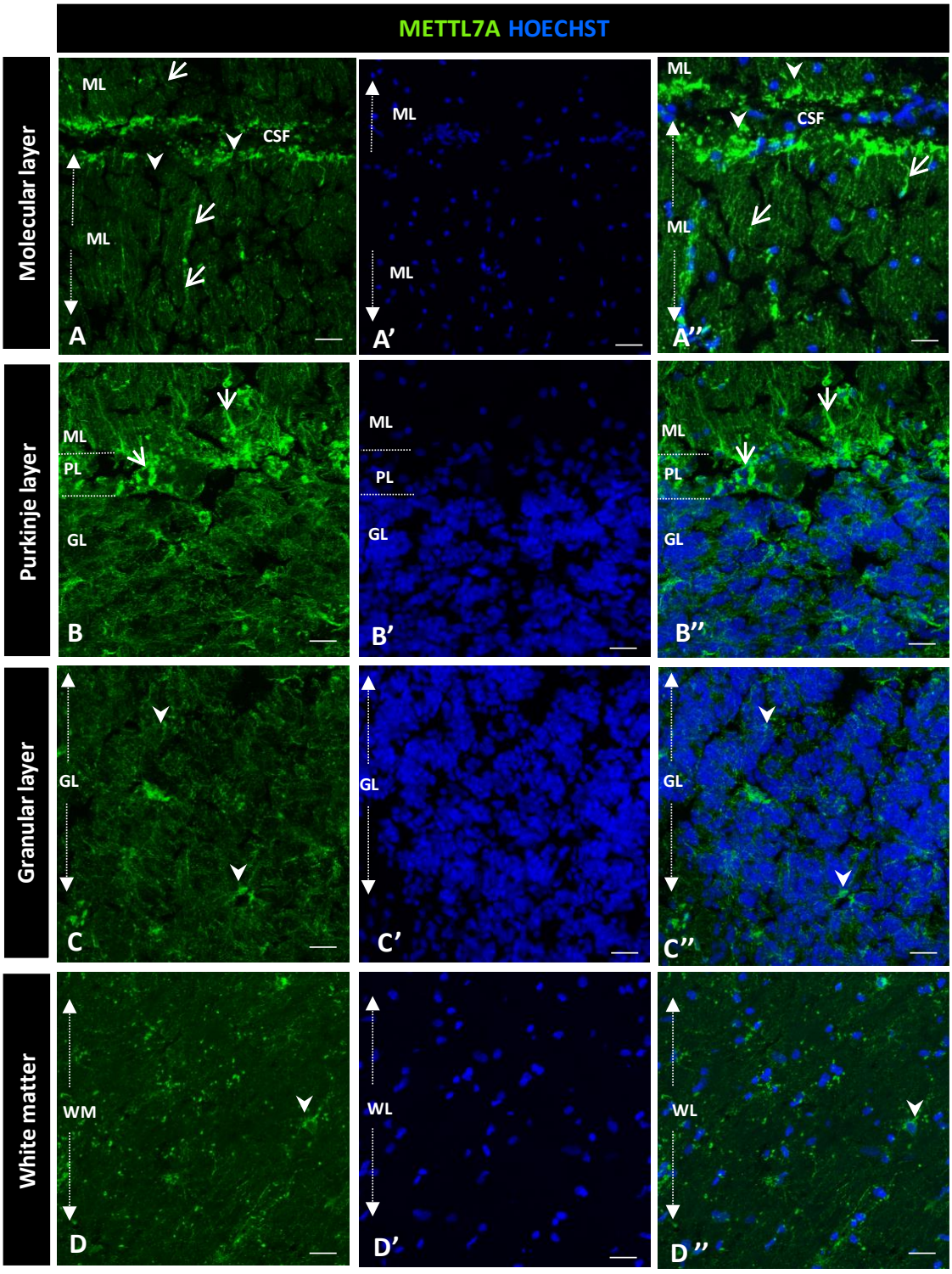
METTL7A HOECHST
Molecular layer
Purkinje layer
Granular layer
White matter
ML
CSF
PL
GL
WM
WL
A
A'
A''
B
B'
B''
C
C'
C''
D
D'
D''

Figure 28. Immunohistochemistry of METTL7A in the human cerebellum using a monoclonal antibody: **A-D.** Panel shows the immunodetection of METTL7A using a monoclonal antibody with a similar expression profile to METTL7A as in **Figure. 5**. **A-A''.** Images show immunodetection of METTL7A in the molecular layer (arrows) and high immunoreactivity in the apical region (arrowheads). **B-B''**. Purkinje layer projection shows reactivity of METTL7A possibly in the Bergmann glia cells (arrows). **C-C''**. Image shows immunoreactivity for METTL7A in the cells of the granular layer (arrows). **D-D''.** Image of white matter shows cells positive for METTL7A (arrowheads). **A', B', C'** and **D'.** Nuclei were stained with Hoechst. **GL**: Granular layer; **PL**: Purkinje layer; **ML**: Molecular layer; **WM**: White matter; **PM**: Pia mater; **CSF**: Cerebrospinal fluid. Tissue thickness 7 µm. Scale bar 4 µm, 20x magnification

5.9.2. Co-immunostaining of METTL7A and GFAP in human cerebellar tissue

To characterize the high immunoreactivity of METTL7A in the molecular layer, a double staining with GFAP for glia cells **(Figure 29** and **Figure 30**) was performed. Our results showed that METTL7A colocalizes with GFAP in the molecular layer where projections of Bergmann glia cells are found (**Figure 29A-A'''**, **B-B''** and **Figure 30A-A'''**). METTL7A also showed a low cytoplasmic signal in GFAP positive cells at the edge of the Purkinje layer, corresponding to the cell body of Bergmann cells (**Figure 29 C-C'''** and **Figure 30B-B'''**) and strong immunoreactivity in the end-feet of Bergmann glia cells at the edge of the molecular layer with intimate contact with the pia matter (**Figure 29B-B''''** and **Figure 30A-A'''**). Both structures contribute to creating a physical barrier that separates cerebellar tissue from cerebrospinal fluid. The granular layer (**Figure 29D-D''''** and **Figure 30C-C'''**) shows the co-expression of METTL7A and GFAP in some astrocytes. **Figure 29E-E'''** and **Figure 30D-D'''** show immunoreactivity of METTL7A and GFAP in white matter and its colocalization in some cells.

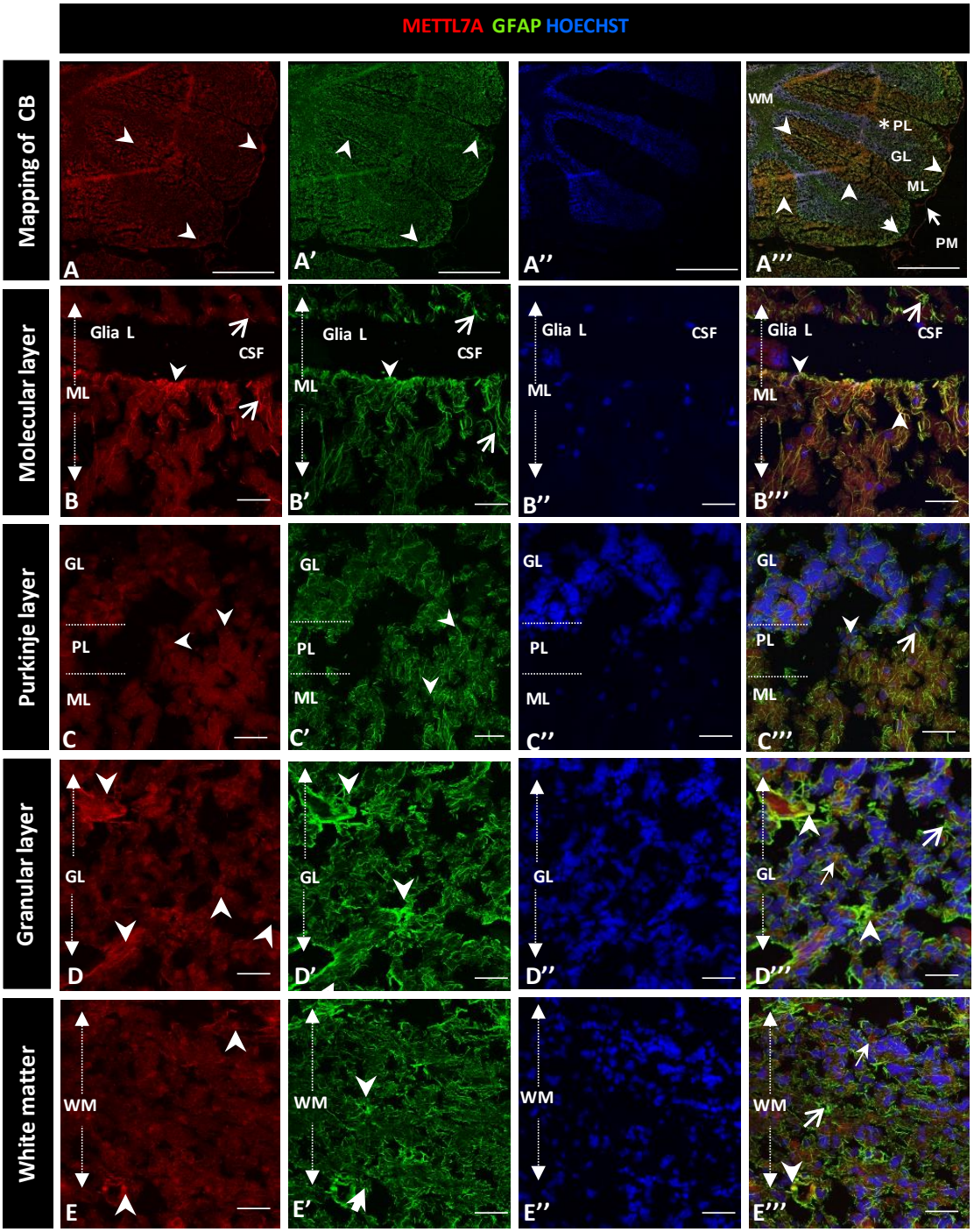
METTL7A GFAP HOECHST
Mapping of CB
Molecular layer
Purkinje layer
Granular layer
White matter
A
A'
A''
A'''
WM
PL
GL
ML
PM
B
B'
B''
B'''
Glia L
CSF
C
C'
C''
C'''
D
D'
D''
D'''
E
E'
E''
E'''

Figure 29. Co-immunodetection of METTL7A and GFAP in the human cerebellum using a polyclonal antibody for METTL7A. Images show the immunodetection of METTL7A using polyclonal antibody AB8021. **A-A'''**. Mapping of the human cerebellum. **A**. Immunodetection of METTL7A (arrowheads). **A'**. Immunoreactivity for GFAP (arrowheads). **A'''**. Image shows the colocalization of both proteins (arrowheads) and immunodetection for GFAP (arrow). **B**. Immunoreactivity of METTL7A distributed across the molecular layer (arrows) and strong immunoreactivity in the apical region (arrowheads). **B'**. High immunodetection of GFAP (green) in the Bergmann glia (arrows) and the apical region (arrowheads). **B'''**. Colocalization of METTL7A and GFAP in the Bergmann glia and strong immunodetection in the apical region (arrowheads). **C**. Immunoreactivity in the Purkinje layer of METTL7A (red) and possibly in the Bergmann glia (arrowheads). **C'**. Note positive cells for GFAP (green) in the Purkinje layer (arrowheads). **C'''**. Colocalization of METTL7A and GFAP in the Purkinje layer and possibly in the cytoplasm of the Bergmann glia (arrowheads). **D**. Low immunoreactivity in the granular layer (arrowheads). **D'**. Strong immunodetection of GFAP in cells of the granular layer. **D'''**. Merge of METTL7A and GFAP in the granular layer; arrowheads indicate colocalization of METTL7A and GFAP and arrows shows positive immunodetection for GFAP. **E**. Panel shows the expression of METTL7A (arrowheads) in white matter. **E'**. Immunodetection for GFAP (arrowheads) in white matter. **E'''**. Merge of METTL7A and GFAP in white matter and their colocalization (arrowheads) and positive expression of GFAP (arrows). **A''**, **B''**, **C''**, **D'' and E''**. Nuclei stained with Hoechst. Tissue thickness 7 µm**. CB:** Cerebellum; **GL**: Granular layer; **PL**: Purkinje layer; **ML**: Molecular layer; **WM**: White matter; **PM**: Pia mater; **Glia L**: Glia limitans; **CSF**: Cerebrospinal fluid. **A.** Scale bar 1 mm, 10x magnification. **B-E**. Scale bar 4 µm, 20x magnification.

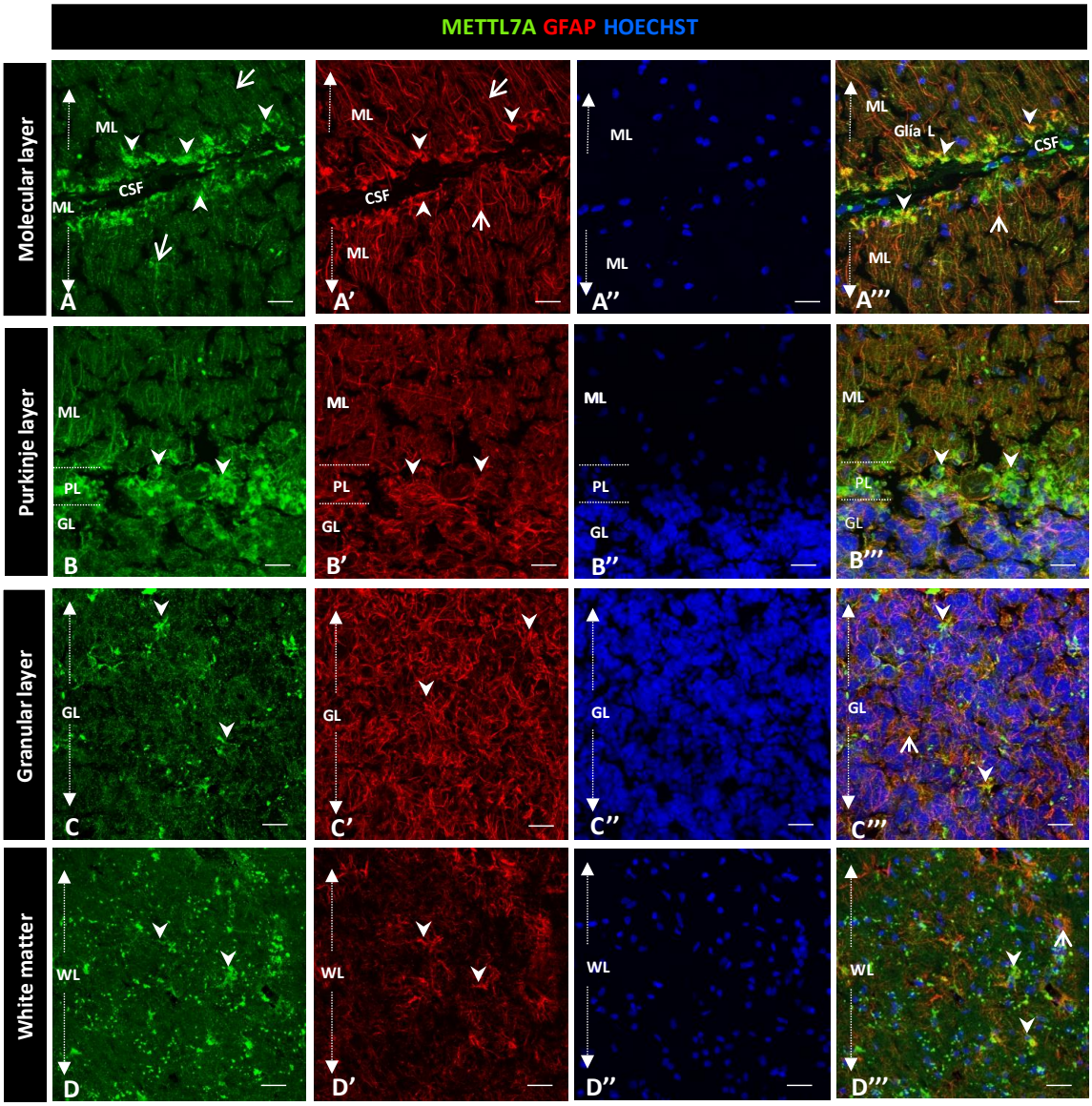
METTL7A GFAP HOECHST
Molecular layer
Purkinje layer
Granular layer
White matter
ML
CSF
Glía L
PL
GL
WL
A
A'
A''
A'''
B
B'
B''
B'''
C
C'
C''
C'''
D
D'
D''
D'''

Figure 30. Co-immunodetection of METTL7A and GFAP in the human cerebellum using a monoclonal antibody for METTL7A. **A**. Image shows immunoreactivity of METLL7A (green) distributed across the molecular layer (arrows) and strong immunoreactivity in the apical region (arrowheads). **A'**. Immunodetection of GFAP (red), which shows strong immunodetection in the Bergmann glia (arrows) in the apical regions of molecular layer (arrowheads). **A'''**. Colocalization of METTL7A and GFAP in the Bergmann glia and strong immunodetection in the apical region of this layer where the Bergmann glia constitutes the glia limitans (arrowheads). **B**. Panel shows the immunoreactivity in the Purkinje layer of METTL7A (green) and possibly in the Bergmann glia (arrowheads). **B'**. Note positive cells for GFAP in the Purkinje layer (arrowheads). **B'''**. Colocalization of METTL7A and GFAP in the Purkinje layer and possibly in the cytoplasm of the Bergmann glia due to its perinuclear immunoreactivity (arrowheads). **C**. Low immunoreactivity in cells of the granular layer (arrowheads). **C'**. Strong immunodetection of GFAP in the cells of the granular layer. **C'''**. Merge of METTL7A and GFAP in the granular layer; arrowheads indicate colocalization of METTL7A and GFAP. Arrows show cells positive for GFAP. **D**. Panel shows the expression of METTL7A in white matter (arrowheads). **D'**. Note cells positive for GFAP (arrowheads) in white matter. **D'''**. Merge of METTL7A and GFAP in white matter shows colocalization of the two proteins (arrowheads) and expression of GFAP (arrows). **A''**, **B''**, **C''**, **D''**. Nuclei stained with Hoechst. **CB:** Cerebellum; **GL**: Granular layer; **PL**: Purkinje layer; **ML**: Molecular layer; **WM**: White matter; **PM**: Pia mater; **Glia L**: Glia limitans; **CSF**: Cerebrospinal fluid. Tissue thickness 7 µm. Scale bar 4 µm, 20x magnification

5.9.3. Co-immunostaining of METTL7A and Tuj1 protein in human cerebellar tissue.

To explore whether METTL7A localizes in neurons, we performed co-immunostaining with Tuj1 as neuronal marker. Our analysis showed no detectable colocalization between METTL7A and Tuj1 in the molecular layer (**Figure 31B-B'''). ** Moreover, our analysis showed that METTL7A is expressed at low levels in the soma and projections of some Tuj1-positive cells (**Figure 31C-C'''**). Thus, the major expression of METTL7A is in astrocytes, in particular, in the *glia limitans* formed by Bergmann glia cells. The granular layer shows low reactivity for METTL7A and Tuj1 (**Figure 31D-D'''**) and white matter cells show reactivity for METLL7A and Tuj1, but not co-expression (**Figure 31E-E'''**).

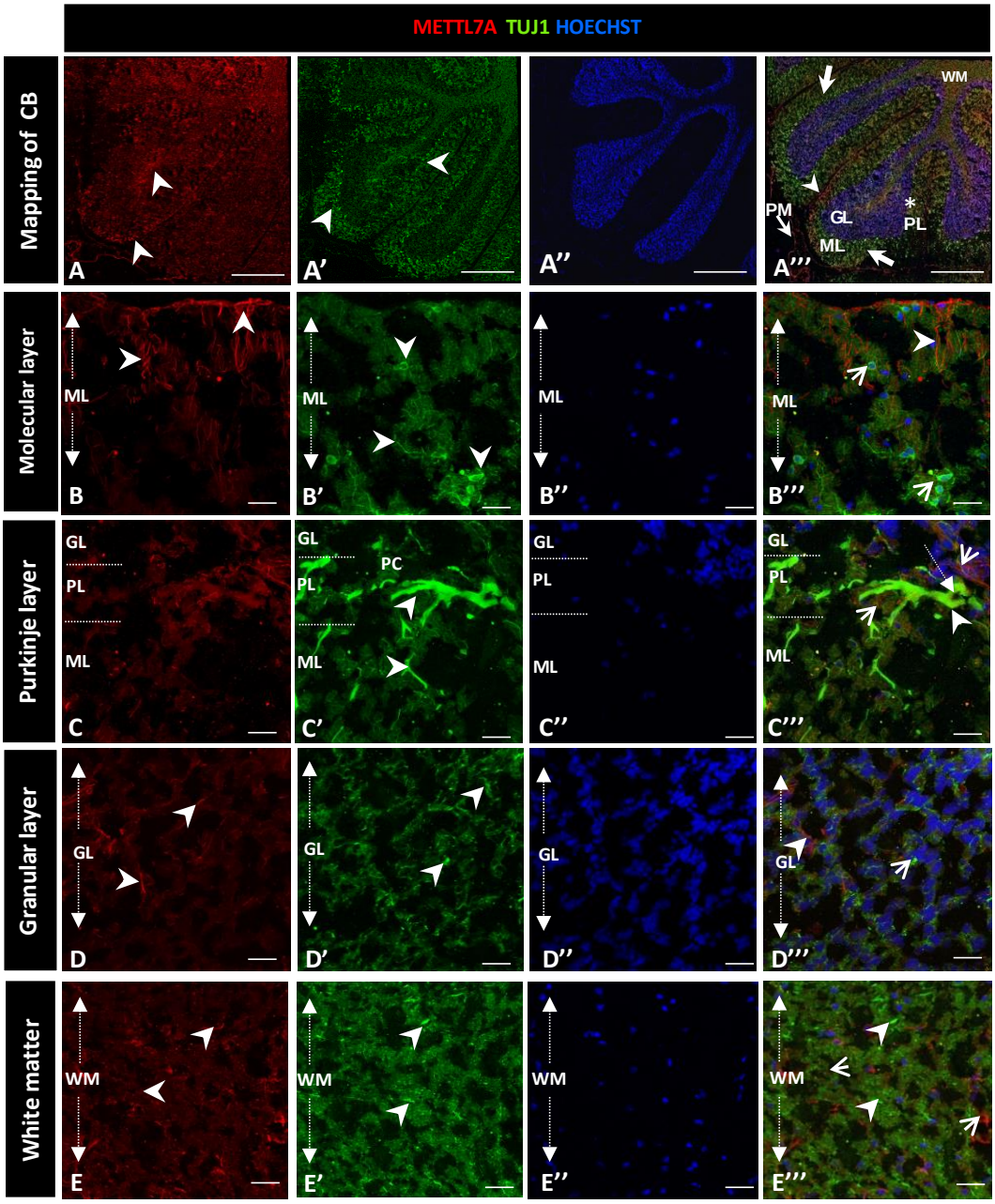
METTL7A TUJ1 HOECHST
Mapping of CB
Molecular layer
Purkinje layer
Granular layer
White matter
A
A'
A''
A'''
WM
PM
GL
ML
PL
B
B'
B''
B'''
C
C'
C''
C'''
PC
D
D'
D''
D'''
E
E'
E''
E'''

Figure 31. Co-immunodetection of METTL7A and Tuj1 in human cerebellum. A-E Image shows the immunodetection of METTL7A using polyclonal antibody AB8021. **A-A'''**. Mapping of adult human cerebellum. **A**. Immunodetection of METTL7A (arrowheads). **A'**. Immunoreactivity for Tuj1 (arrowheads). **A'''**. Merge of METTL7A (arrowheads) and Tuj1 (arrow). **B**. Immunoreactivity of METTL7A distributed across the molecular layer (arrows) and apical region (arrowheads). **B'**. Immunodetection of Tuj1 (arrows) in the molecular layer (arrowheads). **B'''**. Image shows non-colocalization of METTL7A (arrowheads) and Tuj1 (arrows). **C**. Low immunoreactivity in the Purkinje layer of METTL7A (arrowheads). **C'**. Note cells positive for Tuj1 in the Purkinje layer (arrowheads). **C'''**. Positive immunodetection of some Purkinje cells for METTL7A in the cytoplasm (dotted arrow) and immunodetection of Tuj1 in Purkinje cells. **D**. Low immunoreactivity in the granular layer (arrowheads). **D'**. Immunodetection of Tuj1 in the granular layer (arrowheads). **D'''**. Merge of METTL7A and Tuj1 in the granular layer; arrowheads indicate immunodetection of METTL7A and arrows, immunodetection of Tuj1. **A''**, **B''**, **C''**, **D''** and **E''.** Nuclei were stained with Hoechst. **CB**: Cerebellum; **GL**: Granular layer; **PL**: Purkinje layer; **ML**: Molecular layer; **WM**: White matter. Tissue thickness 7 µm. **A.** Scale bar 1 mm, 10x magnification. **B-E.** Scale bar 4 µm, 20x magnification.

5.9.4. Expression of METTL7A in lipid droplets

The classical localization of METTL7A is in the lipid droplets. Thus, we performed Bodipy 493/503 staining with immunodetection of METTL7A in white matter (**Figure 32A-A'''**) due to the presence of cells containing lipid droplets in this region. Furthermore, **Figure 32B-B'''** also shows immunodetection of METTL7A in the cytoplasm of some Purkinje cells, an observation that supports the results displayed in Figure **31C-C '''.**

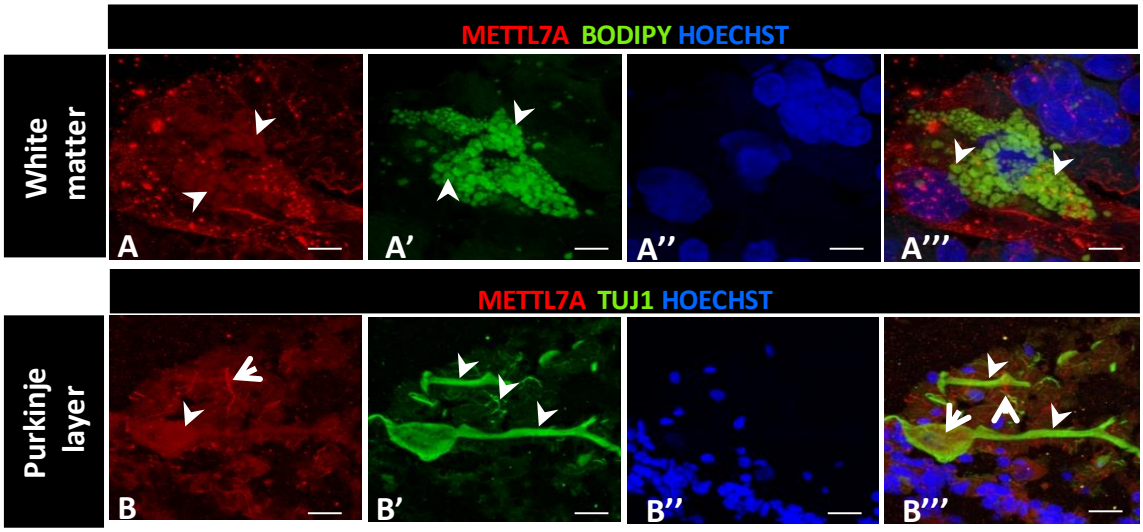

Figure 32. Bodipy stain and immunohistochemistry of METTL7A and Tuj1. Images show Bodipy 493/503 staining with immunodetection of METTL7A in white matter. **A**. Image shows immunodetection of METTL7A in lipid droplets (arrowheads) contained in the cells of white matter. **A'**. Bodipy stain for lipid droplets (arrowheads) in a white matter cell. **A'''**. Merge of METTL7A and bodipy and their colocalization in lipid droplets**. B-B'''**. Images show immunodetection of METTL7A and Tuj1 in a Purkinje cell. **B**. Low immunoreactivity of METTL7A in a Purkinje cell (arrowheads) and fibres in the Purkinje layer (arrow). **B'**. Immunodetection of Tuj1 in a Purkinje cell (arrowheads). **B'''**. Low immunoreactivity of METTL7A in the cytoplasm of a Purkinje cell (arrow), fibre positive for METTL7A (dotted arrow) and immunoreactivity of Tuj1 in a Purkinje cell (arrowheads). **A''** and **B''**. Nuclei were stained with Hoechst. Tissue thickness 7 µm. Scale bar 4 µm. **A-A'''**. 100x magnification. **B-B'''**. 63x magnification.

5.9.5. 3D projection analysis for the characterization of METTL7A

To further characterize METTL7A localization, 3D projection analysis was performed. This method involved creating a solid mask for each channel used to demarcate the surface for each labelling, allowing us to visualize the volume of the labelled structure. Using this procedure, we found that METTL7A was present along the cellular projections of Bergmann cells (**Figure 33A-A'**), in multiple contacts between Bergmann glia cells and Purkinje cells (**Figure 33B-B'**) and in intracellular droplets in some Purkinje neurons (**Figure 33B**). Furthermore, we performed BODIPY 493/503 staining for lipid droplets and immunostaining with METTL7A. In white matter we detected a few lipid droplet-containing cells. The 3D projection showed that the distribution of METTL7A in some lipid droplets detected in the cytoplasm was similar to the distribution observed for lipid droplets in some white matter cells (**Figure 33C-C'**).

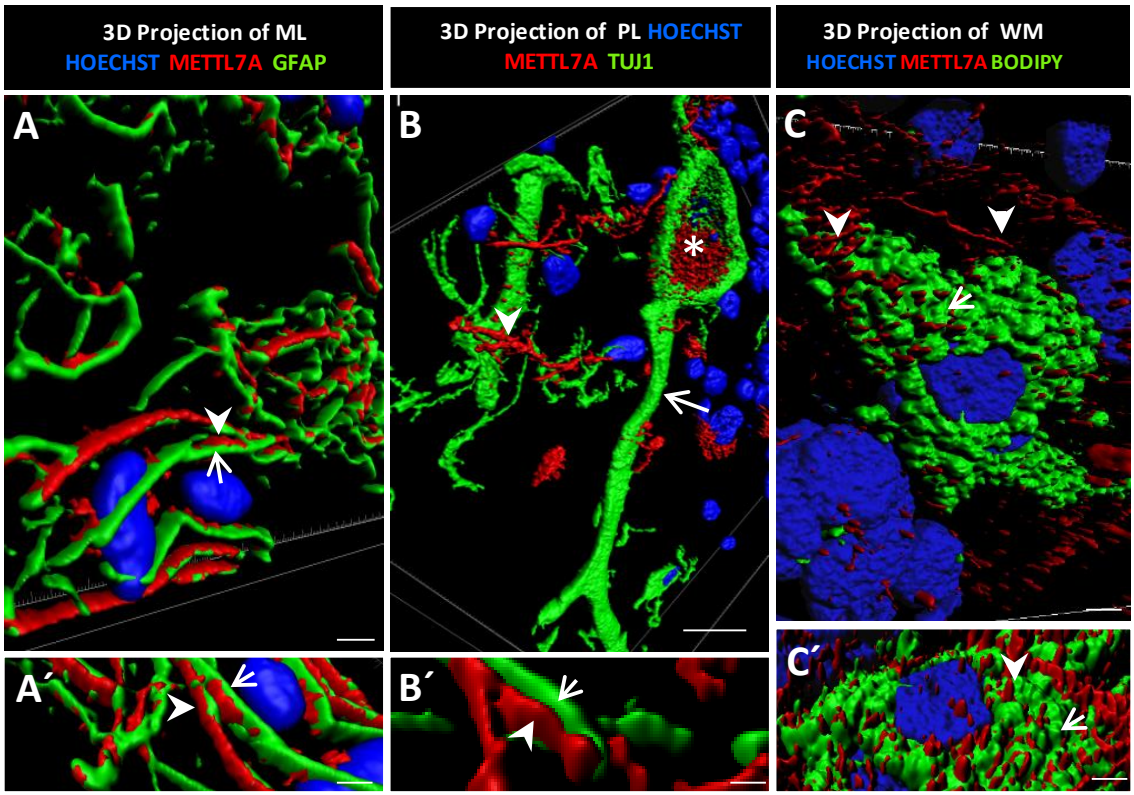

Figure 33. 3D projection model. A-A´. These images show the localization of METTL7A (arrowhead) and GFAP (arrow) **B.** Purkinje cells showed strong reactivity for METTL7A in droplets in their cytoplasm (asterisk). **B´** shows small contacts of Bergmann glia (arrowheads). **C.** A white matter cell. The panel shows a lipid droplet-filled cell which is marked with BODIPY (green) and METTL7A (red). **ML**: Molecular layer, **PL**: Purkinje cell, **WM**: White matter. Tissue thickness 7 µm. **A.** Scale bar 4 µm and **A´.** 3 µm (high magnification 63x). **B.** Scale bar 10 µm (high magnification 63x). **B´**. Scale bar 2 µm (high magnification 63x). **C.** Scale bar 5 µm (high magnification 100x).

VI. DISCUSSION

6.1. Proteomic analysis of *postmortem* cerebellum from schizophrenia and healthy controls

Our study identified and characterized the proteomic alterations for the cerebellar cortex in chronic schizophrenia. We could segregate SZ samples from healthy control samples based on their proteomic profiles, similarly as achieved in gene expression studies (Ramaker *et al.*, 2017) (Naseri *et al.*, 2016). A subset of the molecular findings of this study had been previously related to brain diseases, the main ones being mitochondrial and mental disorders, but also other less represented diseases such as stress. In this context, a study related psychosocial stress mediated by the cortisol with decreased blood flow in the cerebellum and an impairment of retrieval memory (De Quervain *et al.*, 2003). This evidence suggests that the cerebellum is a brain area susceptible to psychosocial stress. This susceptibility could be exacerbated in SZ, thereby contributing to the cognitive symptoms in this disorder.

Here we also observed an enrichment of proteins involved in neurodegenerative diseases. Although the neurodegenerative hypothesis is strongly debated in SZ (Lieberman, 1999b; Pérez-Neri *et al.*, 2006), enrichment in the neurodegenerative disease category in this study could be related to the up-regulation of apoptosis, a biological process also found enriched in our study. NMDA-mediated excitotoxicity has been widely described as causing inflammation, oxidative stress and apoptosis and may be linked to neurodegenerative processes (Armada-Moreira *et al.*, 2020). However, here we observed an enrichment in apoptosis in the cerebellum in a context of NMDA hypofunction. In line with these results are the findings that inhibition of the NMDA receptor in animal studies triggers apoptotic signalling mediated by ERK1/2-CREB (Hansen *et al.*, 2004), raising the possibility that the observed up-regulation of apoptotic proteins could be dependent on the NMDA hypofunction described in SZ (Lisman *et al.*, 2008; Snyder and Gao, 2020). In this context, studies on the inactivation of the NMDA receptor showed the existence of

disseminated apoptotic events in the brain and cerebellum (Ikonomidou *et al.*, 1999; Monti and Contestabile, 2000; Hansen *et al.*, 2004). This type of apoptosis might be responsible for the reduction of grey matter reported in the cerebellum of SZ subjects (He *et al.*, 2019). In contrast to neurodegenerative diseases in which significant apoptotic events and gliosis occurs, in the context of schizophrenia, our findings along with previous studies support a possible low grade, slow progression of apoptosis and/or a higher vulnerability of programmed cell death in the cerebellar neurons in SZ.

In this study, the enrichment of the mitochondrial disease category in the altered proteins could be related to a downregulation of biological processes related to oxidative phosphorylation and TCA, biological processes that were also observed to be enriched in this study. In SZ, altered mitochondrial function has been previously reported (Rajasekaran *et al.*, 2015). This energy imbalance could affect cell growth, motility and signalling in the cerebellum. In this context, our results showed an up-regulation of cytoskeleton organization processes, which could be a compensatory mechanism that increases retrograde transport of damaged mitochondria at the synapsis and the anterograde transport of functional mitochondria towards the synaptic terminals. Furthermore, up-regulation of processes involved in cell signalling pathways could be due to altered vesicle-mediated transport and release of neurotransmitters. Moreover, altered protein expression in axon guidance could contribute to the disruption in neuronal connectivity, which has been suggested in the neurodevelopmental hypothesis in SZ (Weinberger, 1988). Furthermore, our network analyses showed two modules for the down-regulated network, namely energy metabolism and neutrophil degranulation. For the up-regulated network, we found pathway crosstalk between proteins of vesicle-mediated transport, axon guidance, signalling by Rho GTPases, apoptosis, and the cell cycle, suggesting that signalling pathways are dynamic events in which the alteration of one protein could affect several pathways.

6.1.1. Genetic localization of altered proteins and putative transcription programs responsible for changes in the proteomic profile in the cerebellum

Our study revealed that the 250 altered proteins are localized across 185 loci, 54 of which have been previously reported as risk loci for schizophrenia (Ripke *et al.*, 2013; Wong *et al.*, 2014), suggesting that the proteins that are altered in the cerebellum are not widely distributed throughout the human genome. Several loci that we found in the cerebellum have been studied in this disorder. The Xq28 locus has been associated with the X chromosome hypothesis of schizophrenia, which postulates that sex chromosome alterations are more frequent in schizophrenia subjects; in particular, studies found anomalies in the X chromosome (Bache and Delisi, 2018). Furthermore, Xq28 carries gene candidates for schizophrenia such as MEPC2 and ARHGAP (Wong *et al.*, 2014; Bache and Delisi, 2018). We identified 11 potential transcription factors enriched in the cerebellum in chronic schizophrenia which could be responsible, in part, for the altered levels of these 250 altered proteins. These 11 transcription factors could be controlling the expression of the 250 significantly altered proteins, contributing to dysregulation of several biological processes and pathways in schizophrenia. Several studies have implicated these 11 transcription factors in schizophrenia: SP1 (Ben-Shachar, 2009; Fusté *et al.*, 2013, 2016); KLF7 and SP4 (Pinacho *et al.*, 2013; Saia *et al.*, 2014; Pinacho, Saia, Fusté, *et al.*, 2015; Pinacho, Saia, Meana, *et al.*, 2015; J. Chen *et al.*, 2016); EGR1 (Ramaker *et al.*, 2017; Hu *et al.*, 2019); HNF4A (M. P. Vawter, Mamdani and Macciardi, 2011); CTCF (Juraeva *et al.*, 2014; Huo *et al.*, 2019); GABPA (Juraeva *et al.*, 2014); NRF1 (Mcmeekin *et al.*, 2016); NFYA (Smeland *et al.*, 2017); YY1 (Huo *et al.*, 2019); and MEF2A (Mitchell *et al.*, 2018).

6.2.2. Altered biological processes and pathways could be under the transcriptional control of the SP/KLF factor family

The enrichment analysis showed that SP1, KFL7 and SP4 —which belong to the SP/KFL family, which is characterized by having GC boxes and basic transcription elements with highly conserved DNA binding sites (Van Vliet *et al.*, 2006) had the greatest number of target genes. SP1 is a transcription factor that is ubiquitously expressed in the nervous system and the peripheral system. We therefore expected SP1 to be involved in the regulation of multiple processes in the cerebellum. Our results identified categories such as cytoskeleton organization/development, cellular/organelle organization and pathways related to signalling as the categories most enriched for SP1, SP4 and KFL7. The cytoskeleton mediates a large variety of cellular functions, including supporting cellular morphology and cellular activities such as vesicle trafficking, neuronal migration, neurite outgrowth (Zhao *et al.*, 2015). SP1 has been implicated in neurite outgrowth in astrocytes (Hung 2020), while SP4 has been associated with dendritic arborization (Ramos *et al.*, 2007, 2009). KFL7 has been implicated in enhancing axon growth (Laub *et al.*, 2001, 2005), formation of dendritic branching in the hippocampus and altered axon projection in several brain regions (Laub *et al.*, 2005). Moreover, KFL7 has been reported to be involved in the maturation of granular neurons in the cerebellum during early postnatal development (Laub *et al.*, 2005). In this context, our results are line with the functions proposed for SP1, SP4 and KFL7. In the context of schizophrenia, studies performed by our group in the *postmortem* brain have shown altered protein levels of SP1 and SP4 in the hippocampus (Pinacho *et al.*, 2014), cerebellum and prefrontal cortex in chronic schizophrenia (Pinacho *et al.*, 2013). We believe that the dysregulation of KFL7 in schizophrenia could lead to the alteration of the maturation of granular cells and axon growth, while altered expression of SP1 and SP4 could lead to the altered formation of neurites and the dendritic arborization pattern, which could eventually lead to altered cell-cell communication in the inner

cerebellar circuits and the connection of the cerebellum with other regions such as the prefrontal cortex.

The immune response and inflammatory processes involve the activation of complex transcriptional programs. In our study, biological processes and pathways related to the immune response were found to be enriched. The target genes involved in these categories could be under the transcriptional control of SP1 and KLF7. Several members of the Krüppel-like factor family, such as KLF2, KLF4 and KLF6, have been reported to be involved in the immune system and inflammation (Nayak *et al.*, 2013; Date *et al.*, 2014; Luo *et al.*, 2016). Although we have not found any reports about the function of KLF7 in the immune response regulation in the central nervous system, SP1 has been implicated in the activation of interleukin 21 receptors in T cells (Wu *et al.*, 2005), which mediate the activation of several cell types involved in the immune response (Parrish-Novak *et al.*, 2000). Furthermore, SP1 has been implicated in interleukin 12 (IL-12) expression. IL-12 induces the differentiation of T-helper 1 cells (Sun *et al.*, 2006) during the adaptative immune response. SP1 induces the activation of macrophage inflammatory protein-2 (MIP-2), which is involved in recruiting neutrophils to inflammatory regions (Lee *et al.*, 2005). (Lee *et al.*, 2005). In addition, SP1 could increase the levels of the NFκB-blocking anti-inflammatory cytokine IL-10 (Norkina *et al.*, 2007) and has also been implicated in the crosstalk between interferon regulatory factors and NFκB pathways, thereby contributing to the TLR-dependent antiviral response (Iwanaszko and Kimmel, 2015). In schizophrenia, it has been reported that SP1 could interact with the TLR4-MyD88-IκBα-NFκB pathway, which mediates its interaction with NFκB (MacDowell *et al.*, 2017). In addition, altered IL-12 levels have been described in plasma in schizophrenia subjects (Kim *et al.*, 2002).

Thus, SP1 could be an activator of the immune response. The dysregulation in IL-2 expression due to the altered function of SP1 could lead to the dysfunction of the

differentiation of T-helper cells and an altered immune adaptative response in schizophrenia. SP1 could be regulating the mechanisms of innate immunity through the TLR4-MyD88-IκBα-NFκB pathway. These results are interesting from the perspective of the immune hypothesis proposed for schizophrenia.

Apoptotic processes underlie the neurodegenerative hypothesis proposed for schizophrenia. However, the transcriptional program involved in this process is unknown. Our analysis revealed that SP1 and KLF7 could participate in mitochondrial apoptosis. SP1 has a dual function in apoptosis. While some studies have demonstrated that overexpression of SP1 could induce apoptosis, others have reported that the depletion of SP1 increases the sensitivity of cells to DNA damage (Marvel and Leverrier, 2006; Torabi *et al.*, 2018) and eventually leads to apoptosis. On the other hand, it has been reported that depletion of KLF7 increases apoptosis in animal models (Lei *et al.*, 2005). However, we have not found studies that examine in depth the molecular mechanism of SP1 and KLF7 in apoptosis. However, one possibility is that the balance in SP1 expression is crucial for maintaining DNA without leading to cell apoptosis. In the context of schizophrenia, altered expression of SP1 and KLF7 could activate apoptotic signalling pathways in the CNS and contribute to the disseminated apoptosis described in schizophrenia (Jarskog *et al.*, 2005).

Pathways related to transport and the Golgi complex, such as vesicle-mediated and membrane trafficking, were the pathways found to be most enriched for the target genes of SP1, EGR1, HNFA4, and CTCF. Moreover, the pathway most enriched for CTCF was that of Golgi anterograde transport. All these pathways are involved in Golgi apparatus functioning. Protein transport from the endoplasmic reticulum to the Golgi complex involves transport vesicles (Watson and T, 2005). However, we did not find any reports about the possible transcriptional control of SP1, EGR1, HNFA4 and CTCF in transport related to the Golgi apparatus. EGR1, also called Zif286, is an immediate-early gene

whose expression can be induced by several signals such as injury, stress and differentiation (Clements and Wainwright, 2010). EGR1 mediates the expression of several late-response genes implicated in neuronal plasticity (Bahrami and Drabløs, 2016; Duclot and Kabbaj, 2017). Moreover, it is involved in cognitive functions (Beckmann and Wilce, 1997). A transcriptome study in fibroblasts from schizophrenia patients found differentially expressed EGR1 compared to controls (Etemadik *et al.*, 2020). HNFA4 has also been associated with schizophrenia (M. Vawter, Mamdani and Macciardi, 2011). However, its role in this disorder is unknown. CTCF is a molecule involved in chromatin conformational change (Phillips and Corces, 2009). The depletion of CTCF in the hippocampus has been related to deficits in learning and memory, processes implicated in schizophrenia (Sams *et al.*, 2016). However, its role in Golgi anterograde transport or functions associated with the Golgi is unknown.

Our analysis reports that a protein set involved in biological processes related to mRNA processing and mRNA splicing could be under the transcriptional control of SP1 and MEF2A. It has recently been shown that alternative splicing could have a role in schizophrenia (Barry *et al.*, 2014; Saia-Cereda *et al.*, 2017).

Many of the archetypal genes associated with schizophrenia, for example DISC1 (Nakata *et al.*, 2009) and ERBB4 (Law *et al.*, 2007), are aberrantly spliced transcripts. However, the molecular mechanism underpinning this aberrant splicing is unknown. A study in mice showed that Sp1 enhances the transcription of the splicing factor *Slu7*, while depletion of Sp1 repressed *Slu7* expression, thereby affecting alternative splicing processes (Alberstein *et al.*, 2007). MEF2A is a transcription factor implicated in the formation of postsynaptic granule neuron dendritic claws (Shalizi *et al.*, 2006) and has been associated with schizophrenia (Crisafulli *et al.*, 2015; Hilge *et al.*, 2015). However, its role in mRNA processing has not been studied. Thus, more studies are needed regarding the impact of the transcriptional program on the dysfunction of pathways in schizophrenia. In this

doctoral thesis, we report 11 potential transcription factors that could be related to new altered signalling pathways in schizophrenia (**Figure 34**). Together, these findings suggest that the altered function of a limited number of transcription factors could have a significant impact on disseminated pathways through the altered expression of a number of transcriptional targets that have key roles in these pathways.

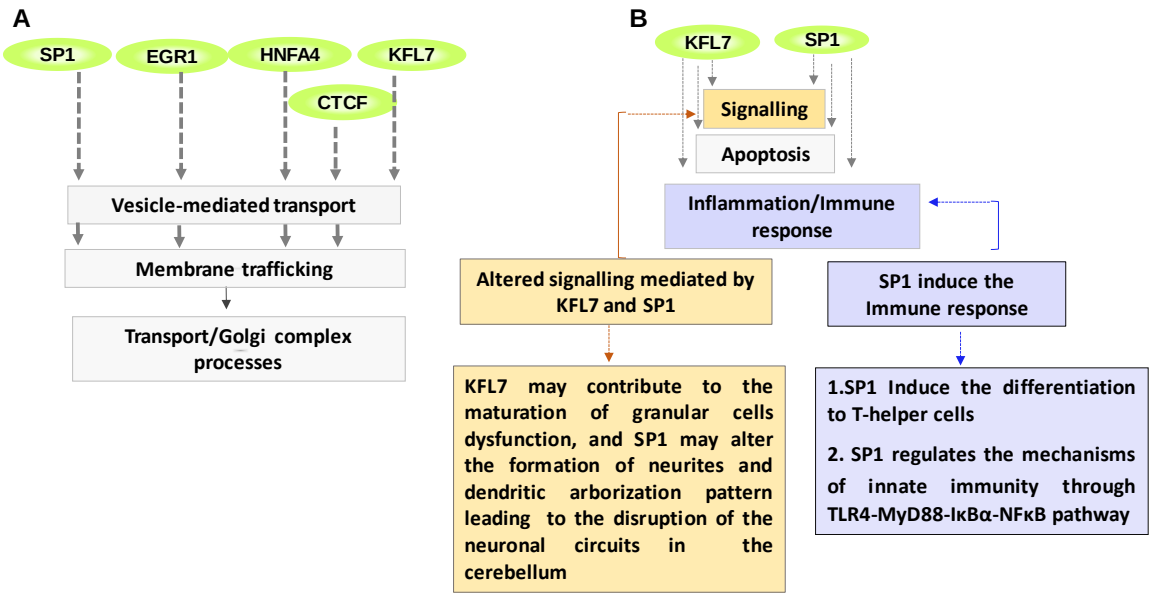

Figure 34. Diagram of the transcriptional program in the cerebellum. **A.** Common pathways categories for SP1, EGR1, HNFA4, KFL7 and CTCF. **B**. Specific pathways categories for KFL7 and SP1.

6.3. Network generation from enriched pathways in the cerebellum

6.3.1. Vesicle-mediated transport pathways

Transport is a critical step for the correct maintenance of biological processes. In neurons, altered transport could limit effectiveness in neuronal communication (Barlan, Rossow and Gelfand, 2013). Defective synaptic transmission and neurotransmitter release (Maher and LoTurco, 2012), decreased in pre-synaptic vesicle proteins (Mirnics *et al.*, 2000; Camargo *et al.*, 2007), and altered levels of proteins involved in synaptic vesicle fusion (Honer, 2002; Mukaetova-Ladinska *et al.*, 2002) have been associated with SZ. However, in our proteomic study we found up-regulated pathways related to vesicle-mediated transport. YWHAZ was found to be up-regulated in our proteomic study and is widely expressed in the cerebellum. Its role as an adaptor protein of extracellular vesicle (EVs) involves the stabilization of vesicles and synapsis (Drago *et al.*, 2017). EVs have various functions: some carry glutamate receptors (GluR2), some oligodendrocyte-derived EVs can be internalized by neurons to protect them from cellular stress (Frühbeis *et al.*, 2013) and neurons may modulate their synaptic activity through the release of EVs with miRNAs that regulate their gene expression (Goldie *et al.*, 2014). We also studied the effect of two *double-hit* SZ murine models on YWHAZ. However, we did not observe any significant changes in YWHAZ in these stress-based models. Other proteomics studies in different brain regions of SZ subjects have shown downregulation of YWHAZ (Martins-de-Souza *et al.*, 2010; Saia-Cereda *et al.*, 2015b). The overexpression of YWHAZ could increase the formation and release of EVs carrying protein or miRNA, which could be a mechanism to compensate for cellular stress in the cerebellum. In addition, our screening of protein expression in cerebellar tissue also showed that ARRB1 and SNX5 proteins from vesicle-mediated transport are expressed only in Purkinje cells. These proteins are involved in desensitization, internalization of G-protein-coupled receptors (GPCRs) (Goodman *et al.*, 1996; Kohout *et al.*, 2001) and recycling of GPCRs to the cell surface

(Villar *et al.*, 2013), respectively. Thus, altered levels of these three proteins could cause defects in the axonal transport of presynaptic vesicles or in the postsynaptic receptor-mediated neurotransmission of Purkinje cells towards deep cerebellar nuclei. This could compromise the efferent signals from the cerebellum to the cortex via the thalamus.

6.3.2. Axon guidance pathway

Defects in neuronal connectivity during development have been proposed as an important cause of the etiopathology of SZ (Chen, Huang and Cheng, 2011; Friston *et al.*, 2016). However, the causes of such abnormalities are still unknown. A study based on the SZ-GWAS database found the axon guidance pathway to be altered in this disorder (Z. Wang *et al.*, 2018). However, the relationship between the axon guidance pathway and SZ has not been well studied. Our proteomic study showed an altered axon guidance pathway in the cerebellum in which CLASP1 was further studied in two murine models. This protein participates in neurite outgrowth by binding at microtubules (Sayas *et al.*, 2019). Since its function has not been studied in SZ, we analysed the effect of the murine models of maternal deprivation combined with social isolation (MD/Iso) or chronic stress (MD/RS) on CLASP1. Our result showed decreased expression of CLASP1 in the MD/Iso model, while our proteomic study in SZ subjects showed an up-regulation. One possible explanation for the up-regulation of CLASP1 in human cerebellum could be the accumulation of this protein in the neuritic growth cone due to a decrease in energy production required for the assembly of CLASP1 at microtubules.

6.3.3. Energy metabolism module

The cerebellum represents 11% human brain weight (Semendeferi and Damasio, 2000) and the distribution of the energy it uses varies between different cell types. The more energy-demanding biological functions in Purkinje cells include the production of action potentials and maintenance of postsynaptic receptors, while granule cells consume more energy to propagate action potentials and support the resting potential (Howarth, Gleeson and Attwell, 2012). In the context of SZ, a study of cerebellar activity showed decreased blood flow in this area during several tasks, including attention, social cognition, emotion and memory (Nopoulos *et al.*, 1999; Koziol *et al.*, 2014). Evidence of mitochondrial dysfunction in SZ includes genetic (Verge *et al.*, 2011), metabolic (Prabakaran *et al.*, 2004), and enzymatic dysfunctions (Maurer, Zierz and Möller, 2001), anatomical abnormalities (Roberts, 2017), and disturbed levels of proteins of glycolysis, TCA cycle, mitochondrial function and oxidative stress (Martins-de-Souza, Gattaz, Schmitt, Novello, *et al.*, 2009; Bubber *et al.*, 2011; Jane A English *et al.*, 2011; Zuccoli *et al.*, 2017). These studies are in line with our results showing a downregulation of pathways involved in TCA cycle/respiratory electron transport and several mitochondrial proteins. In this study, NDUFB9 was observed to be one of the down-regulated proteins in SZ involved in respiratory electron transport. NDUFB9 is widely expressed in the cerebellum and was also observed to be down-regulated in the *double-hit* MD/Iso murine model but not in the MD/RS model. NDUFB9 is involved in the assembly of Complex I. Together with the activity of Complex I, NDUFB9 has been investigated in other brain areas in SZ (Martins-De-Souza *et al.*, 2011; Rollins *et al.*, 2017). Thus, the altered expression of NDUFB9 observed in this study could contribute to reduce energy metabolism in cerebellar cells through the disruption of Complex I in respiratory electron transport and could consequently decrease the propagation action potentials among the major cell types of the cerebellar cortex in chronic SZ.

6.3.4. Neutrophil degranulation module

An imbalance of the immune system is one of the hypotheses underlying SZ (Kinney *et al.*, 2010). Microbial infections generate the release of several proinflammatory cytokines and neutrophil degranulation is one of the first defence barriers against infection (De Oliveira, Rosowski and Huttenlocher, 2016). Our study observed downregulation of several proteins involved in the various processes of the neutrophil degranulation pathway in cerebellar tissue. The altered proteins were related to processes such as transmigration, sequestration of microbes in the autophagosome, and exocytosis of primary and second granules. CD47 was found to be a down-regulated protein expressed only in the granular layer and its inhibition decreased neutrophil transmigration towards injured tissue (Fournier and Parkos, 2012). In addition, we observed altered expression of METTL7A, a hit protein in this pathway. METTL7A, a member of the METTL family of methyltransferases, is of interest as it has been poorly studied; indeed, only one study investigated its role in RhoBTB1 signalling in maintaining Golgi integrity (McKinnon and Mellor, 2017), a function that could be involved in neutrophil degranulation. However, its expression profile in the brain and its function in SZ are completely unknown. In our study, METTL7A was observed to be consistently down-regulated in both SZ human samples and our SZ murine models. In the context of neutrophil degranulation, the altered expression of METTL7A could impair Golgi integrity and contribute to the abnormal formation of secretory granules in neutrophils, altering the first defence barrier of the innate immune response in chronic SZ. We observed a METTL7A localization pattern in the cerebellum that was completely different from its role in neutrophil degranulation described in peripheral cells. Our results revealed that it is expressed in the *glia limitans* in the cerebellum. Therefore, more studies are required to understand the role of this protein in the context of SZ.

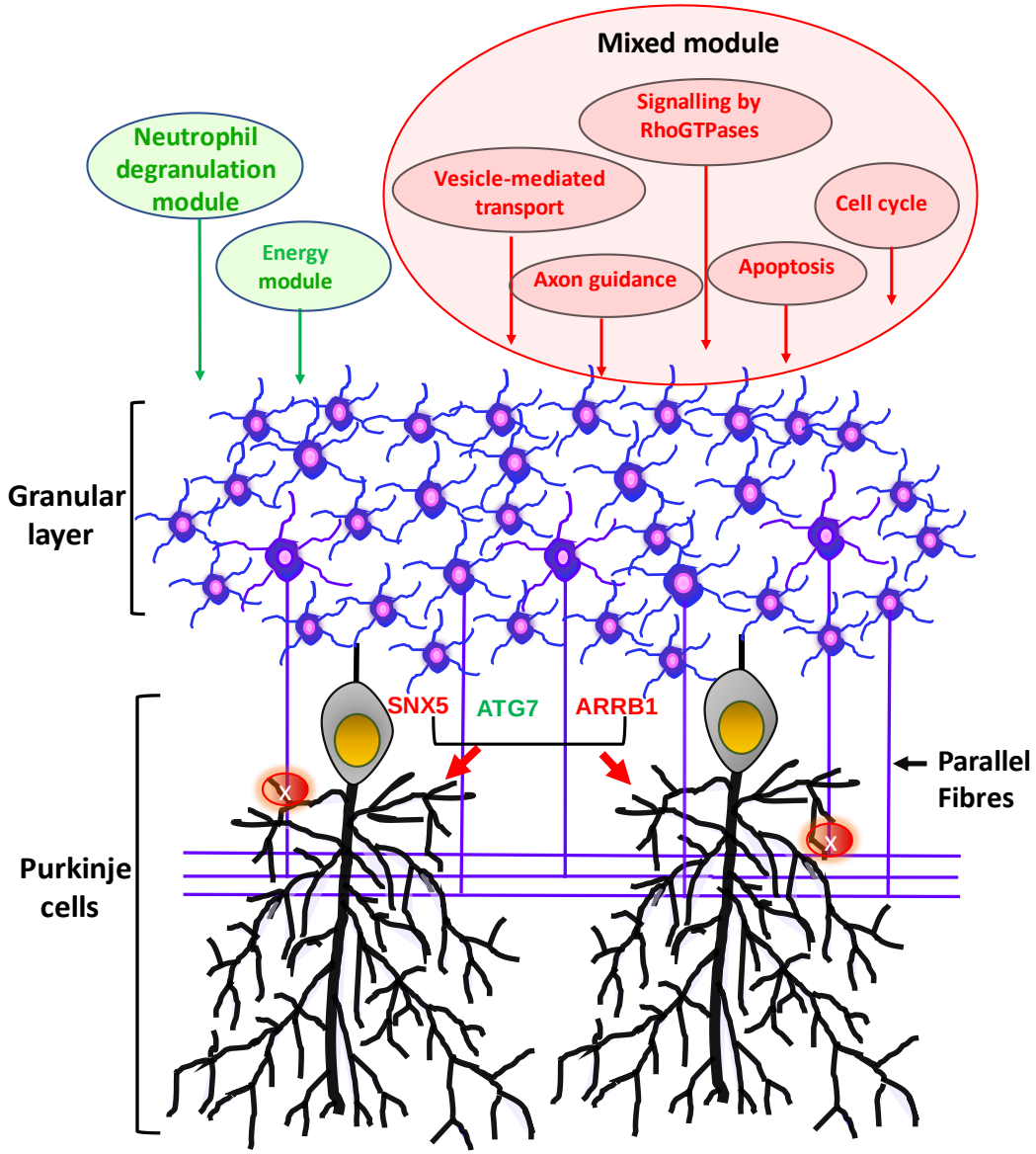

Figure 35. Model of possible contribution of altered networks in the cerebellum. The changes more prominent in the cerebellum may be occurring probability in the granular neurons due to that are the most abundant cells in the cerebellum. Imbalance energy may alter the correct synaptic propagation. Altered pathways in the granular neurons related to axon guidance, vesicle-mediated transport may impact on the Purkinje cells (highlighted red circle in PC) thought of the contacts with parallel fibres from granular neurons. **PC**: Purkinje cell.

SNX5, TG7 and ARRB1 proteins were only expressed in the Purkinje cell. Thus, could have specific functions in this cell type in the cerebellum. SNX5 and ARRB1 are proteins involved in vesicle-mediated transport, and TG7 is implicated neutrophil degranulation.

6.4. The altered expression of METTL7A in *glia limitans* in the cerebellum

We show for the first time the characterization of METTL7A in the human cerebellum. In our study, METTL7A colocalized with the glial marker GFAP in adult human cerebellum, showing high expression in Bergmann glia cells, the *glia limitans superficialis* in the cerebellum. Our result is consistent with a previous transcriptome study which showed that METTL7A is highly expressed in astrocytes (Cahoy *et al.*, 2008). Our result suggests that this protein could have a structural function in astrocytes in brain tissue rather than the typical neutrophil degranulation role of METTL7A assigned by Gene Ontology tools. Thus, the reduction of METTL7A observed here in the cerebellar cortex in SZ patients and in the SZ murine models is more than likely due to a reduction of this protein in astrocytes, and more extensively in Bergmann glia cells. These cells are intimately related to the pia mater in the cerebellum to build the inner cerebrospinal fluid (CSF)-brain barrier. The integrity of this barrier is essential for the correct functioning and homeostasis of the cerebellum (Abbott *et al.*, 2010). The pia mater is separated from cerebellar parenchyma by a physical and immunological barrier formed by the end-feet of the Bergmann glia. These cells separate the cerebellar parenchyma into two immune compartments: the immune-privileged parenchyma in which *glia limitans* release anti-inflammatory factors and the non-immune privileged subpial space towards which these cells secrete pro-inflammatory molecules (Sofroniew, 2015). A pro-inflammatory brain state has been linked to schizophrenia including in the cerebellum (Trépanier *et al.*, 2016), with a possible role of *glia limitans* in this process. The fact that we report a reduction of METTL7A in both SZ patients and in the two stress animal models suggests a possible downregulation of METTL7A linked to stress in schizophrenia, with an impact on the immunological/inflammatory protection of Bergmann glia of brain parenchyma. However, further studies are needed to investigate the role of METTL7A in these cells.

In the context of SZ, a study on the prefrontal cortex (Brodmann area 9) found an increase in the RNA levels of METTL7A (Scarr *et al.*, 2018), while a study on the prefrontal cortex (Brodmann area 46/10) and a proteomic study of the anterior cingulate cortex (Brodmann area 24) observed a decrease in RNA and protein levels in SZ subjects, respectively (Kim *et al.*, 2007; Föcking *et al.*, 2015). Moreover, a previous study reported that METTL7A could be regulated by hormones, specifically testosterone, which is interesting from the point of view of the neurodevelopmental hypothesis. Subtle hormonal imbalances during particular periods of the intrauterine life could alter normal neuronal development (Quartier *et al.*, 2018). Reduced levels of METTL7A found in the cerebellum could therefore be related to hormone dysregulation in SZ patients.

No previous studies are available on the function of METTL7A in the cerebellum. However, other members of the METTL family have been reported to be involved in the correct proliferation of cerebellar granule cell progenitors, Purkinje cell maturation and the Bergmann glia organization pattern during the development of this region (C. Wang *et al.*, 2018), suggesting that METTL7A might also have a role during the development of the cerebellum, with an impact also on Bergmann glia and Purkinje neurons.

In our study, we observed that METTL7A localized also in lipid droplets in white matter cells. This result is in line with a the classical function proposed for METTL7A in lipid droplet formation (Zehmer *et al.*, 2008). Lipid droplet-containing microglia have been described in ageing and linked to inflammation and cognitive decline, both processes also related to schizophrenia (Marschallinger *et al.*, 2020). Here we observed a reduction of METTL7A in grey matter in chronic schizophrenia. Further studies are needed to investigate the possible deregulation of METTL7A in white matter in SZ.

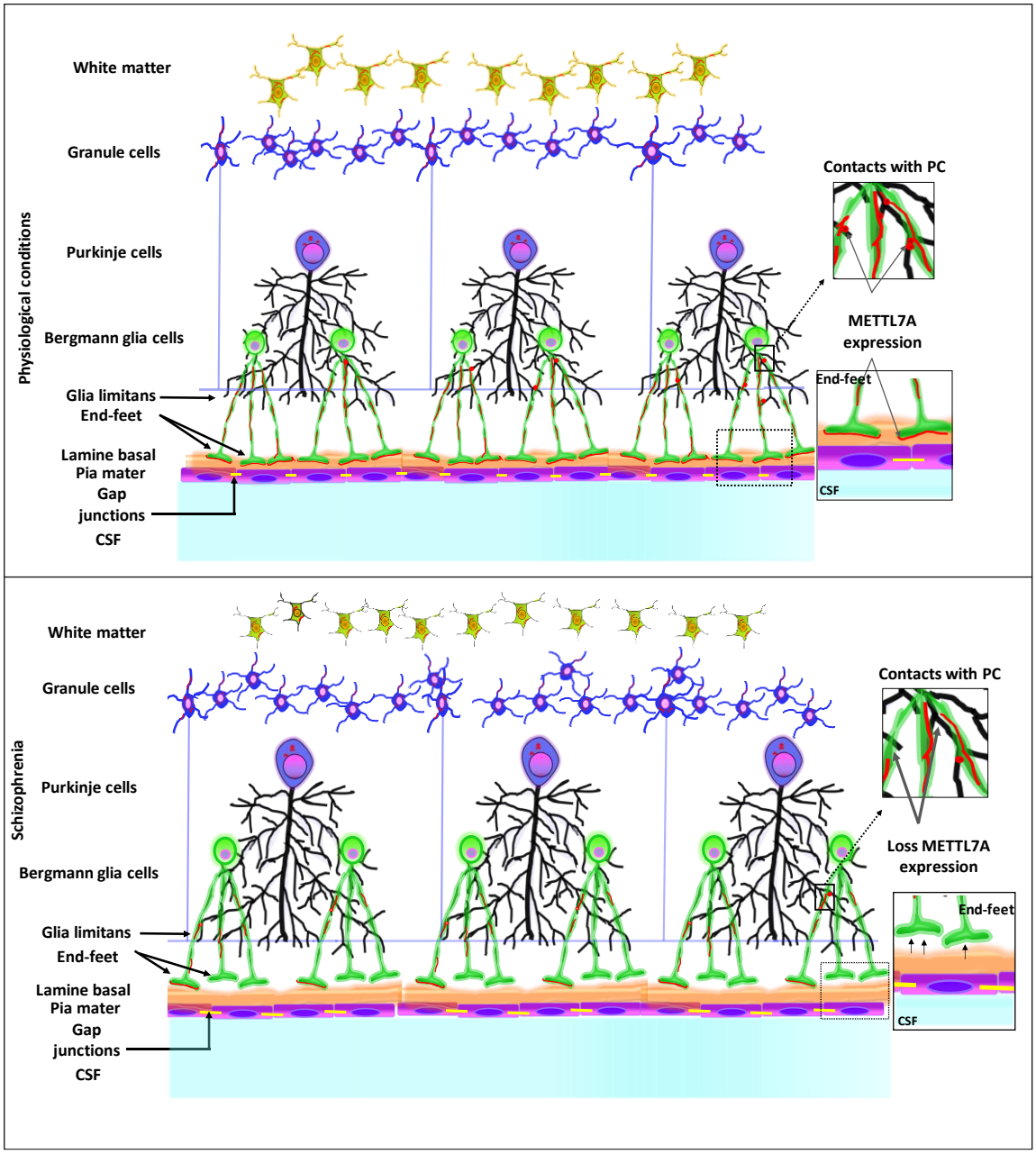

Figure 36. Model of possible contribution of METTL7A in Bergmann glia cells in the cerebellum in schizophrenia. A reduction of METTL7A in end-feet of the Bergmann glia may alter the anchorage of the end-feet to the pia mater, due at are intimately related to the pia mater in the cerebellum to build the inner cerebrospinal fluid (CSF)-brain barrier. The reduction of METTL7A may alterer this barrier and exposed cerebellar parenchyma to the damage molecules. Further METTL7A, have multiples contacts with Purkinje cells, a reduction in the MEETL7A may lead to the disruption in the connectivity of cerebellum with other brain area.

6.5. Correlation analysis between proteins altered in the cerebellum and executive function

In this proteomic study, we identified an altered axon guidance pathway in the cerebellum. DCTN1 was found to be one of the proteins altered in this pathway. Our screening of protein expression showed that DCTN1 is expressed at high levels in mainly Purkinje cells, and our correlation analysis showed that DCTN1 is positively correlated with executive functioning. In neurons, DCTN1 is involved in anterograde and retrograde axonal transport (Hafezparast *et al.*, 2003; Schnapp and Reese, 2006). However, the role of DCTN1 in schizophrenia is not clear. One study in peripheral blood found elevated mRNA levels of DCTN1 in subjects with high delusion stages (Kurian *et al.*, 2011). It would therefore be interesting to investigate DCTN1 in schizophrenia to examine in greater depth the axonal-related functions controlled by DCTN1 that could lead to altered circuit functioning that impacts on cognitive performance in schizophrenia.

6.6. Quantitative proteomic analyses of *postmortem* prefrontal cortex from schizophrenia and healthy controls

Our study has allowed us to identify and characterize the altered proteome profile in the prefrontal cortex in chronic schizophrenia. The unsupervised hierarchical clustering analysis revealed that the proteomic profile detected for each subject did not allow segregation between controls and schizophrenia samples. Although segregation between schizophrenia subjects and controls has been observed in other “omics” gene expression studies of *postmortem* prefrontal cortex (Santarelli *et al.*, 2020), our analysis failed to do so, suggesting that proteomic changes are not sufficient to identify a pathological sample in this region. Although large numbers of proteins are detected with advanced proteomics techniques, much larger numbers of transcripts are detected using microarray strategies. This difference in the method of analysing the functional expression of the genome could explain why proteome profiles detected using current techniques still do not detect in the prefrontal cortex changes in less abundant proteins that may be key to enabling the segregation of schizophrenia subjects from healthy controls.

Our results in the prefrontal cortex revealed small changes compared to the ones observed in the cerebellum. One possible explanation for these differences in the number of altered proteins detected in each region could be that the cerebellum in schizophrenia is a more sensitive area to producing alterations than in the prefrontal cortex. The cerebellum’s long maturation could also allow more changes to accumulate over the time. Alternatively, the high abundance of granule neurons in the cerebellum could make it easier to detect changes in this region compared to the prefrontal cortex where there are not so many histologically distinctive features.

6.6.1. Altered biological processes and pathways in the prefrontal cortex

Our results also showed enrichment of several biological processes implicated in vesicle-mediated transport, processing and antigen presentation via MHC class II, intracellular transport and selenium metabolism. The enriched pathways were directly related to the enriched biological processes. These pathways were related to MHC class II antigen presentation, vesicle-mediated transport, Golgi ER retrograde transport and the immune system. All these enriched categories were found to be down-regulated. The proteome profile in the prefrontal cortex in schizophrenia showed enriched categories related mainly to the immune system, which had previously been reported in proteomic studies in this area (Martins-De-Souza *et al.*, 2009).

Furthermore, our network analyses showed crosstalk between proteins involved in MHC class II antigen presentation, vesicle-mediated transport, Golgi ER retrograde transport and the immune system. Like the network analysis in the cerebellum, our network analysis in the prefrontal cortex showed crosstalk between proteins, supporting the notion that signalling pathways are dynamic events where just one protein can contribute to the dysfunction of several pathways.

6.6.2. Network generation from pathways enriched in the prefrontal cortex

6.6.2.1. Immune system

The immune system is essential for the correct maintenance of brain homeostasis. Similar to our observations in the cerebellum, our results from the proteome of the prefrontal cortex showed enrichment for biological processes and pathways related mainly to the immune response. It is well known that intrauterine or perinatal infections can increase vulnerability to schizophrenia (Brown and Derkits, 2010). Thus, an imbalance in the immune system has been proposed as one possible hypothesis that underlies this disorder (Kinney *et al.*, 2010)**.** The immune response involves major histocompatibility complex

class II antigen presentation (MHC-complex class II). This process is essential in the adaptative immune response (Bondy, 2020). The MHC class II molecule is assembled in the endoplasmic reticulum, transported to the Golgi apparatus and subsequently carried by the endocytic pathway to late endosomes and lysosomes where the MHC class II complexes are loaded with peptides from antigens and sent to the cell surface (Hiltbold and Roche, 2002). Furthermore, in schizophrenia MHC II has been proposed as a risk gene for this disorder (Consortium, 2009). In this context, our study identified an altered MHC-complex class II antigen presentation pathway in the prefrontal cortex in schizophrenia. Our analysis identified proteins that were altered in this pathway such as AP2M, which is involved in MHC II molecule trafficking (McCormick, Martina and Bonifacino, 2005), a process that is crucial in antigen presentation. RAB7 is a Rab GTPase that is involved in the regulation of degradative signalling of autophagosomes (Gutierrez *et al.*, 2004). During infection, the microorganism is internalized into the autophagosome, which fuses with lysosomes for the degradation of its contents (Harrison *et al.*, 2003). Altered expression of RAB7A could lead to the dysfunction of the degradation process, thereby contributing to dysregulation in the innate and adaptive response. Moreover, our analysis identified ACTR1A, an actin-related protein that participates in the dynactin complex (Eckley *et al.*, 1999). A study associated ACTR1A with the regulation of Toll-like receptor 2 (TLR2) signalling (Re and Strominger, 2001). This signalling has an active function in the innate immune response and the recognition of microbial products in dendritic cells in the brain. However, there is no evidence of the role of ACTR1A in the adaptative immune response. Moreover, ACTR1A could interact with DCTN5 since both are involved in the dynactin complex (Eckley *et al.*, 1999; Urnavicius *et al.*, 2015), which is involved in the activity of dynein during several intracellular motility processes (Jaarsma and Hoogenraad, 2015). Dynactin is recruited to the Golgi membrane by RAB 6 and 7 GTPases, which contribute to the motility of Golgi-associated vesicles (Short *et al.*, 2002). In this context, we found altered pathways related to vesicle-mediate transport and Golgi-

to-ER retrograde transport. Altered vesicle-mediated transport could be a reflection of the disruption in RAB6 and RAB7, proteins that are altered in this pathway that affect the recruitment of dynactin to the Golgi membrane. These pathways could be directly related to the immune system. The Golgi apparatus has recently been proposed as a signalling station that facilitates processes related to the innate immune response (Chen and Chen, 2018) and the interface between the Golgi, endoplasmic reticulum and mitochondria has been proposed to form an activity core in inflammasome activation (Chen and Chen, 2018).

Furthermore, a study has shown that palmitoylation in the Golgi apparatus is an essential step for activation of interferon genes such as type I interferon in response to genetic pathogen material (Mukai *et al.*, 2016). In this regard, studies in the *postmortem* prefrontal cortex in schizophrenia subjects also identified an altered glycosylation process in the Golgi apparatus (Bauer *et al.*, 2010; Mueller, Haroutunian and Meador-woodruff, 2014). However, there are no studies that involved altered Golgi apparatus functioning with a dysfunction in the immune response in schizophrenia.

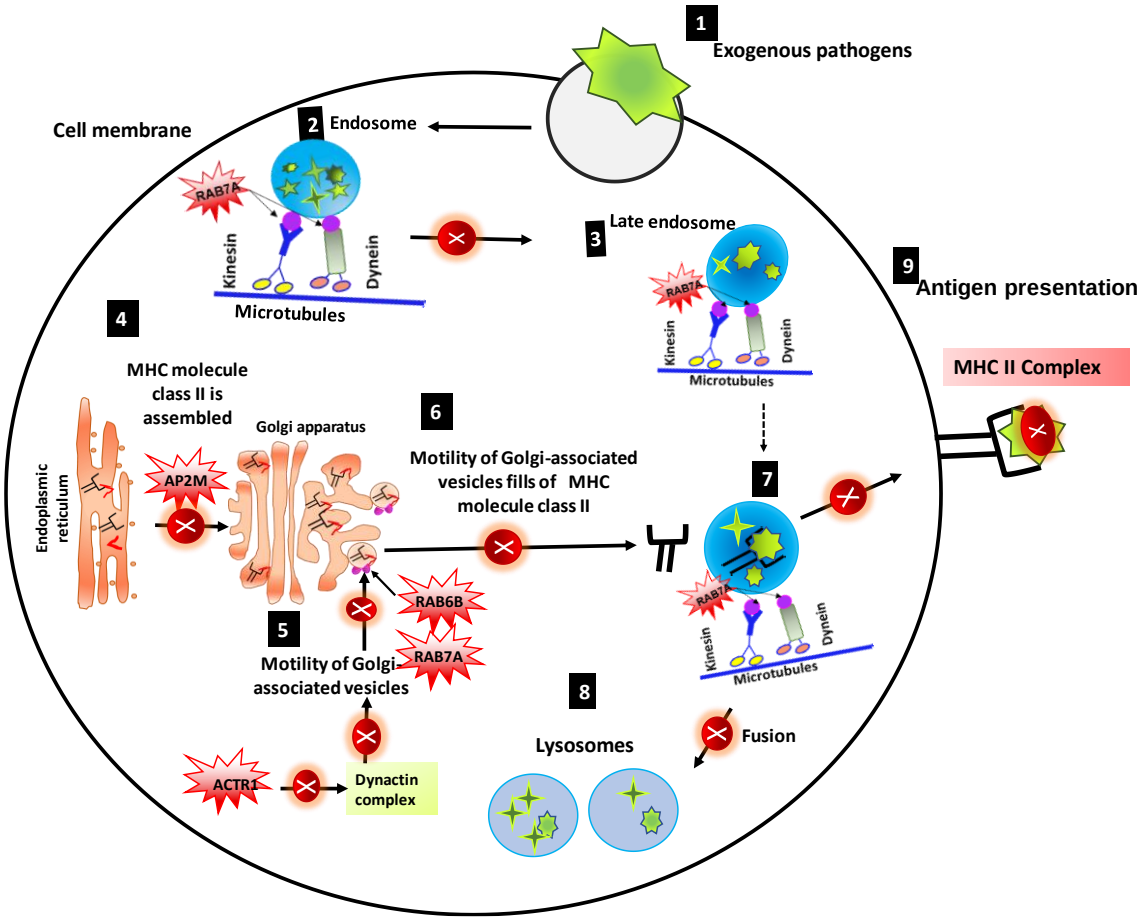

Figure 37. Model of possible contribution of altered immune system network to the dysfunction of the immune response in the prefrontal cortex in schizophrenia. The network analysis showed the integration pathways to into of an immune system module involved mainly in the Major histocompatibility complex class II antigen presentation (MHC class II antigen presentation). In this diagram are marked the steps that could be altered. Also, are highlighted in red the altered proteins in each step. Step 2-3, altered expression of RAB7A could generate disruption in the anchorage between endosome and kinesin-dynein complex, limiting the mobility of endosome. Step 4, APM2 could alter the MHC molecules assembled in the endoplasmic reticulum. Step 5, altered expression of ACTR1 could alter the recruitment of Dynactin complex and together with altered RAB7A and RAB6B expression could damage the correct motility of Golgi-associated vesicles. Step7, Finally altered motility vesicles could contribute to dysfunction in the delivery of MHC II molecules-antigen to the cell surface and contributes to the dysfunction adaptative immune response.

As in the cerebellum, our analysis in the prefrontal cortex also showed dysregulation in proteins related to vesicle-mediated transport. This process is highly related to the immune response. However, we cannot ignore the possibility that the vesicle-mediated transport proteins could be involved in transmission and neurotransmitter release, which are essential for correct neuronal communication (Fei *et al.*, 2008). Dysfunction in neuronal transmission in the prefrontal cortex with other areas such as the cerebellum could lead to dysfunction of the cortico-cerebellar thalamo-cortical circuit. It has also been reported that when neurons are injured, they could activate immune cells such as microglia that are distant from damage site. Vesicle-mediated transport mediates this process by transporting signalling molecules along the axon and inducing the activation of immune cells at a distance (De Jong *et al.*, 2005). This suggests that changes in vesicle-mediated transport in the prefrontal cortex could also affect cerebellar function.

Together, our results showed an altered immune system in two brain regions, the cerebellum and the prefrontal cortex, suggesting that the nervous system could be susceptible to the dysfunction of the immune system in schizophrenia. Moreover, the vesicle-mediated transport pathway was found to be altered in both the cerebellum and the prefrontal cortex, two brain areas that participle in the cortico-cerebellar thalamo-cortical circuit, which has been reported to be altered in schizophrenia. This result suggests a possible alteration in synaptic efficacy and communication between these areas, which could be involved in the impaired cognition reported in schizophrenia subjects.

VII. LIMITATIONS

The use of human *postmortem* brain constitutes a valuable tool in understanding the molecular pathways altered in several psychiatric disorders. However, it has limitations. Firstly, confounding factors such as age, *postmortem* delay, and pH have to be carefully explored. In our proteomic study, we did not find any association between these variables and the significantly altered proteins in the cerebellum and prefrontal cortex. Secondly, the possible effect of laterality in our samples cannot be ruled out. In this study only the right cerebellar hemisphere was available for the control group and this was compared to the left cerebellar hemisphere of schizophrenia patients, while in the prefrontal cortex only 10 right hemispheres and 10 left hemispheres were available for the control group, which were compared to the left prefrontal cortex hemispheres of schizophrenia patients. Thirdly, patients with chronic schizophrenia had been treated with long-term, heterogeneous antipsychotics medications. Fourthly, our study only included men, who do not represent a real population of this disorder. And finally, our study included elderly individuals due to the type of sample available.

VIII. CONCLUSIONS

1

1. Biological functions involving transport and cell communication/signal transduction are enriched in the pilot study of pooled samples from *postmortem* cerebellum.

2. 99 proteins are altered in the pilot study of pooled samples, 68 proteins are new proteins not previously reported in schizophrenia, and 11 proteins from the biological functions of transport and cell communication are the most robust candidates.

3. Proteomic profiling in individual proteomic analyses of *postmortem* cerebellum allowed most of the schizophrenia subjects to be segregated from control individuals, however, this analysis in the prefrontal cortex fails in segregating schizophrenia subjects from controls. This might suggest that the cerebellum is a brain region with more prominent changes in chronic schizophrenia compared to prefrontal cortex.

4. 250 proteins are altered in the proteomic analysis in individual samples of *postmortem* cerebellum and 167 corresponded to new altered proteins not previously reported in the cerebellum in chronic schizophrenia while only 43 proteins are altered in the prefrontal cortex, all of them previously related with schizophrenia.

5. The 250 proteins altered in the cerebellum are distributed across 185 loci, 54 of which are previously reported in schizophrenia and with loci 12q13.3, 16p13.3, 22q12.3, and Xq28 containing a higher number of genes encoding for the most abundant altered proteins. However, the 43 altered proteins in the prefrontal cortex are distributed in 37 loci and only one of them, the loci 8p21.2 with two altered proteins, is previously reported in schizophrenia. This suggests that proteins altered in the cerebellum are concentrated in some genomic regions while in the prefrontal cortex the altered proteins are widely distributed across the genome in chronic schizophrenia.

6. The altered proteins in the cerebellum in schizophrenia are the target genes of just 11 transcription factors: SP1, SP4, EGR1, KLF7, HNF4A, CTCF, MEF2A, GABPA, NRF1, YY1 and NYFA, however, in the prefrontal cortex the altered proteins are not related to a particular transcription program. This suggests that a small set of transcription factors could be responsible for altered molecular signalling in the cerebellum, but not in the prefrontal cortex in chronic schizophrenia.

7. Transport-related pathways are enriched for SP1-, KFL7-, EGR1-, HNF4A- and CTCF--altered targets. The signalling-related pathways are enriched for SP1-, KFL7- and EGR1-altered targets in the cerebellum. Pathways involving inflammatory/immune responses and apoptosis are enriched for SP1- and FKL7-altered targets in the cerebellum. This

suggests that SP1 and FKL7 could play a prominent role in chronic schizophrenia in this region.

8. Energy generation, neutrophil degranulation, vesicle-mediated transport and axonal guidance pathways are enriched in the 250 proteins altered in the cerebellum. This suggests an energy compromise, which could alter correct axonal signalling in the cerebellum in chronic schizophrenia.

9. The immune response and transport pathways are mainly altered in the 43 altered proteins in *postmortem* prefrontal cortex in schizophrenia, suggesting that this region could be an area susceptible to damage due to a failure in immune protection in this region.

10. The network generated by the downregulated pathways consists of two well-differentiated modules, energy and neutrophil degranulation, in the cerebellum while the network generated by the up-regulated pathways consists of a mixed module of different pathways. The network generated in the prefrontal cortex consist in a unique mixed module of immune system pathway.

11. YWHAZ is up-regulated in *postmortem* cerebellum in schizophrenia but not in the double-hit murine models for schizophrenia that used maternal deprivation combined with social isolation or chronic restraint stress as stressors.

12. CLASP1 is up-regulated in *postmortem* cerebellum in schizophrenia but downregulated in the double-hit murine model for schizophrenia that used maternal deprivation combined with social isolation as stressors.

13. NDUFB9 is downregulated in *postmortem* cerebellum in schizophrenia and the double-hit murine model for schizophrenia that used maternal deprivation combined with social isolation as stressors.

14. METTL7A is reduced in *postmortem* cerebellum in schizophrenia and in both double-hit murine models for schizophrenia that used maternal deprivation combined with social isolation or chronic restraint stress as stressors. This suggests that METTL7A could be linked to stress in schizophrenia.

15. METTL7A is located mainly in the end-feet of Bergman glia in *postmortem* cerebellum, indicating a possible role in the protection of cerebellar parenchyma and providing the first evidence of the localization of METTL7A in the human brain.

16. METTL7A is located in the projections of Bergmann glia that are in contact with Purkinje cells in *postmortem* cerebellum. This suggests that altered expression of METTL7A could disrupt signalling mediated by Purkinje cells in the cerebellum.

17. METTL7A is expressed in lipid droplets in white matter cells in *postmortem* cerebellum.

IX. ANNEXES

Note.

The “data set” 1 annex, “data set” 2 annex, containing the quantified proteins and significantly altered proteins in the cerebellum and “data set” 8 annex which corresponds to the quantified and significant altered proteins in the prefrontal cortex**,** are attached in a compressed file “Data set proteomic_Thesis_America Vera

Annex 3

Table 1. Genetic localization of altered proteins in the cerebellum. Loci previously reported in SZ by [a]Repke et al., 2014, study in Europe Population; [b] Li et al., 2017 study in Chinese ancestry cases

Region	Total number	Observated Number	Gene symbold	Previouly reported in SZ
22q12.3	53	4	SYN3;MYH9;TXN2;YWHAH	
12q13.3	57	4	CS;NACA;LRP1;DCTN2	Yes[a]
Xq28	149	4	ATP6AP1;BCAP31;ATP2B3;CD99L2	
16p13.3	238	4	UBE2I;ELOB;NDUFB10;TRAP1	Yes[b]
7p13	41	3	DBNL;PPIA;PGAM2	
6q25.3	43	3	SOD2;TCP1;ACAT2	
1p36.22	61	3	LZIC;CLSTN1;TARDBP	
12q13.12	62	3	GPD1;METTL7A;DIP2B	
17p13.3	68	3	YWHAE;PAFAH1B1;PITPNA	Yes[a-b]
11q13.4	76	3	RPS3;NUMA1;ARRB1	
9q34.11	82	3	CRAT;SPTAN1;SET	
22q11.21	95	3	CRKL;COMT;BCL2L13	
11p15.5	98	3	HRAS;CEND1;SLC25A22	
4q34.2	6	2	SPCS3;GPM6A	Yes[a-b]
4q21.22	13	2	HNRNPDL;COPS4	
13q14.13	16	2	LCP1;TPT1	
2q32.1	19	2	NCKAP1;ITGAV	Yes[a-b]
5q34	22	2	GABRA6;RARS	
2q14.3	24	2	UGGT1;CLASP1	
7q31.1	26	2	DLD;NRCAM	Yes[a-b]
9q31.3	32	2	TXN;GNG10	
15q21.2	33	2	DMXL2;GNB5	
8q22.3	34	2	ATP6V1C1;YWHAZ	Yes[b]
1q23.2	35	2	IGSF8;CADM3	Yes[b]
4q24	35	2	CISD2;PPA2	Yes[a-b]
3q21.3	52	2	MGLL;RPN1	
1p36.12	55	2	HP1BP3;HNRNPR	
6q21	62	2	PREP;MARCKS	Yes[b]
21q22.11	74	2	ATP5PO;SOD1	
17p13.2	75	2	PFN1;C1QBP	
2p23.3	77	2	DPYSL5;RAB10	
2q35	89	2	ARPC2;ATIC	
12q24.31	93	2	CAMKK2;DIABLO	Yes[a-b]
20p13	96	2	SIRPA;IDH3B	
19q13.43	100	2	UBE2M;TRIM28	
17q11.2	104	2	OMG;MYO18A	
17q25.1	107	2	RAB37;ATP5PD	
16q22.1	114	2	DYNC1LI2;SF3B3	Yes[a]
11q13.1	115	2	CAPN1;MACROD1	
14q11.2	121	2	NDRG2;PRMT5	
17q25.3	135	2	ARHGDIA;GPS1	
17p13.1	136	2	ACADVL;TXNDC17	
19q13.2	155	2	ATP1A3;SNRPA	
19q13.33	158	2	SLC17A7;NAPA	Yes[a-b]
11p15.4	188	2	STIM1;EIF4G2	
19p13.3	229	2	SF3A2;CIRBP	
9p23	7	1	PTPRD	
9q21.2	8	1	GNAQ	
10p11.22	9	1	KIF5B	
3q13.12	9	1	CD47	
6q14.3	10	1	SYNCRIP	
5q22.1	11	1	CAMK4	
8q23.1	11	1	ENY2	
10p12.2	12	1	PIP4K2A	
2p24.3	12	1	DDX1	
10q21.2	13	1	ANK3	Yes[b]
11p15.2	13	1	C11orf58	
12q21.1	13	1	RAB21	
13q12.13	13	1	AMER2	

Continuation of annex 3

Region	Total number	Observated Number	Gene symbold	Previouly reported in SZ
16p13.2	13	1	USP7	Yes[a-b]
2p13.2	13	1	CCT7	Yes[a-b]
14q23.2	14	1	PPP2R5E	
2q36.1	14	1	SERPINE2	
8q12.3	14	1	GGH	
9p21.1	14	1	NDUFB6	
11q14.2	15	1	PICALM	
12q21.33	15	1	ATP2B1	Yes[a-b]
22q11.22	15	1	MAPK1	
5q12.1	15	1	NDUFAF2	Yes[a]
7p21.3	15	1	NDUFA4	
3p14.2	16	1	CADPS	Yes[b]
10q23.2	17	1	SNCG	
12q21.2	17	1	NAP1L1	
2q23.3	17	1	CACNB4	
4p13	17	1	UCHL1	
13q32.1	18	1	RAP2A	
18p11.22	18	1	RAB12	
5p15.2	18	1	CMBL	
9q21.32	18	1	HNRNPK	Yes[a-b]
11q25	19	1	VPS26B	Yes[a-b]
1p13.1	19	1	ATP1A1	
5q23.1	19	1	HSD17B4	
7q21.11	19	1	PCLO	Yes[b]
7q31.2	19	1	CAPZA2	
14q32.11	20	1	DGLUCY	
18q22.3	20	1	CYB5A	
21q22.12	20	1	CBR1	
8q21.11	20	1	GDAP1	
Xp22.11	20	1	SMS	
11q13.5	21	1	MAP6	
8p11.23	21	1	ERLIN2	Yes[b]
3q22.3	22	1	MRAS	Yes[a]
3q26.33	22	1	NDUFB5	Yes[a-b]
11q13.3	23	1	CTTN	
12q21.31	23	1	LIN7A	
4q23	23	1	ADH5	
15q15.3	24	1	PDIA3	
1p36.31	24	1	RPL22	
12q24.23	26	1	RAB35	
13q13.3	26	1	SPART	Yes[b]
20p11.23	26	1	SNX5	
2p25.3	26	1	RPS7	
5q23.2	26	1	CSNK1G3	Yes[b]
1q25.1	27	1	PRDX6	
21q21.3	28	1	ATP5PF	
6q13	28	1	RIMS1	Yes[a-b]
7p15.2	28	1	HIBADH	
10q24.1	29	1	PGAM1	
12q24.13	29	1	ERP29	
10p15.1	30	1	AKR1C2	
13q12.11	30	1	PSPC1	Yes[b]
15q22.2	30	1	TPM1	Yes[a-b]
1p22.3	30	1	DDAH1	
7p14.1	30	1	EPDR1	
9q22.31	31	1	IARS	
12q22	32	1	NDUFA12	
2q33.3	32	1	NDUFS1	
3p22.2	32	1	WDR48	Yes[b]
14q23.1	33	1	RTN1	Yes[b]

Continuation of annex 3

Region	Total number	Observated Number	Gene symbold	Previouly reported in SZ
12q15	34	1	RAP1B	
3p21.1	34	1	TKT	Yes[a-b]
3q13.33	34	1	COX17	
2p14	35	1	ACTR2	Yes[b]
5q35.1	35	1	NPM1	
9q22.33	35	1	NANS	Yes[b]
15q25.2	36	1	SH3GL3	Yes[a-b]
16q12.1	37	1	CBLN1	
3p21.2	37	1	TWF2	
4q35.1	37	1	SLC25A4	
9q31.1	37	1	ERP44	
2p13.1	38	1	DCTN1	Yes[b]
16p12.2	39	1	UQCRC2	
18q11.2	39	1	SNRPD1	
3q27.1	39	1	AP2M1	
11q14.1	40	1	PRCP	Yes[b]
5p15.33	40	1	TPPP	
8q22.1	40	1	UQCRB	
5q13.2	41	1	MAP1B	
5q31.2	41	1	HSPA9	Yes[a-b]
8q24.13	41	1	NDUFB9	
10q26.3	42	1	DPYSL4	
2p25.1	44	1	YWHAQ	
7p14.3	44	1	SCRN1	
16p12.3	46	1	THUMPD1	
1q25.3	46	1	ARPC5	
20q11.22	47	1	AHCY	
Xp11.22	47	1	HUWE1	
Xq22.1	47	1	TCEAL6	
22q11.23	49	1	DDT	
10q22.1	51	1	PSAP	
1q41	51	1	MARK1	
3p25.3	52	1	ATG7	
2q33.1	55	1	HSPD1	Yes[a-b]
6q27	55	1	PSMB1	Yes[b]
Xq24	56	1	SLC25A5	
1q21.2	59	1	SV2A	Yes[a-b]
1q22	60	1	NAXE	
2p11.2	63	1	CAPG	
14q12	65	1	GMPR2	Yes[a-b]
15q26.1	65	1	IDH2	Yes[a-b]
1p13.3	66	1	GSTM3	Yes[b]
22q13.2	67	1	POLDIP3	Yes[a-b]
1p34.3	71	1	SFPQ	
2q31.1	71	1	SLC25A12	
3q29	72	1	PAK2	
4p16.3	75	1	ATP5ME	
14q24.3	81	1	TMED10	
9p13.3	81	1	STOML2	
1p36.11	82	1	HMGCL	
Xp11.23	87	1	SYP	
11q23.3	88	1	MCAM	
20q13.12	91	1	YWHAB	
6p22.1	93	1	MOG	Yes[a-b]
17p11.2	95	1	COPS3	Yes[a-b]
20q13.33	96	1	TPD52L2	
19q13.12	97	1	CAPNS1	
17q21.31	102	1	DUSP3	
6p21.33	102	1	LSM2	Yes[b]
5q31.3	109	1	PURA	Yes[b]
17q12	120	1	LASP1	
17q21.2	125	1	ACLY	
8q24.3	126	1	PLEC	Yes[a-b]
1q32.1	128	1	CYB5R1	Yes[b]
7q22.1	137	1	ARPC1A	Yes [b]
3p21.31	164	1	TMA7	Yes [b]

Annex 4

Table 2. Correlation for protein level vs pH in cerebellum in schizophrenia subjects, FDR<0.1

Gene Symbol	*p*-value	FDR-derived significance thresholds	FDR-adjusted *p*-values a.k.a. *q*-values
TRIM28	0,0004	0,0004	0,1005
PGAM1	0,0014	0,0008	0,1689
DGLUCY	0,0024	0,0012	0,2039
HSD17B4	0,0036	0,0016	0,2117
PLEC	0,0043	0,0020	0,2117
RPS3	0,0051	0,0024	0,2117
CSNK1G3	0,0112	0,0028	0,2877
PURA	0,0120	0,0032	0,2877
YWHAB	0,0125	0,0036	0,2877
TXNDC17	0,0133	0,0040	0,2877
HSPD1	0,0140	0,0044	0,2877
TMED10	0,0145	0,0048	0,2877
RAP1B	0,0154	0,0052	0,2877
PAK2	0,0169	0,0056	0,2877
MAP6	0,0174	0,0060	0,2877
TARDBP	0,0184	0,0064	0,2877
NDRG2	0,0209	0,0068	0,3070
RAB12	0,0311	0,0072	0,4302
CISD2	0,0336	0,0076	0,4302
PPA2	0,0370	0,0080	0,4302
CAPN1	0,0374	0,0084	0,4302
BCL2L13	0,0379	0,0088	0,4302
ATP5ME	0,0433	0,0092	0,4302
NCKAP1	0,0435	0,0096	0,4302
MYH9	0,0467	0,0100	0,4302
CD47	0,0493	0,0104	0,4302
UBE2I	0,0499	0,0108	0,4302
CAMKK2	0,0514	0,0112	0,4302
NDUFA12	0,0540	0,0116	0,4302
SLC25A22	0,0553	0,0120	0,4302
YWHAZ	0,0559	0,0124	0,4302
ATP6V1C1	0,0603	0,0128	0,4302
SCRN1	0,0607	0,0132	0,4302
SLC25A4	0,0632	0,0136	0,4302
ATP5PO	0,0642	0,0140	0,4302
AKR1C2	0,0650	0,0144	0,4302
PDIA3	0,0684	0,0148	0,4302
SIRPA	0,0692	0,0152	0,4302
ACTR2	0,0695	0,0156	0,4302
LZIC	0,0714	0,0160	0,4302
ARPC5	0,0745	0,0164	0,4302
SLC17A7	0,0748	0,0168	0,4302
USP7	0,0755	0,0172	0,4302
ATP1A3	0,0757	0,0176	0,4302
PAFAH1B1	0,0819	0,0180	0,4422
HNRNPR	0,0828	0,0184	0,4422
TCP1	0,0833	0,0188	0,4422
PSAP	0,0849	0,0192	0,4422
ERP29	0,0872	0,0196	0,4449
RAP2A	0,0906	0,0200	0,4532
TRAP1	0,0937	0,0204	0,4575
HRAS	0,0952	0,0208	0,4575
GGH	0,0974	0,0212	0,4583
CADPS	0,0991	0,0216	0,4583
NANS	0,1032	0,0220	0,4583
SNRPD1	0,1076	0,0224	0,4583
YWHAE	0,1076	0,0228	0,4583
SF3B3	0,1081	0,0232	0,4583
ARRB1	0,1081	0,0236	0,4583
HNRNPDL	0,1139	0,0240	0,4746
DDX1	0,1194	0,0244	0,4893
CBLN1	0,1245	0,0248	0,5022
CS	0,1301	0,0252	0,5042
CYB5R1	0,1302	0,0256	0,5042
SPCS3	0,1311	0,0260	0,5042
DUSP3	0,1391	0,0264	0,5187
ATG7	0,1457	0,0268	0,5187
MYO18A	0,1469	0,0272	0,5187
LASP1	0,1471	0,0276	0,5187
RAB21	0,1477	0,0280	0,5187
TXN2	0,1480	0,0284	0,5187
YWHAH	0,1504	0,0288	0,5187
PRCP	0,1515	0,0292	0,5187
UGGT1	0,1571	0,0296	0,5258
HMGCL	0,1600	0,0300	0,5258
SOD2	0,1615	0,0304	0,5258
GDAP1	0,1620	0,0308	0,5258
PPIA	0,1712	0,0312	0,5276
LCP1	0,1718	0,0316	0,5276
YWHAQ	0,1719	0,0320	0,5276
TMA7	0,1731	0,0324	0,5276
SNX5	0,1754	0,0328	0,5276
SPART	0,1759	0,0332	0,5276
EPDR1	0,1829	0,0336	0,5276
NDUFB5	0,1842	0,0340	0,5276
TXN	0,1845	0,0344	0,5276
MOG	0,1875	0,0348	0,5276
ATP1A1	0,1887	0,0352	0,5276
CEND1	0,1891	0,0356	0,5276
CYB5A	0,1958	0,0360	0,5276
MAPK1	0,1959	0,0364	0,5276
CACNB4	0,1965	0,0368	0,5276
NDUFAF2	0,2003	0,0372	0,5276
RIMS1	0,2008	0,0376	0,5276
MRAS	0,2009	0,0380	0,5276
DIP2B	0,2062	0,0384	0,5276
PRMT5	0,2068	0,0388	0,5276
IGSF8	0,2086	0,0392	0,5276
SERPINE2	0,2089	0,0396	0,5276
DIABLO	0,2161	0,0400	0,5403
DBNL	0,2212	0,0404	0,5474
CLASP1	0,2249	0,0408	0,5511
PGAM2	0,2279	0,0412	0,5532
DLD	0,2469	0,0416	0,5666
IDH3B	0,2473	0,0420	0,5666
LIN7A	0,2482	0,0424	0,5666
C11orf58	0,2492	0,0428	0,5666
GMPR2	0,2494	0,0432	0,5666
TPD52L2	0,2498	0,0436	0,5666
SET	0,2520	0,0440	0,5666
BCAP31	0,2543	0,0444	0,5666
SYN3	0,2552	0,0448	0,5666
TPPP	0,2576	0,0452	0,5666
AHCY	0,2621	0,0456	0,5666
SYNCRIP	0,2622	0,0460	0,5666
COMT	0,2629	0,0464	0,5666
THUMPD1	0,2719	0,0468	0,5809
VPS26B	0,2770	0,0472	0,5862

Continuation of annex 4

Gene Symbol	*p*-value	FDR-derived significance thresholds	FDR-adjusted *p*-values a.k.a. *q*-values
RAB10	0,2790	0,0476	0,5862
LSM2	0,2816	0,0480	0,5866
DMXL2	0,2851	0,0484	0,5891
NRCAM	0,2897	0,0488	0,5936
GPD1	0,2944	0,0492	0,5940
PIP4K2A	0,2980	0,0496	0,5940
MGLL	0,2984	0,0500	0,5940
CCT7	0,2994	0,0504	0,5940
SV2A	0,3051	0,0508	0,5981
UQCRB	0,3062	0,0512	0,5981
SNRPA	0,3127	0,0516	0,6036
ATIC	0,3174	0,0520	0,6036
DCTN2	0,3181	0,0524	0,6036
RARS	0,3197	0,0528	0,6036
SF3A2	0,3211	0,0532	0,6036
CAPNS1	0,3306	0,0536	0,6168
COX17	0,3350	0,0540	0,6191
NAP1L1	0,3410	0,0544	0,6191
ELOB	0,3422	0,0548	0,6191
SYP	0,3444	0,0552	0,6191
NAPA	0,3465	0,0556	0,6191
SLC25A5	0,3467	0,0560	0,6191
SFPQ	0,3588	0,0564	0,6362
ACADVL	0,3638	0,0568	0,6406
C1QBP	0,3742	0,0572	0,6510
PFN1	0,3750	0,0576	0,6510
PSMB1	0,3796	0,0580	0,6514
PIP4K2A	0,3808	0,0584	0,6514
ERLIN2	0,3831	0,0588	0,6514
RPN1	0,3956	0,0592	0,6682
RPS7	0,4054	0,0596	0,6803
ADH5	0,4173	0,0600	0,6955
SNCG	0,4215	0,0604	0,6979
NPM1	0,4319	0,0608	0,7104
CLSTN1	0,4486	0,0612	0,7306
PCLO	0,4500	0,0616	0,7306
MARCKS	0,4557	0,0620	0,7349
PREP	0,4666	0,0624	0,7477
PSPC1	0,4767	0,0628	0,7591
GPM6A	0,4832	0,0632	0,7645
UCHL1	0,4863	0,0636	0,7646
CAMK4	0,4917	0,0640	0,7683
PPP2R5E	0,4979	0,0644	0,7704
ITGAV	0,5018	0,0648	0,7704
CIRBP	0,5023	0,0652	0,7704
IDH2	0,5090	0,0656	0,7741
ERP44	0,5109	0,0660	0,7741
POLDIP3	0,5189	0,0664	0,7758
PTPRD	0,5191	0,0668	0,7758
CMBL	0,5214	0,0672	0,7758
NACA	0,5442	0,0676	0,8051
GNB5	0,5537	0,0680	0,8098
ATP2B3	0,5539	0,0684	0,8098
CD99L2	0,5580	0,0688	0,8111
ARPC2	0,5644	0,0692	0,8137
NDUFB6	0,5668	0,0696	0,8137
CRAT	0,5752	0,0700	0,8137
SPTAN1	0,5757	0,0704	0,8137
NUMA1	0,5761	0,0708	0,8137
CBR1	0,5901	0,0712	0,8289
HSPA9	0,6068	0,0716	0,8475
TWF2	0,6112	0,0720	0,8488
DYNC1LI2	0,6214	0,0724	0,8552
HNRNPK	0,6226	0,0728	0,8552
GABRA6	0,6422	0,0732	0,8735
TCEAL6	0,6469	0,0736	0,8735
CAPG	0,6484	0,0740	0,8735
UBE2M	0,6499	0,0744	0,8735
SMS	0,6575	0,0748	0,8762
DCTN1	0,6589	0,0752	0,8762
SLC25A12	0,6626	0,0756	0,8765
PITPNA	0,6728	0,0760	0,8835
NDUFS1	0,6750	0,0764	0,8835
RPL22	0,6868	0,0768	0,8893
ARHGDIA	0,6889	0,0772	0,8893
DDAH1	0,6931	0,0776	0,8893
ARPC1A	0,6941	0,0780	0,8893
IGLC3	0,6999	0,0784	0,8893
STOML2	0,7065	0,0788	0,8893
DDT	0,7071	0,0792	0,8893
NDUFB10	0,7079	0,0796	0,8893
ACLY	0,7135	0,0800	0,8903
COPS4	0,7158	0,0804	0,8903
COPS3	0,7204	0,0808	0,8915
UQCRC2	0,7257	0,0812	0,8918
TPM1	0,7277	0,0816	0,8918
GNAQ	0,7375	0,0820	0,8949
DPYSL4	0,7377	0,0824	0,8949
TPT1	0,7410	0,0828	0,8949
ATP5PD	0,7497	0,0832	0,9011
IARS	0,7557	0,0836	0,9039
ATP5PF	0,7627	0,0840	0,9048
ATP6AP1	0,7639	0,0844	0,9048
AMER2	0,7688	0,0848	0,9048
PRDX6	0,7749	0,0852	0,9048
STIM1	0,7786	0,0856	0,9048
NDUFA4	0,7787	0,0860	0,9048
KIF5B	0,7840	0,0864	0,9048
GSTM3	0,7854	0,0868	0,9048
HIBADH	0,7945	0,0872	0,9112
GPS1	0,8104	0,0876	0,9251
PICALM	0,8187	0,0880	0,9303
ENY2	0,8253	0,0884	0,9309
NDUFB9	0,8301	0,0888	0,9309
AP2M1	0,8304	0,0892	0,9309
ATP2B1	0,8354	0,0896	0,9324
WDR48	0,8451	0,0900	0,9389
MCAM	0,8503	0,0904	0,9405
SOD1	0,8564	0,0908	0,9432
EIF4G2	0,8733	0,0912	0,9569
CAPZA2	0,8765	0,0916	0,9569
HP1BP3	0,8805	0,0920	0,9571
CTTN	0,8896	0,0924	0,9628
ANK3	0,8960	0,0928	0,9655
MACROD1	0,9042	0,0932	0,9691
RAB37	0,9071	0,0936	0,9691
METTL7A	0,9130	0,0940	0,9713
MARK1	0,9340	0,0944	0,9747
CRKL	0,9380	0,0948	0,9747
RTN1	0,9423	0,0952	0,9747
GNG10	0,9442	0,0956	0,9747
ACAT2	0,9446	0,0960	0,9747
TKT	0,9447	0,0964	0,9747
RAB35	0,9475	0,0968	0,9747
HUWE1	0,9478	0,0972	0,9747
OMG	0,9513	0,0976	0,9747
DPYSL5	0,9590	0,0980	0,9756
LRP1	0,9600	0,0984	0,9756
CADM3	0,9649	0,0988	0,9766
SH3GL3	0,9734	0,0992	0,9813
MAP1B	0,9828	0,0996	0,9868
NAXE	0,9949	0,1000	0,9949

Annex 5

Table 3. Correlation for protein level vs PMD in the cerebellum in schizophrenia subjects, FDR<0.1

Gene Symbol	*p*-value	FDR-derived significance thresholds	FDR-adjusted *p*-values a.k.a. *q*-values
SPTAN1	0,0027	0,0004	0,4263
SNRPA	0,0073	0,0008	0,4263
ATP5ME	0,0090	0,0012	0,4263
ERP29	0,0108	0,0016	0,4263
ATP5PF	0,0124	0,0020	0,4263
ATP2B3	0,0126	0,0024	0,4263
MARK1	0,0138	0,0028	0,4263
CAPZA2	0,0140	0,0032	0,4263
PSAP	0,0162	0,0036	0,4263
NUMA1	0,0182	0,0040	0,4263
CADM3	0,0188	0,0044	0,4263
GGH	0,0258	0,0048	0,5373
NDRG2	0,0362	0,0052	0,6960
CTTN	0,0418	0,0056	0,7456
BCL2L13	0,0460	0,0060	0,7492
GMPR2	0,0512	0,0064	0,7492
SET	0,0533	0,0068	0,7492
PITPNA	0,0542	0,0072	0,7492
LCP1	0,0595	0,0076	0,7492
RIMS1	0,0599	0,0080	0,7492
PAK2	0,0693	0,0084	0,7895
PCLO	0,0744	0,0088	0,7895
HSPA9	0,0772	0,0092	0,7895
PPIA	0,0831	0,0096	0,7895
ATP1A3	0,0867	0,0100	0,7895
NCKAP1	0,0871	0,0104	0,7895
C1QBP	0,0901	0,0108	0,7895
LRP1	0,0930	0,0112	0,7895
MGLL	0,0939	0,0116	0,7895
HNRNPK	0,0947	0,0120	0,7895
IDH2	0,0984	0,0124	0,7935
CBR1	0,1043	0,0128	0,8149
HSPD1	0,1121	0,0132	0,8312
NDUFAF2	0,1133	0,0136	0,8312
GNAQ	0,1187	0,0140	0,8312
OMG	0,1221	0,0144	0,8312
UQCRC2	0,1269	0,0148	0,8312
TPM1	0,1279	0,0152	0,8312
HIBADH	0,1297	0,0156	0,8312
MARCKS	0,1448	0,0160	0,8904
MAP6	0,1552	0,0164	0,8904
DCTN2	0,1556	0,0168	0,8904
CEND1	0,1603	0,0172	0,8904
ERLIN2	0,1610	0,0176	0,8904
SF3B3	0,1682	0,0180	0,8904
CD47	0,1715	0,0184	0,8904
CYB5A	0,1747	0,0188	0,8904
SIRPA	0,1759	0,0192	0,8904
NDUFB10	0,1822	0,0196	0,8904
ATIC	0,1824	0,0200	0,8904
DCTN1	0,1851	0,0204	0,8904
AMER2	0,2002	0,0208	0,8904
PLEC	0,2028	0,0212	0,8904
ANK3	0,2033	0,0216	0,8904
NDUFB9	0,2070	0,0220	0,8904
UBE2I	0,2083	0,0224	0,8904
COPS4	0,2148	0,0228	0,8904
AKR1C2	0,2227	0,0232	0,8904
COMT	0,2259	0,0236	0,8904
RPS3	0,2262	0,0240	0,8904
MCAM	0,2266	0,0244	0,8904
ARRB1	0,2304	0,0248	0,8904
ARHGDIA	0,2355	0,0252	0,8904
MAPK1	0,2357	0,0256	0,8904
PAFAH1B1	0,2360	0,0260	0,8904
SOD2	0,2369	0,0264	0,8904
ARPC2	0,2388	0,0268	0,8904
TXN	0,2465	0,0272	0,8904
CAPN1	0,2490	0,0276	0,8904
COPS3	0,2549	0,0280	0,8904
GABRA6	0,2560	0,0284	0,8904
UQCRB	0,2564	0,0288	0,8904
HRAS	0,2611	0,0292	0,8942
TCP1	0,2787	0,0296	0,9239
ATP5PD	0,2833	0,0300	0,9239
SNRPD1	0,2858	0,0304	0,9239
PPA2	0,2880	0,0308	0,9239
SLC25A5	0,2886	0,0312	0,9239
ERP44	0,2923	0,0316	0,9239
TRAP1	0,2957	0,0320	0,9239
HNRNPR	0,3192	0,0324	0,9620
IGSF8	0,3200	0,0328	0,9620
CAPG	0,3225	0,0332	0,9620
SNX5	0,3280	0,0336	0,9620
PDIA3	0,3349	0,0340	0,9620
GPM6A	0,3391	0,0344	0,9620
HMGCL	0,3464	0,0348	0,9620
DPYSL4	0,3545	0,0352	0,9620
ATP2B1	0,3564	0,0356	0,9620
RPL22	0,3614	0,0360	0,9620
TPT1	0,3655	0,0364	0,9620
RARS	0,3662	0,0368	0,9620
CIRBP	0,3729	0,0372	0,9620
ADH5	0,3777	0,0376	0,9620
PSPC1	0,3797	0,0380	0,9620
PREP	0,3833	0,0384	0,9620
GNB5	0,3839	0,0388	0,9620
DPYSL5	0,3941	0,0392	0,9620
UCHL1	0,4064	0,0396	0,9620
NACA	0,4187	0,0400	0,9620
RAP1B	0,4213	0,0404	0,9620
NDUFS1	0,4256	0,0408	0,9620
TPD52L2	0,4302	0,0412	0,9620
THUMPD1	0,4314	0,0416	0,9620
AP2M1	0,4329	0,0420	0,9620
PSMB1	0,4337	0,0424	0,9620
PRCP	0,4357	0,0428	0,9620
DYNC1LI2	0,4393	0,0432	0,9620
CS	0,4402	0,0436	0,9620
YWHAH	0,4432	0,0440	0,9620
RAB35	0,4488	0,0444	0,9620
MRAS	0,4535	0,0448	0,9620
TARDBP	0,4555	0,0452	0,9620
ATP1A1	0,4556	0,0456	0,9620
CCT7	0,4642	0,0460	0,9620

Continuation of annex 5

Gene Symbol	*p*-value	FDR-derived significance thresholds	FDR-adjusted *p*-values a.k.a. *q*-
TCEAL6	0,4671	0,0464	0,9620
ATP6AP1	0,4698	0,0468	0,9620
NDUFB5	0,4735	0,0472	0,9620
BCAP31	0,4756	0,0476	0,9620
PURA	0,4801	0,0480	0,9620
WDR48	0,4812	0,0484	0,9620
CRKL	0,4861	0,0488	0,9620
PGAM2	0,4995	0,0492	0,9620
ARPC5	0,5041	0,0496	0,9620
LSM2	0,5052	0,0500	0,9620
SYNCRIP	0,5090	0,0504	0,9620
GPD1	0,5129	0,0508	0,9620
SPART	0,5154	0,0512	0,9620
NRCAM	0,5200	0,0516	0,9620
TXNDC17	0,5239	0,0520	0,9620
SOD1	0,5246	0,0524	0,9620
RPS7	0,5257	0,0528	0,9620
COX17	0,5314	0,0532	0,9620
TXN2	0,5323	0,0536	0,9620
NDUFB6	0,5325	0,0540	0,9620
SCRN1	0,5325	0,0544	0,9620
CLSTN1	0,5393	0,0548	0,9620
TRIM28	0,5396	0,0552	0,9620
GDAP1	0,5412	0,0556	0,9620
RAB10	0,5423	0,0560	0,9620
PGAM1	0,5431	0,0564	0,9620
SERPINE2	0,5471	0,0568	0,9620
IGLC3	0,5522	0,0572	0,9620
RTN1	0,5541	0,0576	0,9620
VPS26B	0,5704	0,0580	0,9794
YWHAQ	0,5761	0,0584	0,9794
PRDX6	0,5782	0,0588	0,9794
DUSP3	0,5818	0,0592	0,9794
SYN3	0,5837	0,0596	0,9794
LZIC	0,5936	0,0600	0,9816
DDAH1	0,5949	0,0604	0,9816
SH3GL3	0,5988	0,0608	0,9816
CAPNS1	0,6095	0,0612	0,9816
DIP2B	0,6113	0,0616	0,9816
DIABLO	0,6154	0,0620	0,9816
CAMK4	0,6219	0,0624	0,9816
C11orf58	0,6259	0,0628	0,9816
MYO18A	0,6328	0,0632	0,9816
TPPP	0,6439	0,0636	0,9816
ITGAV	0,6524	0,0640	0,9816
DDT	0,6573	0,0644	0,9816
ENY2	0,6634	0,0648	0,9816
DLD	0,6639	0,0652	0,9816
STIM1	0,6724	0,0656	0,9816
ACLY	0,6745	0,0660	0,9816
SLC25A4	0,6779	0,0664	0,9816
GPS1	0,6803	0,0668	0,9816
NDUFA4	0,6817	0,0672	0,9816
CSNK1G3	0,6846	0,0676	0,9816
RAB21	0,6863	0,0680	0,9816
RPN1	0,6919	0,0684	0,9816
LASP1	0,6951	0,0688	0,9816
TMA7	0,7011	0,0692	0,9816
MYH9	0,7050	0,0696	0,9816
PICALM	0,7098	0,0700	0,9816
SMS	0,7180	0,0704	0,9816
IARS	0,7182	0,0708	0,9816
CISD2	0,7204	0,0712	0,9816
UBE2M	0,7293	0,0716	0,9816
SV2A	0,7310	0,0720	0,9816
PIP4K2A	0,7372	0,0724	0,9816
CMBL	0,7394	0,0728	0,9816
HSD17B4	0,7458	0,0732	0,9816
ACTR2	0,7496	0,0736	0,9816
UGGT1	0,7511	0,0740	0,9816
PFN1	0,7520	0,0744	0,9816
PTPRD	0,7548	0,0748	0,9816
SNCG	0,7569	0,0752	0,9816
GSTM3	0,7591	0,0756	0,9816
HP1BP3	0,7670	0,0760	0,9816
EIF4G2	0,7671	0,0764	0,9816
MAP1B	0,7679	0,0768	0,9816
RAB12	0,7771	0,0772	0,9816
HNRNPDL	0,7816	0,0776	0,9816
ATG7	0,7856	0,0780	0,9816
ARPC1A	0,7874	0,0784	0,9816
PPP2R5E	0,7915	0,0788	0,9816
DGLUCY	0,7952	0,0792	0,9816
SYP	0,7953	0,0796	0,9816
SFPQ	0,7956	0,0800	0,9816
DMXL2	0,7973	0,0804	0,9816
YWHAB	0,8040	0,0808	0,9816
LIN7A	0,8077	0,0812	0,9816
NDUFA12	0,8130	0,0816	0,9816
SLC25A22	0,8152	0,0820	0,9816
SLC25A12	0,8171	0,0824	0,9816
TWF2	0,8202	0,0828	0,9816
IDH3B	0,8267	0,0832	0,9816
NAP1L1	0,8295	0,0836	0,9816
RAB37	0,8410	0,0840	0,9816
POLDIP3	0,8453	0,0844	0,9816
CYB5R1	0,8471	0,0848	0,9816
TMED10	0,8498	0,0852	0,9816
TKT	0,8513	0,0856	0,9816
CAMKK2	0,8563	0,0860	0,9816
DBNL	0,8581	0,0864	0,9816
HUWE1	0,8598	0,0868	0,9816
CACNB4	0,8659	0,0872	0,9816
METTL7A	0,8671	0,0876	0,9816
CBLN1	0,8677	0,0880	0,9816
SF3A2	0,8720	0,0884	0,9816
NANS	0,8738	0,0888	0,9816
CADPS	0,8756	0,0892	0,9816
KIF5B	0,8824	0,0896	0,9824
NPM1	0,8841	0,0900	0,9824
ACAT2	0,8906	0,0904	0,9852
CLASP1	0,9014	0,0908	0,9897
NAXE	0,9026	0,0912	0,9897
CD99L2	0,9091	0,0916	0,9924
AHCY	0,9230	0,0920	0,9924
NAPA	0,9239	0,0924	0,9924
ACADVL	0,9246	0,0928	0,9924
CRAT	0,9276	0,0932	0,9924
ATP5PO	0,9289	0,0936	0,9924
STOML2	0,9416	0,0940	0,9930
MOG	0,9422	0,0944	0,9930
GNG10	0,9441	0,0948	0,9930
YWHAE	0,9476	0,0952	0,9930
ELOB	0,9496	0,0956	0,9930
RAP2A	0,9533	0,0960	0,9930
EPDR1	0,9610	0,0964	0,9942
USP7	0,9624	0,0968	0,9942
PRMT5	0,9705	0,0972	0,9946
SLC17A7	0,9775	0,0976	0,9946
PIP4K2A	0,9783	0,0980	0,9946
SPCS3	0,9881	0,0984	0,9946
DDX1	0,9881	0,0988	0,9946
MACROD1	0,9904	0,0992	0,9946
ATP6V1C1	0,9906	0,0996	0,9946
YWHAZ	0,9960	0,1000	0,9960

Annex 6

Table 4. Selection of the most robust candidates for each network module in cerebellum. Candidates with the most prominent fold change (FC) and a coefficient of variation (CV) lower than 0.35 are highlighted**.**

	Network Module (STRING)	Gene Name	SD Control	SD SZ	FC (SZ/C)	CV Control	CV SZ
Downregulated Pathways	Energy	CS	0,000245	0,000156	0,858124	0,146703	0,108566
		DLD	0,000142	0,000139	0,835429	0,088079	0,102801
		IDH3B	0,000057	0,000044	0,862722	0,132702	0,117903
		NDUFA4	0,000100	0,000144	0,659902	0,119778	0,259981
		NDUFB5	0,000025	0,000011	0,419620	0,537987	0,564118
		NDUFB6	0,000016	0,000010	0,712555	0,298479	0,250997
		NDUFB9	**0,000118**	**0,000064**	**0,645685**	**0,287949**	**0,240992**
		NDUFB10	0,000167	0,000150	0,754847	0,252435	0,299750
		NDUFS1	0,000211	0,000122	0,870124	0,156132	0,103624
		NDUFA12	0,000052	0,000014	0,690572	0,223932	0,085901
		UQCRB	0,000135	0,000167	0,787754	0,175430	0,274991
		UQCRC2	0,000589	0,000698	0,728364	0,204081	0,331805
		NDUFAF2	0,000011	0,000014	0,746617	0,180762	0,317846
	Neutrophil degranulation	HUWE1	0,000006	0,000005	0,818596	0,134399	0,144893
		ARPC5	0,000003	0,000004	0,831269	0,110751	0,158401
		ACTR2	0,000012	0,000016	0,868430	0,082191	0,122233
		ATG7	0,000004	0,000003	0,689307	0,139422	0,158797
		SIRPA	0,000211	0,000100	0,765766	0,215063	0,133834
		ERP44	0,000008	0,000013	0,821452	0,090543	0,170895
		METTL7A	**0,000037**	**0,000041**	**0,642297**	**0,184852**	**0,319271**
		DBNL	0,000026	0,000023	0,618095	0,368514	0,548538
		RAB37	0,000019	0,000011	0,715510	0,258637	0,202315
		ACLY	0,000061	0,000036	0,839426	0,183041	0,128750
		PRCP	0,000029	0,000017	0,741312	0,240482	0,196913
		PSAP	0,000428	0,000410	0,812950	0,128034	0,150838
		RAP1B	0,000173	0,000092	0,823486	0,168800	0,108220
		CAPN1	0,000015	0,000005	0,739852	0,284967	0,130011
		GGH	0,000030	0,000022	0,691188	0,180875	0,196457
		CD47	0,000137	0,000056	0,778743	0,178230	0,092833

Continuation of annex 6

	Network Module (STRING)	Gene Name	SD Control	SD SZ	FC (SZ/C)	CV Control	CV SZ
Upregulated pathways	Mixed module (Vesicle-mediated transport)	ARPC2	0,000033	0,000032	1,141656	0,095997	0,081326
		DCTN2	0,000053	0,000059	1,293853	0,154151	0,132907
		ARPC1A	0,000020	0,000020	1,297457	0,187044	0,146870
		RAB10	0,000065	0,000080	1,239172	0,207100	0,204896
		DCTN1	0,000036	0,000043	1,329391	0,219815	0,200548
		RAB21	0,000005	0,000011	1,327262	0,130299	0,196626
		SNX5	0,000006	0,000009	1,195561	0,154522	0,179864
		LRP1	0,000013	0,000010	1,152146	0,142467	0,100606
		ARRB1	0,000030	0,000031	1,310383	0,257914	0,203675
		PAFAH1B1	0,000034	0,000024	1,161844	0,132773	0,080726
		COPS4	0,000054	0,000034	1,287955	0,313744	0,155174
		SPTAN1	0,000956	0,001290	1,084858	0,051058	0,063495
		YWHAB	0,000290	0,000346	1,276625	0,166989	0,156221
		YWHAE	0,000435	0,000371	1,121619	0,116823	0,088686
		YWHAH	0,000133	0,000191	1,333372	0,228295	0,246840
		YWHAZ	**0,000516**	**0,000555**	**1,355259**	**0,155762**	**0,123565**
		NAPA	0,000031	0,000051	1,207060	0,098982	0,133873
	Mixed module (Axon guidance)	ARPC2	0,000033	0,000032	1,141656	0,095997	0,081326
		ARPC1A	0,000020	0,000020	1,297457	0,187044	0,146870
		CLASP1	**0,000005**	**0,000011**	**1,365445**	**0,124572**	**0,192996**
		ARRB1	0,000030	0,000031	1,310383	0,257914	0,203675
		MYH9	0,000035	0,000052	1,181797	0,116365	0,148585
		NRCAM	0,000039	0,000041	1,126540	0,064235	0,060120
		PITPNA	0,000032	0,000027	1,291011	0,241082	0,155915
		MAPK1	0,000079	0,000112	1,290899	0,136233	0,149938
		PSMB1	0,000028	0,000035	1,262384	0,177769	0,178623
		DPYSL5	0,000033	0,000037	1,134216	0,113367	0,110560
		SPTAN1	0,000956	0,001290	1,084858	0,051058	0,063495
		YWHAB	0,000290	0,000346	1,276625	0,166989	0,156221
	Mixed module (Apoptosis)	PLEC	0,000193	0,000266	1,285227	0,183287	0,196881
		DIABLO	0,000008	0,000015	1,306865	0,199729	0,272172
		PSMB1	0,000028	0,000035	1,262384	0,177769	0,178623
		SPTAN1	0,000956	0,001290	1,084858	0,051058	0,063495
		YWHAB	0,000290	0,000346	1,276625	0,166989	0,156221
		YWHAE	0,000435	0,000371	1,121619	0,116823	0,088686
		YWHAH	0,000133	0,000191	1,333372	0,228295	0,246840
		YWHAZ	**0,000516**	**0,000555**	**1,355259**	**0,155762**	**0,123565**
	Mixed module (Rho GTPase Effectors)	ARPC2	0,000033	0,000032	1,141656	0,095997	0,081326
		ARPC1A	0,000020	0,000020	1,297457	0,187044	0,146870
		CLASP1	**0,000005**	**0,000011**	**1,365445**	**0,124572**	**0,192996**
		MYH9	0,000035	0,000052	1,181797	0,116365	0,148585
		PAFAH1B1	0,000034	0,000024	1,161844	0,132773	0,080726
		MAPK1	0,000079	0,000112	1,290899	0,136233	0,149938
		YWHAB	0,000290	0,000346	1,276625	0,166989	0,156221
		YWHAE	0,000435	0,000371	1,121619	0,116823	0,088686
		YWHAH	0,000133	0,000191	1,333372	0,228295	0,246840
		YWHAZ	**0,000516**	**0,000555**	**1,355259**	**0,155762**	**0,123565**
	Mixed module (Signalling by Rho GTPases)	ARPC1A	0,000020	0,000020	1,297457	0,187044	0,146870
		CLASP1	**0,000005**	**0,000011**	**1,365445**	**0,124572**	**0,192996**
		ARHGDIA	0,000021	0,000031	1,362667	0,167251	0,181069
		MYH9	0,000035	0,000052	1,181797	0,116365	0,148585
		PAFAH1B1	0,000034	0,000024	1,161844	0,132773	0,080726
		MAPK1	0,000079	0,000112	1,290899	0,136233	0,149938
		YWHAB	0,000290	0,000346	1,276625	0,166989	0,156221
		YWHAE	0,000435	0,000371	1,121619	0,116823	0,088686
		YWHAH	0,000133	0,000191	1,333372	0,228295	0,246840
		YWHAZ	**0,000516**	**0,000555**	**1,355259**	**0,155762**	**0,123565**
	Mixed module (Cell Cycle)	DCTN2	0,000053	0,000059	1,293853	0,154151	0,132907
		DCTN1	0,000036	0,000043	1,329391	0,219815	0,200548
		CLASP1	**0,000005**	**0,000011**	**1,365445**	**0,124572**	**0,192996**
		NUMA1	0,000007	0,000009	1,273833	0,143884	0,143425
		PAFAH1B1	0,000034	0,000024	1,161844	0,132773	0,080726
		MAPK1	0,000079	0,000112	1,290899	0,136233	0,149938
		PSMB1	0,000028	0,000035	1,262384	0,177769	0,178623
		YWHAB	0,000290	0,000346	1,276625	0,166989	0,156221
		YWHAE	0,000435	0,000371	1,121619	0,116823	0,088686
		YWHAH	0,000133	0,000191	1,333372	0,228295	0,246840
		YWHAZ	**0,000516**	**0,000555**	**1,355259**	**0,155762**	**0,123565**

Annex 7

Table 5. Correlation for altered proteins in the cerebellum from vesicle-mediated transport pathway vs FAB total in schizophrenia subjects, FDR<0.1

Gene Symbol	p-value	FDR-derived significance thresholds	FDR-adjusted p-values a.k.a. q-values	Pearsons'r
DCTN1	**0,0028**	**0,0059**	**0,0484**	**0,8333**
DCTN2	0,1374	0,0118	0,5375	0,5040
RAB21	0,1426	0,0176	0,5375	-0,5671
SPTAN1	0,1438	0,0235	0,5375	-0,4971
NAPA	0,1527	0,0294	0,5375	0,4877
YWHAE	0,2313	0,0353	0,6784	-0,4164
ARPC1A	0,3375	0,0412	0,8487	0,3393
YWHAZ	0,3902	0,0471	0,8584	-0,3058
SNX5	0,5060	0,0529	0,9211	0,2390
YWHAH	0,5271	0,0588	0,9211	0,2276
ARPC2	0,6126	0,0647	0,9211	0,1831
COPS4	0,6752	0,0706	0,9211	-0,1520
RAB10	0,6947	0,0765	0,9211	0,1424
ARRB1	0,7904	0,0824	0,9211	-0,0967
PAFAH1B1	0,8471	0,0882	0,9211	-0,0703
YWHAB	0,8807	0,0941	0,9211	-0,0547
LRP1	0,8897	0,1000	0,9211	-0,0506

Annex 8

Table 6. Proteins significantly regulated in *postmortem* prefrontal cortex in schizophrenia

ID Uniprot	Gene symbol	Controls(N)	SZ(N)	Normalized Mean_Controls	Normalized Mean_SZ	Normalized SD_C	Normalized SD_SZ	*p* -value	FDR-derived significance threshold		FDR-adjusted *p* -values	Mol. weight [Da]	Peptide number	Sequence coverage [%]	MS/MS Count
O00154	ACOT7	20	20	1	0,7474	0,1592	0,0915	0,0000	0,0001	*	0,0017	41796	12	45.8	559
P63244	GNB2L1	20	20	1	0,7908	0,1298	0,1166	0,0000	0,0001	*	0,0043	35076	14	75.7	280
B5MDF5	RAN	20	20	1	0,8317	0,1218	0,0984	0,0000	0,0002	*	0,0102	26224	11	48.1	408
P61163	ACTR1A	20	20	1	0,8700	0,0971	0,0723	0,0000	0,0002	*	0,0102	42613	17	57.4	673
C9JFZ1	SYNJ1	20	20	1	0,8588	0,1080	0,0737	0,0000	0,0003	*	0,0102	149.3	36	41	1121
Q9NRW1	RAB6B	20	20	1	0,7972	0,1584	0,0995	0,0000	0,0003	*	0,0102	23461	7	42.8	215
P10915	HAPLN1	20	20	1	0,7840	0,1563	0,1404	0,0000	0,0004	*	0,0134	40165	6	25.7	160
P19174	PLCG1	20	20	1	0,8384	0,1149	0,1161	0,0001	0,0004	*	0,0195	148.53	14	20.2	246
P17612	PRKACA;KIN27	20	20	1	0,8490	0,1206	0,0957	0,0001	0,0005	*	0,0211	40589	13	41.6	384
A0A087WY71	AP2M1	20	20	1	0,8428	0,1295	0,0959	0,0001	0,0005	*	0,0214	49526	17	52.8	544
P53396	ACLY	20	20	1	0,8739	0,0998	0,0913	0,0002	0,0006	*	0,0311	120.84	22	31.2	589
O75533	SF3B1	20	20	1	1,1886	0,1380	0,1502	0,0002	0,0006	*	0,0316	145.83	18	25.2	252
P36543	ATP6V1E1;ATP6V1E2	20	20	1	0,8661	0,1282	0,0842	0,0004	0,0007	*	0,0673	26145	15	68.1	750
P53680	AP2S1	20	20	1	0,8599	0,1106	0,1214	0,0005	0,0007	*	0,0673	17018	6	55.6	288
Q13509	TUBB3	20	20	1	0,8211	0,1350	0,1617	0,0005	0,0008	*	0,0673	50432	13	53.6	982
F8WCF6	ARPC4-TTLL3;ARPC4	20	20	1	0,8226	0,1336	0,1611	0,0005	0,0008	*	0,0673	21058	6	40.9	144
O95352	ATG7	20	20	1	0,8213	0,1455	0,1581	0,0006	0,0009	*	0,0755	77959	12	23.6	131
P53004	BLVRA	20	20	1	0,8214	0,1632	0,1413	0,0007	0,0009	*	0,0764	33428	10	35.8	147
P05198	EIF2S1	20	20	1	0,8269	0,1654	0,1304	0,0008	0,0010	*	0,0783	36112	11	56.2	271
P61204	ARF3	20	20	1	0,7406	0,2521	0,1902	0,0008	0,0010	*	0,0783	20601	5	55.2	174
Q9C040	TRIM2	20	20	1	0,8786	0,1164	0,0941	0,0009	0,0011	*	0,0828	81529	25	58.7	825
P06744	GPI	20	20	1	0,8535	0,1558	0,0893	0,0010	0,0011	*	0,0858	63146	28	64.9	1829
E7EVJ5	CYFIP2	20	20	1	0,8706	0,1414	0,0750	0,0011	0,0012	*	0,0858	142.58	24	29.3	687
F8VZI0	PFKM	20	20	1	0,8680	0,1279	0,1079	0,0011	0,0012	*	0,0858	79642	19	39.9	823
F8W809	TXNRD1	20	20	1	0,8314	0,1854	0,0985	0,0012	0,0013	*	0,0858	54603	13	50	332
Q96I15	SCLY	20	20	1	0,7799	0,2308	0,1588	0,0013	0,0013	*	0,0858	48148	8	36.9	85
Q9NUP9	LIN7C	20	20	1	1,1269	0,0975	0,1302	0,0013	0,0014	*	0,0858	21834	7	60.9	233
P54578	USP14	20	20	1	0,8495	0,1611	0,1050	0,0014	0,0014	*	0,0858	56068	26	69.8	709
Q92896	GLG1	20	20	1	1,2420	0,2139	0,2292	0,0014	0,0015	*	0,0858	134.55	14	17.5	117
P41250	GARS	20	20	1	0,8698	0,1159	0,1238	0,0015	0,0015	*	0,0858	83165	18	40.1	503
E7ESP9	NEFM	20	20	1	0,7763	0,2373	0,1652	0,0015	0,0016	*	0,0858	98.38	63	74.6	3614
P62072	TIMM10	20	20	1	1,3247	0,2931	0,3070	0,0015	0,0016	*	0,0858	10333	4	75.6	97
P07196	NEFL	20	20	1	0,7826	0,2381	0,1480	0,0015	0,0017	*	0,0858	61516	35	63.9	2231
P20700	LMNB1	20	20	1	1,1520	0,1385	0,1436	0,0016	0,0017	*	0,0858	66408	16	38.1	160
P30038	ALDH4A1	20	20	1	0,8116	0,1968	0,1473	0,0016	0,0018	*	0,0858	61719	22	66.8	1073
Q9H993	ARMT1	20	20	1	0,8290	0,1796	0,1344	0,0016	0,0018	*	0,0858	51172	8	28.8	149
Q9BTE1	DCTN5	20	20	1	0,8349	0,1743	0,1289	0,0017	0,0019	*	0,0858	20126	6	50	113
Q12906	ILF3	20	20	1	1,1526	0,1371	0,1485	0,0017	0,0019	*	0,0858	95337	24	50.2	511
Q5M775	SPECC1	20	20	1	1,1574	0,1263	0,1655	0,0018	0,0020	*	0,0858	118.58	18	31.1	186
H3BT71	RBMX;RBMXL2	20	20	1	1,2258	0,2117	0,2129	0,0018	0,0020	*	0,0858	32197	6	23.3	107
P51148	RAB5C	20	20	1	0,8602	0,1526	0,1026	0,0018	0,0021	*	0,0858	23482	6	43.5	127
P51149	RAB7A	20	20	1	0,8700	0,1328	0,1111	0,0018	0,0021	*	0,0872	23489	10	63.8	368
O43390	HNRNPR	20	20	1	1,1514	0,1485	0,1391	0,0020	0,0022	*	0,0906	70942	22	43.4	471

X. REFERENCES

Abbott, N. J. *et al.* (2010) 'Structure and function of the blood-brain barrier', *Neurobiology of Disease*. Elsevier Inc., 37(1), pp. 13–25. doi: 10.1016/j.nbd.2009.07.030.

Akazawa, C. *et al.* (1994) 'Differential expression of five N-methyl-D-aspartate receptor subunit mRNAs in the cerebellum of developing and adult rats', *Journal of Comparative Neurology*, 347(1), pp. 150–160. doi: 10.1002/cne.903470112.

Al-Shammari, A. R. *et al.* (2018) 'Schizophrenia-related dysbindin-1 gene is required for innate immune response and homeostasis in the developing subventricular zone', *npj Schizophrenia*. Springer US, 4(1). doi: 10.1038/s41537-018-0057-5.

Alberstein, M. *et al.* (2007) 'Regulation of transcription of the RNA splicing factor hSlu7 by Elk-1 and Sp1 affects alternative splicing', pp. 1988–1999. doi: 10.1261/rna.492907.Shomron.

Altamura, A. C. *et al.* (2013) 'Neurodevelopment and inflammatory patterns in schizophrenia in relation to pathophysiology', *Progress in Neuro-Psychopharmacology and Biological Psychiatry*. Elsevier B.V., 42, pp. 63–70. doi: 10.1016/j.pnpbp.2012.08.015.

Andreasen, N. C. *et al.* (1996) 'Schizophrenia and cognitive dysmetria : A positron-emission tomography study of dysfunctional prefrontal-thalamic- cerebellar circuitry', 93(September), pp. 9985–9990.

Andreasen, N. C. (1997) 'The evolving concept of schizophrenia: From Kraepelin to the present and future', *Schizophrenia Research*, 28(2–3), pp. 105–109. doi: 10.1016/S0920-9964(97)00112-6.

Andreasen, N. C. *et al.* (1999) 'Defining the phenotype of schizophrenia: Cognitive dysmetria and its neural mechanisms', *Biological Psychiatry*. doi: 10.1016/S0006-3223(99)00152-3.

Andreasen, N. C. *et al.* (2018) '·" Cognitive of " Cognitive Dysmetria " as an Integrative Theory of Dysfunction in Cortical- Schizophrenia : A Dysfunction Subcortical--Cerebellar Circuitry ?', *Network*, (March), pp. 203–218.

Andreasen, N. C. and Pierson, R. (2008) 'The Role of the Cerebellum in Schizophrenia', *Biological Psychiatry*, 64(2), pp. 81–88. doi: 10.1016/j.biopsych.2008.01.003.

Armada-Moreira, A. *et al.* (2020) 'Going the Extra (Synaptic) Mile: Excitotoxicity as the Road Toward Neurodegenerative Diseases', *Frontiers in Cellular Neuroscience*,

14(April), pp. 1–27. doi: 10.3389/fncel.2020.00090.

Avramopoulos, D. (2010) 'Genetics of psychiatric disorders methods: Molecular approaches', *Psychiatric Clinics of North America*. Elsevier Ltd, 33(1), pp. 1–13. doi: 10.1016/j.psc.2009.12.006.

Ayuso-Mateos, J. L. *et al.* (2006) 'Estimating the prevalence of schizophrenia in Spain using a disease model', *Schizophrenia Research*, 86(1–3), pp. 194–201. doi: 10.1016/j.schres.2006.06.003.

Bache, W. K. and Delisi, E. (2018) 'The Sex Chromosome Hypothesis of Schizophrenia : Alive , Dead , or Forgotten ? A Commentary and Review', 02301, pp. 83–89. doi: 10.1159/000491489.

Baharnoori, M., Brake, W. G. and Srivastava, L. K. (2009) 'Prenatal immune challenge induces developmental changes in the morphology of pyramidal neurons of the prefrontal cortex and hippocampus in rats', *Schizophrenia Research*. Elsevier B.V., 107(1), pp. 99–109. doi: 10.1016/j.schres.2008.10.003.

Bahrami, S. and Drabløs, F. (2016) 'Advances in Biological Regulation Gene regulation in the immediate-early response process', *Advances in Biological Regulation*. Elsevier Ltd, 62(7491), pp. 37–49. doi: 10.1016/j.jbior.2016.05.001.

Bailoo, J. D. *et al.* (2016) 'Maternal separation followed by isolation-housing differentially affects prepulse inhibition of the acoustic startle response in C57BL/6 mice', *Developmental Psychobiology*, 58(8), pp. 937–944. doi: 10.1002/dev.21422.

Barlan, K., Rossow, M. J. and Gelfand, V. I. (2013) 'The journey of the organelle: Teamwork and regulation in intracellular transport', *Current Opinion in Cell Biology*. Elsevier Ltd, 25(4), pp. 483–488. doi: 10.1016/j.ceb.2013.02.018.

Barry, G. *et al.* (2014) 'The long non-coding RNA Gomafu is acutely regulated in response to neuronal activation and involved in schizophrenia-associated alternative splicing', (April 2013), pp. 486–494. doi: 10.1038/mp.2013.45.

Barton, R. A. (2012) 'Embodied cognitive evolution and the cerebellum', *Philosophical Transactions of the Royal Society B: Biological Sciences*, 367(1599), pp. 2097–2107. doi: 10.1098/rstb.2012.0112.

Bartos, M., Vida, I. and Jonas, P. (2007) 'Synaptic mechanisms of synchronized gamma oscillations in inhibitory interneuron networks', *Nature Reviews Neuroscience*, 8(1), pp.

45–56. doi: 10.1038/nrn2044.

Bast, T. *et al.* (2000) 'Effects of MK801 and neuroleptics on prepulse inhibition: Re-examination in two strains of rats', *Pharmacology Biochemistry and Behavior*, 67(3), pp. 647–658. doi: 10.1016/S0091-3057(00)00409-3.

Bauer, D. *et al.* (2010) 'Abnormal glycosylation of EAAT1 and EAAT2 in prefrontal cortex of elderly patients with schizophrenia', *Schizophrenia Research*. Elsevier B.V., 117(1), pp. 92–98. doi: 10.1016/j.schres.2009.07.025.

Baumann, O. *et al.* (2015) 'Consensus Paper: The Role of the Cerebellum in Perceptual Processes', *Cerebellum*, 14(2), pp. 197–220. doi: 10.1007/s12311-014-0627-7.

Becker, A. *et al.* (2003) 'Ketamine-induced changes in rat behaviour: A possible animal model of schizophrenia', *Progress in Neuro-Psychopharmacology and Biological Psychiatry*, 27(4), pp. 687–700. doi: 10.1016/S0278-5846(03)00080-0.

Ben-Shachar, D. (2009) 'The interplay between mitochondrial complex I, dopamine and Sp1 in schizophrenia', *Journal of Neural Transmission*, 116(11), pp. 1383–1396. doi: 10.1007/s00702-009-0319-5.

Bernard, J. A., Orr, J. M. and Mittal, V. A. (2017) 'Cerebello-thalamo-cortical networks predict positive symptom progression in individuals at ultra-high risk for psychosis', *NeuroImage: Clinical*. The Authors, 14, pp. 622–628. doi: 10.1016/j.nicl.2017.03.001.

Blake, D. J. *et al.* (2010) 'TCF4, schizophrenia, and pitt-hopkins syndrome', *Schizophrenia Bulletin*, 36(3), pp. 443–447. doi: 10.1093/schbul/sbq035.

Bleuler, M. and Bleuler, R. (1986) 'Dementia praecox oder die Gruppe der Schizophrenien: Eugen Bleuler.', *The British journal of psychiatry : the journal of mental science*, 149, pp. 661–662. doi: 10.1192/bjp.149.5.661.

Bondy, S. C. (2020) 'Aspects of the immune system that impact brain function', *Journal of Neuroimmunology*. Elsevier, 340(December 2019), p. 577167. doi: 10.1016/j.jneuroim.2020.577167.

Bordey, A. and Sontheimer, H. (2003) 'Modulation of glutamatergic transmission by bergmann glial cells in rat cerebellum in situ.', *Journal of neurophysiology*. United States, 89(2), pp. 979–988. doi: 10.1152/jn.00904.2002.

Bostan, A. C. and Strick, P. L. (2018) 'The basal ganglia and the cerebellum : nodes in an integrated network', *Nature Reviews Neuroscience*. Springer US, 19(June). doi:

10.1038/s41583-018-0002-7.

Brown, A. S. *et al.* (2004) 'Elevated Maternal Interleukin-8 Levels and Risk of Schizophrenia in Adult Offspring', *American Journal of Psychiatry*, 161(5), pp. 889–895. doi: 10.1176/appi.ajp.161.5.889.

Brown, A. S. and Derkits, E. J. (2010) 'Prenatal infection and schizophrenia: A review of epidemiologic and translational studies', *American Journal of Psychiatry*, 167(3), pp. 261–280. doi: 10.1176/appi.ajp.2009.09030361.

Bubber, P. *et al.* (2011) 'Abnormalities in the tricarboxylic acid (TCA) cycle in the brains of schizophrenia patients', *European Neuropsychopharmacology*. Elsevier B.V. and ECNP, 21(3), pp. 254–260. doi: 10.1016/j.euroneuro.2010.10.007.

Buckner, R. L. (2013) 'Perspective The Cerebellum and Cognitive Function : 25 Years of Insight from Anatomy and Neuroimaging', *Neuron*. Elsevier Inc., 80(3), pp. 807–815. doi: 10.1016/j.neuron.2013.10.044.

Burdick, K. E. *et al.* (2006) 'Genetic variation in DTNBP1 influences general cognitive ability', *Human Molecular Genetics*, 15(10), pp. 1563–1568. doi: 10.1093/hmg/ddi481.

Byrne, P. (2007) 'Managing the acute psychotic episode', *British Medical Journal*, 334(7595), pp. 686–692. doi: 10.1136/bmj.39148.668160.80.

Cahoy, J. D. *et al.* (2008) 'A transcriptome database for astrocytes, neurons, and oligodendrocytes: A new resource for understanding brain development and function', *Journal of Neuroscience*, 28(1), pp. 264–278. doi: 10.1523/JNEUROSCI.4178-07.2008.

Camargo, L. M. *et al.* (2007) 'Disrupted in Schizophrenia 1 interactome: Evidence for the close connectivity of risk genes and a potential synaptic basis for schizophrenia', *Molecular Psychiatry*, 12(1), pp. 74–86. doi: 10.1038/sj.mp.4001880.

Cao, H. *et al.* (2018) 'Cerebello-thalamo-cortical hyperconnectivity as a state-independent functional neural signature for psychosis prediction and characterization', *Nature Communications*. Springer US, 9(1). doi: 10.1038/s41467-018-06350-7.

Carlsson, A. and Lindqvist, M. (1963) 'Effect of Chlorpromazine or Haloperidol on Formation of 3-Methoxytyramine and Normetanephrine in Mouse Brain', *Acta Pharmacologica et Toxicologica*, 20(2), pp. 140–144. doi: 10.1111/j.1600-0773.1963.tb01730.x.

Carlsson, A., Lindqvist, M. and Magnusson, T. (1957) 'November 30, 1957', l, p. 4710.

Center for Behavioral Health Statistics and Quality (2016) 'IMPACT OF THE DSM-IV TO DSM-5 CHANGES ON THE NATIONAL SURVEY ON DRUG USE AND HEALTH. Substance Abuse and Mental health Services Adminsitration', (June), p. Rockville, MD.

Chan, M. K. *et al.* (2011) 'Evidence for disease and antipsychotic medication effects in post-mortem brain from schizophrenia patients', *Molecular Psychiatry*. Nature Publishing Group, 16(12), pp. 1189–1202. doi: 10.1038/mp.2010.100.

Chen, J. *et al.* (2016) 'Role played by the SP4 gene in schizophrenia and major depressive disorder in the Han Chinese population', *British Journal of Psychiatry*, 208(5), pp. 441–445. doi: 10.1192/bjp.bp.114.151688.

Chen, J. and Chen, Z. J. (2018) 'PtdIns4P on dispersed trans-Golgi network mediates NLRP3 inflammasome activation', *Nature*. Springer US, 564(7734), pp. 71–76. doi: 10.1038/s41586-018-0761-3.

Chen, M. H. *et al.* (2020) 'Cortico-thalamic dysconnection in early-stage schizophrenia: a functional connectivity magnetic resonance imaging study', *European Archives of Psychiatry and Clinical Neuroscience*. Springer Berlin Heidelberg, 270(3), pp. 351–358. doi: 10.1007/s00406-019-01003-2.

Chen, S.-Y., Huang, P.-H. and Cheng, H.-J. (2011) 'Disrupted-in-Schizophrenia 1-mediated axon guidance involves TRIO-RAC-PAK small GTPase pathway signaling', *Proceedings of the National Academy of Sciences*, 108(14), pp. 5861–5866. doi: 10.1073/pnas.1018128108.

Chen, T. *et al.* (2016) 'Tcf4 controls neuronal migration of the cerebral cortex through regulation of Bmp7', *Frontiers in Molecular Neuroscience*, 9(OCT2016), pp. 1–9. doi: 10.3389/fnmol.2016.00094.

Chew, L. J. *et al.* (2005) 'Interferon-γ inhibits cell cycle exit in differentiating oligodendrocyte progenitor cells', *Glia*, 52(2), pp. 127–143. doi: 10.1002/glia.20232.

Cho, R. Y., Konecky, R. O. and Carter, C. S. (2006) 'Impairments in frontal cortical γ synchrony and cognitive control in schizophrenia', *Proceedings of the National Academy of Sciences of the United States of America*, 103(52), pp. 19878–19883. doi: 10.1073/pnas.0609440103.

Choi, H. *et al.* (2015) 'Maturation of metabolic connectivity of the adolescent rat brain', *eLife*, 4(NOVEMBER2015), pp. 1–12. doi: 10.7554/eLife.11571.

Clark, D. *et al.* (2006) 'A proteome analysis of the anterior cingulate cortex gray matter in schizophrenia', *Molecular Psychiatry*, 11(5), pp. 459–470. doi: 10.1038/sj.mp.4001806.

Clark, D. *et al.* (2007) 'Altered proteins of the anterior cingulate cortex white matter proteome in schizophrenia', *Proteomics - Clinical Applications*, 1(2), pp. 157–166. doi: 10.1002/prca.200600541.

Clements, K. M. and Wainwright, P. E. (2010) 'Swim stress increases hippocampal Zif268 expression in the spontaneously hypertensive rat', *Brain Research Bulletin*. Elsevier Inc., 82(5–6), pp. 259–263. doi: 10.1016/j.brainresbull.2010.05.002.

Cohen, S. M. *et al.* (2015) 'The impact of NMDA receptor hypofunction on GABAergic neurons in the pathophysiology of schizophrenia', *Schizophrenia Research*. Elsevier B.V., 167(1–3), pp. 98–107. doi: 10.1016/j.schres.2014.12.026.

Comer, A. L. *et al.* (2020) 'The Inflamed Brain in Schizophrenia: The Convergence of Genetic and Environmental Risk Factors That Lead to Uncontrolled Neuroinflammation', *Frontiers in Cellular Neuroscience*, 14(August). doi: 10.3389/fncel.2020.00274.

Consortium, S. (2009) 'Common variants conferring risk of schizophrenia', 460(August), pp. 3–7. doi: 10.1038/nature08186.

Crespo-facorro, B. *et al.* (2001) 'Neural Basis of Novel and Well-Learned Recognition Memory in Schizophrenia : A Positron Emission Tomography Study', 231, pp. 219–231.

Crisafulli, C. *et al.* (2015) 'Progress in Neuro-Psychopharmacology & Biological Psychiatry A molecular pathway analysis informs the genetic background at risk for schizophrenia', *Progress in Neuropsychopharmacology & Biological Psychiatry*. Elsevier B.V., 59, pp. 21–30. doi: 10.1016/j.pnpbp.2014.12.009.

Date, D. *et al.* (2014) 'Kruppel-like transcription factor 6 regulates inflammatory macrophage polarization', *Journal of Biological Chemistry*, 289(15), pp. 10318–10329. doi: 10.1074/jbc.M113.526749.

Davis, J. *et al.* (2016) 'A review of vulnerability and risks for schizophrenia: Beyond the two hit hypothesis', *Neuroscience and Biobehavioral Reviews*. Elsevier Ltd, 65, pp. 185–194. doi: 10.1016/j.neubiorev.2016.03.017.

Davis, K. L. *et al.* (1991) 'Dopamine in schizophrenia: A review and reconceptualization', *American Journal of Psychiatry*, 148(11), pp. 1474–1486. doi: 10.1176/ajp.148.11.1474.

Decimo, I. *et al.* (2012) 'Meninges : from protective membrane to stem cell niche', 1(2),

pp. 92–105.

Delevich, K. *et al.* (2020) 'Parvalbumin Interneuron Dysfunction in a Thalamo-Prefrontal Cortical Circuit in Disc1 Locus Impairment Mice', *eNeuro*. Society for Neuroscience, 7(2), p. ENEURO.0496-19.2020. doi: 10.1523/ENEURO.0496-19.2020.

Desmond, J. E. *et al.* (1997) 'Lobular patterns of cerebellar activation in verbal working-memory and finger-tapping tasks as revealed by functional MRI', *Journal of Neuroscience*, 17(24), pp. 9675–9685. doi: 10.1523/jneurosci.17-24-09675.1997.

Doherty, J. L., O'Donovan, M. C. and Owen, M. J. (2012) 'Recent genomic advances in schizophrenia', *Clinical Genetics*, 81(2), pp. 103–109. doi: 10.1111/j.1399-0004.2011.01773.x.

Dolan, J. and Bench, C. J. (1993) 'Dorsolateral prefrontal cortex dysfunction in the major psychoses ; symptom or disease specificity ?', pp. 1290–1294.

Donohoe, G. *et al.* (2007) 'Variance in neurocognitive performance is associated with dysbindin-1 in schizophrenia: A preliminary study', *Neuropsychologia*. Elsevier Ltd, 45(2), pp. 454–458. doi: 10.1016/j.neuropsychologia.2006.06.016.

Drago, F. *et al.* (2017) 'ATP modifies the proteome of extracellular vesicles released by microglia and influences their action on astrocytes', *Frontiers in Pharmacology*, 8(DEC), pp. 1–14. doi: 10.3389/fphar.2017.00910.

Druart, M. and Le Magueresse, C. (2019) 'Emerging Roles of Complement in Psychiatric Disorders', *Frontiers in Psychiatry*, 10(August), pp. 1–13. doi: 10.3389/fpsyt.2019.00573.

Duclot, F. and Kabbaj, M. (2017) 'The role of early growth response 1 (EGR1) in brain plasticity and neuropsychiatric disorders', *Frontiers in Behavioral Neuroscience*, 11(March), pp. 1–20. doi: 10.3389/fnbeh.2017.00035.

Eckley, D. M. *et al.* (1999) 'Analysis of Dynactin Subcomplexes Reveals a Novel Actin-related Protein Associated with the Arp1 Minifilament Pointed End', 147(2), pp. 307–319.

Eisenman, L. M. *et al.* (1999) 'Neonatal Borna disease virus infection in the rat causes a loss of Purkinje cells in the cerebellum', *Journal of Neurovirology*. Taylor & Francis, 5(2), pp. 181–189. doi: 10.3109/13550289909022000.

Ellman, L. M. *et al.* (2010) 'Structural brain alterations in schizophrenia following fetal exposure to the inflammatory cytokine interleukin-8', *Schizophrenia Research*. Elsevier B.V., 121(1–3), pp. 46–54. doi: 10.1016/j.schres.2010.05.014.

English, Jane A. *et al.* (2011) 'The neuroproteomics of schizophrenia', *Biological Psychiatry*. Elsevier Inc., 69(2), pp. 163–172. doi: 10.1016/j.biopsych.2010.06.031.

English, Jane A *et al.* (2011) 'The Neuroproteomics of Schizophrenia', *BPS*. Elsevier Inc., 69(2), pp. 163–172. doi: 10.1016/j.biopsych.2010.06.031.

Etemadik, M. *et al.* (2020) 'Transcriptome analysis of fibroblasts from schizophrenia patients reveals differential expression of schizophrenia-related genes', pp. 1–9. doi: 10.1038/s41598-020-57467-z.

Ewald, R. C. and Cline, H. T. (2009) 'Receptors and 1 NMDA Brain Development', pp. 1–15.

Fatemi, S. H. *et al.* (2005) 'Prenatal viral infection in mouse causes differential expression of genes in brains of mouse progeny: A potential animal model for schizophrenia and autism', *Synapse*, 57(2), pp. 91–99. doi: 10.1002/syn.20162.

Fatemi, S. H. and Folsom, T. D. (2009) 'The neurodevelopmental hypothesis of Schizophrenia, revisited', *Schizophrenia Bulletin*, 35(3), pp. 528–548. doi: 10.1093/schbul/sbn187.

Fei, H. *et al.* (2008) 'Trafficking of vesicular neurotransmitter transporters', *Traffic*, 9(9), pp. 1425–1436. doi: 10.1111/j.1600-0854.2008.00771.x.

Feig, S. L. and Haberly, L. B. (2011) 'Surface-Associated Astrocytes , Not Endfeet , Form the Glia Limitans in Posterior Piriform Cortex and Have a Spatially Distributed , Not a Domain , Organization', 1969, pp. 1952–1969. doi: 10.1002/cne.22615.

Flores-Soto, M. E. *et al.* (2012) 'Structure and function of NMDA-type glutamate receptor subunits', *Neurología (English Edition)*, 27(5), pp. 301–310. doi: https://doi.org/10.1016/j.nrleng.2011.10.003.

Flynn, S. W. *et al.* (2003) 'Abnormalities of myelination in schizophrenia detected in vivo with MRI, and post-mortem with analysis of oligodendrocyte proteins', *Molecular Psychiatry*, 8(9), pp. 811–820. doi: 10.1038/sj.mp.4001337.

Föcking, M. *et al.* (2011) 'Common proteomic changes in the hippocampus in schizophrenia and bipolar disorder and particular evidence for involvement of cornu ammonis regions 2 and 3', *Archives of General Psychiatry*, 68(5), pp. 477–488. doi: 10.1001/archgenpsychiatry.2011.43.

Föcking, M. *et al.* (2015) 'Proteomic and genomic evidence implicates the postsynaptic

density in schizophrenia', *Molecular Psychiatry*, 20(4), pp. 424–432. doi: 10.1038/mp.2014.63.

Fournier, B. M. and Parkos, C. A. (2012) 'The role of neutrophils during intestinal inflammation'. Nature Publishing Group, 5(4), pp. 354–366. doi: 10.1038/mi.2012.24.

Friston, K. *et al.* (2016) 'The dysconnection hypothesis (2016)', *Schizophrenia Research*. The Authors, 176(2–3), pp. 83–94. doi: 10.1016/j.schres.2016.07.014.

Frohlich, J. and Van Horn, J. D. (2014) 'Reviewing the ketamine model for schizophrenia', *Journal of Psychopharmacology*, 28(4), pp. 287–302. doi: 10.1177/0269881113512909.

Frühbeis, C. *et al.* (2013) 'Neurotransmitter-Triggered Transfer of Exosomes Mediates Oligodendrocyte–Neuron Communication', *PLOS Biology*. Public Library of Science, 11(7), p. e1001604. Available at: https://doi.org/10.1371/journal.pbio.1001604.

Fujimaki, K. *et al.* (2018) 'Predictors of negative symptoms in the chronic phase of schizophrenia : A cross-sectional study', *Psychiatry Research*. Elsevier Ireland Ltd, 262(April 2017), pp. 600–608. doi: 10.1016/j.psychres.2017.09.051.

Funke, B. *et al.* (2004) 'Report Association of the', *Schizophrenia*, 1, pp. 891–898.

Fusté, M. *et al.* (2013) 'Reduced expression of SP1 and SP4 transcription factors in peripheral blood mononuclear cells in first-episode psychosis', *Journal of Psychiatric Research*. Elsevier Ltd, 47(11), pp. 1608–1614. doi: 10.1016/j.jpsychires.2013.07.019.

Fusté, M. *et al.* (2016) 'Specificity proteins 1 and 4, hippocampal volume and first-episode psychosis', *British Journal of Psychiatry*, 208(6), pp. 591–592. doi: 10.1192/bjp.bp.114.152140.

García-Bueno, B. *et al.* (2016) 'Evidence of activation of the Toll-like receptor-4 proinflammatory pathway in patients with schizophrenia', *Journal of Psychiatry and Neuroscience*, 41(3), pp. E46–E55. doi: 10.1503/jpn.150195.

Gardner, D. M. *et al.* (2010) 'International consensus study of antipsychotic dosing', *American Journal of Psychiatry*, 167(6), pp. 686–693. doi: 10.1176/appi.ajp.2009.09060802.

Ghiani, C. A. and Dell'Angelica, E. C. (2011) 'Dysbindin-containing complexes and their proposed functions in brain: From zero to (too) many in a decade', *ASN Neuro*, 3(2), pp. 109–124. doi: 10.1042/AN20110010.

Gi, H. S. *et al.* (2006) 'Maternal stress produces learning deficits associated with impairment of NMDA receptor-mediated synaptic plasticity', *Journal of Neuroscience*, 26(12), pp. 3309–3318. doi: 10.1523/JNEUROSCI.3850-05.2006.

Gilabert-Juan, J. *et al.* (2013) 'A "double hit" murine model for schizophrenia shows alterations in the structure and neurochemistry of the medial prefrontal cortex and the hippocampus', *Neurobiology of Disease*. Elsevier Inc., 59, pp. 126–140. doi: 10.1016/j.nbd.2013.07.008.

Giovanoli, S. *et al.* (2016) 'Preventive effects of minocycline in a neurodevelopmental two-hit model with relevance to schizophrenia', *Translational Psychiatry*. Nature Publishing Group, 6(4), pp. e772-9. doi: 10.1038/tp.2016.38.

Glantz, L. A. and Lewis, D. A. (2000) 'Decreased Dendritic Spine Density on Prefrontal Cortical Pyramidal Neurons in Schizophrenia', *Archives of General Psychiatry*, 57(1), pp. 65–73. doi: 10.1001/archpsyc.57.1.65.

Goldie, B. J. *et al.* (2014) 'Activity-associated miRNA are packaged in Map1b-enriched exosomes released from depolarized neurons', *Nucleic Acids Research*, 42(14), pp. 9195–9208. doi: 10.1093/nar/gku594.

Goodman, O. B. *et al.* (1996) 'β-Arrestin acts as a clathrin adaptor in endocytosis of the β2-adrenergic receptor', *Nature*, 383(6599), pp. 447–450. doi: 10.1038/383447a0.

Gourzis, P., Katrivanou, A. and Beratis, S. (2002) 'Symptomatology of the initial prodomal phase in schizophrenia', *Schizophrenia Bulletin*, 28(3), pp. 415–429. doi: 10.1093/oxfordjournals.schbul.a006950.

Goyal, N. *et al.* (2008) 'Neuropsychology of prefrontal cortex', *Indian Journal of Psychiatry*, 50(3), p. 202. doi: 10.4103/0019-5545.43634.

Graumann, J. *et al.* (2008) 'Stable isotope labeling by amino acids in cell culture (SILAC) and proteome quantitation of mouse embryonic stem cells to a depth of 5,111 proteins', *Molecular and Cellular Proteomics*, 7(4), pp. 672–683. doi: 10.1074/mcp.M700460-MCP200.

Güntekin, B. *et al.* (2013) 'Beta oscillatory responses in healthy subjects and subjects with mild cognitive impairment', *NeuroImage: Clinical*, 3, pp. 39–46. doi: 10.1016/j.nicl.2013.07.003.

Gutierrez, M. G. *et al.* (2004) 'Rab7 is required for the normal progression of the

autophagic pathway in mammalian cells', *Journal of Cell Science*, 117(13), pp. 2687–2697. doi: 10.1242/jcs.01114.

Haenschel, C. *et al.* (2009) 'Cortical oscillatory activity is critical for working memory as revealed by deficits in early-onset schizophrenia', *Journal of Neuroscience*, 29(30), pp. 9481–9489. doi: 10.1523/JNEUROSCI.1428-09.2009.

Hafezparast, M. *et al.* (2003) 'Mutations in dynein link motor neuron degeneration to defects in retrograde transport', *Science*, 300(5620), pp. 808–812. doi: 10.1126/science.1083129.

Hans, A. *et al.* (2004) 'Persistent, noncytolytic infection of neurons by Borna disease virus interferes with ERK 1/2 signaling and abrogates BDNF-induced synaptogenesis.', *The FASEB journal : official publication of the Federation of American Societies for Experimental Biology*, 18(7), pp. 863–865. doi: 10.1096/fj.03-0764fje.

Hansen, H. H. *et al.* (2004) 'Mechanisms leading to disseminated apoptosis following NMDA receptor blockade in the developing rat brain', *Neurobiology of Disease*, 16(2), pp. 440–453. doi: 10.1016/j.nbd.2004.03.013.

Hansen, K. B. *et al.* (2014) 'Distinct functional and pharmacological properties of triheteromeric GluN1/GluN2A/GluN2B NMDA receptors', *Neuron*, 81(5), pp. 1084–1096. doi: 10.1016/j.neuron.2014.01.035.

Harrison, R. E. *et al.* (2003) 'Phagosomes Fuse with Late Endosomes and/or Lysosomes by Extension of Membrane Protrusions along Microtubules: Role of Rab7 and RILP', *Molecular and Cellular Biology*, 23(18), pp. 6494–6506. doi: 10.1128/mcb.23.18.6494-6506.2003.

He, H. *et al.* (2019) 'Reduction in gray matter of cerebellum in schizophrenia and its influence on static and dynamic connectivity', *Human Brain Mapping*, 40(2), pp. 517–528. doi: 10.1002/hbm.24391.

Hewett, M. *et al.* (2002) 'BiGCaT Bioinformatics\rPharmGKB: the Pharmacogenetics Knowledge Base', *Nucleic Acids Res*, 30(1), pp. 163–165. Available at: http://www.bigcat.nl.

Hilge, J. *et al.* (2015) 'Linkage and whole genome sequencing identify a locus on 6q25 – 26 for formal thought disorder and implicate MEF2A regulation', *Schizophrenia Research*. Elsevier B.V., 169(1–3), pp. 441–446. doi: 10.1016/j.schres.2015.08.037.

Hilker, R. *et al.* (2018) 'Heritability of Schizophrenia and Schizophrenia Spectrum Based on the Nationwide Danish Twin Register', *Biological Psychiatry*. Elsevier Inc, 83(6), pp. 492–498. doi: 10.1016/j.biopsych.2017.08.017.

Hiltbold, E. M. and Roche, P. A. (2002) 'Trafficking of MHC class II molecules in the late secretory pathway', *Current Opinion in Immunology*, 14(1), pp. 30–35. doi: 10.1016/S0952-7915(01)00295-3.

Hochberg, Y. (1995) 'Controlling the False Discovery Rate : a Practical and Powerful Approach to Multiple Testing', (I), pp. 289–300. doi: 10.1111/j.2517-6161.1995.tb02031.x.

Hoff, P. (2015) 'The Kraepelinian tradition', *Dialogues in Clinical Neuroscience*, 17(1), pp. 31–41. doi: 10.5167/uzh-110661.

Holtzman, C. W. *et al.* (2013) 'Stress and neurodevelopmental processes in the emergence of psychosis', *Neuroscience*. IBRO, 249, pp. 172–191. doi: 10.1016/j.neuroscience.2012.12.017.

Honer, W. G. (2002) 'Abnormalities of SNARE Mechanism Proteins in Anterior Frontal Cortex in Severe Mental Illness', *Cerebral Cortex*, 12(4), pp. 349–356. doi: 10.1093/cercor/12.4.349.

Howarth, C., Gleeson, P. and Attwell, D. (2012) 'Updated energy budgets for neural computation in the neocortex and cerebellum', *Journal of Cerebral Blood Flow and Metabolism*. Nature Publishing Group, 32(7), pp. 1222–1232. doi: 10.1038/jcbfm.2012.35.

Howes, O. D. and Kapur, S. (2009) 'The dopamine hypothesis of schizophrenia: version III--the final common pathway.', *Schizophrenia bulletin*, 35(3), pp. 549–62. doi: 10.1093/schbul/sbp006.

Howes, O. D. and Nour, M. M. (2016) 'Dopamine and the aberrant salience hypothesis of schizophrenia', *World Psychiatry*, 15(1), pp. 3–4. doi: 10.1002/wps.20276.

Hu, T. M. *et al.* (2019) 'Functional analyses and effect of DNA methylation on the EGR1 gene in patients with schizophrenia', *Psychiatry Research*, 275(August 2018), pp. 276–282. doi: 10.1016/j.psychres.2019.03.044.

Hughes, C. S. *et al.* (2014) 'Ultrasensitive proteome analysis using paramagnetic bead technology', *Molecular Systems Biology*, 10(10), p. 757. doi: 10.15252/msb.20145625.

Huo, Y. *et al.* (2019) 'Functional genomics reveal gene regulatory mechanisms underlying schizophrenia risk', *Nature Communications*. Springer US, 10(1). doi: 10.1038/s41467-019-08666-4.

Ichikawa-tomikawa, N. *et al.* (2012) 'Laminin α 1 is essential for mouse cerebellar development', *Matrix Biology*. International Society of Matrix Biology, 31(1), pp. 17–28. doi: 10.1016/j.matbio.2011.09.002.

Ikonomidou, C. *et al.* (1999) 'Blockade of NMDA Receptors and Apoptotic Neurodegeneration in the Developing Brain Published by : American Association for the Advancement of Science Stable URL : https://www.jstor.org/stable/2897193 Linked references are available on JSTOR for this artic', 283(5398), pp. 70–74.

Iwanaszko, M. and Kimmel, M. (2015) 'NF- κ B and IRF pathways : cross-regulation on target genes promoter level', ??? ???, pp. 1–8. doi: 10.1186/s12864-015-1511-7.

Jaaro-Peled, H. (2009) *Gene models of schizophrenia: DISC1 mouse models*, *Progress in Brain Research*. Elsevier. doi: 10.1016/S0079-6123(09)17909-8.

Jaarsma, D. and Hoogenraad, C. C. (2015) 'Cytoplasmic dynein and its regulatory proteins in Golgi pathology in nervous system disorders', 9(October), pp. 1–9. doi: 10.3389/fnins.2015.00397.

James, S. L. *et al.* (2018) 'Global, regional, and national incidence, prevalence, and years lived with disability for 354 Diseases and Injuries for 195 countries and territories, 1990-2017: A systematic analysis for the Global Burden of Disease Study 2017', *The Lancet*, 392(10159), pp. 1789–1858. doi: 10.1016/S0140-6736(18)32279-7.

Jang, C. G. and Lee, S. Y. (2001) 'NMDA-type Glutamatergic Modulation in Dopaminergic Activation Measured by Apomorphine-Induced Cage Climbing Behaviors', *Archives of Pharmacal Research*, 24(6), pp. 613–617. doi: 10.1007/BF02975175.

Jarskog, L. F. *et al.* (2000) 'Cortical Bcl-2 protein expression and apoptotic regulation in schizophrenia', *Biological Psychiatry*, 48(7), pp. 641–650. doi: 10.1016/S0006-3223(00)00988-4.

Jarskog, L. F. *et al.* (2005) 'Apoptotic mechanisms in the pathophysiology of schizophrenia', *Progress in Neuro-Psychopharmacology and Biological Psychiatry*, 29(5), pp. 846–858. doi: 10.1016/j.pnpbp.2005.03.010.

Javitt, C. (1991) 'Advances', (October), pp. 1301–1308.

Javitt, D. C. (2010) 'Glutamatergic theories of schizophrenia', *Israel Journal of Psychiatry and Related Sciences*, 47(1), pp. 4–16.

Jentsch, J. D. and Roth, R. H. (1999) 'The Neuropsychopharmacology of Phencyclidine: From NMDA Receptor Hypofunction to the Dopamine Hypothesis of Schizophrenia', *Neuropsychopharmacology*, 20(3), pp. 201–225. doi: https://doi.org/10.1016/S0893-133X(98)00060-8.

De Jong, E. K. *et al.* (2005) 'Vesicle-mediated transport and release of CCL21 in endangered neurons: A possible explanation for microglia activation remote from a primary lesion', *Journal of Neuroscience*, 25(33), pp. 7548–7557. doi: 10.1523/JNEUROSCI.1019-05.2005.

Jourquin, J. *et al.* (2012) 'GLAD4U : deriving and prioritizing gene lists from PubMed literature', *BMC Genomics*. BioMed Central Ltd, 13(Suppl 8), p. S20. doi: 10.1186/1471-2164-13-S8-S20.

Juraeva, D. *et al.* (2014) 'Integrated Pathway-Based Approach Identifies Association between Genomic Regions at CTCF and CACNB2 and Schizophrenia', *PLoS Genetics*, 10(6). doi: 10.1371/journal.pgen.1004345.

Kang, W. S. *et al.* (2012) 'Genetic variants of GRIA1 are associated with susceptibility to schizophrenia in Korean population.', *Molecular biology reports*, 39(12), pp. 10697–10703. doi: 10.1007/s11033-012-1960-x.

Karayiorgou, M., Simon, T. J. and Gogos, J. A. (2010) '22q11.2 microdeletions: Linking DNA structural variation to brain dysfunction and schizophrenia', *Nature Reviews Neuroscience*. Nature Publishing Group, 11(6), pp. 402–416. doi: 10.1038/nrn2841.

Kelly, R. M. and Strick, P. L. (2003) 'Cerebellar loops with motor cortex and prefrontal cortex of a nonhuman primate', *Journal of Neuroscience*, 23(23), pp. 8432–8444. doi: 10.1523/jneurosci.23-23-08432.2003.

Kempton, M. J. *et al.* (2010) 'Progressive lateral ventricular enlargement in schizophrenia : A meta-analysis of longitudinal MRI studies', *Schizophrenia Research*. Elsevier B.V., 120(1–3), pp. 54–62. doi: 10.1016/j.schres.2010.03.036.

Kendler, K. S. *et al.* (1993) 'The Roscommon Family Study. I. Methods, diagnosis of probands, and risk of schizophrenia in relatives.', *Archives of general psychiatry*. United States, 50(7), pp. 527–540. doi: 10.1001/archpsyc.1993.01820190029004.

Khidekel, N. *et al.* (2007) 'Probing the dynamics of O-GlcNAc glycosylation in the brain using quantitative proteomics', *Nature Chemical Biology*, 3(6), pp. 339–348. doi: 10.1038/nchembio881.

Kim, S. *et al.* (2007) 'Suicide candidate genes associated with bipolar disorder and schizophrenia: An exploratory gene expression profiling analysis of post-mortem prefrontal cortex', *BMC Genomics*, 8, pp. 1–10. doi: 10.1186/1471-2164-8-413.

Kim, Y. *et al.* (2002) 'The plasma levels of interleukin-12 in schizophrenia , major depression , and bipolar mania : effects of psychotropic drugs', pp. 1107–1114. doi: 10.1038/sj.mp.4001084.

Kinney, D. K. *et al.* (2010) 'A unifying hypothesis of schizophrenia: Abnormal immune system development may help explain roles of prenatal hazards, post-pubertal onset, stress, genes, climate, infections, and brain dysfunction', *Medical Hypotheses*. Elsevier Ltd, 74(3), pp. 555–563. doi: 10.1016/j.mehy.2009.09.040.

Koechlin, E. and Hyafil, A. (2007) 'Anterior prefrontal function and the limits of human decision-making', *Science*, 318(5850), pp. 594–598. doi: 10.1126/science.1142995.

Kohout, T. A. *et al.* (2001) 'β-Arrestin 1 and 2 Differentially Regulate Heptahelical Receptor Signaling and Trafficking', *Proceedings of the National Academy of Sciences of the United States of America*. National Academy of Sciences, 98(4), pp. 1601–1606. Available at: http://www.jstor.org/stable/3054922.

Koirala, S. and Corfas, G. (2010) 'Identification of novel glial genes by single-cell transcriptional profiling of Bergmann glial cells from mouse cerebellum', *PLoS ONE*, 5(2). doi: 10.1371/journal.pone.0009198.

Kouneiher, F., Charron, S. and Koechlin, E. (2009) 'Motivation and cognitive control in the human prefrontal cortex', *Nature Neuroscience*, 12(7), pp. 939–945. doi: 10.1038/nn.2321.

Koziol, L. F. *et al.* (2014) 'Consensus paper: The cerebellum's role in movement and cognition', *Cerebellum*. doi: 10.1007/s12311-013-0511-x.

Krienen, F. M. and Buckner, R. L. (2009) 'Segregated fronto-cerebellar circuits revealed by intrinsic functional connectivity', *Cerebral Cortex*, 19(10), pp. 2485–2497. doi: 10.1093/cercor/bhp135.

Kroken, R. A. *et al.* (2019) 'Constructing the immune signature of schizophrenia for

clinical use and research; an integrative review translating descriptives into diagnostics', *Frontiers in Psychiatry*, 10(JAN), pp. 1–16. doi: 10.3389/fpsyt.2018.00753.

Krystal, J. H. *et al.* (1994) 'Subanesthetic effects of the noncompetitive NMDA antagonist, ketamine, in humans. Psychotomimetic, perceptual, cognitive, and neuroendocrine responses.', *Archives of general psychiatry*. United States, 51(3), pp. 199–214. doi: 10.1001/archpsyc.1994.03950030035004.

Kurian, S. M. *et al.* (2011) 'Identification of blood biomarkers for psychosis using convergent functional genomics', *Molecular Psychiatry*. Nature Publishing Group, 16(1), pp. 37–58. doi: 10.1038/mp.2009.117.

Laidi, C. *et al.* (2015) 'Cerebellar volume in schizophrenia and bipolar I disorder with and without psychotic features', di, pp. 223–233. doi: 10.1111/acps.12363.

Laub, F. *et al.* (2001) 'Developmental expression of mouse Krüppel-like transcription factor KLF7 suggests a potential role in neurogenesis', *Developmental Biology*, 233(2), pp. 305–318. doi: 10.1006/dbio.2001.0243.

Laub, F. *et al.* (2005) 'Transcription Factor KLF7 Is Important for Neuronal Morphogenesis in Selected Regions of the Nervous System', *Molecular and Cellular Biology*, 25(13), pp. 5699–5711. doi: 10.1128/mcb.25.13.5699-5711.2005.

Law, A. J. *et al.* (2007) 'Disease-associated intronic variants in the ErbB4 gene are related to altered ErbB4 splice-variant expression in the brain in schizophrenia', 16(2), pp. 129–141. doi: 10.1093/hmg/ddl449.

Lawford, B. R. *et al.* (2005) 'The C/C genotype of the C957T polymorphism of the dopamine D2 receptor is associated with schizophrenia', *Schizophrenia Research*, 73(1), pp. 31–37. doi: 10.1016/j.schres.2004.08.020.

Lawrie, S. M., Hall, J. and Johnstone, E. C. (2010) *Schizophrenia and related disorders*. 8th edn, *Companion to Psychiatric Studies*. 8th edn. Elsevier Ltd. doi: 10.1016/b978-0-7020-3137-3.00015-2.

Lee, K. W. *et al.* (2005) 'Sp1-associated activation of macrophage inflammatory protein-2 promoter by CpG-oligodeoxynucleotide and lipopolysaccharide', *Cellular and Molecular Life Sciences*, 62(2), pp. 188–198. doi: 10.1007/s00018-004-4399-y.

Lei, L. *et al.* (2005) 'The zinc finger transcription factor Klf7 is required for TrkA gene expression and development of nociceptive sensory neurons', pp. 1354–1364. doi:

10.1101/gad.1227705.the.

Lemaire, V. *et al.* (2000) 'Prenatal stress produces learning deficits associated with an inhibition of neurogenesis in the hippocampus.', *Proceedings of the National Academy of Sciences of the United States of America*. National Academy of Sciences, 97(20), pp. 11032–7. doi: 10.1073/pnas.97.20.11032.

Leto, K. *et al.* (2016) 'Consensus Paper: Cerebellar Development', *Cerebellum*, 15(6), pp. 789–828. doi: 10.1007/s12311-015-0724-2.

Leutert, M. *et al.* (2019) 'R2-P2 rapid-robotic phosphoproteomics enables multidimensional cell signaling studies', *Molecular Systems Biology*, 15(12), pp. 1–20. doi: 10.15252/msb.20199021.

Lewis, D. A. *et al.* (1999) 'Altered GABA neurotransmission and prefrontal cortical dysfunction in schizophrenia', *Biological Psychiatry*, 46(5), pp. 616–626. doi: 10.1016/S0006-3223(99)00061-X.

Lewis, P. M. *et al.* (2004) 'Sonic hedgehog signaling is required for expansion of granule neuron precursors and patterning of the mouse cerebellum', *Developmental Biology*, 270(2), pp. 393–410. doi: 10.1016/j.ydbio.2004.03.007.

Li, C. T., Yang, K. C. and Lin, W. C. (2019) 'Glutamatergic dysfunction and glutamatergic compounds for major psychiatric disorders: Evidence from clinical neuroimaging studies', *Frontiers in Psychiatry*, 10(JAN), pp. 1–11. doi: 10.3389/fpsyt.2018.00767.

Lieberman, J. A. (1999a) 'Is schizophrenia a neurodegenerative disorder? A clinical and neurobiological perspective', *Biological Psychiatry*, 46(6), pp. 729–739. doi: 10.1016/S0006-3223(99)00147-X.

Lieberman, J. A. (1999b) 'Is schizophrenia a neurodegenerative disorder? A clinical and neurobiological perspective', *Biological Psychiatry*, 46(6), pp. 729–739. doi: 10.1016/S0006-3223(99)00147-X.

Lieberman, J. A. *et al.* (2002) 'Erratum: The early stages of schizophrenia: Speculations on pathogenesis, pathophysiology, and therapeuthic approaches (Biological Psychiatry 50:11 (884-897))', *Biological Psychiatry*, 51(4), p. 346. doi: 10.1016/S0006-3223(02)01310-0.

Limanowski, J., Litvak, V. and Friston, K. (2020) 'Cortical beta oscillations reflect the contextual gating of visual action feedback', *NeuroImage*. Elsevier Inc., 222(June), p.

117267. doi: 10.1016/j.neuroimage.2020.117267.

Lippman, J. J. *et al.* (2008) 'Morphogenesis and regulation of Bergmann glial processes during Purkinje cell dendritic spine ensheathment and synaptogenesis', *Glia*, 56(13), pp. 1463–1477. doi: 10.1002/glia.20712.

Lisman, J. E. *et al.* (2008) 'Circuit-based framework for understanding neurotransmitter and risk gene interactions in schizophrenia', *Trends in Neurosciences*, 31(5), pp. 234–242. doi: 10.1016/j.tins.2008.02.005.

Logue, S. F. and Gould, T. J. (2014) 'The neural and genetic basis of executive function: Attention, cognitive flexibility, and response inhibition', *Pharmacology Biochemistry and Behavior*. Elsevier Inc., 123, pp. 45–54. doi: 10.1016/j.pbb.2013.08.007.

Luo, W. W. *et al.* (2016) 'Krüppel-like factor 4 negatively regulates cellular antiviral immune response', *Cellular and Molecular Immunology*, 13(1), pp. 65–72. doi: 10.1038/cmi.2014.125.

Lutkenhoff, E. *et al.* (2012) 'Structural and functional neuroimaging phenotypes in dysbindin mutant mice', *NeuroImage*. Elsevier Inc., 62(1), pp. 120–129. doi: 10.1016/j.neuroimage.2012.05.008.

Lyne, J. *et al.* (2014) 'Do psychosis prodrome onset negative symptoms predict first presentation negative symptoms?', *European Psychiatry*. Elsevier Masson SAS, 29(3), pp. 153–159. doi: 10.1016/j.eurpsy.2013.02.003.

Lyne, J. *et al.* (2018) 'Negative symptoms of psychosis: A life course approach and implications for prevention and treatment', *Early Intervention in Psychiatry*, 12(4), pp. 561–571. doi: 10.1111/eip.12501.

Mabunga, D. F. N. *et al.* (2019) 'Recapitulation of neuropsychiatric behavioral features in mice using acute low-dose MK-801 administration', *Experimental Neurobiology*, 28(6), pp. 697–708. doi: 10.5607/en.2019.28.6.697.

MacDowell, K. S. *et al.* (2017) 'Differential regulation of the TLR4 signalling pathway in post-mortem prefrontal cortex and cerebellum in chronic schizophrenia: Relationship with SP transcription factors', *Progress in Neuro-Psychopharmacology and Biological Psychiatry*, 79(August), pp. 481–492. doi: 10.1016/j.pnpbp.2017.08.005.

Maher, B. J. and LoTurco, J. J. (2012) 'Disrupted-in-schizophrenia (DISC1) functions presynaptically at glutamatergic synapses', *PLoS ONE*, 7(3), pp. 1–9. doi:

10.1371/journal.pone.0034053.

Malt, E. A. *et al.* (2016) 'A role for the transcription factor Nk2 homeobox 1 in schizophrenia: Convergent evidence from animal and human studies', *Frontiers in Behavioral Neuroscience*, 10(MAR), pp. 1–28. doi: 10.3389/fnbeh.2016.00059.

Manto, M. *et al.* (2012) 'Consensus Paper : Roles of the Cerebellum in Motor Control — The Diversity of Ideas on Cerebellar Involvement in Movement', pp. 457–487. doi: 10.1007/s12311-011-0331-9.

Margari, F. *et al.* (2013) 'Anti-brain autoantibodies in the serum of schizophrenic patients : A case-control study', *Psychiatry Research*. Elsevier, 210(3), pp. 800–805. doi: 10.1016/j.psychres.2013.09.006.

Marín, O. (2016) 'Developmental timing and critical windows for the treatment of psychiatric disorders', *Nature Medicine*. Nature Publishing Group, 22(11), pp. 1229–1238. doi: 10.1038/nm.4225.

Marschallinger, J. *et al.* (2020) 'Lipid-droplet-accumulating microglia represent a dysfunctional and proinflammatory state in the aging brain', *Nature Neuroscience*, 23(2), pp. 194–208. doi: 10.1038/s41593-019-0566-1.

Marshall, C. R. *et al.* (2017) 'Contribution of copy number variants to schizophrenia from a genome-wide study of 41,321 subjects', *Nature Genetics*, 49(1), pp. 27–35. doi: 10.1038/ng.3725.

Martínez-Téllez, R. I. *et al.* (2009) 'Prenatal stress alters spine density and dendritic length of nucleus accumbens and hippocampus neurons in rat offspring', *Synapse*, 63(9), pp. 794–804. doi: 10.1002/syn.20664.

Martins-de-Souza, D., Gattaz, W. F., Schmitt, A., Novello, J. C., *et al.* (2009) 'Proteome analysis of schizophrenia patients Wernicke's area reveals an energy metabolism dysregulation', *BMC Psychiatry*, 9, pp. 1–8. doi: 10.1186/1471-244X-9-17.

Martins-de-Souza, D., Gattaz, W. F., Schmitt, A., Maccarrone, G., *et al.* (2009) 'Proteomic analysis of dorsolateral prefrontal cortex indicates the involvement of cytoskeleton, oligodendrocyte, energy metabolism and new potential markers in schizophrenia', *Journal of Psychiatric Research*. Elsevier Ltd, 43(11), pp. 978–986. doi: 10.1016/j.jpsychires.2008.11.006.

Martins-de-Souza, D. *et al.* (2010) 'Proteome analysis of the thalamus and cerebrospinal

fluid reveals glycolysis dysfunction and potential biomarkers candidates for schizophrenia', *Journal of Psychiatric Research*. Elsevier Ltd, 44(16), pp. 1176–1189. doi: 10.1016/j.jpsychires.2010.04.014.

Martins-De-Souza, D. *et al.* (2009) 'Prefrontal cortex shotgun proteome analysis reveals altered calcium homeostasis and immune system imbalance in schizophrenia', *European Archives of Psychiatry and Clinical Neuroscience*, 259(3), pp. 151–163. doi: 10.1007/s00406-008-0847-2.

Martins-De-Souza, D. *et al.* (2011) 'The role of energy metabolism dysfunction and oxidative stress in schizophrenia revealed by proteomics', *Antioxidants and Redox Signaling*, 15(7), pp. 2067–2079. doi: 10.1089/ars.2010.3459.

Marvel, J. and Leverrier, Y. (2006) 'Overexpression of Sp1 transcription factor induces apoptosis', pp. 7096–7105. doi: 10.1038/sj.onc.1209696.

Mattson, M. P., Keller, J. N. and Begley, J. G. (1998) 'Evidence for synaptic apoptosis', *Experimental Neurology*, 153(1), pp. 35–48. doi: 10.1006/exnr.1998.6863.

Maurer, I., Zierz, S. and Möller, H. J. (2001) 'Evidence for a mitochondrial oxidative phosphorylation defect in brains from patients with schizophrenia', *Schizophrenia Research*, 48(1), pp. 125–136. doi: 10.1016/S0920-9964(00)00075-X.

Maynard, T. M. *et al.* (2001) 'Neural development, cell-cell signaling, and the "two-hit" hypothesis of schizophrenia', *Schizophrenia Bulletin*, 27(3), pp. 457–476. doi: 10.1093/oxfordjournals.schbul.a006887.

McCormick, P. J., Martina, J. A. and Bonifacino, J. S. (2005) 'Involvement of clathrin and AP-2 in the trafficking of MHC class II molecules to antigen-processing compartments', *Proceedings of the National Academy of Sciences of the United States of America*, 102(22), pp. 7910–7915. doi: 10.1073/pnas.0502206102.

McGrath, J. *et al.* (2008) 'Schizophrenia: A concise overview of incidence, prevalence, and mortality', *Epidemiologic Reviews*, 30(1), pp. 67–76. doi: 10.1093/epirev/mxn001.

McKinnon, C. M. and Mellor, H. (2017) 'The tumor suppressor RhoBTB1 controls Golgi integrity and breast cancer cell invasion through METTL7B', *BMC Cancer*. BMC Cancer, 17(1), pp. 1–9. doi: 10.1186/s12885-017-3138-3.

Mcmeekin, L. J. *et al.* (2016) 'Cortical PGC-1 α -Dependent Transcripts Are Reduced in Postmortem Tissue From Patients With Schizophrenia', 42(4), pp. 1009–1017. doi:

10.1093/schbul/sbv184.

Mednick, S. A. *et al.* (1988) 'Adult Schizophrenia Following Prenatal Exposure to an Influenza Epidemic', *Archives of General Psychiatry*, 45(2), pp. 189–192. doi: 10.1001/archpsyc.1988.01800260109013.

Meldrum, B. S. (2000) 'Glutamate as a neurotransmitter in the brain: Review of physiology and pathology', *Journal of Nutrition*, 130(4 SUPPL.), pp. 1007–1015. doi: 10.1093/jn/130.4.1007s.

Metzner, C., Zurowski, B. and Steuber, V. (2019) 'The Role of Parvalbumin-positive Interneurons in Auditory Steady-State Response Deficits in Schizophrenia', *Scientific Reports*, 9(1), pp. 1–16. doi: 10.1038/s41598-019-53682-5.

Meyer-Lindenberg, A. *et al.* (2002) 'Reduced prefrontal activity predicts exaggerated striatal dopaminergic function in schizophrenia', *Nature Neuroscience*, 5(3), pp. 267–271. doi: 10.1038/nn804.

Meyer, J. M. *et al.* (2009) 'Inflammatory Markers in Schizophrenia: Comparing Antipsychotic Effects in Phase 1 of the Clinical Antipsychotic Trials of Intervention Effectiveness Study', *Biological Psychiatry*. Elsevier Inc., 66(11), pp. 1013–1022. doi: 10.1016/j.biopsych.2009.06.005.

Michaelovsky, E. *et al.* (2019) 'Risk gene-set and pathways in 22q11.2 deletion-related schizophrenia: a genealogical molecular approach', *Translational Psychiatry*. Springer US, 9(1). doi: 10.1038/s41398-018-0354-9.

Middleton, F. A. (2002) 'Basal-ganglia "Projections" to the Prefrontal Cortex of the Primate', *Cerebral Cortex*, 12(9), pp. 926–935. doi: 10.1093/cercor/12.9.926.

Middleton, F. A. and Strick, P. L. (2001) 'Cerebellar projections to the prefrontal cortex of the primate', *The Journal of neuroscience : the official journal of the Society for Neuroscience*. Society for Neuroscience, 21(2), pp. 700–712. doi: 10.1523/JNEUROSCI.21-02-00700.2001.

Milardi, D. *et al.* (2019) 'The Cortico-Basal Ganglia-Cerebellar Network : Past , Present and Future Perspectives', 13(October), pp. 1–14. doi: 10.3389/fnsys.2019.00061.

Millar, J. K. *et al.* (2000) 'Disruption of two novel genes by a translocation co-segregating with schizophrenia', *Human Molecular Genetics*, 9(9), pp. 1415–1423. doi: 10.1093/hmg/9.9.1415.

Miller, B. J. *et al.* (2011) 'Meta-analysis of cytokine alterations in schizophrenia: Clinical status and antipsychotic effects', *Biological Psychiatry*. Elsevier Inc., 70(7), pp. 663–671. doi: 10.1016/j.biopsych.2011.04.013.

Mirnics, K. *et al.* (2000) 'Molecular Characterization of Schizophrenia Viewed by Microarray Analysis of Gene Expression in Prefrontal Cortex', *Neuron*. Elsevier, 28(1), pp. 53–67. doi: 10.1016/S0896-6273(00)00085-4.

Mitchell, A. C. *et al.* (2018) 'MEF2C transcription factor is associated with the genetic and epigenetic risk architecture of schizophrenia and improves cognition in mice', *Molecular Psychiatry*. Nature Publishing Group, 23(1), pp. 123–132. doi: 10.1038/mp.2016.254.

Monte, A. S. *et al.* (2017) 'Two-hit model of schizophrenia induced by neonatal immune activation and peripubertal stress in rats: Study of sex differences and brain oxidative alterations', *Behavioural Brain Research*. Elsevier, 331(May), pp. 30–37. doi: 10.1016/j.bbr.2017.04.057.

Monti, B. and Contestabile, A. (2000) 'Blockade of the NMDA receptor increases developmental apoptotic elimination of granule neurons and activates caspases in the rat cerebellum', *European Journal of Neuroscience*, 12(9), pp. 3117–3123. doi: 10.1046/j.1460-9568.2000.00189.x.

Moran, P. *et al.* (2016) 'Gene × Environment Interactions in Schizophrenia: Evidence from Genetic Mouse Models', *Neural Plasticity*, 2016. doi: 10.1155/2016/2173748.

Morris, J. A. *et al.* (2003) 'DISC1 (Disrupted-In-Schizophrenia 1) is a centrosome-associated protein that interacts regulation and loss of interaction with mutation', 12(13), pp. 1591–1608. doi: 10.1093/hmg/ddg162.

Moskowitz, A. and Heim, G. (2011) 'Eugen Bleuler's Dementia Praecox or the Group of Schizophrenias (1911): A centenary appreciation and reconsideration', *Schizophrenia Bulletin*, 37(3), pp. 471–479. doi: 10.1093/schbul/sbr016.

Mostaid, M. S. *et al.* (2017) 'Meta-analysis reveals associations between genetic variation in the 5' and 3' regions of Neuregulin-1 and schizophrenia', *Translational Psychiatry*. Nature Publishing Group, 7(1). doi: 10.1038/tp.2016.279.

Mouaffak, F. *et al.* (2011) 'Association of Disrupted in Schizophrenia 1 (DISC1) missense variants with ultra-resistant schizophrenia', *Pharmacogenomics Journal*, 11(4), pp. 267–273. doi: 10.1038/tpj.2010.40.

Mueller, T. M., Haroutunian, V. and Meador-woodruff, J. H. (2014) 'N -Glycosylation of GABA A Receptor Subunits is Altered in Schizophrenia', *Neuropsychopharmacology*. Nature Publishing Group, pp. 528–537. doi: 10.1038/npp.2013.190.

Mukaetova-Ladinska, E. B. *et al.* (2002) 'Loss of synaptic but not cytoskeletal proteins in the cerebellum of chronic schizophrenics', *Neuroscience Letters*, 317(3), pp. 161–165. doi: https://doi.org/10.1016/S0304-3940(01)02458-2.

Mukai, K. *et al.* (2016) 'Activation of STING requires palmitoylation at the Golgi', *Nature Communications*. Nature Publishing Group, 7(May). doi: 10.1038/ncomms11932.

Müller, N. *et al.* (1997) 'Soluble IL-6 receptors in the serum and cerebrospinal fluid of paranoid schizophrenic patients', *European Psychiatry*, 12(6), pp. 294–299. doi: 10.1016/S0924-9338(97)84789-X.

Müller, N. and Ackenheil, M. (1995) 'Immunoglobulin and albumin content of cerebrospinal fluid in schizophrenic patients: Relationship to negative symptomatology', *Schizophrenia Research*, 14(3), pp. 223–228. doi: 10.1016/0920-9964(94)00045-A.

Murray, C. J. L. *et al.* (1996) 'The Global burden of disease : a comprehensive assessment of mortality and disability from diseases, injuries, and risk factors in 1990 and projected to 2020 : summary / edited by Christopher J. L. Murray, Alan D. Lopez'. World Health Organization (Global burden of disease and injury series, volume 1), p. Published by the Harvard School of Public Health o.

Nair, V. D., Savelli, J. E. and Mishra, R. K. (1998) 'Modulation of dopamine D2 receptor expression by an NMDA receptor antagonist in rat brain', *Journal of Molecular Neuroscience*, 11(2), pp. 121–126. doi: 10.1385/JMN:11:2:121.

Najjar, S. *et al.* (2017) 'Neurovascular Unit Dysfunction and Blood–Brain Barrier Hyperpermeability Contribute to Schizophrenia Neurobiology: A Theoretical Integration of Clinical and Experimental Evidence', *Frontiers in Psychiatry*, 8(May). doi: 10.3389/fpsyt.2017.00083.

Nakata, K. *et al.* (2009) 'DISC1 splice variants are upregulated in schizophrenia and associated with risk polymorphisms', pp. 37–40.

Naseri, N. N. *et al.* (2016) 'Novel Metabolic Abnormalities in the Tricarboxylic Acid Cycle in Peripheral Cells From Huntington's Disease Patients', *PLOS ONE*. Public Library of Science, 11(9), p. e0160384. Available at: https://doi.org/10.1371/journal.pone.0160384.

Nayak, L. *et al.* (2013) 'Kruppel-like factor 2 is a transcriptional regulator of chronic and acute inflammation', *American Journal of Pathology*. American Society for Investigative Pathology, 182(5), pp. 1696–1704. doi: 10.1016/j.ajpath.2013.01.029.

Neill, J. C. *et al.* (2010) 'Animal models of cognitive dysfunction and negative symptoms of schizophrenia: Focus on NMDA receptor antagonism', *Pharmacology and Therapeutics*. Elsevier Inc., 128(3), pp. 419–432. doi: 10.1016/j.pharmthera.2010.07.004.

Nopoulos, P. C. *et al.* (1999) 'An MRI study of cerebellar vermis morphology in patients with schizophrenia: Evidence in support of the cognitive dysmetria concept', *Biological Psychiatry*, 46(5), pp. 703–711. doi: 10.1016/S0006-3223(99)00093-1.

Norkina, O. *et al.* (2007) 'Acute alcohol activates STAT3, AP-1, and Sp-1 transcription factors via the family of Src kinases to promote IL-10 production in human monocytes.', *Journal of leukocyte biology*. United States, 82(3), pp. 752–762. doi: 10.1189/jlb.0207099.

Nyffeler, M. *et al.* (2006) 'Maternal immune activation during pregnancy increases limbic GABAA receptor immunoreactivity in the adult offspring: Implications for schizophrenia', *Neuroscience*, 143(1), pp. 51–62. doi: 10.1016/j.neuroscience.2006.07.029.

O'Donnell, B. F. *et al.* (1995) 'Increased Rate of P300 Latency Prolongation with Age in Schizophrenia: Electrophysiological Evidence for a Neurodegenerative Process', *Archives of General Psychiatry*, 52(7), pp. 544–549. doi: 10.1001/archpsyc.1995.03950190026004.

O'Donovan, M. C. *et al.* (2008) 'Identification of loci associated with schizophrenia by genome-wide association and follow-up', *Nature Genetics*, 40(9), pp. 1053–1055. doi: 10.1038/ng.201.

De Oliveira, S., Rosowski, E. E. and Huttenlocher, A. (2016) 'Neutrophil migration in infection and wound repair: Going forward in reverse', *Nature Reviews Immunology*. Nature Publishing Group, 16(6), pp. 378–391. doi: 10.1038/nri.2016.49.

Van Den Oord, E. J. C. G. *et al.* (2003) 'Identification of a high-risk haplotype for the dystrobrevin binding protein 1 (DTNBP1) gene in the Irish study of high-density schizophrenia families', *Molecular Psychiatry*, 8(5), pp. 499–510. doi: 10.1038/sj.mp.4001263.

Orlovska-Waast, S. *et al.* (2019) 'Cerebrospinal fluid markers of inflammation and

infections in schizophrenia and affective disorders: a systematic review and meta-analysis', *Molecular Psychiatry*. Springer US, 24(6), pp. 869–887. doi: 10.1038/s41380-018-0220-4.

Overwalle, F. Van *et al.* (2020) *Consensus Paper : Cerebellum and Social Cognition*. The Cerebellum.

Owen, M. J., Williams, N. M. and O'Donovan, M. C. (2004) 'The molecular genetics of schizophrenia: New findings promise new insights', *Molecular Psychiatry*, 9(1), pp. 14–27. doi: 10.1038/sj.mp.4001444.

Palesi, F. *et al.* (2017) 'Contralateral cortico-ponto- cerebellar pathways reconstruction in humans in vivo : implications for reciprocal cerebro-cerebellar structural connectivity in motor and non-motor areas', (May), pp. 1–13. doi: 10.1038/s41598-017-13079-8.

Papaleo, F. *et al.* (2012) 'Dysbindin-1 modulates prefrontal cortical activity and schizophrenia-like behaviors via dopamine/D2 pathways', *Molecular Psychiatry*, 17(1), pp. 85–98. doi: 10.1038/mp.2010.106.

Parker, K. L. *et al.* (2017) 'Delta-frequency stimulation of cerebellar projections can compensate for schizophrenia-related medial frontal dysfunction', *Molecular Psychiatry*. Nature Publishing Group, 22(5), pp. 647–655. doi: 10.1038/mp.2017.50.

Parrish-Novak, J. *et al.* (2000) 'Interleukin 21 and its receptor are involved in NK cell expansion and regulation of lymphocyte function', *Nature*, 408(6808), pp. 57–63. doi: 10.1038/35040504.

Pascual-Leone, A. *et al.* (1996) 'The role of the dorsolateral prefrontal cortex in implicit procedural learning.', *Experimental brain research*. Germany, 107(3), pp. 479–485. doi: 10.1007/BF00230427.

Pathan, M. *et al.* (2015) 'FunRich: An open access standalone functional enrichment and interaction network analysis tool', *Proteomics*, 15(15), pp. 2597–2601. doi: 10.1002/pmic.201400515.

Pennington, K. *et al.* (2008) 'Prominent synaptic and metabolic abnormalities revealed by proteomic analysis of the dorsolateral prefrontal cortex in schizophrenia and bipolar disorder', *Molecular Psychiatry*, 13(12), pp. 1102–1117. doi: 10.1038/sj.mp.4002098.

Pérez-Neri, I. *et al.* (2006) 'Possible mechanisms of neurodegeneration in schizophrenia', *Neurochemical Research*, 31(10), pp. 1279–1294. doi: 10.1007/s11064-

006-9162-3.

Petrides, M. (2000) ‘The role of the mid-dorsolateral prefrontal cortex in working memory’, pp. 44–54.

Peyroux, E. *et al.* (2019) ‘Subthreshold social cognitive deficits may be a key to distinguish 22q11.2DS from schizophrenia’, *Early Intervention in Psychiatry*, 13(2), pp. 304–307. doi: 10.1111/eip.12557.

Pfaff, D. W. (2013) ‘Neuroscience in the 21st century: From basic to clinical’, *Neuroscience in the 21st Century: From Basic to Clinical*, pp. 1–3111. doi: 10.1007/978-1-4614-1997-6.

Phillips, J. E. and Corces, V. G. (2009) ‘Review CTCF : Master Weaver of the Genome’. doi: 10.1016/j.cell.2009.06.001.

Picard, H. *et al.* (2008) ‘The role of the cerebellum in schizophrenia: An update of clinical, cognitive, and functional evidences’, *Schizophrenia Bulletin*, 34(1), pp. 155–172. doi: 10.1093/schbul/sbm049.

Pinacho, R. *et al.* (2011) ‘The transcription factor SP4 is reduced in postmortem cerebellum of bipolar disorder subjects: Control by depolarization and lithium’, *Bipolar Disorders*, 13(5–6), pp. 474–485. doi: 10.1111/j.1399-5618.2011.00941.x.

Pinacho, R. *et al.* (2013) ‘Analysis of Sp transcription factors in the postmortem brain of chronic schizophrenia: a pilot study of relationship to negative symptoms.’, *Journal of psychiatric research*, 47(7), pp. 926–934. doi: 10.1016/j.jpsychires.2013.03.004.

Pinacho, R. *et al.* (2014) ‘Increased SP4 and SP1 transcription factor expression in the postmortem hippocampus of chronic schizophrenia.’, *Journal of psychiatric research*, 58, pp. 189–96. doi: 10.1016/j.jpsychires.2014.08.006.

Pinacho, R., Saia, G., Fusté, M., *et al.* (2015) ‘Phosphorylation of transcription factor specificity protein 4 is increased in peripheral blood mononuclear cells of first-episode psychosis’, *PLoS ONE*, 10(4), pp. 1–14. doi: 10.1371/journal.pone.0125115.

Pinacho, R., Saia, G., Meana, J. J., *et al.* (2015) ‘Transcription factor SP4 phosphorylation is altered in the postmortem cerebellum of bipolar disorder and schizophrenia subjects’, *European Neuropsychopharmacology*. Elsevier, 25(10), pp. 1650–1660. doi: 10.1016/j.euroneuro.2015.05.006.

Pinacho, R. *et al.* (2016) ‘Altered CSNK1E, FABP4 and NEFH protein levels in the

dorsolateral prefrontal cortex in schizophrenia', *Schizophrenia Research*. Elsevier B.V., 177(1–3), pp. 88–97. doi: 10.1016/j.schres.2016.04.050.

Pletnikov, M. V *et al.* (2008) 'Inducible expression of mutant human DISC1 in mice is associated with brain and behavioral abnormalities reminiscent of schizophrenia', 1, pp. 173–186. doi: 10.1038/sj.mp.4002079.

Prabakaran, S. *et al.* (2004) 'Mitochondrial dysfunction in schizophrenia : evidence for compromised brain metabolism and oxidative stress', pp. 684–697. doi: 10.1038/sj.mp.4001511.

Pycock, C. J., Kerwin, R. W. and Carter, C. J. (1980) 'Effect of lesion of cortical dopamine terminals on subcortical dopamine receptors in rats', *Nature*, 286(5768), pp. 74–77. doi: 10.1038/286074a0.

Quartier, A. *et al.* (2018) 'Genes and Pathways Regulated by Androgens in Human Neural Cells, Potential Candidates for the Male Excess in Autism Spectrum Disorder', *Biological Psychiatry*. Elsevier Inc, 84(4), pp. 239–252. doi: 10.1016/j.biopsych.2018.01.002.

De Quervain, D. J. F. *et al.* (2003) 'Glucocorticoid-induced impairment of declarative memory retrieval is associated with reduced blood flow in the medial temporal lobe', *European Journal of Neuroscience*, 17(6), pp. 1296–1302. doi: 10.1046/j.1460-9568.2003.02542.x.

Radakovits, R. *et al.* (2009) 'Regulation of Radial Glial Survival by Signals from the Meninges', 29(24), pp. 7694–7705. doi: 10.1523/JNEUROSCI.5537-08.2009.

Ragland, J. D. *et al.* (2007) 'Neuroimaging of cognitive disability in schizophrenia: Search for a pathophysiological mechanism', *International Review of Psychiatry*, 19(4), pp. 417–427. doi: 10.1080/09540260701486365.

Rajasekaran, A. *et al.* (2015) 'Mitochondrial dysfunction in schizophrenia: Pathways, mechanisms and implications', *Neuroscience and Biobehavioral Reviews*. Elsevier Ltd, 48, pp. 10–21. doi: 10.1016/j.neubiorev.2014.11.005.

Ramaker, R. C. *et al.* (2017) 'Post-mortem molecular profiling of three psychiatric disorders', *Genome Medicine*. Genome Medicine, 9(1), pp. 1–12. doi: 10.1186/s13073-017-0458-5.

Ramos, B. *et al.* (2007) 'Transcription factor Sp4 regulates dendritic patterning during

cerebellar maturation', *Proceedings of the National Academy of Sciences of the United States of America*, 104(23), pp. 9882–9887. doi: 10.1073/pnas.0701946104.

Ramos, B. *et al.* (2009) 'Sp4-dependent repression of neurotrophin-3 limits dendritic branching', *Molecular and Cellular Neuroscience*. Elsevier Inc., 42(2), pp. 152–159. doi: 10.1016/j.mcn.2009.06.008.

Rapoport, J. L., Giedd, J. N. and Gogtay, N. (2012) 'Neurodevelopmental model of schizophrenia: Update 2012', *Molecular Psychiatry*. Nature Publishing Group, 17(12), pp. 1228–1238. doi: 10.1038/mp.2012.23.

Re, F. and Strominger, J. L. (2001) 'Activate Human Dendritic Cells *', 276(40), pp. 37692–37699. doi: 10.1074/jbc.M105927200.

Reiner, A. and Levitz, J. (2018) 'Glutamatergic Signaling in the Central Nervous System: Ionotropic and Metabotropic Receptors in Concert', *Neuron*. Elsevier Inc., 98(6), pp. 1080–1098. doi: 10.1016/j.neuron.2018.05.018.

Reis-de-Oliveira, G. *et al.* (2020) 'Digging deeper in the proteome of different regions from schizophrenia brains', *Journal of Proteomics*. Elsevier, 223(January), p. 103814. doi: 10.1016/j.jprot.2020.103814.

Remington, G. *et al.* (2016) 'Treating Negative Symptoms in Schizophrenia: an Update', *Current Treatment Options in Psychiatry*. Current Treatment Options in Psychiatry, 3(2), pp. 133–150. doi: 10.1007/s40501-016-0075-8.

Ribolsi, M. *et al.* (2014) 'Abnormal Asymmetry of Brain Connectivity in Schizophrenia', *Frontiers in Human Neuroscience*, 8, p. 1010. doi: 10.3389/fnhum.2014.01010.

Ridderinkhof, K. R. *et al.* (2004) 'The Role of the Medial Frontal Cortex in Cognitive Control', *Science*. American Association for the Advancement of Science, 306(5695), pp. 443–447. doi: 10.1126/science.1100301.

Riley, B. *et al.* (2010) 'Replication of association between schizophrenia and ZNF804A in the Irish Case-Control Study of Schizophrenia sample', *Molecular Psychiatry*, 15(1), pp. 29–37. doi: 10.1038/mp.2009.109.

Ripke, S. *et al.* (2013) 'Genome-wide association analysis identifies 13 new risk loci for schizophrenia'. doi: 10.1038/ng.2742.

Roberts, R. C. (2017) 'Postmortem studies on mitochondria in schizophrenia', *Schizophrenia Research*. Elsevier B.V., 187, pp. 17–25. doi:

10.1016/j.schres.2017.01.056.

Roca, M., Escanilla, A., Monje, A., Baño, V., Planchat, L., Costa, J., et al. (2008) 'Banco de tejidos neurológicos de Sant Joan de Déu-Serveis de Salut Mental para la investigación de las enfermendades mentales. La importancia de un programa de donación en vida.', *Psiquiatr. Biol.*, 15, 73–79.

Rollins, B. L. *et al.* (2017) 'Mitochondrial Complex I Deficiency in Schizophrenia and Bipolar Disorder and Medication Influence', *Molecular Neuropsychiatry*, 3(3), pp. 157–169. doi: 10.1159/000484348.

Rosato, M. *et al.* (2019) 'Combined cellomics and proteomics analysis reveals shared neuronal morphology and molecular pathway phenotypes for multiple schizophrenia risk genes', *Molecular Psychiatry*. Springer US. doi: 10.1038/s41380-019-0436-y.

Russell, T. A. *et al.* (2000) 'Exploring the social brain in schizophrenia: Left prefrontal underactivation during mental state attribution', *American Journal of Psychiatry*, 157(12), pp. 2040–2042. doi: 10.1176/appi.ajp.157.12.2040.

Saia-Cereda, V. M. *et al.* (2015a) 'Proteomics of the corpus callosum unravel pivotal players in the dysfunction of cell signaling, structure, and myelination in schizophrenia brains', *European Archives of Psychiatry and Clinical Neuroscience*. Springer Berlin Heidelberg, 265(7), pp. 601–612. doi: 10.1007/s00406-015-0621-1.

Saia-Cereda, V. M. *et al.* (2015b) 'Proteomics of the corpus callosum unravel pivotal players in the dysfunction of cell signaling, structure, and myelination in schizophrenia brains', *European Archives of Psychiatry and Clinical Neuroscience*. doi: 10.1007/s00406-015-0621-1.

Saia-Cereda, V. M. *et al.* (2017) 'The Nuclear Proteome of White and Gray Matter from Schizophrenia Postmortem Brains', *Molecular Neuropsychiatry*, 3(1), pp. 37–52. doi: 10.1159/000477299.

Saia, G. *et al.* (2014) 'Phosphorylation of the transcription factor Sp4 is reduced by NMDA receptor signaling', *Journal of Neurochemistry*, 129(4), pp. 743–752. doi: 10.1111/jnc.12657.

Saito, R. *et al.* (2020) 'Comprehensive analysis of a novel mouse model of the 22q11.2 deletion syndrome: a model with the most common 3.0-Mb deletion at the human 22q11.2 locus', *Translational Psychiatry*. Springer US, 10(1). doi: 10.1038/s41398-020-0723-z.

Sams, D. S. *et al.* (2016) 'Neuronal CTCF Is Necessary for Basal and Experience-Dependent Gene Regulation , Memory Article Neuronal CTCF Is Necessary for Basal and Experience-Dependent Gene Regulation , Memory', *CellReports*. ElsevierCompany., 17(9), pp. 2418–2430. doi: 10.1016/j.celrep.2016.11.004.

Santarelli, D. M. *et al.* (2020) 'Schizophrenia-associated MicroRNA – Gene Interactions in the Dorsolateral Prefrontal Cortex', *Genomics, Proteomics & Bioinformatics*. Elsevier B.V., 17(6), pp. 623–634. doi: 10.1016/j.gpb.2019.10.003.

Sayas, C. L. *et al.* (2019) 'Distinct Functions for Mammalian CLASP1 and -2 During Neurite and Axon Elongation', 13(January), pp. 1–17. doi: 10.3389/fncel.2019.00005.

Scambler, P. J. (2000) 'The 22q11 deletion syndromes', *Human Molecular Genetics*, 9(16 REV. ISS.), pp. 2421–2426. doi: 10.1093/hmg/9.16.2421.

Scarr, E. *et al.* (2018) 'Changed gene expression in subjects with schizophrenia and low cortical muscarinic M1 receptors predicts disrupted upstream pathways interacting with that receptor', *Molecular Psychiatry*. Nature Publishing Group, 23(2), pp. 295–303. doi: 10.1038/mp.2016.195.

Schlösser, R. *et al.* (1998) 'Functional magnetic resonance imaging of human brain activity in a verbal fluency task', *Journal of Neurology Neurosurgery and Psychiatry*, 64(4), pp. 492–498. doi: 10.1136/jnnp.64.4.492.

Schmahmann, J. D. (2004) 'Disorders of the Cerebellum ':, pp. 367–378.

Schmahmann, J. D. (2010) 'The Role of the Cerebellum in Cognition and Emotion : Personal Reflections Since 1982 on the Dysmetria of Thought Hypothesis , and Its Historical Evolution from Theory to Therapy', pp. 236–260. doi: 10.1007/s11065-010-9142-x.

Schnapp, B. J. and Reese, T. S. (2006) 'Dynein is the motor for retrograde axonal transport of organelles.', *Proceedings of the National Academy of Sciences*, 86(5), pp. 1548–1552. doi: 10.1073/pnas.86.5.1548.

Schneider, M. *et al.* (2014) 'Psychiatric disorders from childhood to adulthood in 22q11.2 deletion syndrome: Results from the international consortium on brain and behavior in 22q11.2 deletion syndrome', *American Journal of Psychiatry*, 171(6), pp. 627–639. doi: 10.1176/appi.ajp.2013.13070864.

Schubert, K. O., Föcking, M. and Cotter, D. R. (2015) 'Proteomic pathway analysis of the

hippocampus in schizophrenia and bipolar affective disorder implicates 14-3-3 signaling, aryl hydrocarbon receptor signaling, and glucose metabolism: Potential roles in GABAergic interneuron pathology', *Schizophrenia Research*. Elsevier B.V., 167(1–3), pp. 64–72. doi: 10.1016/j.schres.2015.02.002.

Seeman, P. (1987) 'Dopamine receptors and the dopamine hypothesis of schizophrenia', *Synapse*, 1(2), pp. 133–152. doi: 10.1002/syn.890010203.

Semendeferi, K. and Damasio, H. (2000) 'The brain and its main anatomical subdivisions in living hominoids using magnetic resonance imaging', *Journal of Human Evolution*, 38(2), pp. 317–332. doi: 10.1006/jhev.1999.0381.

Shalev, U. and Weiner, I. (2001) 'Gender-dependent differences in latent inhibition following prenatal stress and corticosterone administration', *Behavioural Brain Research*, 126(1–2), pp. 57–63. doi: 10.1016/S0166-4328(01)00250-9.

Shalizi, A. *et al.* (2006) 'A Calcium-Regulated MEF2 Sumoylation Switch Controls Postsynaptic Differentiation', *Science*, 311(5763), pp. 1012 LP – 1017. doi: 10.1126/science.1122513.

Short, B. *et al.* (2002) 'The Rab6 GTPase Regulates Recruitment of the Dynactin Complex to Golgi Membranes', 12(02), pp. 1792–1795.

Siegenthaler, J. A. and Pleasure, S. J. (2011) 'We have got you " covered ": how the meninges control brain development', *Current Opinion in Genetics & Development*. Elsevier Ltd, 21(3), pp. 249–255. doi: 10.1016/j.gde.2010.12.005.

Skokou, M. *et al.* (2012) 'Active and prodromal phase symptomatology of young-onset and late-onset paranoid schizophrenia ', 5(3), pp. 150–159.

Slifstein, M. *et al.* (2015) 'Deficits in prefrontal cortical and extrastriatal dopamine release in schizophrenia a positron emission tomographic functional magnetic resonance imaging study', *JAMA Psychiatry*, 72(4), pp. 316–324. doi: 10.1001/jamapsychiatry.2014.2414.

Smalla, K. H. *et al.* (2008) 'A comparison of the synaptic proteome in human chronic schizophrenia and rat ketamine psychosis suggest that prohibitin is involved in the synaptic pathology of schizophrenia', *Molecular Psychiatry*, 13(9), pp. 878–896. doi: 10.1038/mp.2008.60.

Smeland, O. B. *et al.* (2017) 'Identification of genetic loci jointly influencing schizophrenia

risk and the cognitive traits of verbal-numerical reasoning, reaction time, and general cognitive function', *JAMA Psychiatry*, 74(10), pp. 1065–1075. doi: 10.1001/jamapsychiatry.2017.1986.

Snyder, M. A. and Gao, W. J. (2020) 'NMDA receptor hypofunction for schizophrenia revisited: Perspectives from epigenetic mechanisms', *Schizophrenia Research*. Elsevier B.V., 217, pp. 60–70. doi: 10.1016/j.schres.2019.03.010.

Sofroniew, M. V. (2015) 'Astrocyte barriers to neurotoxic inflammation', *Nature Reviews Neuroscience*. Nature Publishing Group, 16(5), pp. 249–263. doi: 10.1038/nrn3898.

Stark, K. L. *et al.* (2008) 'Altered brain microRNA biogenesis contributes to phenotypic deficits in a 22q11-deletion mouse model', *Nature Genetics*, 40(6), pp. 751–760. doi: 10.1038/ng.138.

Straub, R. E. *et al.* (2002) 'Genetic variation in the 6p22.3 Gene DTNBP1, the human ortholog of the mouse dysbindin gene, is associated with schizophrenia', *American Journal of Human Genetics*, 71(2), pp. 337–348. doi: 10.1086/341750.

Sullivan, P. F., Kendler, K. S. and Neale, M. C. (2003) 'Schizophrenia as a Complex Trait: Evidence from a Meta-analysis of Twin Studies', *Archives of General Psychiatry*, 60(12), pp. 1187–1192. doi: 10.1001/archpsyc.60.12.1187.

Sun, H. J. *et al.* (2006) 'Transcription factors Ets2 and Sp1 act synergistically with histone acetyltransferase p300 in activating human interleukin-12 p40 promoter', *Acta Biochimica et Biophysica Sinica*, 38(3), pp. 194–200. doi: 10.1111/j.1745-7270.2006.00147.x.

Sun, X. *et al.* (2018) 'Genetic variant for behavioral regulation factor of executive function and its possible brain mechanism in attention deficit hyperactivity disorder', *Scientific Reports*. Springer US, 8(1), pp. 1–9. doi: 10.1038/s41598-018-26042-y.

Takahashi, T. and Suzuki, M. (2018) 'Brain morphologic changes in early stages of psychosis: Implications for clinical application and early intervention', pp. 9–11. doi: 10.1111/pcn.12670.

Takai, H. *et al.* (2003) 'Distribution of N-methyl-D-aspartate receptors (NMDARs) in the developing rat brain', *Experimental and Molecular Pathology*, 75(1), pp. 89–94. doi: 10.1016/S0014-4800(03)00030-3.

Tanaka, S. (2008) 'Dysfunctional GABAergic inhibition in the prefrontal cortex leading to

"psychotic" hyperactivation', *BMC Neuroscience*, 9, pp. 12–14. doi: 10.1186/1471-2202-9-41.

Teffer, K. and Semendeferi, K. (2012) *Human prefrontal cortex. Evolution, development, and pathology.* 1st edn, *Progress in Brain Research*. 1st edn. Elsevier B.V. doi: 10.1016/B978-0-444-53860-4.00009-X.

Thiselton, D. L. *et al.* (2008) 'AKT1 Is Associated with Schizophrenia Across Multiple Symptom Dimensions in the Irish Study of High Density Schizophrenia Families', *Biological Psychiatry*, 63(5), pp. 449–457. doi: 10.1016/j.biopsych.2007.06.005.

Torabi, B. *et al.* (2018) 'Caspase cleavage of transcription factor Sp1 enhances apoptosis', *Apoptosis*. Springer US, 23(1), pp. 65–78. doi: 10.1007/s10495-017-1437-4.

Trépanier, M. O. *et al.* (2016) 'Postmortem evidence of cerebral inflammation in schizophrenia: A systematic review', *Molecular Psychiatry*, 21(8), pp. 1009–1026. doi: 10.1038/mp.2016.90.

Tropea, D. *et al.* (2018) 'Mechanisms underlying the role of DISC1 in synaptic plasticity', 14(April 2017), pp. 2747–2771. doi: 10.1113/JP274330.

Tyanova, S. *et al.* (2016) 'The Perseus computational platform for comprehensive analysis of (prote)omics data', *Nature Methods*, 13(9), pp. 731–740. doi: 10.1038/nmeth.3901.

Uhlén, M. *et al.* (2015) 'Tissue-based map of the human proteome', *Science*, 347(6220). doi: 10.1126/science.1260419.

Uno, Y. and Coyle, J. T. (2019) 'Glutamate hypothesis in schizophrenia', *Psychiatry and Clinical Neurosciences*, 73(5), pp. 204–215. doi: 10.1111/pcn.12823.

Urnavicius, L. *et al.* (2015) 'The structure of the dynactin complex and its interaction with dynein', *Science*, 347(6229), pp. 1441 LP – 1446. doi: 10.1126/science.aaa4080.

Ursu, S. *et al.* (2011) 'Prefrontal cortical deficits and impaired cognition-emotion interactions in schizophrenia', *American Journal of Psychiatry*, 168(3), pp. 276–285. doi: 10.1176/appi.ajp.2010.09081215.

Van, L., Boot, E. and Bassett, A. S. (2017) 'Update on the 22q11.2 deletion syndrome and its relevance to schizophrenia', *Current Opinion in Psychiatry*, 30(3), pp. 191–196. doi: 10.1097/YCO.0000000000000324.

Varela, F. *et al.* (2001) 'The brainweb: Phase synchronization and large-scale

integration', *Nature Reviews Neuroscience*, 2(4), pp. 229–239. doi: 10.1038/35067550.

Vawter, M., Mamdani, F. and Macciardi, F. (2011) 'An integrative functional genomics approach for discovering biomarkers in schizophrenia', (December). doi: 10.1093/bfgp/elr036.

Vawter, M. P., Mamdani, F. and Macciardi, F. (2011) 'An integrative functional genomics approach for discovering biomarkers in Schizophrenia', *Briefings in Functional Genomics*, 10(6), pp. 387–399. doi: 10.1093/bfgp/elr036.

Velásquez, E. *et al.* (2017) 'Synaptosomal Proteome of the Orbitofrontal Cortex from Schizophrenia Patients Using Quantitative Label-Free and iTRAQ-Based Shotgun Proteomics', *Journal of Proteome Research*, 16(12), pp. 4481–4494. doi: 10.1021/acs.jproteome.7b00422.

Verge, B. *et al.* (2011) 'Mitochondrial DNA (mtDNA) and schizophrenia', *European Psychiatry*. Elsevier Masson SAS, 26(1), pp. 45–56. doi: 10.1016/j.eurpsy.2010.08.008.

Vidal-Domènech, F. *et al.* (2020) 'Calcium-binding proteins are altered in the cerebellum in schizophrenia', *PLoS ONE*, 15(7), pp. 1–22. doi: 10.1371/journal.pone.0230400.

Villar, V. A. M. *et al.* (2013) 'Novel role of sorting nexin 5 in renal D1 dopamine receptor trafficking and function: Implications for hypertension', *FASEB Journal*, 27(5), pp. 1808–1819. doi: 10.1096/fj.12-208439.

Vizcaíno, J. A. *et al.* (2016) '2016 update of the PRIDE database and its related tools', *Nucleic Acids Research*, 44(D1), pp. D447–D456. doi: 10.1093/nar/gkv1145.

Van Vliet, J. *et al.* (2006) 'Human KLF17 is a new member of the Sp/KLF family of transcription factors', *Genomics*, 87(4), pp. 474–482. doi: 10.1016/j.ygeno.2005.12.011.

Vol, N. I., Beckmann, A. M. and Wilce, P. A. (1997) 'e r g a m o n Egr TRANSCRIPTION FACTORS IN THE NERVOUS SYSTEM Abstract--The'.

Wang, C. *et al.* (2018) 'METTL3-mediated m 6 A modification is required for cerebellar development', pp. 1–29.

Wang, J. *et al.* (2013) 'WEB-based GEne SeT AnaLysis Toolkit (WebGestalt): update 2013.', *Nucleic acids research*, 41(Web Server issue), pp. 77–83. doi: 10.1093/nar/gkt439.

Wang, Z. *et al.* (2018) 'Axon guidance pathway genes are associated with schizophrenia risk', *Experimental and Therapeutic Medicine*, 16(6), pp. 4519–4526. doi:

10.3892/etm.2018.6781.

Watanabe, M. *et al.* (1992) 'Developmental changes in distribution of nmda receptor channel subunit m rim as', *NeuroReport*, pp. 1138–1140. doi: 10.1097/00001756-199212000-00027.

Watson, P. and T, D. J. S. (2005) 'ER-to-Golgi transport : Form and formation of vesicular and tubular carriers', 1744, pp. 304–315. doi: 10.1016/j.bbamcr.2005.03.003.

Weinberger, D. R. (1988) 'Implications of Normal Brain Development for the Pathogenesis of Schizophrenia', *Archives of General Psychiatry*, 45(11), p. 1055. doi: 10.1001/archpsyc.1988.01800350089019.

Weiss, I. C. *et al.* (2004) 'Effect of social isolation on stress-related behavioural and neuroendocrine state in the rat', *Behavioural Brain Research*, 152(2), pp. 279–295. doi: 10.1016/j.bbr.2003.10.015.

Weller, R. O. *et al.* (2018) 'The meninges as barriers and facilitators for the movement of fluid , cells and pathogens related to the rodent and human CNS', *Acta Neuropathologica*. Springer Berlin Heidelberg, 135(3), pp. 363–385. doi: 10.1007/s00401-018-1809-z.

Wesseling, H. *et al.* (2013) 'A combined metabonomic and proteomic approach identifies frontal cortex changes in a chronic phencyclidine rat model in relation to human schizophrenia brain pathology', *Neuropsychopharmacology*. Nature Publishing Group, 38(12), pp. 2532–2544. doi: 10.1038/npp.2013.160.

Whalley, L. J. *et al.* (1984) 'Schneider's First-Rank Symptoms of Schizophrenia: An Association With Increased Growth Hormone Response to Apomorphine', *Archives of General Psychiatry*, 41(11), pp. 1040–1043. doi: 10.1001/archpsyc.1983.01790220030005.

Whitford, T. J. *et al.* (2010) 'Corpus Callosum Abnormalities and Their Association Schizophrenia', *BPS*. Elsevier Inc., 68(1), pp. 70–77. doi: 10.1016/j.biopsych.2010.03.025.

Wisco, J. J. *et al.* (2007) 'Abnormal cortical folding patterns within Broca ' s area in schizophrenia : Evidence from structural MRI', *Schizophrenia Research*. Elsevier B.V., 94(1), pp. 317–327. doi: 10.1016/j.schres.2007.03.031.

Wiser, A. K. *et al.* (1998) 'circuits cause " cognitive dysmetria " in schizophrenia', 9(8),

pp. 1895–1900.

Wolf, C. *et al.* (2011) 'Dysbindin-1 genotype effects on emotional working memory', *Molecular Psychiatry*. Nature Publishing Group, 16(2), pp. 145–155. doi: 10.1038/mp.2009.129.

Wong, E. H. M. *et al.* (2014) 'Common Variants on Xq28 Conferring Risk of Schizophrenia in Han Chinese', 40(4), pp. 777–786. doi: 10.1093/schbul/sbt104.

Woods, B. T. (1998) 'Is schizophrenia a progressive neurodevelopmental disorder? Toward a unitary pathogenetic mechanism', *American Journal of Psychiatry*, 155(12), pp. 1661–1670. doi: 10.1176/ajp.155.12.1661.

Working, S. and Consortium, G. (2014) 'Biological insights from 108 schizophrenia-associated genetic loci'. doi: 10.1038/nature13595.

Wu, Y., Yao, Y. and Luo, X. (2017) 'SZDB : A Database for Schizophrenia Genetic Research', 43(2), pp. 459–471. doi: 10.1093/schbul/sbw102.

Wu, Z. *et al.* (2005) 'Interleukin-21 Receptor Gene Induction in Human T Cells Is Mediated by T-Cell Receptor-Induced Sp1 Activity', *Molecular and Cellular Biology*, 25(22), pp. 9741–9752. doi: 10.1128/mcb.25.22.9741-9752.2005.

Ye, B. *et al.* (2011) 'Differential regulation of dendritic and axonal development by the novel Krüppel-like factor dar1', *Journal of Neuroscience*, 31(9), pp. 3309–3319. doi: 10.1523/JNEUROSCI.6307-10.2011.

Yosef, B. Y. and H. (1995) 'Controlling the False Discovery Rate : a Practical and Powerful Approach to Multiple Testing', *Journal of the royal stadtstical society*, 57;1, pp. 289–300. doi: 10.1111/j.2517-6161.1995.tb02031.x.

Zehmer, J. K. *et al.* (2008) 'Identification of a novel N-terminal hydrophobic sequence that targets proteins to lipid droplets', *Journal of Cell Science*, 121(11), pp. 1852–1860. doi: 10.1242/jcs.012013.

Zhang, J.-M. and An, J. (2009) 'NOT RIGHT REFERENCECytokines, Inflammation and Pain', *Int Anesthesiol Clin.*, 69(2), pp. 482–489. doi: 10.1097/AIA.0b013e318034194e.Cytokines.

Zhang, Y. *et al.* (2015) 'Polymorphisms in MicroRNA Genes and Genes Involving in NMDAR Signaling and Schizophrenia: A Case-Control Study in Chinese Han Population', *Scientific Reports*. Nature Publishing Group, 5(August), pp. 1–9. doi:

10.1038/srep12984.

Zhang, Y. *et al.* (2016) 'Cortical grey matter volume reduction in people with schizophrenia is associated with neuro-in fl ammation', *Nature Publishing Group*. Nature Publishing Group, (September), pp. 1–10. doi: 10.1038/tp.2016.238.

Zhao, Z. *et al.* (2015) 'Transcriptome sequencing and genome-wide association analyses reveal lysosomal function and actin cytoskeleton remodeling in schizophrenia and bipolar disorder', (August 2014), pp. 563–572. doi: 10.1038/mp.2014.82.

Zuccoli, G. S. *et al.* (2017) 'The energy metabolism dysfunction in psychiatric disorders postmortem brains: Focus on proteomic evidence', *Frontiers in Neuroscience*. doi: 10.3389/fnins.2017.00493.

van Zyl, P. J., Dimatelis, J. J. and Russell, V. A. (2016) 'Behavioural and biochemical changes in maternally separated Sprague–Dawley rats exposed to restraint stress', *Metabolic Brain Disease*, 31(1), pp. 121–133. doi: 10.1007/s11011-015-9757-y.